

The palynology and stratigraphy of the Cambrian
Nolichucky Shale and associated formations at
Thorn Hill, Tennessee, USA.

by

Brian E. Pedder



Thesis submitted for the degree of Doctor of Philosophy

Palynology Research Facility, Department of Animal
and Plant Sciences, University of Sheffield

September 2012

Acknowledgements

I gratefully acknowledge the receipt of a PhD scholarship funded by NERC Open CASE award NE/F013833/1 held in the Department of Animal and Plant Sciences of the University of Sheffield and the Palaeontology Department of the Natural History Museum, London. I would like to express my sincere thanks to the following people: Professor Charles Wellman for his supervision throughout my PhD; Dr. Susanne Feist-Burkhardt and Dr. Tim Potter from the Natural History Museum, London for their continued support and advice; Dr. Adrian Rushton from the Natural History Museum, London and Professor John Taylor from the Indiana University of Pennsylvania for identifying trilobites; Dr. Gabrielle Kennaway from the Natural History Museum, London for TEM analysis; Professor Paul Strother and Dr. John Beck from the Western Observatory, Boston College, Massachusetts, USA for their invaluable expertise, support and advice during Field work in the USA; Dr. John Williams and his extraordinary Index of Palaeopalynology (JWIP) at the Natural History Museum, London; Dr. Alex Ball and Dr. Lauren Howard from the Electron Microscope Unit, EMMA Division, Mineralogy Department, Natural History Museum, London for their technical advice and support regarding SEM analysis.

Abstract

A detailed palynological and stratigraphic study was undertaken on the Cambrian Nolichucky Shale, Maynardville Limestone and Copper Ridge Dolomite (Conasauga Group), as exposed at Thorn Hill, northeastern Tennessee, USA. The majority of palynological samples show low abundance and diversity. Fifty two acritarch taxa (fifteen assigned to species; twenty six left in open nomenclature; eleven new forms), two problematica and four invertebrate components are described. Based upon trilobite biostratigraphy and stable carbon isotope chemostratigraphy, the stratigraphic position of the Cambrian Series 3/Furongian (Marjuman/Steptoean; *Aphelaspis* Zone/*Crepicephalus* Zone) boundary is broadly indentified within the uppermost section of the Nolichucky Shale. The first record of SPICE identified using organic residues is also reported, the onset of which is coincident with the *Aphelaspis* Zone/*Crepicephalus* Zone boundary). Recovered acritarchs have little immediate, comparative, stratigraphic value but some forms (Acritarch sp. 1 and Acritarch sp. 2) may have future potential use as biostratigraphic markers for shallow marine upper Cambrian Series 3 units. Palynofacies data and sedimentology indicate that the acritarch abundance peak in the Nolichucky Shale may represent maximum water depth within a transgressive/regressive cycle. Based on TEM analysis of vesicle wall ultrastructure, *Peteinosphaeridium?* sp. 1, *Peteinosphaeridium?* sp. 2, and Acritarch sp. 2 are interpreted as belonging to the Class *Chlorophyceae*. The vesicle wall ultrastructure of Acritarch sp. 1 is trilaminar, consisting of a central alveolar layer bounded by two, thin, electron dense layers and is comparable to that of diapause egg cases of extant branchiopods. Based upon wall ultrastructure, vesicle size and surface ornament, recalcitrant wall biochemistry and evidence of co-occurrence of branchiopod-type crustaceans, Acritarch sp. 1 is interpreted as being the egg case of a Cambrian branchiopod-type crustacean, and as such represents the earliest evidence for diapause-type dormancy in the fossil record.

Contents

Chapter 1

Introduction	1
--------------	---

Chapter 2

Cambrian Period and geological setting	3
2.1. The Cambrian world	3
2.1.1. Introduction	3
2.1.2. Cambrian time scales	3
2.1.3. Global boundary Stratotype Section and Point (GSSP) definitions	5
2.1.4. Cambrian Palaeogeography	7
2.1.5. Cambrian Palaeoenvironment	8
2.1.5.1. Palaeoclimate	8
2.1.5.2. Atmospheric composition	10
2.1.6. Chemostratigraphy	13
2.1.6.1. Introduction	13
2.1.6.2. Strontium	14
2.1.6.3. Carbon	16
2.2. Geology of the Cambrian of North America	19
2.2.1. Laurentia and the North American craton	19
2.2.2. Cambrian geological history and stratigraphy of the United States	20
2.2.2.1. Introduction	20
2.2.2.2. Cratonic sequences and the Sauk Sequence	22
2.2.2.3. Biostratigraphy and North American Cambrian time scales	23
2.2.2.4. Chemostratigraphy: Steptoean positive isotope carbon excursion (SPICE)	29
2.3. The Thorn Hill section, Tennessee	30
2.3.1. Introduction	30
2.3.2. Cambrian formations at Thorn Hill	30
2.3.3. Palaeoenvironments and facies	36
2.3.4. Biostratigraphy	39
2.3.5. Chemostratigraphy	41
2.3.6 Sample collection at Thorn Hill	43

2.3.6.1 Definition of units	43
2.3.6.2 Sampling	43
2.4 The Chief Joseph Highway section, Wyoming	46
2.4.1 Location and geology	46

Chapter 3

Materials and methods	49
3.1. Materials	49
3.1.1 Introduction	49
3.2 Methods	49
3.2.1. Cleaning	49
3.2.2. Acid maceration	50
3.2.3. Sieving	51
3.2.4. Removal of Iron sulphide (pyrite)	51
3.2.5. Heavy liquid separation	51
3.2.6. Oxidation	51
3.2.7. Staining	51
3.2.8. Light microscopy (LM): slide preparation, analysis and imaging	52
3.2.9. Scanning electron microscopy (SEM)	53
3.2.10. Transmission electron microscopy (TEM)	53
3.2.10.1. TEM: specimen selection, preparation, analysis and imaging	53
3.2.10.2. Modifications to the standard TEM protocol	55
3.2.11. Carbon isotope analysis	56
3.3. Sample data	57

Chapter 4

Systematics	63
4.1. Introduction	63
4.2. Species list	63
4.3. Systematics: Acritarchs and Problematica	65
4.4. Invertebrates	129
4.4.1. Introduction	129
4.4.2. Descriptions	129

Chapter 5

Review of Cambrian palynology	135
5.1. Introduction	135
5.2. Terreneuvian and Cambrian Series 2	135
5.3. Cambrian Series 3 and Furongian	140
5.4. Small Carbonaceous Fossils (SCFs)	145

Chapter 6

Stratigraphy	147
6.1. Introduction	147
6.2. Trilobite biostratigraphy	148
6.2.1. Introduction	148
6.2.2. Trilobite biostratigraphy of the Nolichucky Shale	148
6.3. Carbon isotope stratigraphy	150
6.3.1. Introduction	150
6.3.2. Results	151
6.3.3. Discussion	153
6.4. Combined trilobite and carbon isotope stratigraphy	156
6.5. Palynomorphs and biostratigraphy	157
6.6. Conclusion	160

Chapter 7

Palynofacies and palaeoenvironment	163
7.1 Sedimentology and palaeoenvironmental interpretation	163
7.2 Palynofacies	164
7.2.1 Classification	164
7.2.1.1 Acritarchs	164
7.2.1.2 Sphaeromorph acritarchs	164
7.2.1.3 Cells and cryptospores	164
7.2.1.4 Amorphous organic matter (AOM)	165
7.2.1.5 Inertinite	165
7.2.1.6 Cuticular fragments	165

7.2.1.7 Plates	165
7.2.1.8 Spines	166
7.2.1.9 Filaments	166
7.2.1.10 Graptolite cuticle	166
7.2.1.11 Problematica	166
7.3 Discussion	166
7.4. Conclusion	167

Chapter 8

Large spinose acritarchs from the Cambrian of the USA: biological Affinities	169
8.1. Introduction	169
8.2. Algal affinities of acritarchs	170
8.3. Acritarch size in the Ediacaran and Cambrian Periods	172
8.4. Large vesicle size and metazoan affinities	173
8.5. Crustacean affinities of acritarchs	175
8.5.1. Copepods, branchiopods and their egg cases	175
8.5.2. Comparisons between copepod/branchiopod eggs and acritarchs	177
8.6. Ultrastructure of copepod and branchiopod egg cases	179
8.6.1. Copepod egg cases	179
8.6.2. Branchiopod egg cases	180
8.7. TEM analysis of acritarchs from the USA	181
8.7.1. Introduction	181
8.7.2. TEM descriptions	182
8.8. Discussion	183
8.8.1. Acritarch sp. 1	183
8.8.2. Acritarch sp. 2, <i>Peteinosphaeridium?</i> sp. 1 and <i>Peteinosphaeridium?</i> sp. 2.	188
8.9. Conclusion	189

Chapter 9

Conclusions	191
References	193

Chapter 1.

Introduction

Cambrian Laurentia was a palaeocontinental landmass made up of what is now North America (Canada and the U.S.A), Greenland, Svalbard and northwest Scotland. In the United States Cambrian rocks are predominantly Cambrian Series 3 (middle Cambrian) to Furongian (late Cambrian) in age with only a few sections from the Terreneuvian and Cambrian Series 2 (collectively lower Cambrian). The sections are often incomplete with numerous unconformities of one form or another and are dominated by limestone and siliciclastic lithologies (Lochman-Balk 1971). Perhaps it is not surprising then, that as yet, only seven papers have been published relating to the Cambrian palynology of the United States. Of these only two describe and illustrate palynomorph assemblages, including acritarchs, cell clusters and filaments (Wood & Clendening 1982; Wood & Stephenson 1989) whilst the others are either concerned with the morphology and ultrastructure of cryptospores (Strother et al. 2004; Taylor & Strother 2008; 2009) or erect individual acritarch genera (Clendening & Wood 1981; Strother 2008). Consequently our knowledge and understanding of U.S. Cambrian palynology, in particular the palaeogeographic and temporal distribution of the acritarchs, is somewhat lacking and determined systematic study is long overdue.

Similarly, there have been few palynological studies (acritarchs) on Laurentian units in Canada, although these studies are more comprehensive (Dean & Martin, 1982; Baudet et al., 1989; Martin, 1992; Nowlan et al. 1995). A number of other studies have focused more on microscopic components of invertebrates such as *Wiwaxia* sclerites (Butterfield 1990b; Harvey et al. 2011) and evidence for the feeding mechanisms of Cambrian crustaceans (Harvey & Butterfield, 2008; Harvey et al. 2012). These types of study are of course important in determining the evolution and phylogenetic relationships of various invertebrates, and one of the key aspects of this is the understanding of their palaeogeographic and temporal distributions. It has been shown that the occurrence of microscopic recalcitrant remains of arthropods and other invertebrates (e.g. spines, plates and feeding mechanisms) appear to be more abundant than their macrofossil equivalents (Harvey et al. 2011) and that the reasons for this are most likely related to taphonomy. Given this, it is clear that the

palaeogeographic and temporal distributions of known arthropods might be better recorded via the occurrences of their microscopic recalcitrant remains in palynological residues.

This thesis examines the palynology of the Nolichucky Shale, Maynardville Limestone and Copper Ridge Formations as exposed in road cuttings and creeks at Thorn Hill in northeast Tennessee, U.S.A. The Nolichucky Shale represents deposition within a shallow, carbonate rimmed, intracratonic basin (the Conasauga intrashelf shale basin) and consists primarily of shale with subsidiary interbedded limestones and flat-pebble conglomerates (Byerly, 1986; Glumac & Walker, 2000). It has been dated using trilobites as Cambrian Series 3 to Furongian in age (Derby, 1965; Sundberg, 1989) and the onset of the Steptoean positive carbon isotope excursion (SPICE), which is coincident with the onset of the Furongian, has been recorded in carbonates in the uppermost part of the Nolichucky Shale at Thorn Hill (Glumac & Walker, 1998).

The main focus of this thesis is on the description and recording of acritarchs found in the Nolichucky Shale at Thorn Hill with some additional work on microscopic, recalcitrant, invertebrate components. Both standard and low-energy palynological techniques (e.g., processing without centrifuging) have been used for palynomorph extraction, the latter to reduce potential damage to larger specimens, in particular invertebrate components. Light microscope, SEM and TEM analysis have been used for acritarch analysis. Also, to enable a stronger stratigraphic framework, stable carbon isotope ratios were recorded in all samples, and trilobites were collected where possible.

It is the aim of this thesis to present a comprehensive palynological analysis of viable palynomorphs extracted from the Nolichucky Shale, Maynardville Limestone and Copper Ridge Dolomite, and with the additional trilobite and chemo-stratigraphic data, give a multi-contextual (acritarchs and invertebrate components) and mutually supportive stratigraphic framework for the various palynomorph groups.

Chapter 2

The Cambrian Period and geological setting

The first part of this chapter gives a brief introduction to the Cambrian world: its palaeoenvironment, palaeogeography and the global time scales in use today. The second part gives a more detailed account of the Cambrian geology of the USA. The stratigraphy (sequence-, chemo- and bio-) and the sedimentological and structural evolution of the North American Craton are all discussed and the chronostratigraphic time scales used are described. A detailed account of the sample site at Thorn Hill, including location, stratigraphy and palaeoenvironmental context are given at the end.

2.1 The Cambrian World

2.1.1 Introduction

The Cambrian Period, as we understand it today, spanned approximately 54 million years from 542 Ma to 488 Ma (Gradstein et al., 2004). It is probably best known for the “Cambrian explosion”, an astonishing exponential surge of biotic innovation and complexity that oversaw the evolution of the first mineralised metazoan skeletons and the appearance of, amongst many other fauna, the trilobites. Our understanding of the Cambrian biota has been much aided by the discovery of Fossil Konservat Lagerstätten, including the Burgess Shale in Canada (Briggs et al., 1994; Conway Morris, 1998) and the Chengjiang biota from China (Hou et al., 1999; Zhang et al., 2001). Studies of fossils from these sites of exceptional preservation have revealed how diverse and complex metazoan life became during the Cambrian. All of these discoveries, however, and the events and organisms they represent are bound to the marine realm, and although the possibility of terrestrial Cambrian metazoan life (animals, plants or fungi) should not be ruled out, the evidence for its existence is problematic (see Strother, 2000; Retallack, 2011).

Thus the Cambrian period represents a unique time in Earth history during which the world’s biota underwent major changes in a relatively short period of time, just prior to the metazoan colonisation of land in the Ordovician.

2.1.2 Cambrian time scales

The Cambrian has traditionally been divided into three series/epochs: lower/early; middle/middle; upper/late (Fig. 2.1). However, the inherent difficulties of correlating the traditional series boundaries globally and the uneven time durations as represented by the three series have, over the past few decades, prompted major concerns. The lower Cambrian series, for example, was shown to represent more time than once thought resulting in it taking up the majority of Cambrian time

SYSTEMS	SERIES	STAGES	BOUNDARY HORIZONS	AGE (Ma)	
Ordovician	Lower	Tremadocian			
Cambrian	Upper	Stage 10	FAD of <i>Iapetognathus fluctivagus</i> (GSSP)	488.3	
		Stage 9			
		Paibian			
	Middle	Series 3	Guzhangian	FAD of <i>Glyptagnostus reticulatus</i> (GSSP)	499
			Drumian	FAD of <i>Lejopyge laevigata</i> (GSSP)	503
			Stage 5	FAD of <i>Ptychagnostus atavus</i> (GSSP)	506.5
			Stage 4		
	Lower	Series 2	Stage 3		
			Stage 2	FAD of Trilobites	
			Fortunian		
		Terreneuvian		FAD of <i>Trichophycus pedum</i> (GSSP)	542
	Ediacaran				

Figure 2.1 The most recent chronostratigraphic subdivisions of the Cambrian System. Ratified series and stage boundaries are indicated with ‘GSSP’. The old Cambrian timescale is to the left. FAD = first appearance datum.

(Landing et al., 1998). In fact the lower Cambrian series represents approximately 29 million years (myr) whereas the middle and upper Cambrian series represent approximately 12 myr and 13 myr respectively (Gradstein et al., 2004). Also, the

lack of an internationally agreed, global stage scheme for the Cambrian System has inevitably led to the development and entrenchment of localised chronostratigraphic schemes. There are now numerous regional stage schemes in use for most continents, the most notable and well studied being those of Australia, Baltica, southern China, Kazakhstan, North America and Siberia, none of which can be applied globally.

Attempts to address this unsatisfactory state of affairs have been made by the International Subcommission on Cambrian stratigraphy (ISCS) and the traditional three series system has been replaced by a new four series subdivision (Babcock et al., 2005) (Fig. 2.1). The new, lower two series (Terreneuvian and Series 2) approximately correspond to the traditional lower Cambrian with the FAD (first appearance datum) of trilobites marking the base of Series 2 (yet to be ratified); the new Series 3 approximately corresponds to the traditional middle Cambrian and the new uppermost series, the Furongian, corresponds to the Hunanian Series (traditional upper Cambrian) of South China (Peng & Babcock, 2001; Babcock & Peng, 2007). The system is further subdivided into ten stages: the lower two series having two stages each and the upper two series three stages each; this reflects an increase in the number of globally correlatable events recognised in the Cambrian system. It should be noted, however, that most of these subdivisions have yet to be formally defined and ratified and the Cambrian time scale as it stands currently, is unfinished. Completion in terms of defining all Cambrian internal subdivisions (series and stages) is tentatively expected in 2012. For a full discussion see Babcock & Peng (2007). For North American time scales see chapter 2.2.3.3.

2.1.3 Global boundary Stratotype Section and Point (GSSP) definitions

The following are all the Global boundary Stratotype Section and Point (GSSP) definitions for the Cambrian System that have been, or are close to being, ratified by the International Commission on Stratigraphy (ICS) and the International Union of Geological Sciences (IUGS) as of March 2012. For a more detailed discourse see Gradstein (2004).

Precambrian-Cambrian boundary: base of Fortunian Stage, Terreneuvian Series, Cambrian System, Palaeozoic Era and Phanerozoic Eon 542 Ma

The GSSP for the Precambrian-Cambrian boundary is defined as the point where the trace fossil *Trichophycus pedum* (originally *Phycodes pedum*) first appears in the

coastal cliff-section, 2.4m above the base of Member 2 in the Chapel Island Formation, at Fortune Head on the Burin Peninsular, SE Newfoundland, Canada (47°4'34.47"N, 55°49'51.71"W), (Brasier et al., 1994; Landing, 1994; Gehling et al., 2001; Landing et al., 2007). It was ratified in 1992.

Drumian Stage 506.5 Ma

The GSSP for the base of the Drumian Stage (Cambrian Stage 6) is defined as the base of the limestone unit (calcsiltite) situated 62 m above the base of the Wheeler Formation within the Stratotype Ridge section in the Drum Mountains, Utah, USA (39°30.705'N, 112°59.489'W), (Babcock et al., 2007). The GSSP horizon contains the first appearance of the cosmopolitan agnostid trilobite *Ptychagnostus atavus* which marks the base of the *P. atavus* Zone. A secondary global event marker is a major negative carbon isotope excursion referred to as the Drumian carbon isotope excursion (DICE), which is found just above the GSSP (Babcock et al., 2004, 2007; Zhu et al., 2006). It was ratified in 2006.

Guzhangian Stage 503 Ma

The proposed GSSP for the base of the Guzhangian Stage (Cambrian Stage 7) is defined as the point at which the cosmopolitan agnostid trilobite *Lejopyge laevigata* first appears in the road cut-section situated on the south bank of the Youshui River (Fengtian Reservoir) in the Wuling Mountains, 121.3m above the base of the Huaqiao Formation in the Luoyixi section, Guzhang County, Hunan Province, China (28°43.20'N, 109°57.88'W) (Peng et al. 2006a, 2006b; Bagnoli et al., 2008). It was ratified in 2008.

Furongian Series & Paibian Stage 499 Ma

The GSSP for the base of the Furongian Series and Paibian Stage is defined as the point at which the cosmopolitan agnostid trilobite *Glyptagnostus reticulatus* first appears, 369m above the base of the Huaqiao Formation in the Paibi section, NW Hunan Province, China (28°23.37'N, 109°31.54'E), (Peng et al., 2004). This broadly coincides with the onset of a major positive carbon isotope excursion referred to as the Steptoean positive carbon isotope excursion (SPICE) (Peng et al., 2004). It was ratified in 2003.

Cambrian-Ordovician boundary: base of Tremadocian Stage and Ordovician System 488.3 Ma

The GSSP for the Cambrian-Ordovician boundary is defined as the point at which the conodont *Iapetognathus fluctivagus* first appears, as found in the coastal platform at Green Point, in the Gros Morne National Park, western Newfoundland, at the 108.1m level, within bed 23, in the measured section (Lower Broom Point Member, Green Point Formation), (49°40'58.5"N, 57°57'55.09"W). This is 4.8m below the earliest planktonic graptolites (Cooper et al., 2001). It was ratified in 2000. It should be noted that the appearance of the oldest planktonic graptolites belonging to the *Rhabdinopora flabelliformis* species group is very close to the formal boundary as defined by conodonts. This is significant in international correlation because many regions around the globe do not have conodont-bearing limestones.

2.1.4 Cambrian Palaeogeography

Palaeocontinental reconstructions for the Late Neoproterozoic to Early Palaeozoic have been produced by numerous workers with varied results (e.g., McKerrow et al., 1992, Torsvik & Rehnström, 2001; Cocks & Torsvik, 2002, 2006; Scotese, 2002), the main differences being mostly due to the lack of reliable palaeomagnetic data on some of the continental blocks (Meert & Lieberman, 2004). However, it is generally agreed that during the Cambrian there were five major continents (Fig. 2.2): Baltica (composed of northern Europe and Russia west of the Urals), China (China and

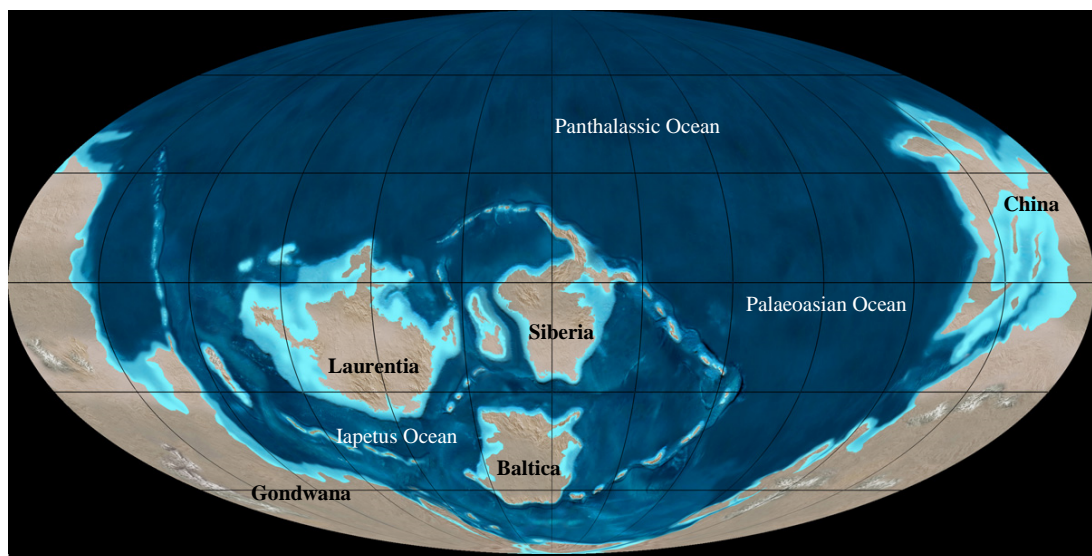


Figure 2.2 A palaeogeographic reconstruction for the Cambrian Period, approximately 500 Ma (Guzhangian/Furongian boundary). After Ron Blakey, NAU Geology.

parts of eastern south-east Asia), Gondwana (Africa, Antarctica, Australia, Florida U.S.A., India and parts of the Middle East and southern Europe), Laurentia (North America, Greenland, northwestern Ireland and Scotland) and Siberia (Russia east of the Ural Mountains and parts of central Asia). There were also smaller landmasses including Avalonia (composed of England, Wales, eastern Newfoundland, Belgium and northern France) and Kazakhstania (situated to the east of Siberia). Notable oceans included the Panthalassic, which occupied most of the northern hemisphere, the Palaeoasian and the Iapetus situated between Laurentia and Baltica.

A particular problem has been the latitudinal positioning of Laurentia during the Cambrian Period (Symons & Chiasson, 1991; Pisarevsky et al., 2000). The general consensus, however, is that Laurentia was situated at high, southerly palaeolatitudes during the Late Neoproterozoic (Meert & Lieberman, 2004) before moving rapidly north: by the early Furongian Laurentia was situated equatorially or at least at low latitudes, where it remained throughout the Early Palaeozoic (Scotese, 2002).

2.1.5 Cambrian Palaeoenvironment

2.1.5.1 Palaeoclimate

Evidence for the palaeoclimate during the Cambrian comes from a wide variety of sources which viewed as a whole is strongly suggestive of a warm world, free of polar ice caps and with rising sea levels. In fact the occurrence of glaciation in the Cambrian has been reported only once, on Avalonia from successions in New Brunswick, Canada (Landing & MacGabhann, 2010). Frakes et al. (1992) place the Cambrian period in the early Palaeozoic “warm mode” which lasted from the earliest Cambrian to the Hirnantian glaciations of the Late Ordovician (530-458 Ma), and Brasier (1992) argued that the Cambrian experienced a move towards ‘greenhouse conditions’ after the Ediacaran Varanger-Marinoan ice ages (605-585). According to these authors the Cambrian was a warm to greenhouse world sandwiched between two major glaciations. Evidence supporting these views is as follows:

1) *Carbonates and reefs*. The global geographical spread of carbonates from low palaeolatitudes (~20°) in the Ediacaran to palaeolatitudes as high as ~50° in the Cambrian (Ziegler et al., 1981) and the appearance and spread of major reef builders, such as archaeocyathan sponges, from the Siberian platform to China, Antarctica and south Australia (Brasier, 1992).

2) *Evaporites*. The development during the Cambrian (Terreneuvian and Series 2), of massive halogenic deposits in Siberia and southern Asia as well as smaller deposits in the Americas, central Australia and Morocco (Frakes et al. 1992). Brasier (1992) suggests that the occurrences of these saline formations are evidence for the development of warm saline bottom waters, undiluted by absent glacial meltwaters. Furthermore, he argued that these nutrient-rich and mineral-saturated water masses might be the source for the major phosphorite formations deposited around Gondwana during the late Ediacaran and Terreneuvian.

3) *Sea level*. Haq & Schutter (2010) determined sea level for most of the Palaeozoic based on sequence stratigraphic data. For the latest Neoproterozoic through to Early Ordovician time interval they used sections in Oman, southern California, the southern Canadian Rockies and Australia. They estimated that sea level at the beginning of the Cambrian was slightly higher than it is today, and that long term sea level rose steadily throughout the Cambrian and into the Ordovician. They noted, however, with reference to comparisons between sea levels past and present, that the further one goes back in time the less reliable the data becomes. Even so, the steady rise in sea level and the lack of evidence for ice caps or major glaciations are compelling indicators for a warming climate during the Cambrian.

4) *Modelling of atmospheric CO₂*. Attempts to understand the Cambrian climate using CO₂ modelling techniques has been slightly undermined by the lack of reliable proxies with which to test them: the proxies we have only go as far back as the Ordovician. However, Royer (2006) made a comparison between the 'best guess predictions' of CO₂ output from the geochemical carbon cycle model GEOCARB III (Berner & Kothavala, 2001) and proxy data obtained from the literature: the GEOCARB III covered the Cambrian to Neogene time interval whilst the proxies covered the Ordovician to Neogene (Fig. 2.3). The two compare reasonably well with the majority of proxies lying within the errors provided by GEOCARB III and the major secular trends being clearly apparent in both. This is mutually supportive for both proxies and the model and gives some validity to the GEOCARB CO₂ output data for the Cambrian. The GEOCARB III model predicts very high (4000+ ppm) CO₂ levels for the Cambrian supporting the idea of a warm or even greenhouse climate.

Other modelling studies on atmospheric CO₂ have been carried out by Berner (1991, 1998, 2006b), Berner & Kothavala (2001) and Royer et al. (2001), all with similar results (see section 2.1.5.2 on atmospheric composition).

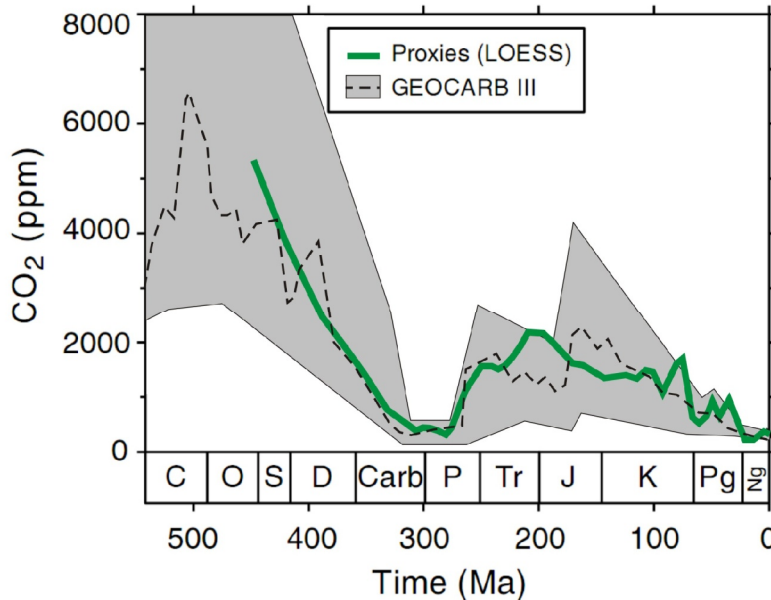


Figure 2.3 Atmospheric CO₂ curve for the Phanerozoic. Dashed line is the best guess predictions of GEOCARB III; solid green line is the proxy record calibrated to the timescale of Gradstein et al. (2004). From Royer (2006b).

2.1.5.2 Atmospheric composition

The principle gases in the Phanerozoic atmosphere in terms of volume and mass were nitrogen (N₂) and oxygen (O₂) (Berner, 2006b), and carbon dioxide (CO₂) in terms of its effect on climate.

Carbon dioxide (CO₂). As previously discussed, atmospheric CO₂ levels have been estimated by Royer (2006b) using the geochemical cycle model GEOCARB III and CO₂ proxies (Fig. 2.3).

For the Cambrian these estimates came out at around 3000-6000 ppm which equate to an atmospheric CO₂ concentration of around 0.3-0.6 % by volume, far greater than CO₂ levels today which are around 0.039 %. Berner & Kothavala (2001), who developed GEOCARB III, obtained RCO₂ values of 16-26 (Fig. 2.4) (RCO₂ being the ratio of the mass of atmospheric CO₂ at a past time to that of the present) equating to around 6000-10,000 ppm or 0.6-1.0 % by volume. Berner (2006b) then

formulated a new model, GEOCARBSULF, by combining GEOCARB III with an isotope mass balance model for O₂ (Berner 2001) and new isotopic data for carbon

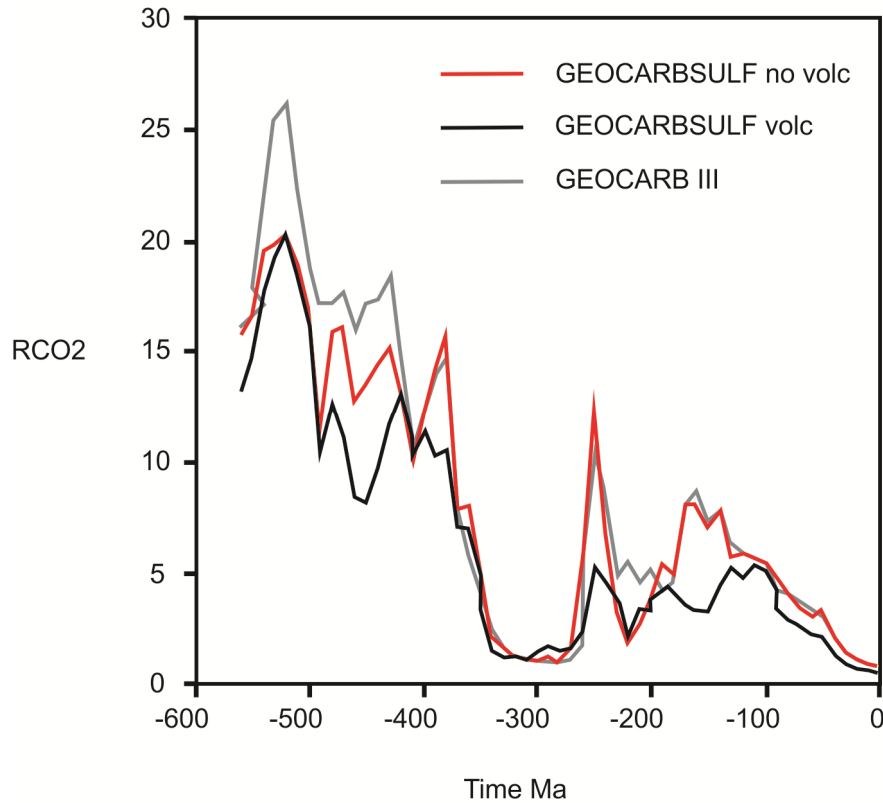


Figure 2.4 Plot of RCO₂ vs. time for GEOCARB (Berner & Kothavala 2001) and GEOCARBSULF modelling. RCO₂ is the ratio of the mass of atmospheric CO₂ at a past time to that at present (weighted mean for the past million years). The terms (volc) and (no volc) refer to the addition or non-addition of variable volcanic weathering to the modelling. From Berner (2006b).

and sulphur. This gave atmospheric CO₂ concentrations in the Cambrian of around 6000-8000 ppm. The main result obtained from GEOCARBSULF is that no majorly significant differences exist between it and earlier GEOCARB CO₂ vs. time curves (Figure 2.4). All the models estimate that atmospheric CO₂ levels during the Cambrian were the highest seen in the Phanerozoic and all had broadly similar trajectories

Oxygen (O₂). A number of studies have been undertaken to discern the levels of atmospheric O₂ through the Phanerozoic (e.g. Berner & Canfield, 1989; Berner 2001, 2006b; Berner et al., 2003; Bergman et al., 2004) with varied results for

Cambrian O₂ levels. Bergman et al. (2004) using the biogeochemical cycling COPSE model (carbon-oxygen-phosphorus-sulphur-evolution) returned Cambrian O₂ levels of around 5% (Fig. 2.5) whilst Berner (2006b), using the GEOCARBSULF model, got higher O₂ levels of around 15-22% (Fig. 2.6).

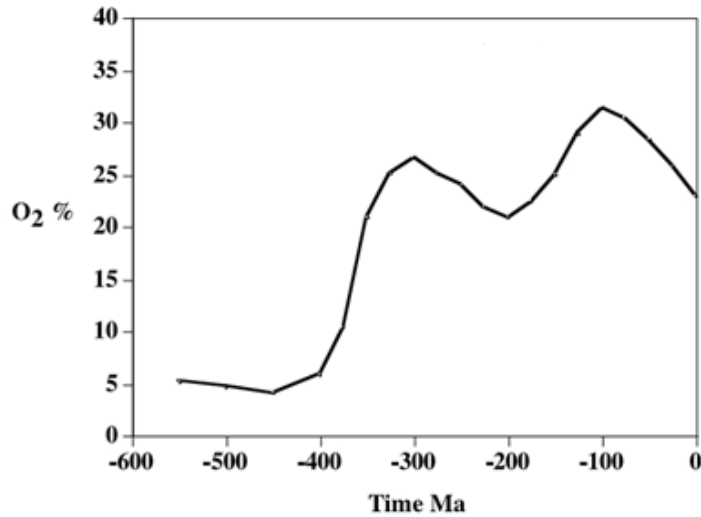


Figure 2.5 Plot of O₂ vs. time. From Bergman et al. (2004).

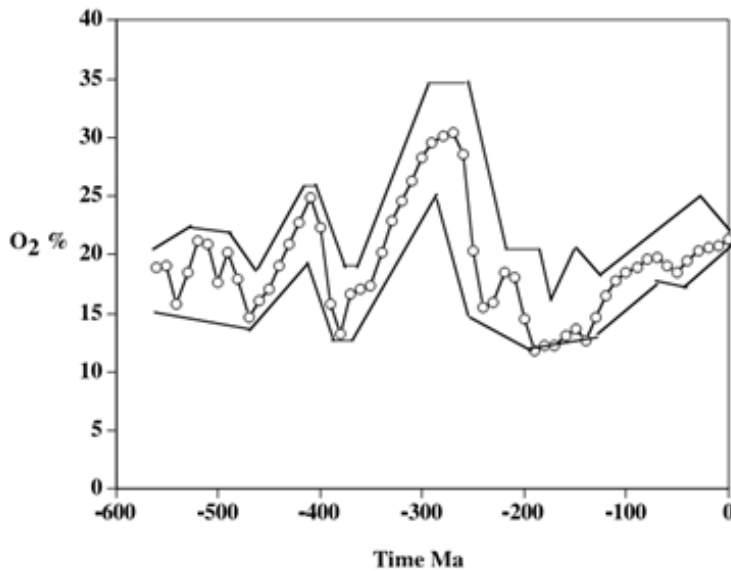


Figure 2.6 Plot of O₂ vs. time for the standard GEOCARNSULF model. From Berner (2006a). The envelope represents a crude estimate of the range of error based on a sensitivity study.

The differences lie in a number of assumptions incorporated, or not, into the respective models. Bergman et al. (2004) assume that the weathering rates of pyrite and organic material are proportional to atmospheric O₂ levels and that the rate of burial of marine organic matter is limited by land derived phosphate supply. These assumptions are challenged by Berner (2006) and are not incorporated into his GEOCARBSULF model.

Nitrogen (N₂). Berner (2006b), using the isotope mass balance model (Berner 2001) and GEOCARBSULF (Berner 2006a), estimates that the mass of atmospheric N₂ actually remains roughly the same throughout the whole Phanerozoic (Fig. 2.7). However, because the mass of atmospheric O₂ has varied quite considerably through the Phanerozoic and given that nitrogen and oxygen make up around 99% of the atmosphere by volume, then the concentration of atmospheric N₂ will also have varied through time (Berner, 2006a). Even so, during the Cambrian the mass of atmospheric O₂ varied only relatively slightly resulting in atmospheric N₂ concentrations varying only slightly also, at around 77-84%.

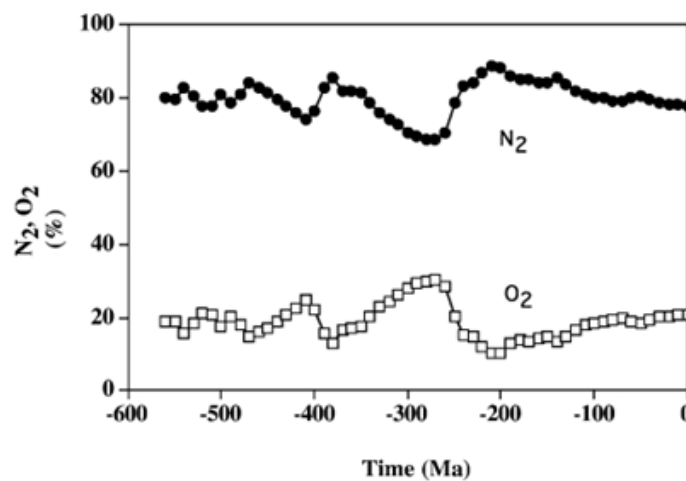


Figure 2.7 Plot of Atmospheric N₂ and O₂ concentrations vs. time. Note the symmetry of the two curves resulting from N₂ and O₂ making up 99% of the Earth's atmosphere by volume. From Berner (2006b).

2.1.6 Chemostratigraphy

2.1.6.1 Introduction

Much of our understanding of Cambrian ocean chemistry is the result of isotope studies, particularly carbon, strontium and oxygen (Ebner et al., 2001). Even so,

although strontium and carbon isotope curves have been determined for the Cambrian, the causes of variations in the various isotope abundances are often difficult to discern (Montañez et al., 2000). Strontium isotope curves for the Cambrian, or Cambrian divisions, have been determined by Montañez et al. (1996; 2000) and Ebner et al. (2001); carbon isotope curves by Runnegar and Saltzman (1998); Montañez et al. (2000); Saltzman et al. (1998; 2000); Zhu et al. (2006); Ahlberg et al. (2008); Kouchinsky et al. (2008), among others.

2.1.6.2 Strontium

Strontium in the oceans is derived from continental weathering and the interaction between sea water and basalt at mid-ocean ridges (Montañez et al., 1996). Strontium isotope values within the oceans are the net result of a complex interplay between the two. The present day seawater $^{87}\text{Sr}/^{86}\text{Sr}$ value is 0.709174 (Montañez et al., 2000).

Montañez et al. (1996) linked increasing $^{87}\text{Sr}/^{86}\text{Sr}$ ratios with increasing continental weathering during regression and decreasing $^{87}\text{Sr}/^{86}\text{Sr}$ ratios to decreasing continental weathering during transgressions. Montañez et al. (2000) looked at Cambrian Series 2 to Furongian deposits in the Great Basin (western US) and southern Canadian Rockies. They suggested the Cambrian experienced periods of significant perturbations in the global Sr and C cycles; in fact they recorded the highest $^{87}\text{Sr}/^{86}\text{Sr}$ value recorded in Earth history, with a $^{87}\text{Sr}/^{86}\text{Sr}$ value of 0.70940 at approximately 498 Ma. A secular rise in $^{87}\text{Sr}/^{86}\text{Sr}$ values from Stage 2 to Stage 5, with a notable increase in the rate of rise of values during Stage 5, is comparable to that observed in the Cenozoic, which has been interpreted as being the result of uplift and continental weathering of the Himalaya-Tibetan Plateau (Richter et al., 1992). This suggests a similar tectonic control during this part of the Cambrian whereby uplift and consequent erosion resulted in an increase in the ^{87}Sr riverine influx. A decrease in $^{87}\text{Sr}/^{86}\text{Sr}$ values during Cambrian Stage 5 and the Drumian is interpreted as being the result of continental rifting along the margins of Gondwana and western Laurentia and the interaction of seawater with subaqueous rift basalts (Curtis et al., 1999). The subsequent rise in $^{87}\text{Sr}/^{86}\text{Sr}$ values during the Guzhangian and Paibian stages is interpreted as a response to the accumulated effects of simultaneous orogenic events in Antarctica and Australia (Curtis & Storey, 1996).

The Cambrian strontium isotope curve we have (Fig. 2.8) is the result of multiple studies (Gradstein et al., 2004) and generally documents a decline in values at the beginning of the Cambrian followed by a rise from Stage 2 to the base of the Furongian before declining again towards the Cambrian-Ordovician boundary. Specifically high resolution strontium isotope curves calibrated to carbon isotope stratigraphy and biostratigraphy have been produced for the Cambrian Series 3 in Australia by Donnelly et al. (1988) and for the Cambrian-Ordovician boundary by Ebneith et al. (2001). The use of strontium isotope stratigraphy in conjunction with other stratigraphic curves has proved useful in highlighting global events. In Siberia and Mongolia, for example, Brasier et al. (1996) used $^{87}\text{Sr}/^{86}\text{Sr}$ measurements to document a major hiatus during the Terreneuvian.

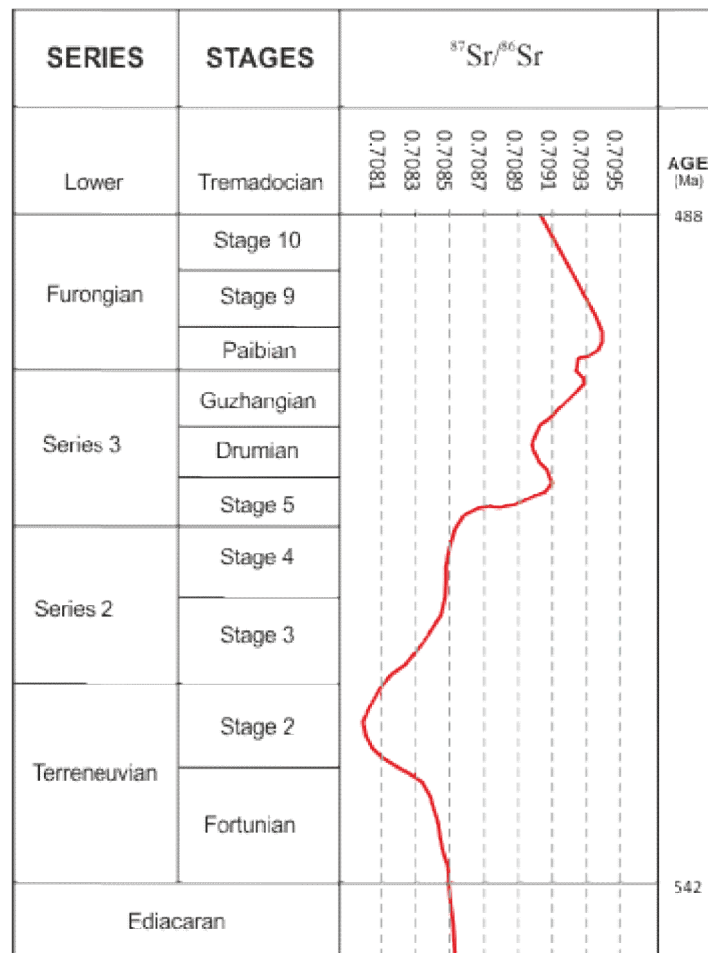


Figure 2.8 Strontium isotope curve through the Cambrian Period. Curve for the Guzhangian and Paibian from Montañez et al. (2000); curve for the remaining from Ebneith et al. (2001).

2.1.6.3 Carbon

Carbon isotope stratigraphy takes advantage of the natural variations that occur between the two stable isotopes of carbon, ^{13}C and ^{12}C . The present, total, global carbon reservoir is estimated to be 98.89% ^{13}C and 1.11% ^{12}C (Hoefs, 1987). However, the distribution of ^{13}C and ^{12}C throughout the various carbon reservoirs (e.g. carbonate rocks, biosphere) is moderated by numerous fractionation processes e.g. photosynthesis. These processes alter the carbon isotope ratios by preferentially concentrating one carbon isotope at the expense of the other in any given reservoir, and because different reservoirs obtain carbon via differing fractionation processes, with differing fractionation factors, the carbon isotope ratios of many reservoirs are different from each other. Furthermore, if the carbon isotope ratio of one reservoir changes, it can affect that of another.

In the marine-derived, sedimentary rock record the two main sources of carbon are shale and carbonates. In shale, carbon is preserved in biodegraded biogenic compounds and the non-decayed corpses of marine organisms, most notably phytoplankton, and is collectively known as total organic carbon (TOC). This carbon (organic) is derived through primary productivity in the marine biosphere where phytoplankton preferentially concentrate the lighter carbon isotope ^{12}C through photosynthesis. In carbonate rocks, carbon (inorganic) is a molecular component of calcium and magnesium carbonates. This carbon is gained through a chemical exchange reaction involving dissolved CO_2 – bicarbonate – carbonate, and its isotope ratio represents that of the sea water it was derived from. Because organic and inorganic carbon are derived via different processes they consequently have different stable carbon isotope signatures (TOC ^{13}C values range from approximately -18 ‰ to <-30 ‰ and carbonate ^{13}C values from +2 ‰ to -0.5 ‰) and both record temporal fluctuations in the carbon cycle in their respective host rock. Consequently, the analysis of carbon isotopes present in suites of shales or carbonates can elucidate changes occurring in the carbon cycle at the time those rocks were formed (Glumac & Spivak-Birndorf, 2002; Glumac & Walker, 1998; Saltzman et al., 1998).

During the Cambrian, oceans were isotopically light in carbon as compared to the rest of the Phanerozoic where the oceans were, on the whole, isotopically heavier and predominantly positive (Gradstein et al. 2004). Montañez et al. (2000) provide a record of ^{13}C values through Cambrian Series 3, where they record a major negative

shift (-4%) just prior to a major trilobite extinction at the Cambrian Series 2/Series 3 boundary. It is associated with a rapid rise in sea level and is interpreted as being the result of a drop in primary productivity and biomass production, in response to flooding of shallow carbonate platforms by anoxic waters depleted in ^{13}C . The return to positive values being the reverse; a drop in sea level during Cambrian Stage 5 followed by recovery of surface water primary productivity.

Brasier (1993) and Saltzman et al. (1998) reported a major carbon isotope excursion in Laurentian, Furongian (Steptoean) rocks in the Great Basin in the western U.S. It has subsequently been reported in Australia, China, Kazakhstan (Runnegar & Saltzman, 1998; Saltzman et al., 2000), Scandinavia (Ahlberg et al., 2008) and Siberia (Kouchinsky et al., 2008) (Fig. 2.9). It represents a global oceanographic event and is now recognised as one of the largest positive carbon isotope excursions recorded in the Phanerozoic and signifies a major perturbation in the global carbon cycle during the Furongian (Saltzman et al., 2000). It lasted approximately 3.5 million years (Saltzman et al., 2004) and began about 500 Ma (Runnegar & Saltzman, 1998). It has a maximum ^{13}C value = $+4\%$ to $+5\%$ Vienna Pee Dee belemnite (VPDB), globally. It is known as the **Steptoean Positive Isotope Carbon Excursion** (Saltzman et al., 1998) or **SPICE**.

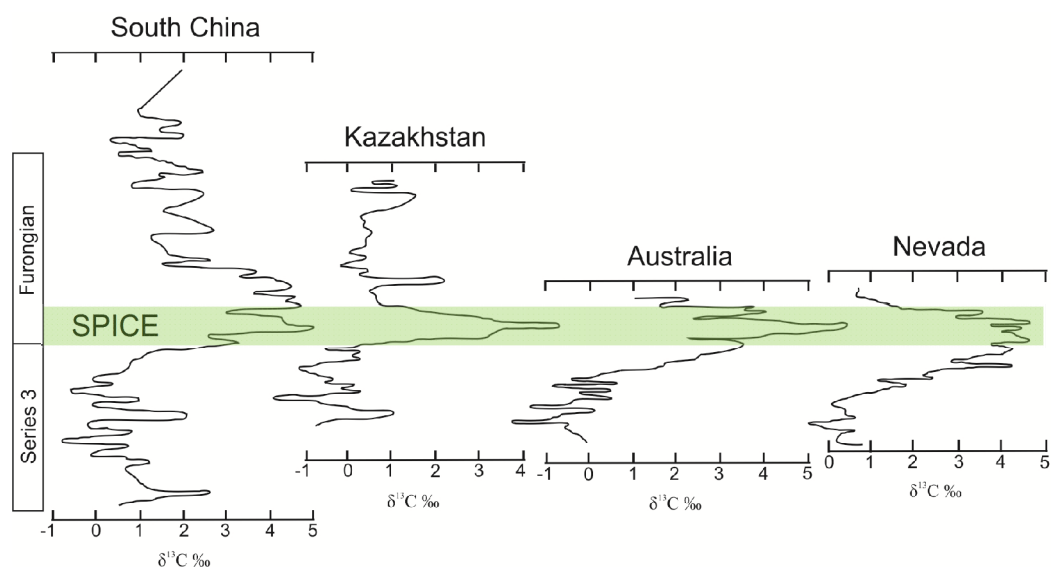


Figure 2.9 Global record of SPICE which is highlighted in green. From Saltzman et al. (2004).

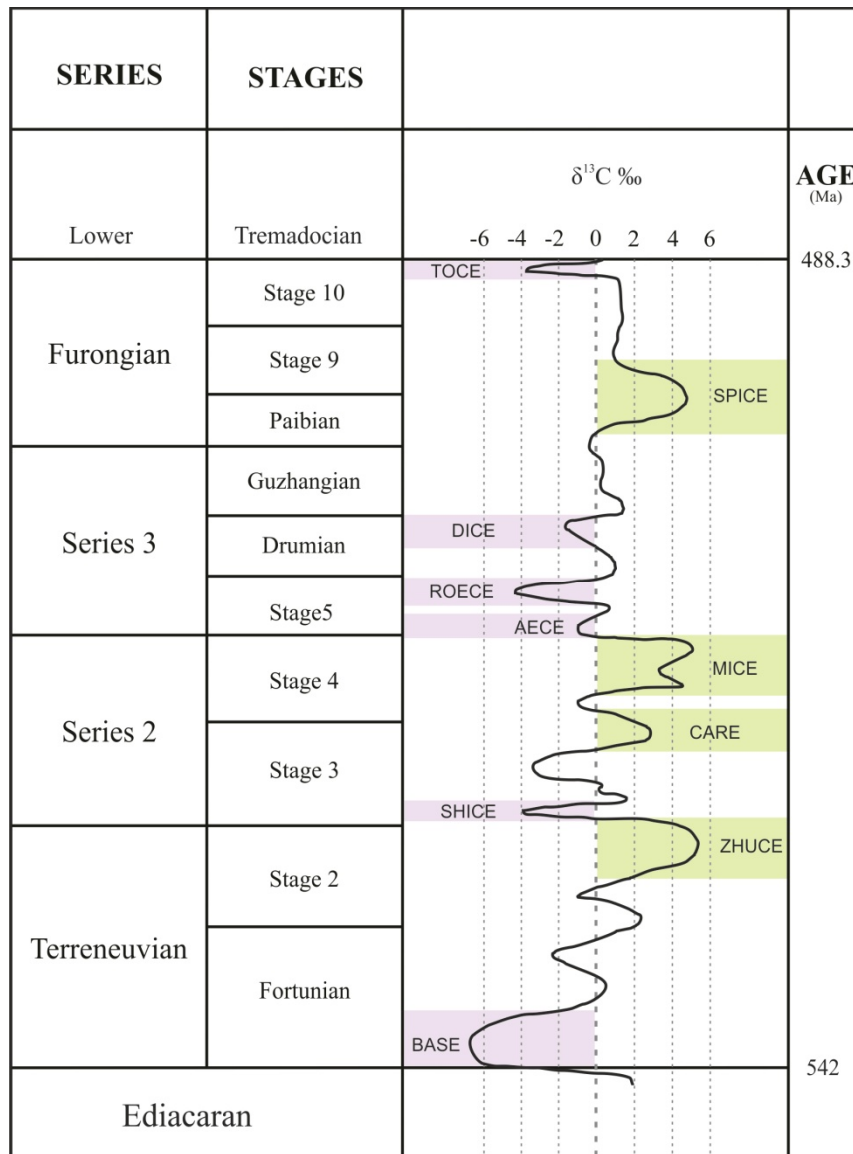


Figure 2.10 Carbon isotope curve for the Cambrian Period with isotope events as proposed by Zhu et al. (2006). Negative excursions in pink; positive excursions in green. TOCE = Top of Cambrian Excursion; SPICE = Steptoean Positive Isotope Carbon Excursion; DICE = Drumian Isotope Carbon Excursion; ROECE = Redlichiid-Olenellid Extinction Carbon isotope Excursion; AECE = Archaeocyathid Extinction Carbon isotope Excursion; MICE = MINGXINSI Carbon isotope Excursion; CARE – Cambrian Arthropod Radiation isotope Excursion; SHICE = SHIYANTOU Carbon isotope Excursion; ZHUCE = ZHUJIAQING Carbon isotope Excursion; BASE = BASAL Cambrian carbon Excursion. From Zhu et al. (2006).

Detailed stratigraphic correlation between SPICE curves and *in situ* trilobite assemblages has proved a valuable tool in international and regional correlation and has confirmed previous global correlations based on trilobites, particularly the agnostid trilobite *Glyptagnostus reticulatus* (Saltzman et al., 1998, 2000; Zhu et al., 2006). The FAD of this species is the GSSP marker for the bases of the

Furongian Series and Paibian Stage in the global time scale (Gradstein et al. 2004; Peng et al. 2004). Globally, the start of SPICE has been recorded as being coincident or very close to a worldwide mass extinction of trilobites at the base of *Glyptagnostus reticulatus* zone (Saltzman et al., 2000). The SPICE maximum and the return to background values both occur between the FAD of *Glyptagnostus reticulatus* and the FAD of *Irvingella* in the Paibian. Other carbon isotope excursions have now been reported, many associated with global biotic and oceanographic events or the occurrence of Lagerstätten deposits (Zhu et al., 2006) (Fig. 2.10). However, their utility as global stratigraphic markers has yet to be tested.

2.2 Geology of the Cambrian of North America

This chapter deals with the formation of the North American craton, the subsequent Cambrian deposition of sediments upon its shores and their geological history and stratigraphy.

2.2.1 Laurentia and the North American craton

Cambrian Laurentia was a palaeocontinental landmass made up of what is now North America, Greenland, Svalbard and northwest Scotland. At its core was the North American Craton, a precise definition of which is difficult to pin down because the craton's boundaries were, and are, continually subject to change through tectonic accretion and erosion (Sloss, 1988). However, notwithstanding the vagaries of plate tectonics, the North American craton is generally taken as the more or less stable interior of the North American continent, upon which most North American Phanerozoic sediments were deposited. It is pre-Phanerozoic in age, composed mostly, but not exclusively, of metamorphic and igneous rocks and has, as a whole, remained essentially stable over the past 600 million years (Sloss, 1988). The midcontinent province, situated between the Appalachian-Ouachita fold belt in the east and the Rocky Mountains in the west, has remained relatively stable for approximately the past one billion years (Hinze & Braille, 1988).

There are two terms commonly found in the literature that are often confused with the term North American craton, but in fact refer to specific parts of it. For the sake of clarity these are the Canadian Shield, which refers to the exposed part of the craton, and the Laurentian Platform, that part of the craton buried beneath Phanerozoic deposits.

Most of the North American craton was formed between 2.0 and 1.6 billion years ago by the accretion of cratonic masses formed during the Archaean (Wicander & Monroe, 2007). Between 1.3 and 1.0 billion years ago Laurentia became part of the first recognised supercontinent, Rodinia (Dalziel, 1992; Torsvik et al., 1996). During this event, the final stage of Laurentian, Proterozoic continental accretion occurred with the Grenville Orogeny (Wicander & Monroe, 2007), affecting the eastern boundary areas of the Laurentian Craton. At 750 Ma Rodinia began to fragment (Dalziel et al., 1994) only to have the continents reform around 650 Ma into another supercontinent, Pannotia (Scotese, 2002). Throughout this whole period, Baltica and Laurentia remained attached until around 600 Ma, when they finally rifted to form the Iapetus Ocean (Torsvik et al., 1996). By 550 Ma, at the very end of the Neoproterozoic Era and just before the onset of the Cambrian Period and Phanerozoic Eon, Pannotia was fragmented (Scotese, 2002) and the North American craton had reached its Phanerozoic form (Sloss, 1988).

2.2.2 Cambrian geological history and stratigraphy of the United States

2.2.2.1 Introduction

From the Late Ediacaran through to the Early Ordovician, the North American craton was subject to a series of transgressive/regressive cycles that deposited swathes of sediments across its Precambrian surface (Sloss, 1988). Collectively these cycles are known as the Sauk sequence (Sloss, 1963, 1964, 1988). During periods of regression those sediments underwent weathering and erosion, resulting in a series of Cambrian formations bounded by unconformities. Consequently, the North American Cambrian system is riddled with hiatuses, and the majority of Cambrian deposits are incomplete and lie unconformably upon Precambrian basement (Lochman-Balk, 1971). Most sections are Series 3 to Furongian in age but exceptions are found on the western and eastern fringes of the craton where more extensive Cambrian sections are found. One such example is the Thorn Hill section in north eastern Tennessee, where an almost complete Cambrian succession is exposed (Byerly et al., 1986). Other examples are found in the Lake Superior Basin in Minnesota and Wisconsin where early Cambrian non-marine sediments outcrop around the shores of Lake Superior (Lochman-Balk, 1971), in the Southern Oklahoma Aulacogen where groups of igneous and sedimentary rocks have been dated as early and middle Cambrian (Terreneuvian, Series 2 & 3) (Ham et al., 1964)

and in Arizona where lower-middle Cambrian sequences are exposed in the Grand Canyon (Tonto Group consisting of the Tapeats Sandstone, Bright Angel Shale and Mauv Limestone). All of these sites are pre-Furongian intracratonic basins (Fig. 2.11) (Lochman-Balk, 1971).

As a result of Proterozoic tectonics, the Precambrian surface upon which Cambrian sediments were deposited, had considerable topographic relief which had a major influence on the Phanerozoic geology of the USA (Lochman-Balk, 1971; Baars, 1988; Bunker et al., 1988). In the US the most dramatic element inherited from the Proterozoic was the Transcontinental Arch (Fig. 2.11), a major tectonic high running south west across the craton from Ontario, Canada to Chihuahua, Mexico. It was approximately 2,250 km long and 960-1300 km wide (Lochman-Balk, 1971) and acted as a major boundary against the transgressing Cambrian seas and was the main part of the craton that remained emergent throughout the Cambrian Period. However, during the Late Sunwaptan the arch subsided and divided into two sections, the Siouxi Arch to the north and the Sierra Grande Arch to the south (Lochman-Balk, 1971). Other significant tectonic highs were the Cambridge Arch (Black Hills)-Central Kansas Uplift (Bunker et al., 1988) which cut across the Transcontinental Arch; the Adirondack and Ozark Domes; the Northern Michigan Highlands and the Wisconsin Highlands; and Montana in and around north west Montana (Fig. 2.10) (Lochman-Balk, 1971). All of these positive elements were exposed to subaerial erosion and acted as major sources of sediment for the seas throughout most of the Cambrian Period (Lochman-Balk, 1971). Most of the craton, however, consisted of stable, vastly expansive shelves submerged below epeiric seas (Lochman-Balk, 1971) which received sediment from the craton and/or developed vast carbonate platforms. Cambrian sections across the craton range in thickness from 0 to 5,000 m, the variations being the result of local relief of the Proterozoic surface (Milici & De Witt, 1988) and the effects of regressive oceans and consequential erosion. The most common Cambrian rock types are fine to coarse sandstones, many of which are transgressive, and carbonates and dolomites (Lochman-Balk, 1971). Shales are less common, occurring both as thin subsidiary units within larger clastic or carbonate sequences, and as larger, less common intra-formational units. Other significant rock types are flat pebble conglomerates (Myrow et al., 2004) and oolites, and glauconite is common (Lochman-Balk, 1971). Most Cambrian rocks have avoided significant

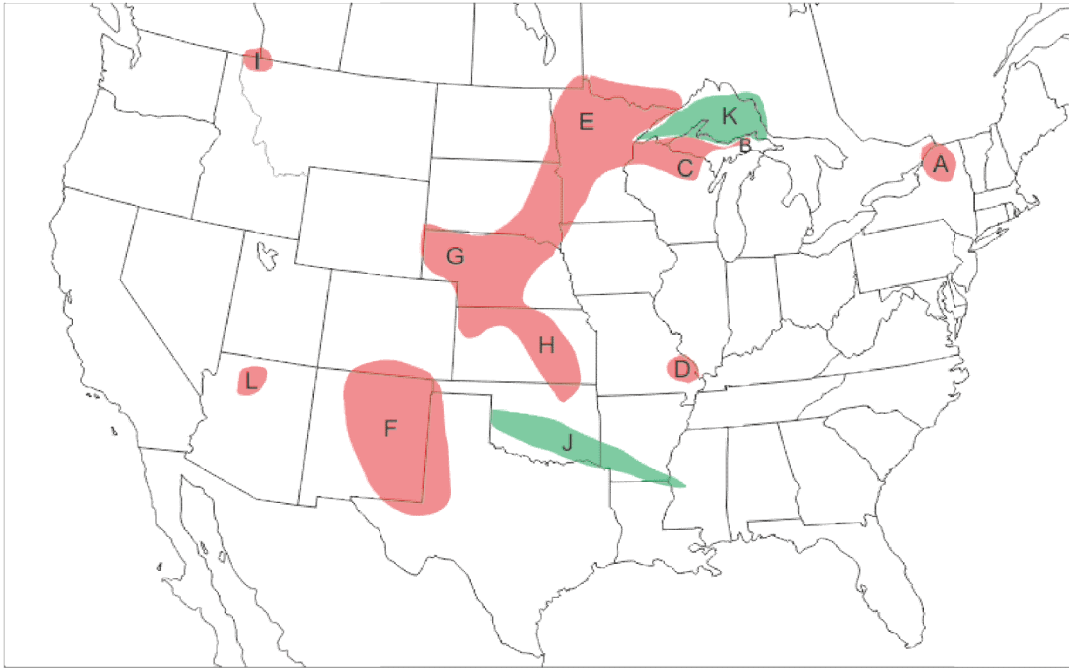


Figure 2.11 Tectonic framework for the Cambrian craton of the US. Highs in red; major Cambrian intracratonic basins in green. A: Adirondack Dome; B: Michigan Highlands; C: Wisconsin Highlands; D: Ozark Dome; E: Siouxia Arch; F: Sierra Grande Arch; G: Cambridge Arch; H: Kansas Highlands; I: Montania; J: Oklahoma Aulacogen; K: Lake Superior Basin; L: Grand Canyon. The Transcontinental Arch consists of F, G and E.

metamorphism, though it is apparent in eastern parts of the Appalachian region (Palmer, 1971) amongst other places. Structural deformation of Cambrian units as a result of orogenic events is most noticeable, not surprisingly, in the Rocky Mountain and Appalachian regions. Here the structural tectonic frameworks are the result of deformation during the Laramide (Late Cretaceous - Eocene) and Sevier (Early Cretaceous - Eocene) orogenies in the west (Baars, 1988) and the Taconic (Ordovician), Acadian (Devonian) and Alleghenian (Carboniferous) orogenies in the east (Palmer, 1971).

2.2.2.2 Cratonic sequences and the Sauk Sequence

Although the stratigraphic application of interregionally extensive rock units in North America was first discussed during the 1940s (Longwell, 1949; Sloss et al., 1949), it was not until the 1960s that the concept and utility of explicitly defined ‘cratonic sequences’ across North America were proposed (Sloss, 1963). Sloss (1963) divided the late Ediacaran to present sedimentary record of the North American craton into six interregional rock-stratigraphic units separated by

unconformities. The unconformities are manifest across all areas of the cratonic interior where regressive/transgressive cycles had their maximum effect. Towards the cratonic fringes, however, the unconformities become less significant and begin to disappear as they are subsumed within more extensive sedimentary units, whose structures are the result of more locally-controlled events. In such cases biostratigraphy becomes a more useful correlative tool (Sloss 1988).

For the Cambrian Period it is the Sauk sequence that is most pertinent representing the Late Ediacaran to the Early Ordovician. The system itself rests unconformably between Precambrian units at its base and Early Ordovician units at its top belonging to the overlying Tippecanoe sequence, and represents in general terms a gradual encroachment upon the craton (Sloss, 1988). However, although the cratonic margins were tectonically quiescent through the Cambrian (Lochman-Balk, 1971) the craton did experience warping, initiating regressions and transgressions resulting in unconformities and major changes in sediment deposition within the Sauk sequence. It has therefore been subsequently divided into three sequential subsequences, Sauk I, II and III, each representing discrete and definable stratigraphic packages separated either by unconformities or correlatable conformable intervals. Their temporal ranges are as follows: Sauk I represents the Ediacaran to early Cambrian; Sauk II the middle Cambrian to earliest late Cambrian; Sauk III the mid-late Cambrian to Early Ordovician. The Sauk sequence was terminated by a major regression in the Early Ordovician (Sloss, 1963, 1988; Lochman-Balk 1971).

2.2.2.3 Biostratigraphy and North American Cambrian time scales

In North America the trilobites are by far the most widely used fossil group for Cambrian biostratigraphy, although archaeocyathans and conodonts have also been used (Gradstein et al., 2004). Trilobites are relatively common and evolved quickly through time enabling the development of high-resolution, stratigraphic subdivisions, particularly in the Guzhangian to Furongian deposits (Gradstein et al., 2004; Taylor, 2006). Also, three upper Cambrian facies belts are apparent, generally concentrically arranged around the craton and within which distinct trilobite assemblages can be recognised. These are the Inner Detrital (nearshore clastics), Middle Carbonate (shallow platform carbonates) and Outer Detrital (off-platform deep water) facies belts (Palmer, 1960). However, the geochronological and chronostratigraphic subdivision of the North American Cambrian system, and indeed

Laurentia as a whole, has had a difficult history and undergone a number of developmental changes over the past half century. The reasons are three-fold:

1) Due to the severity of regressions upon the craton many Cambrian units are simply missing either through erosion or non-deposition. This is particularly acute with Terreneuvian to Cambrian Series 2 (old lower Cambrian) units and Cambrian Series 3 (old middle Cambrian) units. In fact the majority of Cambrian units of the North American system are Guzhangian to Furongian in age (Lochman-Balk, 1971), but even many of these sections are truncated and/or show evidence of internal unconformities of one nature or another (Glumac & Spivak-Birndorf, 2002).

2) The rate and nature of transgression upon the craton was such that many Cambrian units are diachronous (time-transgressive) (Lochman-Balk, 1971). Harris (1964), for example, used facies analysis to show that the Rome Formation is of early Cambrian age in Tennessee and of middle Cambrian age in eastern Kentucky where it overlies Precambrian crystalline basement. The diachronous nature of units hinders the assignation of stratigraphic reference points that are simultaneously biostratigraphically and chronostratigraphically unique. Palmer (1965), in an attempt to resolve this issue, developed the concept of the biomere. He defined it as “a regional biostratigraphic unit bounded by abrupt non-evolutionary changes in the dominant elements of a single phylum which were not related to physical discontinuities in the sedimentary record”. In other words, over a period of time, complex, shallow shelf, faunal communities are replaced by low diversity, outer shelf trilobite fauna which then evolve themselves (Gradstein et al., 2004). The resultant biomere, therefore, has a unique faunal content but not a unique age: it is potentially diachronous. However, it has been criticised precisely because it is unclear as to whether observed faunal changes within a biomere are the result of evolutionary changes or lateral migration (Taylor, 2006). As a result the biomere concept has been through numerous revisions (Palmer, 1979, 1984; Stitt, 1975; Taylor, 1997) and, although specific biomerics are occasionally referred to in the literature, it is not universally accepted. For a full discussion of the biomere concept see Taylor (2006).

3) The Cambrian faunal province of Laurentia is distinct from that of the rest of the Cambrian world (Gradstein et al., 2004) and workers have necessarily created their own regional biostratigraphic schemes, normally based on trilobite faunal zones

(Palmer, 1998). This has been further complicated by the diachronous nature of many trilobite faunas and their extinction horizons. Also, for many years there was no complete regional stage name nomenclature for Laurentia and the traditional Laurentian lower Cambrian was depleted of stages (Palmer, 1960). Consequently, correlating the Cambrian North American System globally has proved tricky at best and some confusion exists over the nomenclature (Geyer & Palmer, 1995; Palmer, 1998). For example, Robison (1988) in northern Greenland found *Lejopyge* Zone agnostids, which are middle Cambrian in the old global timescale, co-occurring with polymeroid trilobites from the *Cedaria* Zone which is upper Cambrian in the traditional Laurentian timescale.

The Saint Croixan Series. This Series contains the first formally recognised stages of the Laurentian Cambrian; the Dresbachian, Franconian and Trempealeauan Stages of Howell et al. (1944) (Fig. 2.12). They specifically divide the traditional middle and upper Cambrian. Each stage has a marine transgression at its base and a regression at its top. The series contains eight trilobite assemblage zones which are, in ascending order: *Cedaria*, *Crepicephalus*, *Aphelaspis*, *Dunderbergia*, *Elvinia*, *Conaspis*, *Ptychaspis-Prosaukia* and the *Saukia* zones. Each of these trilobite assemblage zones is bounded by turnover events (Lochman-Balk, 1971). The Series was described from sections in the upper Mississippi Valley region in Wisconsin and Minnesota and occupies an interior cratonic position. Consequently it is not representative of the whole craton and outer cratonic sites have necessarily had extended faunal zones attributed (Palmer, 1965). Because the type section of the Saint Croixan Series is incomplete with inadequate fauna (Ludvigsen & Westrop, 1985) it is now regarded as essentially obsolete. However, because the stages of the Saint Croixan Series are so prevalent, even in some modern literature, it is noted here.

Modern Cambrian Stages. Ludvigsen and Westrop (1985) proposed three new upper Cambrian stages based upon biomes as redefined by Palmer (1979), and used them as stages in subsequent papers (e.g. Westrop, 1986; Ludvigsen et al., 1989). These are the Marjuman, Steptoean and Sunwaptan stages, each separated by laterally extensive trilobite extinction horizons (Ludvigsen & Westrop, 1985; Taylor, 2006). Palmer (1998) then proposed a series of six regional stages for the Cambrian trilobite-bearing rocks of Laurentia with regional trilobite extinctions as boundaries (Figs. 2.12; 2.13). No stages were designated for pre-trilobite Cambrian Laurentia

(defined in the new global time scale as the Terreneuvian Series). Palmer (1998) also suggested four regional series. Ascending they are: Millardan, Lincolnian, Waucoban and Begadean. Each of the youngest three series accommodates two stages with the oldest series, the Begadean, accommodating pre-trilobite Laurentian Cambrian time. These names, however, have not been fully adopted.

Palmer's stages (1998) (see Fig. 2.12) are listed below with, where possible, tentative correlation to the global timescale from Cocks et al. (2010).

Montezuman Stage (Palmer, 1998). Base defined as the FAD of trilobites and can be tentatively correlated with the base of the global Series 2 and global Stage 3.

Dyeran Stage (Palmer, 1998). No precise correlation to the global time scale available.

Delamaran Stage (Palmer, 1998). No precise correlation to the global time scale available.

Marjuman Stage (Ludvigsen & Westrop, 1985; emended Palmer, 1998). This extends from below the base of the Drumian Stage up to the base of the Furongian Series.

Steptoean Stage (Ludvigsen & Westrop, 1985). The base is defined as the base of the *Aphelaspis* Zone. The cosmopolitan species *Glyptagnostus reticulatus* is present in basal beds of the Steptoean in basinal facies (Palmer, 1998; Gradstein et al., 2004). The FAD of *Glyptagnostus reticulatus* marks the onset of the Furongian in international correlation (Gradstein et al., 2004) and therefore the base of the Steptoean can be placed in the lower Furongian. This means part of the upper Marjuman must be in the Guzhangian Stage of Cambrian Series three. The Steptoean closely correlates with the Paibian Stage and also embraces the Sauk II-III discontinuity (Palmer, 1981).

Global standard Series & Stages		Modern North American Stages (Ludvigsen & Westrop, 1985; Palmer, 1998)	Laurentian Series nomenclature proposed by Palmer, (1998)	Saint Croixan Series (Howell et al 1944)	Super-sequence
Lower Ord.	Tremadocian	Skullrockian	IBEXIAN		SAUK III
	Stage 10			Trempealeauan	
Furongian	Stage 9	Sunwaptan	MILLARDAN	Franconian	Hiatus
	Paibian	Steptoean			
	Guzhangian	Marjuman			
Drumian					
Stage 5	Delameran	Hiatus			
Series 2	Stage 4	Dyeran	WAUCOBAN		
	Stage 3	Montezuman			
Terreneuvian	Stage 2	Unnamed	BEGADEAN		SAUK I
	Fortunian				
Ediacaran					

Figure 2.12 Cambrian, Laurentian, stratigraphical sub-divisions, including modern North American stages, the Laurentian Series names of Palmer (1998), the Saint Croixan Series and the SAUK sequence. Tentatively correlated to the global timescale.

Modern North American Stages (Ludvigsen & Westrop, 1985; Palmer, 1998)	Shallow shelf North American faunal zones (trilobites). From Taylor (2006)	GTS
Skullrockian	<i>Missisquoia</i>	Furongian
Sunwaptan	<i>Saukia</i> <i>Ellipsocephaloides</i> <i>Saratogia</i> <i>Taenicephalus</i>	
Steptoean	<i>Elvinia</i> <i>Dunderbergia</i> <i>Dicanthopyge</i> <i>Aphelaspis</i>	
		?
Marjuman	<i>Crepicephalus</i> <i>Cedaria</i> <i>Bolaspidella</i> <i>Ehmeniella</i>	Series 3
	<i>Glossopleura</i>	

Figure 2.13 North American shallow shelf faunal zones (trilobites) for Cambrian Series 3 and the Furongian. Blue line indicates approximate position of the Cambrian Series 3/Furongian boundary. GTS = Global time scale; Tre = Tremadocian. Not to any scale.

Sunwaptan Stage (Ludvigsen & Westrop, 1985). Base is taken at the *Irvingella major* Zone. The Sunwaptan roughly coincides with the very upper Paibian, global Stage 9 and a lower portion of global Stage 10.

Skullrockian Stage (Ross et al., 1997). The upper part of the Skullrockian is Ordovician and its lower part Cambrian. The Skullrockian Stage is the lowest stage of the Ibexian Series and their concomitant base occurs within Cambrian global Stage 10.

2.2.2.4 Chemostratigraphy: the Steptoean positive isotope carbon excursion (SPICE)

The SPICE event in North America has been recorded in Nevada and Utah in the Great Basin, Wyoming, Iowa, western Newfoundland (Brasier, 1993; Saltzman et al., 1998, 2000, 2004) and Tennessee in the southern Appalachians (Glumac & Walker, 1998). A Furongian carbon isotope excursion in the Great Basin was first detected by Brasier (1993) and was subsequently confirmed and named by Saltzman et al. (1998). In the Great Basin, Brasier (1993) recorded SPICE within the Pterocephaliid biomere (Palmer, 1984) and the equivalent Steptoean Stage (Ludvigsen & Westrop, 1985; Palmer, 1998).

Saltzman et al. (1998) looked at sections in Nevada and Utah and recorded the SPICE event as starting at the base of the *Aphelaspis* Zone, reaching its maximum in the upper half of the *Dunderbergia* Zone before levelling out to background ^{13}C values in the latter half of the *Elvinia* Zone. It begins, peaks and ends within the Pterocephaliid biomere and the Steptoean Stage. They also noted that the SPICE maximum is approximately coincident with a regionally extensive and distinctive influx of siliciclastic debris onto carbonate platforms across the Great Basin.

Saltzman et al. (2004) compared isotope data and trilobite biostratigraphy from three Laurentian basins in northern Utah, central Iowa and western Newfoundland. They showed that the SPICE maximum is consistently well correlated to the middle of the Steptoean Stage (*Dunderbergia* Zone) and occurs during maximum regression associated with the Sauk II-Sauk III boundary on the North American craton. They also noted that associated with the regression are distinctive influxes of quartz sand into carbonate platform settings and that this lithological marker might be used to predict the position of the SPICE maximum.

Glumac & Walker (1998) compared their SPICE curve from the Cambrian Thorn Hill section in Tennessee with that of Saltzman et al. (1998) from the Great Basin. The tighter constraint on biostratigraphy and lithostratigraphy of the Great Basin sections informed the less well constrained biostratigraphy of the Tennessee section resulting in a more detailed chronostratigraphic framework (see chapter 2.3.5). Their study also recorded the coincident nature of the SPICE maximum and an influx of siliciclastic debris.

2.3 The Thorn Hill section, Tennessee

2.3.1 Introduction

The Thorn Hill section is a well exposed succession of rocks situated in Grainger County in the NE-SW trending Valley and Ridge Province of northeastern Tennessee (Figs. 2.14, 2.15). It extends for 14 km along U.S. 25-E from War Ridge to Poor Valley Ridge and is one of the best exposures of lower to middle Palaeozoic rocks in North America, ranging from the Cambrian through to the Carboniferous (Byerly et al., 1986). The section is 3,326 m thick and exposed in an imbricate thrust sheet (Copper Creek fault block) bounded by two major thrust faults, the Copper Creek Fault to the northwest and the Saltville Fault to the southeast (both trending approximately NE-SW); the lower to middle Cambrian Rome Formation is the hanging wall for both faults (Fig. 2.15). The strata dip at around 35-40° to the southeast with a strike of 058-086° (ENE-WSW). The stratigraphy represents deposition within a shallow, carbonate rimmed, intracratonic basin (the Conasauga intrashelf shale basin) that was subject to transgressive/regressive cycles (Milici & De Witt, 1988; Glumac & Walker, 2000). The basin formed part of a passive continental margin along the eastern side of Laurentia. During the Cambrian the exposed craton was situated to the west of the basin, supplying terrigenous clastic sediment; to the east was situated a gently westward sloping, westward prograding carbonate bank that sat between the basin, and the Iapetus ocean to the east (Markello & Read, 1982; Hasson & Haase, 1988; Glumac & Walker, 2000). Today the basin extends from eastern Tennessee to western Virginia.

2.3.2 Cambrian formations at Thorn Hill

The Thorn Hill section is divided into three sequences by regionally extensive unconformities: Sequence I: Cambrian to early Ordovician; Sequence II: Middle Ordovician to Early Devonian and Sequence III: Late Devonian to early Mississippian (Walker & Byerly, 1985; Byerly et al., 1986). Only Sequence I will be discussed here with greater emphasis placed upon the studied formations: the Nolichucky Shale and the Maynardville Limestone.

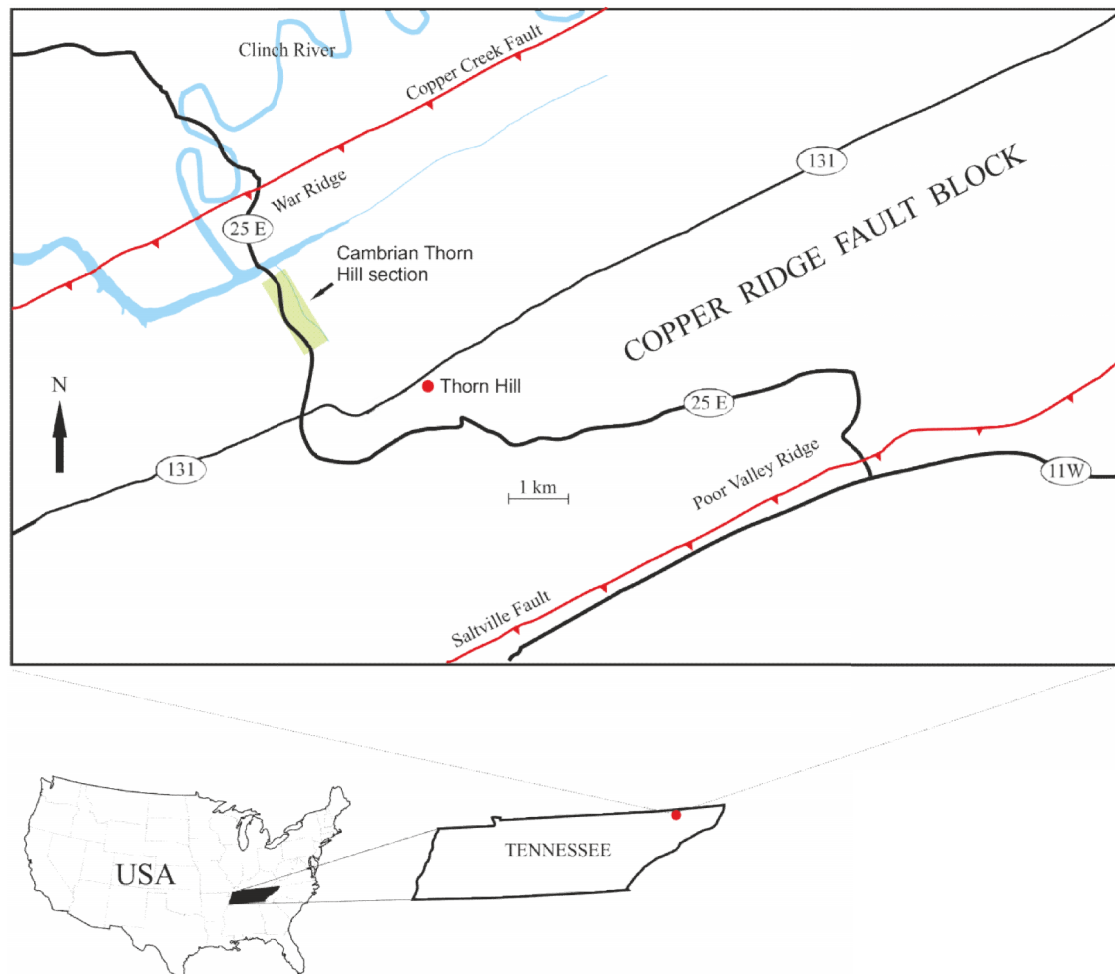


Figure 2.14 The Thorn Hill section extends for approximately 14 km along Highway 25E from the junction with Highway 11W at Poor Valley Ridge to War Ridge. It is situated on the Copper Ridge fault block between the Saltville and Copper Ridge faults. The worked Cambrian section at Thorn Hill is exposed just northwest of the town of Thorn Hill and is highlighted in green.

Sequence I includes the Rome Formation (lower to middle Cambrian), the Conasauga Group (middle to upper Cambrian) and the Knox Group (uppermost Cambrian to Lower Ordovician). Generally the lithologies change from terrigenous clastic rocks, as represented by the Rome Formation at the base, to carbonate rocks of the Knox Group at the top, with a transitional facies, the Conasauga Group, sandwiched between (Byerly et al., 1986). The stratigraphy has generally been interpreted as representing a gradually subsiding basin subject to transgression

(Rome Formation), followed by regression (Knox Group) with the Conasauga Group representing the transition between the two (Markello & Read, 1982; Walker & Byerly, 1985; Glumac & Walker 2000). The effects of the changes in relative sea level resulted in the development of a carbonate bank during sea level fall, and the flooding of the carbonate bank and deposition of shales during a sea level rise.

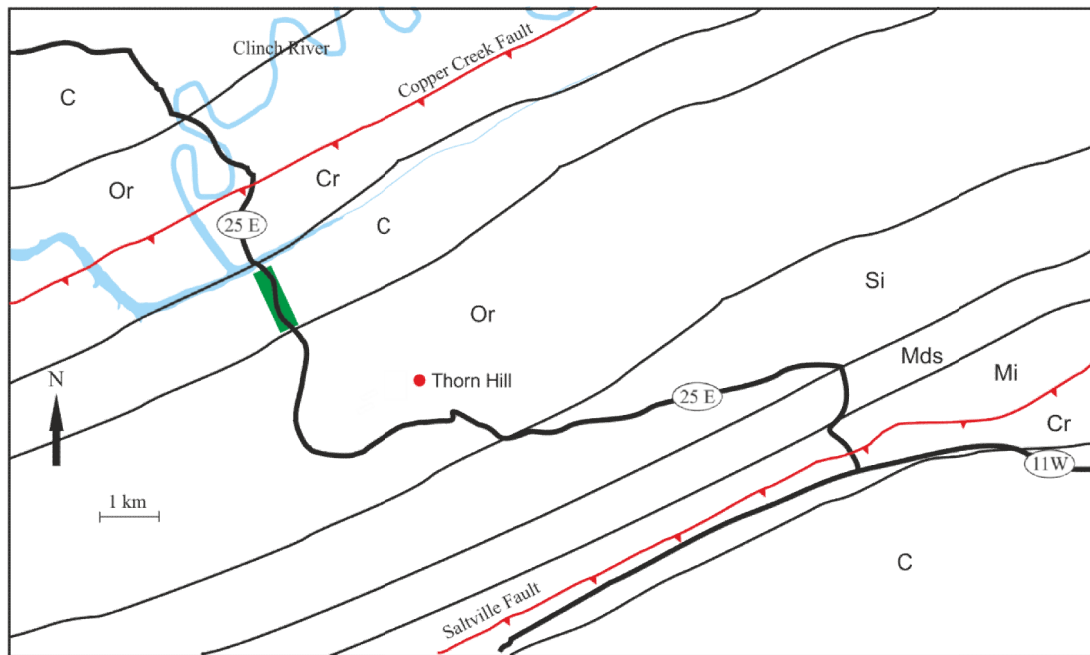


Figure 2.15 Simplified geological map of the Thorn Hill section. The worked section is highlighted in Green. Cr = Cambrian Series 1-2: Rome Formation; C = Cambrian Series 3-Furongian: Pumpkin Valley Shale, Rutledge Limestone, Rogersville Shale, Maryville Limestone, Nolichucky Shale, Maynardville Limestone, and lowermost Copper Ridge Dolomite. Or = Ordovician; Si = Silurian; Mds = Devonian and basal Mississippian; Mi = Mississippian

Rome Formation: Up to about 305 m thick regionally and 128 m thick at Thorn Hill. Heterogeneous assemblage of generally reddish (from iron oxide) with subordinate green (from glauconite) shales, sandstones, thin dolomites and occasional conglomerates. It contains desiccation cracks, algally laminated dolostones, vugs, ripple marks and bioturbation (Byerly et al., 1986). It is mostly unfossiliferous.

The Conasauga Group:

At Thorn Hill the Conasauga Group is 592 m thick and consists of alternating carbonate (mostly limestone) and siliciclastic (mostly shale) units known as Grand Cycles (Aitken, 1966; 1981; Glumac & Walker, 2000). Each cycle consists of a

lower, recessive and predominantly shaly unit succeeded by an upper predominantly carbonate unit. Each Grand cycle is terminated by flooding of the carbonate unit and

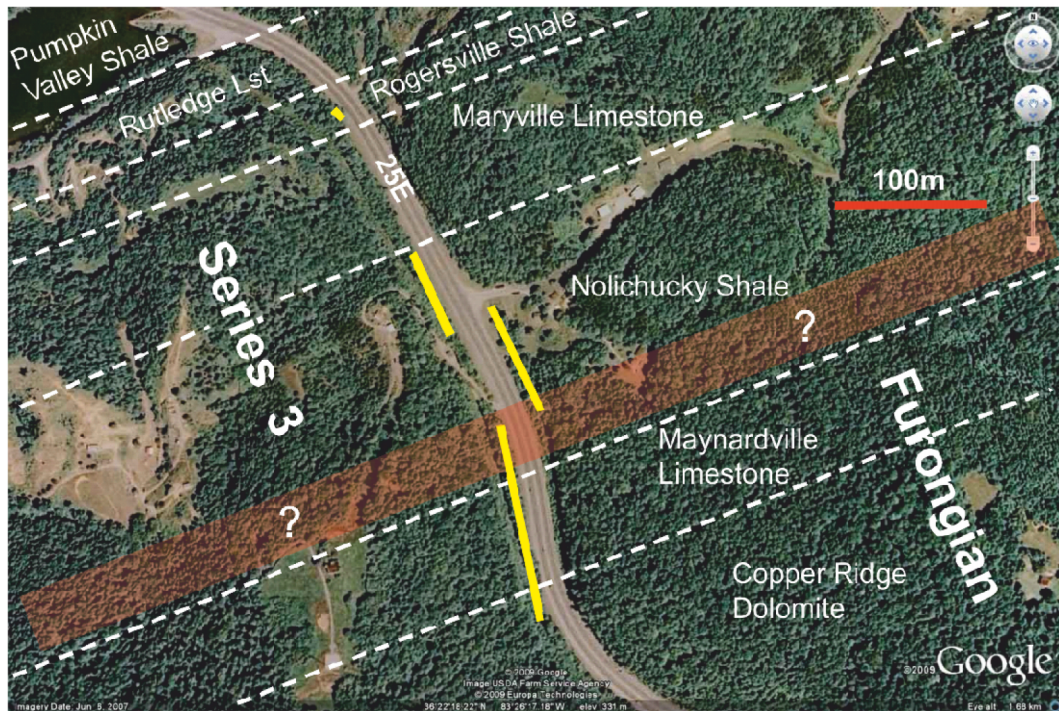


Figure 2.16 Aerial view of the Thorn Hill Cambrian site showing the positions of the Cambrian Formations. Yellow lines denote sampling areas. The position of the Cambrian Series 3/Furongian boundary is not known at Thorn Hill: the red area with question marks indicates the zone within which the boundary most likely lies, in the uppermost part of the Nolichucky Shale.

the initiation of shale deposition. This is followed by recovery and aggradation of the carbonate bank (Aitken 1966, 1978). There are five Grand Cycle couplets at Thorn Hill: Pumpkin Valley Shale/Rutledge Limestone; Rogersville Lower Shale Member/Craig Limestone; Rogersville Upper Shale Member/Maryville Limestone; Nolichucky Lower Shale Member/Nolichucky Middle Limestone Member; Nolichucky Upper Shale member/Maynardville Limestone. Below lies the Rome Formation which grades upwards into the Conasauga Group, and above it lies the Copper Ridge Dolomite. At Thorn Hill the Conasauga Group is divided into six formations: Pumpkin Valley Shale; Rutledge Limestone; Rogersville Shale; Maryville Limestone; Nolichucky Shale; Maynardville Limestone (Figs. 2.16, 2.17)

1. *Pumpkin Valley Shale*: 70-115 m thick regionally and approximately 109 m thick at Thorn Hill. Consists of olive and purple shales (Byerly et al. 1986; Palmer, 1971).

Series	GROUPS	FORMATIONS	MEMBERS	Relative sea level Rising ← → Falling
L. O.	Knox Group	Copper Ridge Dolomite		
Furongian	Conasauga Group	Maynardville Limestone		
			Upper Shale	
		Nolichucky Shale	Middle Limestone	
			Lower Shale	
		Maryville Limestone		
			Upper Shale	
		Rogersville Shale	Craig Limestone	
			Lower Shale	
Series 3		Rutledge Limestone		
		Pumpkin Valley Shale		
Series 1 - 2		Rome Formation		

Figure 2.17 Generalised vertical section showing the Rome Formation and Conasauga and Knox Groups of Sequence I at Thorn Hill. The five grand cycles are highlighted in alternating green & pink. Not to scale.

2. *Rutledge Limestone*: Up to 150 m thick regionally and 54 m thick at Thorn Hill. Consists of externally massive limestones with internally thick laminated to thin-bedded limestone ribbon rocks and dolostones. Occasional trilobite fragments are present (Byerly et al. 1986).

3. *Rogersville Shale*: Up to 80 m thick regionally and 27 m thick at Thorn Hill. Consists of three parts, the lower and upper Shale Members separated by the Craig Limestone Member (Byerly et al., 1986). The shales consist of grey-green, laminated silty clay shale with subordinate intercalations of fine-grained limestone. Trilobites and inarticulate brachiopods are present. The Craig Limestone is predominantly fine-grained clayey dolostone.

4. *Maryville Limestone*: Up to 200 m thick regionally and 169 m thick at Thorn Hill. Consists of alternating progradational and transgressive facies: progradational facies characterized by mottled and ribboned limestone with high micrite content and thin interlaminae of clayey dolostone; transgressive facies characterized by terrigenous quartz silt and interbeds of silty clay shale. The upper transgressive facies of the Maryville grades into the overlying Nolichucky Shale. (Byerly et al., 1986).

5. *Nolichucky Shale*: Up to 225 m thick regionally and 197 m thick at Thorn Hill. It is regionally composed of three interfingering shale and limestone units, the Nolichucky Lower Shale Member, the Middle Limestone Member (also known as the Bradley Creek Limestone) and the Nolichucky Upper Shale Member (Hasson & Haase, 1988). The Lower and Upper Nolichucky Shale Members are lithologically similar (Markello & Read, 1981; Hasson & Haase, 1988). They consist of silty, grey to olive green-grey to brown, laminated shale with locally interbedded oolitic limestones and limestone flat pebble conglomerates (Byerly et al., 1986). There are scattered layers of trilobite and phosphatic brachiopod debris. Most of the shale has high carbonate content (Markello & Read, 1981). The Bradley Creek Limestone consists of thick thrombolitic build-ups or bioclastic rudites and packstones. At Thorn Hill much of the Nolichucky is recessed and obscured by overgrowth and deep weathering.

6. *Maynardville Limestone*: 50-110 m thick regionally and 54 m thick at Thorn Hill. The Maynardville conformably overlies the Nolichucky Shale and the contact is at the base of the first thick limestone unit above the Nolichucky Shale (Glumac, 1997;

Glumac & Walker, 1998). The Maynardville Limestone is divided into two sections, lower and upper. The Low Hollow Member (upper) and the Chances Branch Dolomite Member (lower) are terms occasionally used in the literature (Byerly et al., 1986). The lower section consists of centimetre scale ribbon rocks; shaly ribbon rocks and non-shaly ribbon rocks composed of bioturbated lime mudstone and peloidal packstone (Glumac & Walker, 1997; 2000). These are interbedded with dark grey shale intercalations, silts and occasional beds of flat pebble conglomerates and stromatolitic laminae (Byerly et al., 1986; Glumac & Walker 1997, 2000).

The upper section is more dolomitic, finer-grained and contains more stromatolitic laminae than the lower section. It consists of alternating couplets of basal coarser grained deposits grading upward into finer grained material, and microbial (stromatolites) deposits (Glumac & Walker 1997; 2000).

Knox Group

The Knox Group overlies the Conasauga Group and is a sequence of carbonate shelf deposits measuring up to 915 m thick regionally, and deposited during the Late Cambrian and Early Ordovician in the southern Appalachians (Milici & De Witt, 1988). It represents a major change in sedimentation during the close of Sequence I whereby the grand cycles of the Conasauga were replaced by shallow water deposition of the Knox Group that continued into the Ordovician. It represents the transition from a passive margin setting to a convergent margin setting (Read, 1989) and the boundary between the Conasauga and Knox groups is coincident with the craton-wide Sauk II-Sauk III sequence boundary (Glumac & Walker, 2000).

Copper Ridge Dolomite: 270 to 531 m thick regionally and 307 m thick at Thorn Hill. The Copper Ridge Dolomite is the uppermost Cambrian formation in the region and the lowermost formation of the Knox Group. It consists of oolitic chert and dolomite, nodular chert and abundant algal stromatolites. It lies conformably above the Maynardville Limestone (Glumac & Walker, 1998). The only reported fossil from the Copper Ridge is the Upper Furongian (Sunwaptan Stage) gastropod *Scaevogyra* (Palmer, 1971).

2.3.3 Palaeoenvironments and facies

The generally accepted view of the Cambrian deposits at Thorn Hill and other related coeval deposits, is one of a shallow intracratonic basin setting, situated on the

edge of the cratonic shelf. On the eastern margin of the basin was a carbonate platform with a basin-ward (westward) sloping ramp. The upper parts of the ramp were dominated by shallow subtidal to subtidal carbonates, occasionally subaerially exposed. Shales dominated the lower portions of the ramp. The alternation between the two resulted in the Grand Cycle deposits at Thorn Hill.

The Rome Formation: Supratidal to subtidal. The fossils and sedimentary structures suggest deposition in supratidal to shallow subtidal settings. Supratidal conditions are evidenced by the presence of desiccation cracks and algally laminated dolostone. The presence of red laminated shales and silts suggest subtropical weathering in a mudflat setting. Glauconite suggests sluggish sedimentation (Byerly et al., 1986).

The Pumpkin Valley Shale, Rutledge Limestone, Rogersville Shale and Maryville Limestone: These have all been interpreted as subtidal (Byerly et al. 1986). There is no evidence for either subaerial exposure (Byerly et al., 1986) or for the presence of ribbon rocks, which in the Cambrian are normally interpreted as shallow subtidal deposits (Osleger & Read, 1991; Chow & James, 1992).

The Nolichucky Shale has been interpreted as being deposited in shallow to moderate water depths ranging from 5 to 50 m (Weber, 1988), with the deposition of the Nolichucky lower Shale Member corresponding to the period of maximum flooding of the carbonate platform (Weber, 1988). The gradual transition from the Nolichucky to the Maynardville represents a shift from fine siliciclastic to carbonate dominated sedimentation and reflects the shallowing or infilling of the Conasauga intrashelf basin and the cratonward (westward) progradation of the carbonate platform. The Middle Limestone Member represents a fall in sea level to that which might sustain carbonate deposition (Markello & Read, 1982).

The lower section of the Maynardville Limestone is interpreted as lower subtidal and the upper section as upper peritidal (Glumac & Walker, 2000). Generally the Maynardville represents deposition on a gently sloping subtidal ramp with localised shoal and lagoonal environments, and represents upward shallowing from entirely subtidal to predominantly peritidal settings (Glumac & Walker, 2000). The subtidal environments were laterally linked to broad, semi-arid carbonate tidal flats, characterised by a variety of peritidal environments (upper Maynardville/Copper Ridge) (Glumac & Walker, 1998).

The lower Maynardville is dominated by subtidal ribbon rocks, centimetre scale limestone layers alternating with shale or calcareous siltstone and argillaceous dolostone. There are broadly two types: shaly ribbon rocks with layers of flat pebble conglomerates that were deposited in a storm dominated shallow subtidal ramp; and ribbon rocks composed of bioturbated lime mudstone and peloidal packstone interbedded with calcareous siltstone and argillaceous dolostone. These latter represent deposition in less agitated, shallow subtidal lagoonal environments. This interpretation is supported by the paucity of skeletal allochems and the abundance of micritic and peloidal sediment. (Glumac & Walker, 1997).

The beginning of the upper section of the Maynardville is represented by a gradual transition from ribbon rocks into microbially laminated deposits (stratiform stromatolites), and marks a change from entirely subtidal to predominantly peritidal carbonate deposition in response to progressive carbonate-platform aggradation and shallowing (Glumac & Walker, 1998). Peritidal deposits contain a variety of extensively dolomitized lithofacies among which centimetre-scale, graded couplets predominate. The alternating couplets consist of basal coarser grained material grading upward into finer grained material or microbial (stromatolites) deposits. The couplets are interbedded with a variety of microbial deposits (Glumac & Walker, 1998) and represent storm-, wave- and tidal-dominated shallow subtidal to intertidal settings. The establishment of a wide restricted tidal flat is evidenced by laterally extensive thick, uniform microbial laminates in the lower part of the peritidal succession, and there is a general shoreward transition from thrombolites through digitate, columnar and domal stromatolites to microbial laminites (stratiform stromatolites) (Glumac & Walker, 2000). This represents a decrease in water turbulence from subtidal to supratidal environments (Glumac & Walker, 1997). Desiccation cracks indicate occasional subaerial exposure. The variety of peritidal settings ranging through the vertical succession from supratidal to shallow subtidal reflect a complex pattern of subtle, laterally shifting microenvironments on a broad, laterally extensive platform.

The Maynardville grades conformably upward into the peritidal deposits of the Copper Ridge Dolomite. The occurrence of quartz sand in the carbonate platform deposits containing the Maynardville–Copper Ridge transition is interpreted as an eastward migration of siliciclastic source areas in response to sea level lowering and

subaerial exposure of the craton. These conditions were established during the craton-wide late Steptoean (Dresbachian/Franconian or Sauk II-Sauk III subsequence boundary) unconformity (Lochman-Balk, 1971; Osleger & Read, 1993).

The lower Maynardville consists of subtidal carbonates and shales similar to the rest of the Conasauga Group deposits, whereas the peritidal carbonates from the upper Maynardville resemble deposits of the overlying Knox Group. Thus the Maynardville represents a transitional unit between the Conasauga and the Knox sedimentary successions (Glumac & Walker, 2000).

2.3.4 Biostratigraphy

Early biostratigraphic work on the Cambrian of the Southern Appalachians was undertaken by Resser (1938). Rasetti (1965) made a study of the trilobites in northeastern Tennessee. He reported *Cedaria* and *Crepicephalus* zone fauna from the Nolichucky Shale and found the Copper Ridge Dolomite to be “almost totally barren”; Palmer (1971) concurred. At Thorn Hill Rasetti noted that the Nolichucky Shale was not “particularly fossiliferous”. However, his section at Thorn Hill is one adjacent to the section worked by the present author and apparently had few well exposed sections. Other studies include Bridge (1956); Palmer (1962), Derby (1965) and Sundberg (1989).

Derby (1965) undertook a biostratigraphic study of the trilobites at the Lee Valley section, situated approximately 26 km to the northeast of Thorn Hill and in the same fault block and consisting of the same units (Glumac & Walker, 1997). He looked at the Maryville Limestone, Nolichucky Shale and Maynardville Limestone and assigned the formations as follows: Upper Maryville to the lower *Bolaspidella* zone; Nolichucky Shale to the upper *Bolaspidella*, *Cedaria*, *Crepicephalus* and lower *Aphelaspis* zones; Maynardville Limestone to the upper *Aphelaspis* zone (Fig. 2.15). He recorded a Trempealeauan fauna from the upper part of the Copper Ridge Dolomite.

Sundberg (1989) studied trilobites at Thorn Hill but focused on the middle Cambrian formations. He assigned the formations as follows: Pumpkin Valley Shale, Rutledge Limestone and lowermost Rogersville Shale to the *Glossopleura* zone; the remaining Rogersville Shale and lowermost Maryville Limestone to the *Ehmaniella* zone; the majority of the Maryville to the *Bolaspidella* zone (Fig. 2.15).

	Formations	Old stages	Modern stages	Faunal zones	GTS
KNOX GROUP	Copper Ridge Dolomite	Tremp.	Sunwaptan	<i>Saukia</i>	Furongian
		Franconian		<i>Taenicephalus</i>	
	SAUK III		Steptoean	<i>Irvingella major</i>	
UPPER CONASAUGA GROUP	SAUK II	Dresbachian		<i>Elvinia</i>	
	Maynardville Limestone		<i>Dunderbergia</i>		
			<i>Aphelaspis</i>		
	Nolichucky Shale		Marjuman	<i>Crepicephalus</i>	
Maryville Limestone	<i>Cedaria</i>				
				<i>Bolaspidella</i>	Series 3
				?	

Figure 2.18 Generalised trilobite biostratigraphy and stages for Cambrian Series 3 and the Furongian at Thorn Hill and other coeval Conasauga Basin sections in the southern Appalachians. Blue line indicates approximate position of the Cambrian Series 3/Furongian boundary. Not to scale. After Derby (1965) and Glumac & Walker (1998). Tremp. = Trempealeuan; GTS = Global time scale.

The two studies combined (Derby, 1965; Sundberg, 1989) give a reasonable, general biostratigraphic account of the middle and upper Cambrian formations in this part of Tennessee. Ultimately, however, at Thorn Hill the biostratigraphy of the Nolichucky Shale, Maynardville Limestone and Copper Ridge Dolomite is poorly constrained

and the positions of the faunal zones within Cambrian Series 3 and the Furongian, relative to the measured stratigraphy at Thorn Hill, are unknown. Given the biostratigraphy of Derby (1965) and Sundberg (1989), the Maryville Limestone and the majority of the Nolichucky Shale lie within the Marjuman stage and the uppermost part of the Nolichucky Shale and the Maynardville Limestone lie within the Steptoean.

This places the upper part of the Nolichucky Shale and the overlying Maynardville Limestone in the global Furongian Series and places the base of the Furongian somewhere in the upper part of the Nolichucky Shale.

2.3.5 Chemostratigraphy

As noted earlier, carbon isotope stratigraphy has proved a useful correlative tool in Global and North American Cambrian stratigraphy (Saltzman et al., 1998; 2004). Glumac and Walker (1998) recorded a positive carbon isotope excursion (SPICE) in carbonates sampled from the uppermost Nolichucky Shale, Maynardville Limestone and Copper Ridge Dolomite at Thorn Hill (Figure 2.16). Their sampled section at Thorn Hill represents the upper part of the section sampled for this project (see chapter 6.3). The excursion recorded by Glumac and Walker (1998) at Thorn Hill lies within approximately 80 m of section and has a maximum ^{13}C value = +4‰ to +5‰ Vienna Peedee belemnite (VPDB). It begins within the uppermost 20 m of the Nolichucky Shale, ends approximately 25-30 m into the Copper Ridge Dolomite and has its maximum around the Maynardville Limestone/Copper Ridge Dolomite boundary. Saltzman et al. (1998) recorded the SPICE in the Great Basin in Nevada and Utah in sections through the *Pterocephaliid* biomere/Steptoean Stage, and recognised a major siliciclastic influx coincident with the SPICE maximum.

By correlating the SPICE curve and sedimentation profile from Thorn Hill with those from the Great Basin in Nevada and Utah, Glumac & Walker (1998) were able to show that the lowermost Knox Group (Copper Ridge Dolomite) in the southern Appalachians is early Franconian or late Steptoean in age, and that the Maynardville Limestone/Copper Ridge Dolomite boundary is equivalent to the Dresbachian/Franconian boundary and the Sauk II-Sauk III hiatus. Furthermore, SPICE is greater than 200 m in the Great Basin (Saltzman et al., 1998) whereas at Thorn Hill it is only about 80 m, indicating a lower sedimentation rate. Saltzman et

al (2004) further confirmed the coincident nature of the Sauk II-Sauk III boundary and the SPICE maximum in studied sections in Utah, Iowa and Newfoundland.

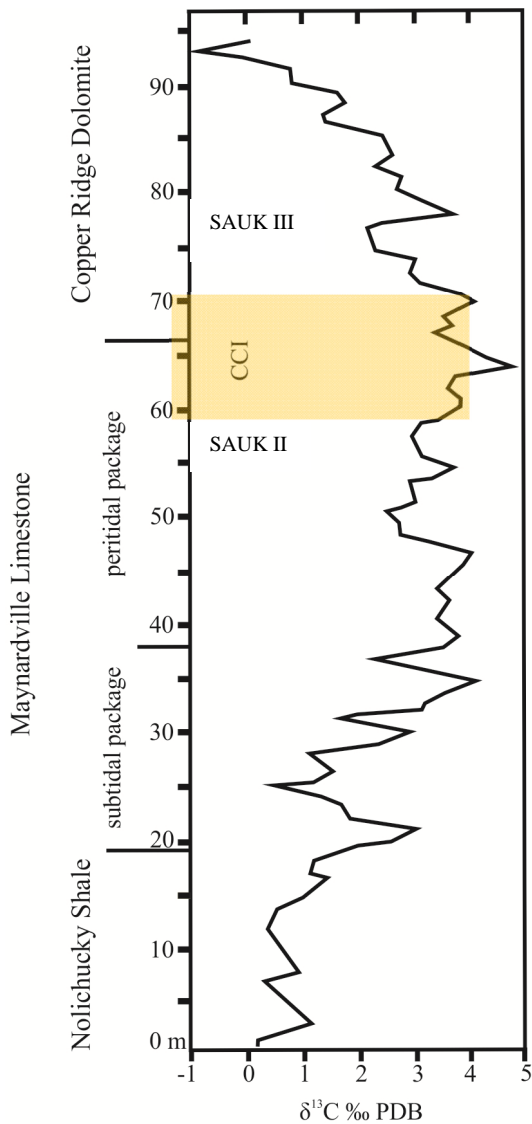


Figure 2.19 The SPICE curve at Thorn Hill. Note the position of the correlatable conformable interval (CCI) at the Maynardville Limestone/ Copper Ridge Dolomite boundary. This marks the influx of quartz sands and represents the Sauk II- Sauk III subsequence boundary and the SPICE maximum. From Glumac and Walker (1998).

Given that the biostratigraphy of the Nolichucky Shale, Maynardville Limestone and Copper Ridge Dolomite at Thorn Hill is poorly constrained, the carbon isotope study of Glumac & Walker (1998) makes a useful contribution to the stratigraphy of both Thorn Hill and the region as a whole in providing a more detailed chronostratigraphic framework.

2.3.6 Sample collection at Thorn Hill

2.3.6.1 Definition of units

Samples were collected from the Rogersville Shale, Nolichucky Shale, Maynardville Limestone and Copper Ridge Dolomite. The units were initially identified using lithological, stratigraphical and geographical information from Byerly et al. (1986) and Glumac (unpublished Ph.D. thesis 1997). In particular, the units defined by Glumac (1997) were of invaluable use in locating the boundary between the Nolichucky Shale and the Maynardville Limestone.

The Rogersville Shale is towards the northern end of the section and was identified using the lithostratigraphic and geographical data from Byerly et al. (1986). It is situated at the first bend along Highway 25E travelling south from Indian Creek (Fig. 2.20). It sits between two limestone formations (the Rutledge and Maryville Limestones) and consists of three members: the Upper Shale Member, Lower Shale Member and the centrally positioned Craig Limestone. The base of the Nolichucky Shale is defined as the base of the first major shale unit occurring stratigraphically above the Maryville Limestone. The base of the Maynardville Limestone is defined as the base of the first major carbonate unit stratigraphically above the Nolichucky Shale. The base of the Copper Ridge Dolomite is defined as the base of the first major carbonate unit stratigraphically above the Maynardville Limestone, which possesses a 'massive' appearance.

2.3.6.2 Sampling

53 samples were collected from outcrop at Thorn Hill: forty six from the Nolichucky Shale, five from the Maynardville Limestone and one each from the Copper Ridge Dolomite and Rogersville Shale (Figs. 2.20, 2.21). Sedimentary logs were made for all Formations except the Rogersville Shale, which was sampled at the very end of the field trip. The one sample from the Rogersville Shale was taken from a point 1.20 m below the Rogersville Shale/Maryville Limestone boundary.

The Cambrian Thorn Hill section is exposed along Highway 25E and outcrops occur on both sides of the road. On the western side of Highway 25E the outcrop is found in both a road cutting and along the waste ground at the side of the road. On the eastern side of the road, the outcrop is found in the Forked Deer Creek which runs

parallel to Highway 25E (Fig. 2.20). The units defined by Glumac were again invaluable in correlating the units between these two sections.

Sample labels followed by a fraction (i.e. 26½, 28½, 33 , 33) indicate samples collected at the end of the field trip, after all other samples had been labelled.

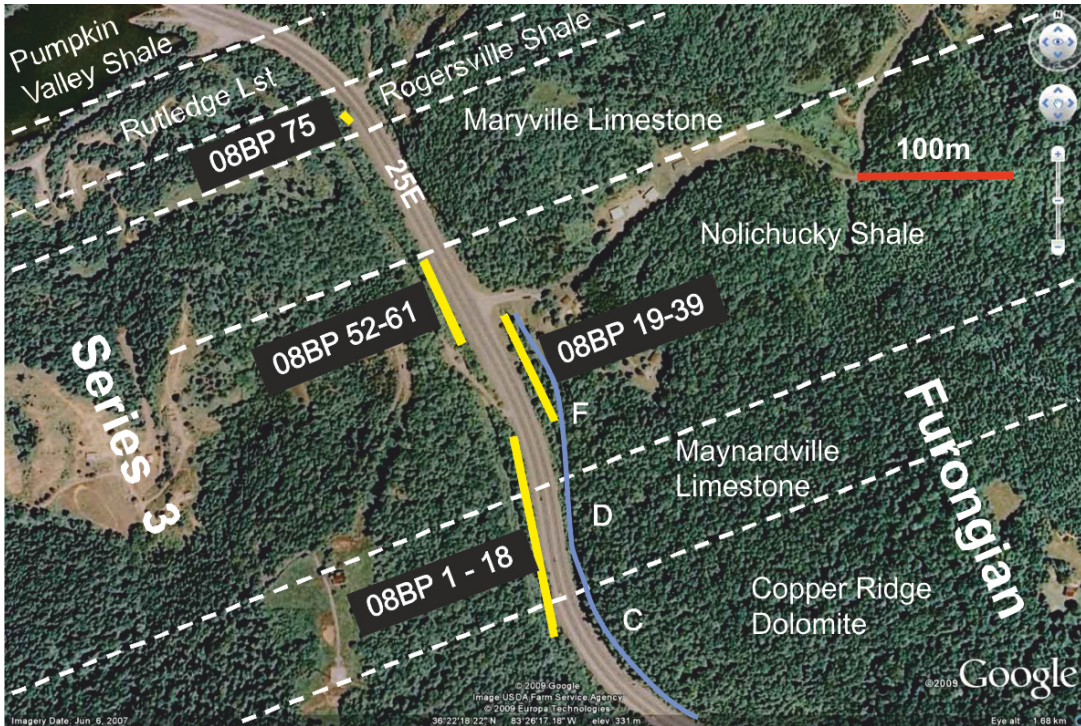


Figure 2.20 Sampling areas in the Cambrian section at Thorn Hill. Samples 08BP 1-18, 08BP 52-61 and 08BP 75 were collected from the road cutting on the western side of Highway 25E, whilst samples 08BP 19-39 were collected from Forked Deer Creek which ran on the eastern side of, and parallel to, Highway 25E. F D C = Forked Deer Creek.

It was deemed necessary to collect extra samples if possible, where large unsampled stratigraphic gaps existed. In such instances a new sample was labelled with the number of the preceding sample followed by a fraction. Thus, sample 08BP-26½, represents one sample collected stratigraphically between samples 08BP-26 and 08BP-27; 08BP-28½ represents one sample collected stratigraphically between samples 08BP-28 and 08BP-29; samples 08BP-33 and 08BP-33 represent two samples collected between samples 08BP-33 and 08BP-34 (Fig. 2.21).

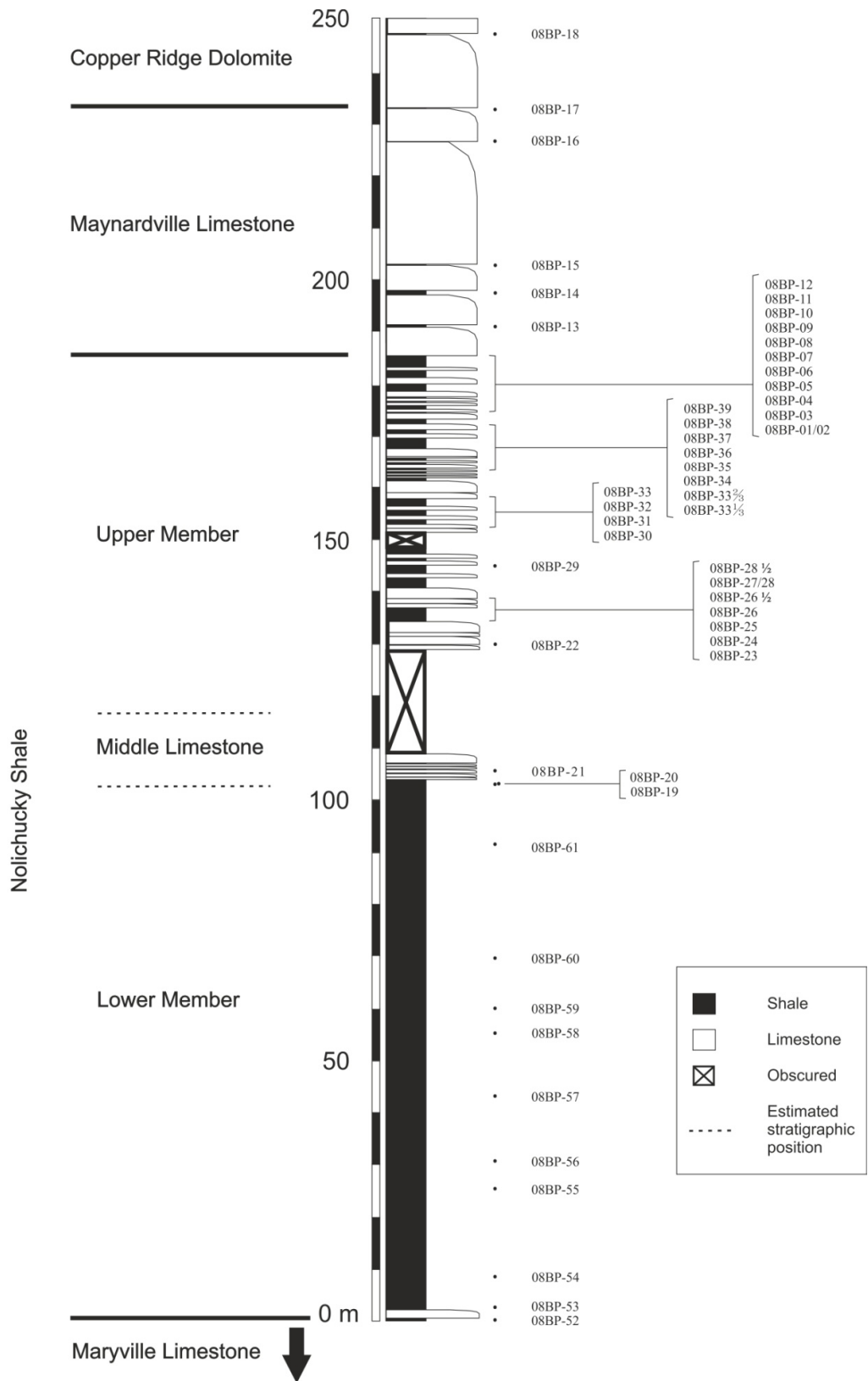


Figure 2.21 Composite sedimentary log and sample points for the Nolichucky Shale, Maynardville Limestone and Copper Ridge Dolomite at Thorn Hill. The boundaries for the upper Nolichucky, lower Nolichucky and middle Limestone Members are estimated.

2.4 The Chief Joseph Highway section, Wyoming

2.4.1 Location and geology

The Chief Joseph Highway (CJH) section is situated in the Absaroka mountain range, on the east side of Crandall Road on Wyoming Highway 296, (otherwise known as the Chief Joseph Scenic Highway) in Park County, northwest Wyoming, USA (Coords: 44°45'29.18"N 109°24'8.31"W) (Fig. 2.22). It is 23 km northwest of Cody. The section forms part of the Park Shale (Guzhangian), the uppermost member of the Gros Ventre Formation and represents deposition in a shallow marine, low-energy environment (Middleton et al., 1980). It is a relatively small, isolated outcrop with a stratigraphic thickness of approximately 9.5 m and consists of pale green shales, alternating with thinly bedded limestones and flat pebble conglomerates (Fig. 2.23). Above it lies the Pilgrim Limestone which marks the base of the Furongian Series. At and around the studied section the Pilgrim Limestone was inaccessible and so the distance between the top of the studied section and the base of the Pilgrim Limestone was estimated to be 20-30 m.

Seven samples were collected at the CJH section (09BP-43 to 09BP-49) but only two were considered for this project, 09BP-44 and 09BP-49. These two samples contained two new forms of unusually large acritarchs ($>100 \mu\text{m}$) which in the opinion of the present author made them worthy of further study. Furthermore, one of the forms is also recorded for this project from the Nolichucky Shale at Thorn Hill.

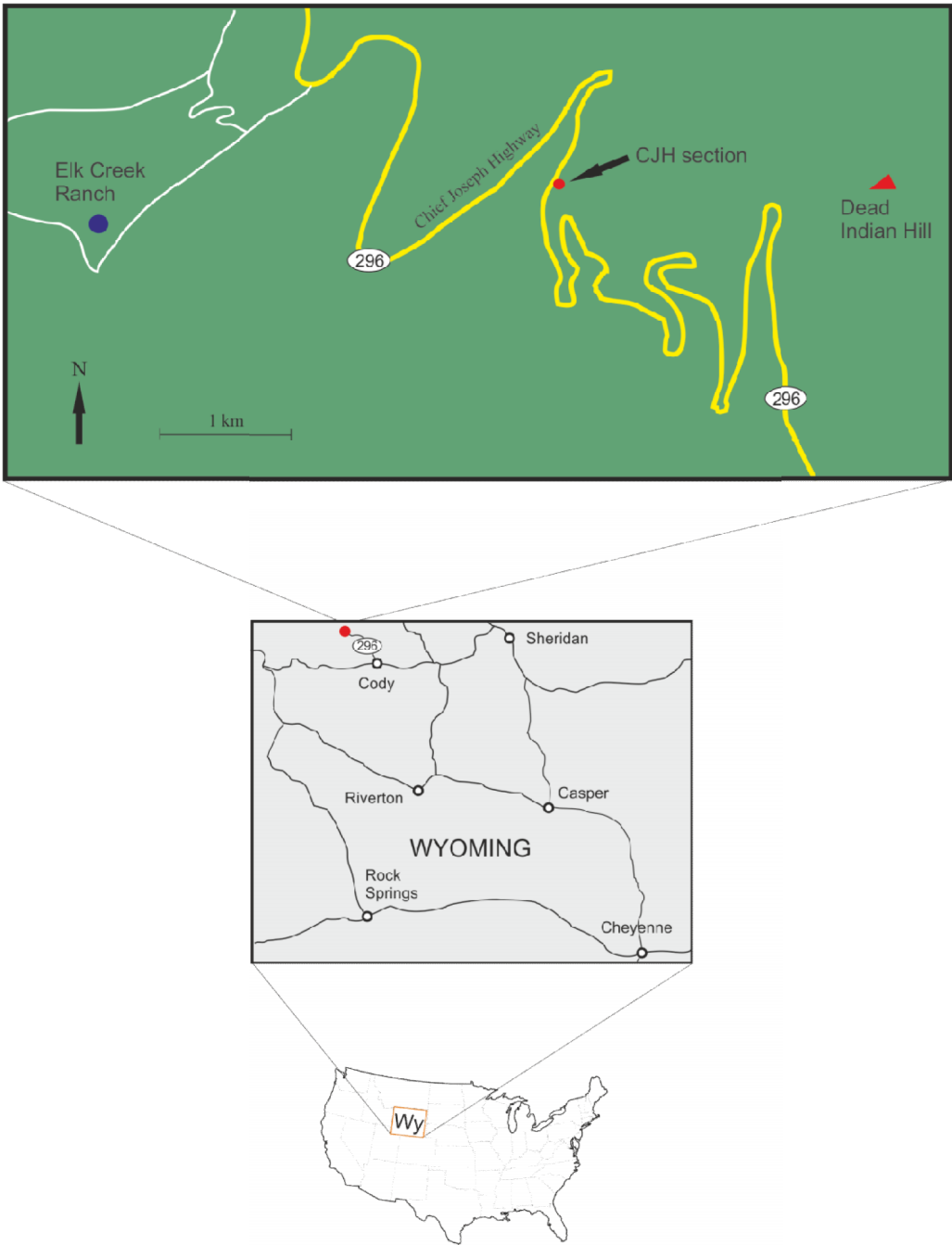


Figure 2.22 Location map for the Chief Joseph Highway section in northwest Wyoming.

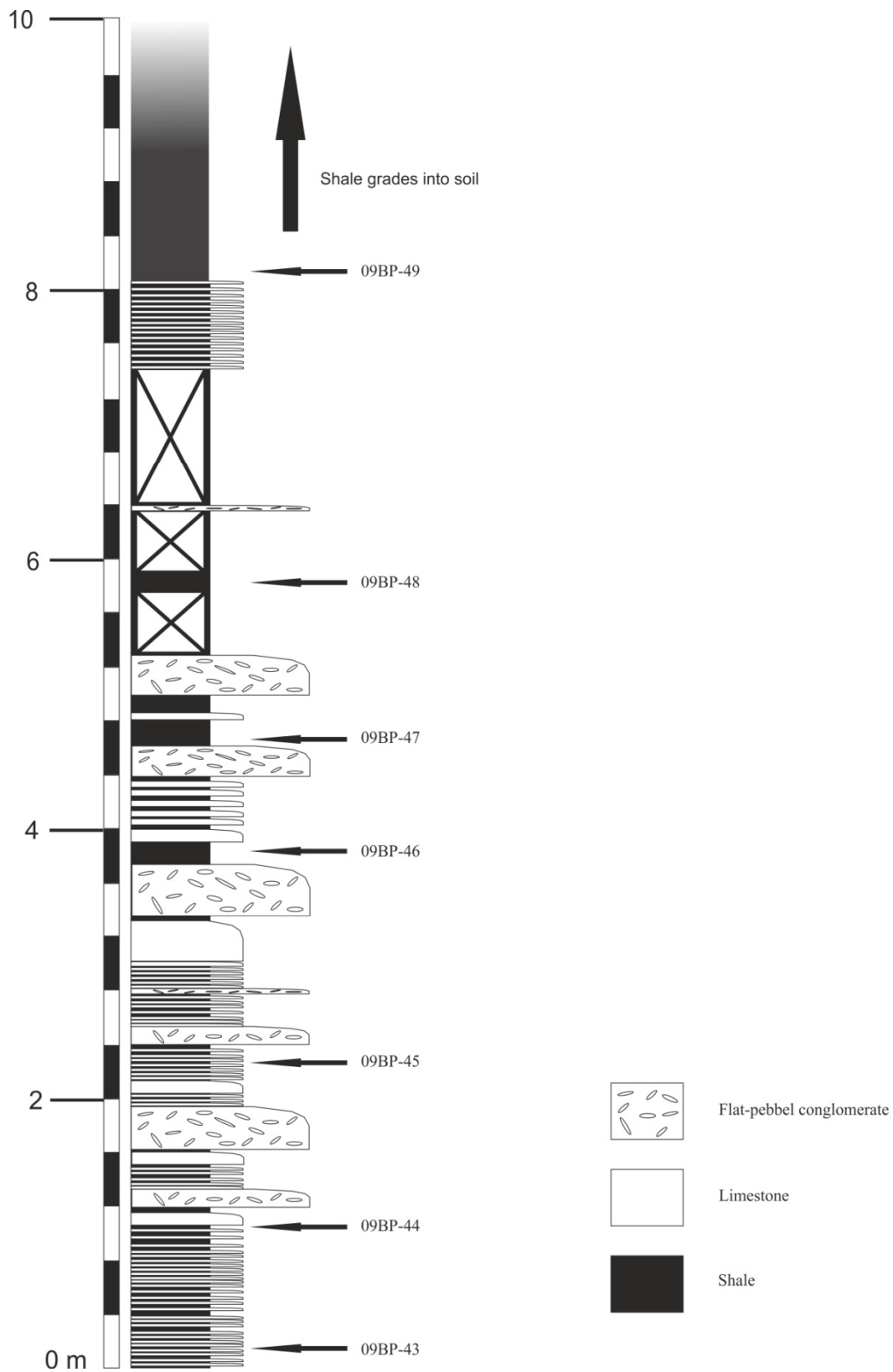


Figure 2.23 Sedimentary log and sample points for the Gros Ventre section along the Chief Joseph Highway.

Chapter 3

Materials and Methods

3.1 Materials

3.1.1 Introduction

Samples were collected for palynological and carbon isotope analysis during two field trips to the USA in 2008 and 2009. Samples were collected from the Cambrian outcrops at Thorn Hill in Tennessee in 2008 and from a small, single outcrop along the Chief Joseph Highway in northwest Wyoming in 2009. Shales, siltstones and calcareous mudstones were collected. In each case fresh, unweathered material or the least weathered material available was collected and placed into a breathable, cotton, draw string bag and labelled with a unique field-sample identification. Where possible trilobites were collected for biostratigraphic application.

All materials (rock, residue, slides and SEM stubs) are curated in the Centre for Palynology, Department of Animal & Plant Sciences, University of Sheffield under the title “Pedder 2012”. Slides are labelled with the prefix BEP-TH (B.E. Pedder, Thorn Hill) or BEP-CJH (B.E. Pedder, Chief Joseph Highway).

3.2 Methods

3.2.1 Cleaning

Two cleaning techniques were utilised depending on the size and/or solubility of a sample. Where individual pieces of a sample were large enough they were scraped with a knife in order to remove weathered material and surface contaminants. They were then gently scrubbed with a moderately stiff brush under running warm water to remove any remaining contaminants. Where the sample comprised of small (<1 cm) pieces, a quantity of sample was placed in a sieve and held under a gentle flow of warm water whilst being gently agitated. Where samples showed a high degree of solubility or disintegration on contact with water, the above techniques were applied though moderated accordingly (i.e. more gently) so as not to lose good material.

After a sample was cleaned it was placed in one or more petri dishes and left to dry. Where necessary, in order to increase the surface area of material and thus enhance the acid maceration process, samples were reduced to pea-sized pieces by crushing using a pestle and mortar. Initially, approximately 20 g of each sample were transferred to polythene bottles for acid maceration. However, if it became apparent that the quantities of organic matter yielded were insufficient the amount of subsequent samples processed was increased accordingly. Precise weights of each sample were recorded before enough water was added to just cover the sample in order to reduce potential contamination and prevent overly effervescent reactions with the addition of HCl. After this all processing was carried out in fume cupboards.

3.2.2. Acid maceration

38 % Hydrochloric acid (HCl) was used to remove carbonates. A few drops of HCl were added to samples to test for the presence of, and strength of reaction with, carbonates. More HCl was then added incrementally until any reactions ceased and the samples left for twenty four hours. A minimum of 50 ml HCl was added to every sample, including those showing little or no reaction. This was done to reduce the formation of precipitates which might hinder sieving later on. Each sample was then diluted with warm water and left to settle for eight hours before being carefully decanted. This process was repeated until the supernatant liquor became colourless. If, after the first HCl treatment, the colour of the liquor was a deep yellow or orange, the process was repeated. No more than two treatments were given to any one sample.

After the final decant 100 ml of 40 % hydrofluoric acid (HF) was added to remove silicates. The samples were left to digest for between one and two weeks and agitated once a day in order to mix non-digested rock with fresh acid. After digestion was achieved each sample was diluted with water, left to settle for eight hours and then carefully decanted. This was repeated until the samples become pH neutral.

During HF treatment, some samples developed precipitates (calcium/magnesium fluoride) in large quantities which had to be removed. Larger precipitated particles (>0.5 cm) were discarded after decanting off the organic portion. Any remaining precipitates or carbonates were removed by gently boiling the samples for five minutes in 50 ml of 38 % HCl. The samples were then diluted with water and decanted until pH neutral. Where necessary a quarter of each sample of organic

residue was set aside at this point for carbon isotope analysis (see section on carbon isotope analysis).

3.2.3 Sieving

A 5 μm nylon mesh was used to remove fine particles and prevent the loss of small palynomorphs. A 10 μm nylon mesh was used where sieving with a 5 μm nylon mesh proved impossible or too time consuming: this was the case for four samples. Samples containing large ($>50 \mu\text{m}$) palynomorphs were top-sieved at 63 μm to concentrate the larger specimens. This was done before heavy liquid separation.

3.2.4 Removal of Iron sulphide (pyrite)

Any residue containing iron sulphide was placed in a 250 ml glass beaker with 50 ml of 68 % nitric acid. After ten minutes the contents of the beaker were poured into approximately 800 ml of water contained in a 1 L beaker. This was then sieved until the residue was Ph neutral.

3.2.5 Heavy liquid separation

Mineral grains sufficiently denser than organic material and still remaining after acid treatments were removed by heavy liquid separation using zinc chloride (specific gravity 1.95). The residue was placed in a 50 ml centrifuge tube (occupying not more than the conical section of the tube). Zinc chloride, along with a few drops of HCl, was added giving a total volume of 45 ml. It was centrifuged at 2200 r.p.m. for 10 minutes. The less dense portion of residue at the top of the centrifuged sample was diluted with warm water and transferred using a pipette to a 1l beaker containing 500 ml of warm water and a few drops of HCl. This solution was then gently mixed and sieved until pH neutral. In some cases, to prevent damage to large palynomorphs residues of $>63 \mu\text{m}$ were not centrifuged. The residue was transferred to a 7 ml vial.

3.2.6 Oxidation

Oxidation was not required for any of the samples processed. However, oxidation would have inevitably occurred in those samples treated for pyrite using nitric acid.

3.2.7 Staining

Where the observation (and photography) of palynomorphs was impeded by high degrees of transparency the palynomorphs were stained with Safranin O stain. Approximately 15 ml of Safranin O stain was added to the organic residue in a sieve

and the stain/residue mix swirled around to ensure thorough mixing. The sieve contents were then rinsed and drained making sure all excess stain was removed. The residue was transferred to a 7 ml vial.

3.2.8 Light microscopy (LM): slide preparation, analysis and imaging

After all treatments were completed, the residue was transferred to a 7 ml vial and left for a minimum of four hours to settle. Excess water was then removed using a pipette and enough 1 % PVA solution added to give a sufficient density of palynomorphs per unit area of slide (i.e. neither too cluttered nor too sparse). The mixture was shaken gently to keep the residue in suspension immediately before being pipetted on to 22 mm x 32 mm cover slips arranged on a cold warm-plate. The warm-plate was then switched on to evaporate off the water and leave the residue adhered to the cover slip as a strew mount.

Blank slides were arranged and heated on a hot-plate in preparation for mounting. A small amount of Petropoxy 154 Epoxy resin was placed on a slide and allowed to heat. After a few seconds the cover slip was inverted and lowered onto the mounting resin; this was done carefully so as to avoid air bubbles being trapped beneath it.

A minimum of three slides were prepared for each sample and all slides were labelled with a unique slide number (e.g., BEP-0001), sieve size. All light Microscope logging and analysis was carried out using an Olympus BH-2 binocular light microscope with x10 eyepieces, x10, x20 and x40 Olympus DPlan objectives, and a x100 Olympus DPlan oil immersion objective. All light microscope imaging was carried out on a Leica DMRX microscope with digital interference contrast (DIC), using Leica 100x, 63x and 40x Plan-Fluortar oil immersion objectives, and Leica 20x and 10x objectives. The microscope was equipped with a Leica DFC290 digital camera. All imaging was carried out in the Palaeontology Department, Natural History Museum, Cromwell Road, London.

All observed acritarchs were recorded in all samples except samples 09BP-44 and 09BP-49. The full complement of palynomorphs in these two samples were not recorded due to lack of time.

Counts for absolute abundance were taken by counting 200 specimens on a slide consisting of a known weight of residue. The area containing the 200 specimens was measured and converted to a percentage of the whole slide area. Assuming uniform

distribution across a slide and that percentage area is equivalent to percentage weight, the number of specimens per gram was calculated.

3.2.9 Scanning electron microscopy (SEM): stub preparation, analysis and imaging

Specimens, residues and SEM stubs were prepared at the University of Sheffield before being transported to the Natural History Museum, London for SEM analysis.

SEM stubs were prepared by gluing a 13 mm glass disc to a “0.5 inch aluminium pin stub” using slow-drying araldite. After the glue had cured any excess glue was removed from the stub edge with a scalpel. A small portion of residue was rinsed through with deionised water in a 5µm sieve before being transferred to a 7 mm vial. A drop of the mixture was then placed on a stub and allowed to dry at room temperature in a contaminant-free, ventilated Perspex box. Where necessary individual specimens were picked and mounted individually on stubs. (For picking details see section 4.2.10).

All SEM analysis and imaging was carried out on a Philips XL30 Field Emission Scanning Electron Microscope in the Electron Microscope Unit, EMMA Division, Mineralogy Department, Natural History Museum, Cromwell Road, London.

3.2.10 Transmission electron microscopy (TEM)

3.2.10.1 TEM: specimen selection, preparation, analysis and imaging

Specimens were selected and collected at the University of Sheffield before being transported to the Natural History Museum, London for TEM preparation and analysis.

For specimen selection a quantity of residue was transferred to a glass petri dish containing, deionised water. The mixture was gently agitated and left to settle. Individual specimens were identified and selected using a stereo microscope and collected and transferred to a 7mm vial (containing acidified deionised water) using a glass micropipette. Specimens were then transported to the Natural History Museum, London.

The specimens were prepared using a modified standard TEM protocol (Kennaway et al. 2008). The modifications are discussed towards the end of this section.

Selected cells were picked from the acidified water and transferred into a watch glass containing deionised water. After three rinses in deionised water (3x15 minutes) the cells were encapsulated in agarose.

Encapsulation of specimens. A 2% solution (water) of IX ultra low temperature gelling agarose (Sigma) coloured with alcian blue was made up for embedding the samples. A small drop of agarose (~150 µl) was pipetted onto a microscope slide and a single cell pipetted into the middle of the agarose droplet. Care was taken not to introduce any more water than was necessary to expel the specimen from the pipette. The slide was covered with damp tissue and placed in a refrigerator for approximately 15 minutes to gel. The firm gel was trimmed into a small block approximately 2-3 mm³ with the cell at the centre of the block.

Fixation. Primary fixation in gluteraldehyde and secondary fixation with osmium tetroxide were omitted from this protocol.

Dehydration. The blocks were dehydrated using an acetone series (25 %, 50 %, 70 %, 80 % 90 % 100 % and 100 % over a molecular sieve). The specimens were dehydrated on a rotary mixer at room temperature. To change solutions the acetone was pipetted from the glass vials containing the blocks and a new solution added. The dehydration series began with the samples left for one hour in both the 25 % and the 50 % acetone and continued overnight in 70 % acetone. For the final steps (80 %, 90 %, 100 % and 100 %) dehydration times were reduced to thirty minutes for each solution.

Infiltration of resin and embedding. The epoxy resin TAAB 812 was introduced gradually into the dehydrated agarose blocks. Infiltration was carried out in two steps. For the initial infiltration, a mixture of TAAB 812 resin and acetone, in a 1: 1 mixture of resin: acetone, was used. The samples were infiltrated overnight on a rotary mixer at room temperature. The resin: acetone mixture was removed the following day and fresh 100 % resin added and left to infiltrate for 6-8 hours at room temperature. The samples were then transferred into labelled, flat-bottomed BEEM capsules, filled with fresh resin and left to stand for two hours to allow air in the resin to rise to the surface of the BEEM capsules. The resin was polymerised at 70 °C for 36 hours.

Shaping the specimen block. A trapezoidal cutting face (mesa) was cut by hand using a single edged razor blade while observing the process under the microtome microscope. The resin blocks were trimmed so that the specimen was at the centre of the mesa. The size of the mesa was kept to a few millimetres.

Ultramicrotomy. The mesa was trimmed with glass knives and semi thin sections (~ 500 nm) cut until the specimen was exposed on the surface face of the block. A final section of approximately 150 nm was cut with a new glass knife to achieve a mirror surface on the mesa in preparation for cutting ultra-thin sections with a diamond knife. A Microstar diamond knife was used to cut ultra-thin silver sections (~ 65-70nm) on a Reichert Ultracut S Ultramicrotome. The sections were picked up on formvar coated slot grids (1 x 2 mm). Counter staining of sectioned material with uranyl acetate and lead citrate (Reynolds 1963) was omitted.

TEM. The grids were examined on a Hitachi H-7100 at 100 KV Transmission Electron Microscope. Micrographs were taken with an Orius SC 600A1 digital camera and Gatan digital micrograph software. All TEM specimen preparation and imaging was undertaken by Dr Gabrielle M. Kennaway at the Electron Microscope Unit, EMMA Division, Mineralogy Department, Natural History Museum, London.

3.2.10.2 Modifications to the standard TEM protocol

Although the acritarch cells were large enough to see with a dissecting microscope the cells were encapsulated in agarose because of the numerous manipulations of the TEM protocol and the fragile nature of the fossil material. Encapsulating cells smaller than 50 μm in agarose reduces the number lost during the protocol, and an alcian blue stained gel helps locate small cells which are often difficult to see once embedded in resin. Agarose forms a transparent gel which is essential when orientation of a specimen is required.

Three modifications to the standard protocol were made to prepare acritarchs for TEM. The first was the omission of primary and secondary fixation and the second to omit counter staining sectioned material. These modifications were introduced because fossilised organic material does not require stabilising and there were no observable changes, no increase in electron density of the material and no increase in ultrastructural information after fixation and counter staining.

The third modification was an increase in dehydration times. TAAB 812 is a relatively safe epoxy resin to use but does not infiltrate well if dehydration of the sample is not complete. The problem is caused by the agarose gel which is largely made up of water. It was found that with standard dehydration times (~15 minutes for each step) a layer of dehydrated agarose formed on the surface of the gel and prevented further dehydration from within the block. Increasing dehydration times, especially of the initial stages, ensured a more thorough dehydration throughout the gel block. The refractory nature of the fossilised organic material meant that prolonged dehydration did not affect the structure of the material.

Spurr resin, which may be carcinogenic, was better at infiltrating a gel which may still contain some water post dehydration.

3.2.11 Carbon isotope analysis

An aliquot of one quarter of unsieved, unoxidised residue was taken from each sample for carbon isotope analysis. These samples had been treated with HCl and HF to remove all carbonate and silicate material respectively, and rendered pH neutral: they had not been centrifuged. The residue was placed in a polythene bottle and then diluted with deionised water and left to settle for eight hours before being carefully decanted. This was repeated two further times to ensure the removal of all unwanted acids and dissolved products. The residue was transferred to a 7 ml vial.

Carbon isotope preparation and analysis. In order to oxidise samples a few grams of each were loaded into a small tin capsule and placed in an oven at 1000 °C in an oxygenated atmosphere. The tin burns exothermically raising the temperature to approximately 1800 °C. To ensure complete oxidation the combustion products were passed through a bed of chromium oxide at 1000 °C using a helium carrier gas. To complete the combustion and remove any sulphur, the products were passed through a 15 cm layer of copper oxide followed by a layer of silver wool. The sample was moved to a second furnace containing copper at 600 °C to absorb any excess oxygen and reduce any nitrogen oxides to elemental nitrogen. A trap containing anhydrous magnesium perchlorate was used to remove any water before the gas stream was passed into a gas chromatograph (GC) where the CO₂ was isolated. It was then passed into a mass spectrometer where the isotopic species ¹²CO₂ and ¹³CO₂ were ionised, separated by mass using a magnetic field and then detected separately.

Isotope values were obtained on an ANCA GSL 20-20 Mass Spectrometer (made by Sercon PDZ Europa), incorporating the Isotope-ratio mass spectrometry (IRMS) technique. The IRMS technique involves the coupling of a preparation system with a stable isotope mass spectrometer allowing the measurement of the total carbon in a sample as well as its ^{13}C levels. Isotope values are reported as ^{13}C in permil (‰) relative to an in-house beet sugar standard which has been calibrated against the PDB standard. The error on the PDB standard is +/- 0.2. All carbon isotope analysis was carried out by Heather Walker in the Department of Animal and Plant Sciences at the University of Sheffield.

3.3 Sample data

The following table (3.1) lists all the samples taken at the Thorn Hill and Chief Joseph Highway sections.

Table 3.1

Sample	Formation	Depth above Nolichucky shale/Maryville Lmst boundary	Lithology
08BP-18	Copper Ridge Dolomite	247.3	Pale-medium grey calcareous mudstone
08BP-17	Maynardville Limestone	233	Medium grey mudstone, bioturbated
08BP-16	Maynardville Limestone	226.85	Medium-grey shale/mudstone, some bioturbation
08BP-15	Maynardville Limestone	203.1	Pale olive-grey mudstone
08BP-14	Maynardville Limestone	197.55	Dark grey shale/mudstone
08BP-13	Maynardville Limestone	190.75	Dark grey, smooth shale/mudstone
08BP-12	Nolichucky Shale	185	Dark grey, smooth shale/mudstone

Sample	Formation	Depth above Nolichucky shale/Maryville Lmst boundary	Lithology
08BP-11	Nolichucky Shale	184.55	Dark grey blocky mudstone
08BP-10	Nolichucky Shale	183.35	Dark grey shale with layers of fine calcareous, fossiliferous hash
08BP-09	Nolichucky Shale	182.3	Dark grey shale/mudstone
08BP-08	Nolichucky Shale	180.35	Dark grey, smooth shale/mudstone
08BP-07	Nolichucky Shale	180.15	Dark grey, smooth shale/mudstone
08BP-06	Nolichucky Shale	179	Dark slaty grey shale
08BP-05	Nolichucky Shale	178.75	Dark slaty grey, smooth shale
08BP-04	Nolichucky Shale	177.55	Dark grey, slaty grey shale
08BP-03	Nolichucky Shale	176.95	Dark grey, slaty grey shale
08BP-01/08BP-02	Nolichucky Shale	175.15	Dark grey, slaty grey shale, slightly rough texture
08BP-39	Nolichucky Shale	172.85	Dark grey, smooth shale
08BP-38	Nolichucky Shale	171.11	Dark grey, smooth shale
08BP-37	Nolichucky Shale	169.4	Dark grey, smooth shale

Sample	Formation	Depth above Nolichucky shale/Maryville Lmst boundary	Lithology
08BP-36	Nolichucky Shale	168.8	Dark grey, smooth shale
08BP-35	Nolichucky Shale	168.5	Dark grey shale
08BP-34	Nolichucky Shale	167.9	Dark grey shale
08BP-33	Nolichucky Shale	165.1	Medium-dark grey, smooth shale
08BP-33	Nolichucky Shale	163.8	Medium-dark grey, smooth shale
08BP-33	Nolichucky Shale	157.5	Medium-dark grey, smooth shale
08BP-32	Nolichucky Shale	154.85	Medium-dark grey, smooth shale
08BP-31	Nolichucky Shale	154.7	Medium grey mudstone
08BP-30	Nolichucky Shale	153.2	Medium grey mudstone
08BP-29	Nolichucky Shale	144.9	Medium grey mudstone
08BP-28½	Nolichucky Shale	139	Pale-medium olive green to grey shale/mudstone
08BP-27/08BP-28	Nolichucky Shale	138.1	Pale-medium olive green to grey shale/mudstone
08BP-26½	Nolichucky Shale	137.5	Pale-medium olive grey shale/mudstone

Sample	Formation	Depth above Nolichucky shale/Maryville Lmst boundary	Lithology
08BP-26	Nolichucky Shale	136.1	Medium grey calcareous mudstone
08BP-25	Nolichucky Shale	135.85	Medium grey calcareous mudstone
08BP-24	Nolichucky Shale	135.3	Medium grey calcareous mudstone
08BP-23	Nolichucky Shale	135.1	Medium grey calcareous mudstone
08BP-22	Nolichucky Shale	129.8	Medium grey calcareous mudstone
08BP-21	Nolichucky Shale	106.2	Very pale creamy-grey shale/mudstone
08BP-20	Nolichucky Shale	103.45	Very pale creamy-grey shale/mudstone. Lots of bioturbation
08BP-19	Nolichucky Shale	103.3	Very pale creamy-grey shale/mudstone
08BP-61	Nolichucky Shale	91.8	Pale olive-brown-grey shale/mudstone
08BP-60	Nolichucky Shale	69.5	Pale olive-brown-grey shale/mudstone
08BP-59	Nolichucky Shale	60	Pale olive-brown-grey shale/mudstone
08BP-58	Nolichucky Shale	56.2	Pale olive-grey shale/mudstone
08BP-57	Nolichucky Shale	43.2	Medium olive-grey, fissile shale

Sample	Formation	Depth above Nolichucky shale/Maryville Lmst boundary	Lithology
08BP-56	Nolichucky Shale	30.6	Pale olive-grey, blocky shale. Trilobites plentiful.
08BP-55	Nolichucky Shale	27.8	Pale-medium brown-grey shale/mudstone. Some bioturbation
08BP-54	Nolichucky Shale	8.4	Medium olive-grey, calcareous shale. Trilobites plentiful
08BP-53	Nolichucky Shale	2.65	Medium grey, smooth, fissile shale
08BP-52	Nolichucky Shale	0.1	Medium dark-grey shale
08BP-76	Rogersville Shale	1.20 m below the upper Rogersville Shale boundary	Dark grey shale
09BP-44	Upper Gros Ventre	1.08 m above the base of the section	Green-grey calcareous shale
09BP-49	Upper Gros Ventre	8.15 m above the base of the section	Green-grey calcareous shale

Chapter 4

Systematics

4.1 Introduction

This chapter presents the taxonomy of acritarchs, problematica and invertebrate components recovered from the Rogersville Shale, Nolichucky Shale, Maynardville Limestone and Copper Ridge Dolomite at Thorn Hill, Tennessee, USA. It also presents two form-species recovered from the Gros Ventre Formation as exposed along the Chief Joseph Highway in Wyoming, USA. Acritarchs are arranged in alphabetical order.

4.2 Species list

Acritarchs

Apodastoides cf. *verobturus* Grey, 2005

Auritusphaera bifurcata Strother, 2008

Auritusphaera cf. *bifurcata* Strother, 2008

Auritusphaera sp. 1

Auritusphaera sp. 2

Auritusphaera sp. 3

Caldariola sp. 1

Cerebrophaera cf. *buickii* Butterfield, 1994

Comasphaeridium brachyspinosum (Kirjanov, 1974), Moczyłowska & Vidal, 1988

Comasphaeridium mackenzianum Baudet, Aitken & Vanguetaine, 1989

Corollasphaeridium wilcoxianum Martin in Dean & Martin, 1982 emend. Martin, 1992

Comasphaeridium sp. 1

Comasphaeridium sp. 2

Cymatiogalea cf. *virgulta* Martin in Martin & Dean, 1988

Cymatiosphaera sp. 1

Cymatiosphaera? sp.

Fimbriaglomerella membranacea (Kirjanov, 1974) Moczyłowska & Vidal, 1988

Granomarginata squamacea Volkova, 1968

Leiosphaeridia kulgunica Jankauskas, 1980
Leiosphaeridia minutissima (Naumova, 1949) emend. Jankauskas, in Jankauskas et al., 1989
Leiosphaeridia sp. 1
Leiosphaeridia sp. 2
Leiosphaeridia sp. 3
Liepaina plana Jankauskas & Volkova, 1979
Lophosphaeridium tentativum Volkova, 1968
Lophosphaeridium truncatum Volkova, 1969
Lophosphaeridium variabile Volkova, 1974
Lophosphaeridium sp. 1
Lophosphaeridium sp. 2
Micrhystridium spp.
Navifusa actinomorpha (Maithy) Hofmann & Jackson 1994
Navifusa sp. 1
Navifusa sp. 2
Peteinosphaeridium? sp. 1
Peteinosphaeridium? sp. 2
Rhopaliophora? sp. 1
Symplassosphaeridium cf. *cambriense* Slavíková, 1968
Thymadora kerke Clendening & Wood, 1981
Timofeovia cf. *pentagonalis* (Vanguetaine, 1974) Vanguetaine, 1978
Virgatasporites rudii Combaz, 1967
Virgatasporites sp. 1
Acritarch sp. 1
Acritarch sp. 2
Acritarch sp. 3
Acritarch sp. 4
Acritarch sp. 5
Acritarch sp. 6
Acritarch sp. 7
Acritarch sp. 8
Acritarch sp. 9
Acritarch sp. 10

Acritarch sp. 11

Problematica

Problematica 1

Problematica 2

Invertebrates

Branchiopod-type Mandibles (mouthparts)

Branchiopod-type limbs

Copepod-type Mandibles (mouthparts)

Wiwaxia sclerites

4.3 Systematics: Acritarchs and Problematica

Incertae Sedis

Group **ACRITARCHA** Evitt, 1963

Genus *Apodastoides* Zhang, Yin, Xiao & Knoll, 1998, emend

Grey, 2005

Type species: *Apodastoides basileus* Zhang, Yin, Xiao and Knoll 1998; by original designation.

Apodastoides cf. *verobturatus* Grey, 2005

Plate 1, Figs 1, 2

- cf. 2003 *Apodastoides* sp. nov. Grey et al., fig 4, B.
- cf. 2005 *Apodastoides verobturatorus* Grey sp. nov. p. 201-203, figs. 10B, 43B, 82, 83 A-E, 84 A-E, 85-87.
- cf. 2006 *Apodastoides verobturatorus* Willman et al., p. 25, pl. I, 1-2.
- cf. 2008 *Apodastoides verobturatorus* Willman & Moczyłowska, fig. 7, A.

Description: Vesicle thin-walled, laevigate and originally spherical to subspherical and bearing approximately forty or more widely and quasi-regularly spaced processes. Processes are of variable length on an individual specimen, thin, hollow, flexible, wiry, cylindrical and laevigate; they gently taper before terminating in a blunt, rounded tip which is occasionally slightly swollen. A distinctive, opaque plug separates individual processes from the vesicle interior and often remains after a process has detached. No excystment structure observed.

Dimensions: 4 specimens. Vesicle diameter 25-40 μm ; process length 3-10 μm ; width & height of plug 1 μm .

Occurrence in this study: Nolichucky Shale: sample 08BP-57.

Remarks: *Apodastoides verobturatorus* Grey, 2005 has previously only been recorded from the Ediacaran of south Australia (Grey et al., 2003; Grey, 2005; Willman et al., 2006; Willman & Moczyłowska, 2008). A few specimens were recorded in the Nolichucky Shale conforming to the diagnosis of *Apodastoides verobturatorus* Grey, 2005 in all but size and process number. The Nolichucky specimens are smaller and have fewer processes than that stated in the diagnosis, although confusingly, it is stated in the remarks section that the holotype has 'about 40' processes, similar to the Nolichucky specimens. In the diagnosis of *A. verobturatorus* (Grey, 2005) there is no stipulation as to size other than the vesicle being 'large'. However, in the same paper (Grey, 2005) the emended generic diagnosis of *Apodastoides* maintains the vesicle size of $>100 \mu\text{m}$ as first stated by Zhang et al. (1998), despite having specimens of *A. verobturatorus* clearly smaller than 100 μm (see Grey, 2005, Fig. 86, p. 205). In any case the sizes of the Nolichucky specimens are relatively smaller than other recorded specimens.

Apodastoides is the only genus described from the Proterozoic that includes species with basally-plugged processes. The most obvious genus to allocate a species with plugged processes is *Baltisphaeridium*, but when Zhang et al. (1998) first proposed *Apodastoides* it was stated that the large vesicle size, distinctive processes and stratigraphical gap between the occurrences of *Apodastoides* and *Baltisphaeridium*, were such that a new genus was warranted. Because the Nolichucky specimens are relatively small and of Cambrian age (although reworking should not be ruled out) it could be suggested that transferring the species *A. verobturatus* to the genus *Baltisphaeridium* may be a valid consideration. However, the Nolichucky specimens show no evidence of a double wall as described by Zang in his emended diagnosis of *Baltisphaeridium* (in Gravestock et al, 2001), and the process plugs appear to be primary features as opposed to being ‘preservational phenomenon’, also outlined by Zang (in Gravestock et al., 2001). Furthermore, the low number of Nolichucky specimens, the possibility of reworking, the distinctive processes and plugs and the confusion surrounding a definitive diagnosis of *Baltisphaeridium* (Wicander et al. 1999), would gender such a move inappropriate.

Genus *Auritusphaera* Strother 2008, emend.

Type species: *Auritusphaera bifurcata* Strother 2008, p. 208-210, pl. 1: 1-7; 2: 1-6.

Original diagnosis: Flattened spherical vesicle, wall unilayered, and thin to moderate in thickness; numerous heteromorphic processes nearly evenly spaced over entire vesicle, solid, slightly tapered, finger-like, short, with rounded distal tips; processes distally simple or bifurcate; processes sometimes expanded at base and may merge into one another, forming partial muri that impart a reticulate to coarsely granular appearance to the wall.

Emended diagnosis: Vesicle circular to subcircular in outline, wall unilayered, and thin to moderate in thickness; vesicle surface reticulate, divided into psilate to granulate, concave, polygonal fields, the edges of which form sharp ridges with processes positioned at ridge intersections; the process-vesicle contact angular to

confluent. Processes homomorphic or heteromorphic, solid, short or long, distally simple, acuminate, evexate or bifurcate; processes sometimes expanded at base and may merge into one another, sometimes accentuating ridge apexes.

Remarks: *Auritusphaera* Strother 2008 emend. differs from *Micrhystridium* Deflandre 1937 emend. Sarjeant & Stancliffe 1994 in having a vesicle surface divided into polygonal fields and from *Skiagia* Downie 1982 in not having funnel-shaped process tips. The fields present on *Auritusphaera* Strother 2008 emend. represent sculptured features of the vesicle wall. This differs from the fields present on both *Timofeevia* Vanguetaine 1978 and *Cristallinium* Vanguetaine 1978 which represent separate conjoined plates.

The monospecific genus *Auritusphaera* Strother 2008 was erected to accommodate small forms with short, solid, heteromorphic processes whose bases sometimes expand and merge resulting in a reticulate or coarsely granular vesicle wall. The type species, *Auritusphaera bifurcata* Strother 2008, possesses simple, acicular processes and bifurcate processes, all of which merge at their bases to form a reticulate vesicle surface. At Thorn Hill five forms have been recovered, including *A. bifurcata*, all of which possess a distinctive, reticulate, vesicle surface with approximately evenly distributed processes. They clearly differ, however, in the morphology of their processes. In SEM the nature of the reticulation and its similarity between the five forms is clearly apparent; the reticulation is a sculptured surface, subdivided into concave, polygonal fields, the edges of which form sharp ridges with processes positioned at ridge intersections. Furthermore, the field ridges frequently extend onto process stems to form narrow fibrils or furrows. It should be noted that although the reticulate structure is seen in light microscope, the finer details are not. It is the opinion of the present author that the generic concept for *Auritusphaera* should be concerned with the nature of the vesicle surface and the presence of evenly distributed, solid, processes. Species concepts should be determined by the nature of the processes. Furthermore, that the five forms found at Thorn Hill represent different species of the same genus.

Auritusphaera bifurcata Strother, 2008

Plate 1, Figs 3-6

2008 *Auritusphaera bifurcata* Strother, sp. nov. p. 208-210, pls. 1, 2.

Description: A species of *Auritusphaera* with a vesicle bearing numerous, finger-like, short, solid, processes, the majority of which are simple, slightly tapering and accompanied by a bifurcate processes. Process terminations acicular to evexate occasionally truncated. Occasionally specimens occur in clusters. Partial rupture observed in a few specimens, otherwise no excystment structure observed.

Dimensions: 58 specimens. Vesicle diameter 14-26 μm (av. 19.7 μm); process length $\sim 1 \mu\text{m}$; width of fields 1-1.5 μm .

Occurrence in this study: Nolichucky Shale: samples 08BP-19, 08BP-20, 08BP-11.

Remarks: Specimens recovered from the Nolichucky Shale at Thorn Hill have slightly shorter processes than those described by Strother (2008) which are recorded as $\sim 2 \mu\text{m}$, although many processes illustrated in that paper do appear closer to 1 μm . Occasionally two adjacent processes are orientated such that one crosses in front of the other giving the impression of a single, bifurcate process, and consequently care must be taken when taxonomically assigning specimens.

Previous records: Northeastern Tennessee, Furongian, USA, Nolichucky Shale (Strother 2008).

Auritusphaera cf. *bifurcata* Strother, 2008

Plate 2, Figs 1, 2

Description: As *Auritusphaera bifurcata* Strother, 2008 but without bifurcate processes.

Dimensions: 22 specimens. Vesicle diameter 15-23 μm (av. 18.5 μm); process length $\sim 1 \mu\text{m}$.

Occurrence in this study: Nolichucky Shale: samples 08BP-61, 08BP-19, 08BP-20, 08BP-24, 08BP-26.

Remarks: *Auritusphaera* cf. *bifurcata* occurs in low numbers and has a very low abundance relative to *A. bifurcata*. It differs from *A. bifurcata* in not having bifurcate processes; in all other respects the two taxa are the same. In light microscope bifurcate processes of *Auritusphaera bifurcata* are only observed in the peripheral region of the vesicle where processes extend outward from the vesicle edge and are clearly discerned; bifurcate processes situated inward of the vesicle periphery are difficult, if not impossible to observe. Furthermore, only a few bifurcate processes occur on any one specimen. Given this, it is only inevitable that specimens without observed bifurcate processes will be encountered; this does not mean unequivocally that there are no bifurcate processes present, but merely that they may not have been observed. Alternatively it might be that *A. cf. bifurcata* and *A. bifurcata* actually represent variant forms, though whether this is the case will need to be determined by future work.

Auritusphaera sp. 1

Plate 2, Figs 3, 4

Description: A species of *Auritusphaera* with a vesicle bearing numerous, slightly flattened, short, solid, simple, slightly tapering, acuminate or evexate processes of varying lengths. Frequently processes are absent, possibly broken, from ridge intersections or resemble very short, rounded stubs. Occasionally specimens occur in clusters. Partial rupture observed in a few specimens, otherwise no excystment structure observed.

Dimensions: 83 specimens. Vesicle diameter 18-31 μm (av. 22.7 μm); process length <1-3 μm (av. 2 μm); width of fields 0.5- 1.5 μm .

Occurrence in this study: Nolichucky Shale: samples 08BP-60, 08BP-61, 08BP-19, 08BP-20, 08BP-22, 08BP-24, 08BP- 25, 08BP-26, 08BP-26½.

Remarks: *Auritusphaera* sp. 1 differs from *Auritusphaera bifurcata* Strother (2008) primarily in not having bifurcate processes, but also in having a slightly larger vesicle and processes with varying dimensions, many of which are either longer than those recorded on *A. bifurcata* or resembling short stubs. Variation of process length and the absence of some processes at ridge intersections, emphasises the presence of longer processes which extend outward from the vesicle periphery and can give the impression of there being fewer processes.

Auritusphaera sp. 2

Plate 2, Figs 5, 6; Plate 3, Fig 1

Description: A species of *Auritusphaera* with a vesicle bearing numerous, slightly flattened, solid, simple, slightly tapering, acuminate to evexate processes of varying lengths. The majority of processes are short and stub-like, the others longer, thin and gently tapering; longer processes are straight, curved or slightly sinuous. Partial rupture observed in a few specimens, otherwise no excystment structure observed.

Dimensions: 18 specimens. Vesicle diameter 17-24 μm (av. 19.8 μm); process length <0.5-6 μm ; width of fields \sim 1 μm .

Occurrence in this study: Nolichucky Shale: sample 08BP-57.

Remarks: *Auritusphaera* sp. 2 differs from other species of *Auritusphaera* in possessing relatively long, acicular processes.

Auritusphaera sp. 3

Plate 3, Figs. 2-4

Description: A species of *Auritusphaera* with a vesicle bearing numerous solid processes of varying lengths. The majority of processes are short and stub-like, the others longer, flat, approximately parallel sided or gently widening before flaring distally; process terminations oblate or bifid. No excystment structure observed.

Dimensions: 30 specimens. Vesicle diameter 20-26 μm (av. 22.2 μm); <0.5-5; width of fields 1-2 μm .

Occurrence in this study: Nolichucky Shale: samples 08BP-19, 08BP-20.

Remarks: *Auritusphaera* sp. 3 differs from other species of *Auritusphaera* in possessing relatively long, flat processes which frequently flare distally into bifid terminations.

Genus *Caldariola* Molyneux *in* Molyneux & Rushton, 1988

Type species: *Caldariola glabra* (Martin 1973) Molyneux *in* Molyneux & Rushton, 1988

Caldariola sp. 1

Plate 3, Figs 5, 6; Plate 4, Figs 1, 2

Description: Vesicle hemispherical with large polar pylome the width of which is equal to, or greater than the vesicle depth. Vesicle laevigate to slightly granulate. Pylome with thickened rim, operculum flat, discoidal and unornamented.

Dimensions: 12 specimens. Vesicle depth 25-60 μm (av. 40.2 μm). Width of pylome 35-113 (av. 59.8 μm).

Occurrence in this study: Nolichucky Shale: samples 08BP-52, 08BP-53, 08BP-55, 08BP-26, 08BP-32, 08BP-36, 08BP-39, 08BP-6, 08BP-9, 08BP-10.

Remarks: *Caldariola* sp. 1 has an approximately hemispherical vesicle outline and possesses a large polar excystment opening (pylome) closed by an operculum. As such it conforms to characteristics of the galeate acritarchs as defined by Servais & Eiserhardt (1995) and additionally having a smooth vesicle, conforms to the generic diagnosis of the monospecific genus *Caldariola* Molyneux *in* Molyneux & Rushton

1988, to which it is tentatively assigned. *Caldariola glabra* (Martin, 1973) Molyneux in Molyneux & Rushton 1988 is the only species assigned to the genus *Caldariola* and is commonly found at the Tremadoc-Arenig boundary interval (Montenari & Servais, 2000). It has also been reported from the Furongian (Volkova, 1989). At Thorn Hill *Caldariola* sp. 1 is found in older, Cambrian Series 3 and lowermost Furongian units. *Caldariola* sp. 1 differs from *Caldariola glabra* (Martin, 1973) Molyneux in Molyneux & Rushton 1988 in being larger, and having a relatively larger and less rigid pylome which lacks a distinctive lip, and from *Leiosphaeridia* Eisenack 1958 emend. Downie & Sarjeant 1963; emend. Turner 1984 in lacking a definitive spherical form.

Genus *Cerebrospira* Butterfield, 1994

Type species: *Cerebrospira buickii* Butterfield, 1994

Cerebrospira cf. *buickii* Butterfield, 1994

Plate 4, Fig 3

cf. 1991 *Leiosphaeridia* sp. cf. *L. atava* Knoll et al. p. 558, fig. 21.2-21.3.

cf. 1994 *Cerebrospira buickii* Butterfield et al., p. 30, fig. 12.

cf. 1996 *Cerebrospira* sp. Grey & Cotter, p. 75, fig. 3 (d, g).

cf. 1999 *Cerebrospira buickii* Cotter, p. 69-70, fig. 6 (D, G).

Description: Originally spherical vesicle with prominent wrinkles regularly and tightly arranged. The wrinkles are sinuous and interfingering, the curved nature of which imparts an undulation to the vesicle outline; secondary folds are absent. A small, opaque, approximately circular inner body is present. The vesicle wall is translucent with a psilate surface; an outer envelope is absent.

Dimensions: 2 specimens. Vesicle diameter 52-78 μm ; width of wrinkles 1 μm ; width of inner body 15 μm .

Occurrence in this study: Nolichucky Shale: Sample 08BP-29.

Remarks: *Cerebrophaera buickii* Butterfield 1994 has previously been reported from the Neoproterozoic Svanbergfjellet Formation (700-750 Ma) of northeastern Spitsbergen (Butterfield et al., 1994) and Neoproterozoic strata in the western Officer Basin of South Australia (e.g., Eyles et al., 2007). Two specimens were recorded from the Nolichucky Shale which correspond to the diagnosis of *Cerebrophaera buickii* Butterfield 1994 in all but size, with the Nolichucky Shale specimens being much smaller (the diagnosis stipulates a vesicle diameter of 100-1000 μm) and the presence of a small, opaque inner body. This latter exception might be the result of contamination, but because only two specimens were observed it is impossible to state with confidence. One of the specimens is slightly degraded resulting in a low density of wrinkles. However, many of the wrinkles present on this specimen are clearly the same as those described and illustrated by Butterfield (*in* Butterfield et al., 1994), and furthermore the vesicle outline bears an undulation, being the result of the underlying, wrinkling nature of the vesicle wall. Both specimens are without outer membranes and this is common in the specimens recorded by Cotter (1999), and conforms to the generic diagnosis of Butterfield (*in* Butterfield et al., 1994) which states an outer thin-walled envelope is sometimes present.

Genus *Comasphaeridium* Staplin, Jansonius & Pocock, 1965

Type species: *Comasphaeridium cometes* (Valensi, 1949) Staplin, Jansonius & Pocock, 1965

Comasphaeridium brachyspinosum (Kirjanov, 1974), Moczyłowska & Vidal, 1988

Plate 4, Figs 4, 5

- 1974 *Baltisphaeridium brachyspinosum* Kirjanov, pp. 120-121, pl. 7 (1).
- 1979 *Baltisphaeridium brachyspinosum* Kirjanov, 1974; Volkova et al., pl. 10 (15).
- 1986 *Comasphaeridium brachyspinosum* (Kirjanov, 1974); comb. nov.; Moczyłowska & Vidal, fig. 9 (a,b).
- 1988 *Comasphaeridium brachyspinosum* (Kirjanov, 1974) Moczyłowska & Vidal, p. 3, pl. 1 (4).
- 1994 *Filisphaeridium brachyspinosum* (Kirjanov, 1974) comb. nov.; Sarjeant & Stancliffe, p. 29.
- 2000 *Comasphaeridium brachyspinosum* (Kirjanov, 1974) Moczyłowska & Vidal, 1988, Talyzina & Moczyłowska, pl. II, figs. 5-7.

Description: Vesicle subcircular to suboval in outline, bearing numerous, densely arranged, solid, thin, filiform, tapering processes of equal length. Processes slightly thickened proximally and acuminate distally. No excystment structure observed.

Dimensions: 31 specimens. Vesicle diameter 8-21 μm (av. 12 μm); process length 1.5-4 μm (av. 2 μm).

Occurrence in present study: Nolichucky Shale: samples 08BP-22, 08BP-26, 08BP-28½, 08BP-29, 08BP-32, 08BP-9.

Remarks: This form conforms to the diagnosis of *Comasphaeridium brachyspinosum* (Kirjanov, 1974) Moczyłowska & Vidal 1988. However, vesicle size is significantly smaller than previously recorded e.g., Moczyłowska & Vidal (1988) recorded a mean vesicle diameter of 50.8 μm ; Moczyłowska (1991) recorded vesicle diameters of 21-39 μm ; and Hagenfeldt (1989a) recorded vesicle diameters of 24-33 μm . It differs from *C. strigosum* (Jankauskas) Downie 1982 in having relatively shorter processes which are slightly thicker proximally, and from *C. mollicum* Moczyłowska & Vidal 1988 in having processes which are not differentiated.

Selected previous records: Siberian Platform, lower Cambrian (Volkova et al., 1979; Rudavskaya & Vassileva, 1984. Sweden, lower Cambrian (Vidal, 1981b, c;

Moczyłowska & Vidal, 1986; Hagenfeldt, 1989a). East Greenland, lower Cambrian (Moczyłowska & Vidal, 1986). Poland, lower Cambrian (Moczyłowska, 1991). Estonia, lower Cambrian (Talyzina & Moczyłowska, 2000).

Comasphaeridium mackenzianum Baudet, Aitken & Vanguestaine, 1989

Plate 4, Fig 6: Plate 5, Figs 1, 2

- 1989 *Comasphaeridium mackenziana* n. sp. Baudet, Aitken & Vanguestaine, p. 138-140, pl. 1 (14-17).
- 2001 *Comasphaeridium mackenzianum* Baudet, Aitken & Vanguestaine, 1989, Moczyłowska et al., fig. 5 (c).
- 2002 *Comasphaeridium mackenzianum* Baudet, Aitken & Vanguestaine, 1989, Moczyłowska, fig. 5 (4).
- 2011 *Comasphaeridium mackenzianum* Baudet, Aitken & Vanguestaine, 1989, Palacios et al. text-fig. 5 (F).

Description: Vesicle small, circular to subcircular in outline bearing numerous, filiform, flexible processes. Processes taper to acuminate tips and are differentiated or partly so. Process length 75-110% of vesicle diameter. Occasionally occurs in clusters. No excystment structure observed.

Dimensions: 11 specimens. Vesicle diameter 5-9 μm (av. 6 μm); maximum process length 3-10 μm (av. 6 μm).

Occurrence in present study: Nolichucky Shale: samples 08BP-57, 08BP-59, 08BP-60, 08BP-61, 08BP-29.

Remarks: This is a very small form occurring in low numbers in the Nolichucky Shale. It differs from *Heliosphaeridium coniferum* (Downie, 1982) Moczyłowska 1991 in possessing solid processes and from *C. gogense* (Downie, 1982) Sarjeant & Stancliffe 1994 in having acuminate process terminations. The original specific name *C. mackenziana* (Baudet, Aitken & Vanguestaine, 1989) was corrected to *C. mackenzianum* by Sarjeant & Stancliffe (1994, p. 26).

Previous records: Northwest Canada, early Cambrian (Baudet et al., 1989). Newfoundland, Canada, early Cambrian (Palacios et al., 2011). North Greenland, early Cambrian (Vidal & Peel, 1993). Sweden, early Cambrian (Moczyłowska, 2002; Moczyłowska et al., 2001).

Comasphaeridium sp. 1

Plate 5, Fig 3

Description: Vesicle approximately ellipsoidal to circular in outline and bearing numerous, densely arranged, solid, thin, sinuous, flexible, variably entangled processes. Processes are of variable length (10-34% of vesicle diameter) and thickness, gently taper to a point and some processes have truncated terminations resulting from breakage. Proximally the processes are not thickened. No excystment structure observed.

Dimensions: 4 specimens. Maximum vesicle diameter 22-41 μm (av. 33 μm); process length 5-14 μm ; process width $<0.5 \mu\text{m}$.

Occurrence in this study: Nolichucky Shale: sample 08BP-59.

Remarks: The four specimens of *Comasphaeridium* sp. 1 are degraded and/or broken making taxonomic assignment difficult. All four specimens are broadly similar in vesicle size and process lengths and also co-occur within the same sample. It differs from *Comasphaeridium strigosum* (Jankauskas) Downie 1982 in having longer processes of variable length and thickness, not thickened proximally. However, it might be that these differences are the result of taphonomic effects and the form is necessarily left on open nomenclature.

Comasphaeridium sp.2

Plate 5, Figs 4, 5

Description: Vesicle small and rigid, circular to subcircular in outline, bearing numerous very densely arranged, solid, long, thin, flexible, gently tapering

processes. Processes are of approximately equal length and 44-110% of the vesicle diameter. Processes are densely arranged proximally and partially differentiate distally. No excystment structure observed.

Dimensions: 3 specimens. Vesicle diameter 9-11 μm ; process length 4-11 μm .

Occurrence in present study: Nolichucky Shale: samples 08BP-59, 08BP-22, 08BP-28½.

Remarks: Two of the three specimens found at Thorn Hill have process lengths approximately equal to the vesicle diameter. The third specimen has a process length 44% of the vesicle diameter. What all three have in common however, are processes which are very numerous, thin, gently tapering and with bases that are not noticeably expanded. As such, and given that only three specimens were recovered, they are grouped together as *Comasphaeridium* sp. 2. It differs from *C. mackenzianum* in having more numerous, relatively thinner, longer processes.

Genus *Corollasphaeridium* Martin in Dean & Martin, 1982
emend. Yin, 1986

Type species: *Corollasphaeridium wilcoxianum* Martin in Dean & Martin, 1982 by original designation

Corollasphaeridium wilcoxianum Martin in Dean & Martin, 1982
emend. Martin 1992

Plate 13, Fig 1

1982 *Corollasphaeridium wilcoxianum* gen. et sp. nov. Martin in Dean & Martin, p. 136, Pl. 1, figs. 15, 16.

1986 *Corollasphaeridium normalisum* sp. nov. Yin, p. 337, Pl. 88, figs. 1, 2, 4, 6, 9, 15; Text fig. 123.

1986 *Corollasphaeridium wilcoxianum* Martin, 1982. Yin, p. 338, Pl. 88, figs. 12, 14.

1992 *Corollasphaeridium wilcoxianum* Martin in Dean & Martin, 1982, emend.
Martin, p. 25, Pl. 6, figs. 2-4, 8, 10-16.

Description: Vesicle originally elongate in lateral view and circular to subcircular in transverse view. The hollow vesicle is dome-shaped in the antapical region with seven, conical, broad-based, hollow, secondary processes arranged quasi-regularly around a larger, central, but in all other aspects similar, primary process; all the processes have acuminate terminations and connect freely with the vesicle interior. At the opposite end (apical pole) vestiges of a collarete remain attached to the base of the antapical dome, which is open to the surrounding environment. One or two thin ridges or fibrils run transversely down the sides of each and all of the processes and extend onto the vesicle surface and collarete vestiges. Anastomosing fibrils were not observed. Operculum not observed.

Dimensions: 1 specimen. Basal width of vesicle 24 μm ; length of primary process 24 μm ; basal width of primary process 5 μm extending to 15 μm ; length of secondary processes 15-20 μm ; basal width of secondary processes 3-7 μm . Total lateral length 36 μm .

Occurrence in this study: Nolichucky Shale: sample 08BP-33 .

Remarks: Despite the absence of most of the collarete enough still remains, notably with clearly visible fibrils, to infer its previous position, and consequently this form is assigned to *Corollasphaeridium wilcoxianum* Martin in Dean & Martin, 1982 emend. Martin 1992.

Previous records: Wilcox Pass, Alberta, Canada, Furongian-Tremadoc(?), basal silty member of the Survey Peak Formation (Dean & Martin, 1982; Martin, 1992). Jilin Province, China, Furongian (Stage 10)-Tremadoc(?), Xiaoyangqiao section, (Yin, 1986; Chen et al., 1988).

Genus *Cymatiogalea* Deunff, 1961 emend. Deunff, Górká &
Rauscher, 1974

Type species: *Cymatiogalea margaritata* Deunff, 1961

Cymatiogalea cf. *virgulta* Martin in Martin & Dean, 1988

Plate 6, Figs 1, 2

cf. 1988 *Cymatiogalea virgulta* sp. nov. Martin in Martin & Dean, Pl. 6, Figs.
1, 2.

Description: Vesicle subcircular in outline, laevigate and divided into polygonal fields or plates delineated by low suture-ridges. Processes appear to be solid and are simple, acuminate, bifurcate, occasionally to the second order and/or digitate. They are situated at the angles and along the edges of plates with normally one process situated between plate-angles. One partially attached plate has concave edges and is devoid of processes at three neighbouring plate-angles and may represent an operculum. No distinct pylome or membranes were observed. Excystment possibly via detached operculum.

Dimensions: 1 specimen. Vesicle diameter 29 μm ; process length 2-4 μm ; field width ~16 μm .

Occurrence in present study: Nolichucky Shale: sample 08BP-34.

Remarks: This form possesses polygonal fields or plates with processes situated at their corners and edges and is therefore comparable to *Timofeevia pentagonalis* (Vanguetaine, 1974) Vanguetaine 1978 and *Cymatiogalea virgulta*. However, the presence of a suspected operculum precludes assignment to *T. pentagonalis*. *Cymatiogalea* cf. *virgulta* differs from *C. virgulta* in having solid processes, and because no unequivocal pylome/operculum was observed it is left in open nomenclature. The absence of membranes, given their delicate nature, may be the result of low preservation potential. That there are polygonal plates delineated by

processes and a possible operculum, comparison to *C. virgulta* is justified. It should be noted that *Cymatiogalea* ? sp. 1 occurs just above the base of the Furongian, and as such would represent an early form of galeate acritarch. Given this, and its similarity to *Timofeevia pentagonalis*, it might represent a form transitional between *Timofeevia* and the galeates.

Genus *Cymatiosphaera* O. Wetzel 1933 ex Deflandre, 1954

Type species: *Cymatiosphaera radiata* O. Wetzel, 1933

Cymatiosphaera sp. 1

Plate 6, Figs 3, 4

Description: Overall form polygonal in outline, vesicle subcircular to polygonal in outline and often difficult to discern. Vesicle laevigate to shagreenate and divided into polygonal fields by lists orientated approximately perpendicular to the vesicle surface. Lists are supported by solid, thin, cylindrical processes situated at list intersections. Distal edges of lists smooth, concave, occasionally parallel, rarely convex. Approximately 9-12 fields are situated in the peripheral region of the vesicle. No excystment structure observed.

Dimensions: 24 specimens. Whole specimen diameter 7-17 μm (av. 14 μm); vesicle diameter 6-11 μm (av. 10 μm); height of lists 1-4 μm (av. 3 μm); μm (av. μm); width of fields 2-3 μm .

Occurrence in present study: Nolichucky Shale: samples 08BP-59, 08BP-22, 08BP-24, 08BP-26, 08BP-26½, 08BP-28½, 08BP-29, 08BP-30, 08BP-32.

Remarks: *Cymatiosphaera* sp. 1 has very small dimensions which differentiates it from the vast majority of other species of *Cymatiosphaera*. It differs from *Cymatiosphaera pusilla* Moczyłowska, 1991 in having relatively smaller, more

numerous lists, and from species of *Fimbriaglomerella* in not possessing an outer membrane.

Cymatiosphaera? sp.

Plate 6, Fig 5

Description: Vesicle subcircular in outline, bearing numerous leaf-like processes of which approximately 30-40 are observed at the vesicle periphery. Vesicle divided into polygonal fields by thickened ridges or muri. Processes consist of an opaque, rod-like, central column supporting a transparent membrane which can extend beyond the end of processes. Some membranes appear arch-shaped whilst others connect between processes with a concave distal edge. No excystment structure observed.

Dimensions: 3 specimens: Maximum overall diameter 66-83 μm (av. 72.3 μm); vesicle diameter 30-50 μm (av. 41.7 μm); process length 5-20 μm ; width of fields 5-7 μm .

Occurrence in this study: Nolichucky Shale: samples 08BP-52, 08BP-54, 08BP-57.

Remarks: Only three specimens of this acritarch were found. The morphology of the processes/membranes and their connections with each other and the vesicle surface is difficult to discern due to either poor preservation or thick crowding of processes which obscures features. Consequently this form cannot be confidently assigned. The closest taxon would be the genus *Cymatiosphaera* O. Wetzel ex Deflandre, 1954, but the unclear nature of the membranes precludes this assignment and the form is left in open nomenclature.

Genus *Fimbriaglomerella* Loeblich & Drugg, 1968

Type species: *Fimbriaglomerella divisa* Loeblich & Drugg 1968

Fimbriaglomerella membranacea (Kirjanov 1974) Moczyłowska &
Vidal, 1988

Plate 6, Fig 6; Plate 7, Figs 1, 2

- 1974 *Cymatiosphaera ? membranacea* Kirjanov, sp. nov., p. 121, pl. 7: 2, 3.
1979 *Cymatiosphaera ? membranacea* Kirjanov, 1974, Volkova et al., p.25, pl. 16:
1, 2.
1986 Non *Cymatiosphaera ? membranacea* Kirjanov, Moczyłowska & Vidal,
Fig. 10: A, B.
1988 *Fimbriaglomerella membranacea* (Kirjanov, 1974) comb. nov
Moczyłowska & Vidal, 1988, p. 3-4, pl 1: 5-9.
1989 ? *Fimbriaglomerella membranacea* (Kirjanov) Moczyłowska & Vidal,
1988, pl. 1: 16-18.

Description: Vesicle small, circular to subcircular in outline, laevigate to shagreenate and robust. Lists, orientated perpendicular to the vesicle surface, connect the vesicle to an outer, thin, surrounding membrane, and narrow polygonal fields are occasionally observed where lists connect to the outer membrane. Lists are thickened at intersections where they appear to be supported by short, solid cylindrical processes. Outer membrane can impart a smooth, wavy outline to specimens. No excystment structure observed.

Dimensions: 12 specimens. Vesicle diameter 10-18 μm (av. 13 μm); height of membranes 1-2 μm (av. ~1 μm).

Occurrence in this study: Nolichucky Shale, 08BP-24, 08BP-3.

Remarks: The Thorn Hill specimens conform to the diagnosis of *Fimbriaglomerella membranacea* (Kirjanov 1974) Moczyłowska & Vidal 1988 but are significantly smaller than specimens recorded by Kirjanov (1974), and Moczyłowska & Vidal (1988) whose specimens have vesicles measuring 22-28 μm . The Thorn Hill specimens have vesicle dimensions which correspond to those of *Fimbriaglomerella*

minuta (Jankauskas, 1979) Moczyłowska & Vidal 1988. However, the Thorn Hill specimens differ in possessing a robust vesicle with more numerous fields.

Previous records: See Occurrence and stratigraphic range, Moczyłowska (1991).

Additional previous records.

Cambrian Series 1 and 2: Spain (Palacios & Vidal, 1992; Liñán et al. 2006); Czech republic (Vavrdová & Bek, 2001); Cambrian Series 3: China (Yang & Yin, 2001), USA (Wood & Stephenson, 1989).

Genus *Granomarginata* Naumova, 1961

Type species: *Granomarginata prima* Naumova, 1961

Granomarginata squamacea Volkova, 1968

Plate 7, Figs 3, 4

Synonymy: See Moczyłowska (1991, 1998).

1968 *Granomarginata squamacea* Volkova, sp. nov., Volkova, p. 25. pl. 4: 14-19; 10: 4, 5; 11: 11.

1969 *Granomarginata squamacea* Volkova, Volkova, 1969b, p. 231, pls. 47: 5, 17; 49: 12.

1978 *Granomarginata squamacea*, Tynni, p. 48, pl. 6:47, 48.

1978 *Annulum difeminatum* Fombella 1978, n. sp., Fombella, p. 249-250, pl. 3: 18, 19.

1979 *Granomarginata squamacea* Volkova 1968, Volkova et al., p. 19, pl. 18: 5-9.

1979 *Granomarginata squamacea* Volkova 1968, Fombella, pls. 1: 2, 3; 3: 40.

1980 *Granomarginata squamacea* Volkova 1968, Moczyłowska, p. 472, pl. 2: 5-7.

1981 *Granomarginata squamacea* Volkova 1968., Moczyłowska, Fig. 5J, L.

1982 *Granomarginata squamacea* Volkova 1968, Downie, p. 279, Fig. 11K.

1983 *Annulum squamacea* (Volkova, 1968) comb. n., Martin & Dean, p. 359-360, pl.43.1, Figs. 4, 7-12.

1983 *Granomarginata squamacea* Volkova 1968, Vanguetaine & Van Looy, pl. 1: 10.

1986 *Granomarginata squamacea* Volkova 1968, Moczyłowska & Vidal, Fig. 8G.

1987 *Granomarginata squamacea* Volkova 1968, Knoll & Swett, p.917, Fig. 8.18, non Fig. 8.11.

Description: Vesicle circular to subcircular in transverse outline, originally lenticular, surrounded by a sponge-like material which extends outward from around the equatorial margin of the vesicle to form a rim. The outer edge of specimens is often irregular and disfigured. Occasionally the sponge-like material has a slightly filamentous appearance. Excystment by partial rupture.

Dimensions: 54 specimens. Overall diameter 10-45 μm (av. 26.3 μm); vesicle diameter 5-28 μm (av. 15.2 μm); thickness of surrounding material 3-24 μm (av. 11.1 μm).

Occurrence in this study: Nolichucky Shale: samples 08BP-55, 08BP-59, 08BP-61, 08BP-21, 08BP-25, 08BP-26½, 08BP-29, 08BP-32, 08BP-33, 08BP-33 , 08BP-37, 08BP-38, 08BP-3, 08BP-5, 08BP-9; Maynardville Limestone: 08BP-17.

Remarks: This is a common species at Thorn Hill occurring in nearly half of all samples. A few specimens exhibited a narrow rim reminiscent of *Granomarginata prima* Naumova, 1961, but the irregular nature of specimen outlines suggests the rim thickness is probably the result of deterioration.

Previous records: This is a common species occurring in the Neoproterozoic and throughout the Cambrian. See Occurrence and stratigraphic range, Moczyłowska (1991, 1998).

Additional previous records.

Cambrian Series 1 and 2: Missouri & Arkansas, North America, Bonnetterre & Davis Formations (Wood & Stephenson, 1989).

Genus *Leiosphaeridia* (Eisenack 1958) Downie & Sarjeant,
1963 emend. Turner, 1984

1958 *Leiosphaeridia* Eisenack, p. 2

1963 *Leiosphaeridia* Eisenack emend.; Downie & Sarjeant, p. 95

1984 *Leiosphaeridia* Eisenack emend.; Turner, p. 116

Type species: *Leiosphaeridia baltica* Eisenack, 1958

Remarks: The division of the genus *Leiosphaeridia* (Eisenack 1958) Downie & Sarjeant, 1963 emend. Turner, 1984 into form species or groups has proven difficult due to the simplicity of the form, and yet numerous validly published species exist. Its most obvious characteristics, size and wall thickness, have been utilised by some workers, most notably Jankauskas (*In: Jankauskas et al., 1989*) who divided the genus into four forms: 1) *Leiosphaeridia jacutica*: thick-walled & >70 μm ; 2) *Leiosphaeridia crassa*: thick-walled & <70 μm ; 3) *Leiosphaeridia tenuissima*: thin-walled & >70 μm ; 4) *Leiosphaeridia minutissima*: thin-walled & <70 μm . This system has been widely applied in Proterozoic populations (e.g. Butterfield & Chandler, 1992; Grey, 2005) but less so in the Cambrian, possibly due to the arbitrary nature of the generic division which fails to take into account similar form-populations with size-ranges that straddle the 70 μm size boundary. This is the case with the Thorn Hill *Leiosphaeridia* populations and consequently the Jankauskas divisions are only applied in part.

Another consideration is excystment. Sphaeromorphs with and without pylomes and sphaeromorphs exhibiting excystment via median split have all been recorded. The original diagnosis by Eisenack (1958) and subsequent emendations by Downie & Sarjeant (1963) and Turner (1994), all state that a pylome may or may not be present; dehiscence is not discussed. Turner (1984) separated forms with an operculate pylome, which he retained in *Leiosphaeridia*, from those which excysted via median split for which he erected the genus *Dichotisphaera* Turner 1984. Colbath & Grenfell (1995) dismissed this idea arguing that the type species

Leiosphaeridia baltica Eisenack 1958 did not exhibit a pylome, and that only those species showing dehiscence by partial splitting or unknown dehiscence mechanism be included in the genus *Leiosphaeridia*; consequently they considered *Dichotisphaera* Turner 1984 to be a junior synonym of *Leiosphaeridia*. Quintavalle & Playford (2006) concurred with this view that “*Leiosphaeridia* sensu stricto should only include forms with excystment via a median split”. This view is not accepted here: sphaeromorphic forms with pylomes or which excyst via median split are treated as species of *Leiosphaeridia*.

Leiosphaeridia kulgunica Jankauskas, 1980

Plate 7, Figs 5, 6

1980 *Leiosphaeridia kulgunica* Jankauskas 1980, sp. nov. Jankauskas. Pl. 1, figs 1-3.

2007 *Leiosphaeridia kulgunica* Jankauskas 1980. Leiming & Xunlai. Fig. 2-2.

Description: Vesicle circular to subcircular in outline, thick-walled, folds absent or few, slightly translucent, shagreenate to slightly granulate and possessing a pylome with a width approximately 27-35 % of the vesicle diameter. Pylome resembles a simple aperture. Operculum subcircular, unornamented and observed on one specimen.

Dimensions: 7 specimens. Vesicle diameter 21-62 μm (av. 48.7 μm); pylome width 7-20 μm (av. 15.5 μm).

Occurrence in this study: Nolichucky Shale: samples 08BP-52, 08BP-53, 08BP-55, 08BP-61, 08BP-29.

Remarks: This is a rare species at Thorn Hill and quite unusual in being slightly translucent, although not a diagnostic feature. As far as the present author is aware *Leiosphaeridia kulgunica* Jankauskas 1980 has not been recorded in the Cambrian Period and is limited to the Proterozoic. If this is the case this would be the first record of this species in the Cambrian. It differs from *Leiosphaeridia ketchenata*

Turner 1984 in having a smaller pylome, from *Tasmanites* Newton 1885 in not having pores and *Caldariola* Molyneux in Molyneux & Rushton 1988 in having a spherical form.

Selected previous records: Neoproterozoic: North China, Dongjia Formation (Leiming & Xunlai, 2007); East Siberia, Russia, (Stanevich et al., 2005; Veis et al., 2003); Northern India, (Bhat et al., 2009).

Leiosphaeridia minutissima (Naumova 1949) emend. Jankauskas
in Jankauskas et al., 1989

Plate 8, Figs 1, 2

- 1949 *Leiotriletes minutissimus*; Naumova, pl. 1, fig. 1.
1989 *Leiosphaeridia minutissima* (Naumova 1949) emend. Jankauskas; Jankauskas et al., p. 79-80, pl. 9, figs. 1-4, 11.
1992 *Leiosphaeridia minutissima* (Naumova 1949) emend. Jankauskas; Butterfield & Chandler, text-figs. 3, A-I; 5, C
1999 *Leiosphaeridia minutissima* (Naumova 1949) emend. Jankauskas; Cotter, p. 76, fig. 8F.

Description: Small, circular to sub-circular in outline, thin-walled, unornamented, folds few to common, vesicle laevigate to shagreenate and very pale brown to clear. Rarely found with inclusions. Excystment by median split, the resultant dehiscence segments being ellipsoidal to hemispherical in shape; aperture situated along the longitudinal axis with commonly folded or rolled edges.

Dimensions: Complete vesicles: 108 specimens. Vesicle diameter 8-36 μm (av. 13.9 μm). Excysted hemispheres: 21 specimens. Hemisphere length 11-34 μm (av. 17.8 μm).

Occurrence in this study: Rogersville Shale: 76 Rg; Nolichucky Shale: 08BP-55, 08BP-19, 08BP-21, 08BP-24, 08BP-26, 08BP-33, 08BP-9.

Remarks: This species was emended by Jankauskas (1989) to accommodate originally spherical forms that are thin-walled and $<70\ \mu\text{m}$ in diameter. Butterfield & Chandler (1992) recorded this form in northwest Baffin Island where approximately 15 per cent of the population consistently exhibited medial split release structures, where the edges of hemispheres exhibited distinctive folds or rolls. Their size-frequency analysis produced a unimodal distribution (slightly skewed) suggesting the population was monospecific, and with a mean vesicle diameter of $10.6\ \mu\text{m}$ ($17.5\ \mu\text{m}$ for excysted hemispheres) placed them within the form taxon *Leiosphaeridia minutissima* Jankauskas (1989). A group of thin-walled sphaeromorphs recorded at Thorn Hill also correspond to the diagnosis of *L. minutissima* with some excysted, hemispherical specimens exhibiting apertural folds. Also the Thorn Hill specimens show a unimodal distribution (Fig. 4.1) which is moderately skewed to the right, similar to that of Butterfield & Chandler (1992). Furthermore, given that the average length of the dehisced segments is greater than the diameter of the original spherical form, the relative sizes of complete specimens (av. $13.9\ \mu\text{m}$) and excysted hemisphere (av. $17.8\ \mu\text{m}$), are such as to suggest that both are from the same population. The folded nature of the hemisphere edges was also recorded by Cotter (1999). Excysted forms of *L. minutissima* at Thorn Hill are morphologically similar to species belonging to the genus *Schizofusa* Yan Yuzhong, 1982, in particular *Schizofusa risoria* Grey 2005. Both have ellipsoidal shapes with enhanced apertural edges, but the Thorn Hill specimens are much smaller.

Previous records: This form has been reported globally from the Mesoproterozoic through to the Cambrian, e.g. Mesoproterozoic (~1250 Ma): Baffin Island, Canada, Agu Bay Formation (Butterfield & Chandler, 1992). Neoproterozoic (~800 Ma): Western Officer Basin, Australia, Steptoe, Kanpar, Browne & Hussar Formations, (Cotter et al., 1999); Western Officer Basin, Australia, Ediacaran, Pertatataka Formation, (Grey, 2005). Cambrian Series 1 and 2: Czech Republic (Steiner & Fatka, 1996).

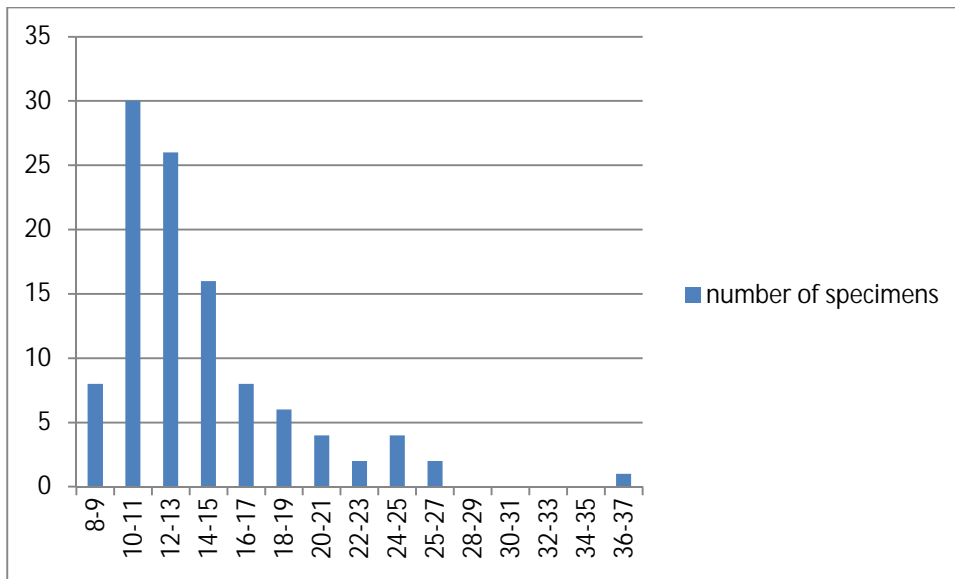


Figure 4.1 Size-frequency distribution of complete specimens of *L. minutissima* at Thorn Hill. Vertical axis: vesicle diameter (μm); Horizontal axis: number of specimens. Number of specimens 108.

Leiosphaeridia sp. 1

Plate 8, Figs 3, 4

Description: Small to medium sized, smoothly circular to sub-circular in outline, thick-walled, unornamented, folds mostly absent, when present are few and rounded; shagreenate to slightly granulate and dark brown; excystment by partial rupture or median split.

Dimensions: 73 specimens. vesicle diameter 20-82 μm (av. 39.3 μm).

Occurrence in this study: Nolichucky Shale: 08BP-52, 08BP-19, 08BP-22 08BP-24, 08BP-26½, 08BP-29, 08BP-31, 08BP-34, 08BP-39, 08BP-1, 08BP-7, 08BP-9.

Remarks: This form possesses a thick, robust vesicle wall that resists folding and splitting and maintains a smooth, approximately circular outline. Other than size there is little variation between specimens. Its size range (20-82 μm) straddles the 70 μm size boundary that separates the thick-walled specimens *Leiosphaeridia crassa* (Naumova, 1949) Jankauskas in Jankauskas et al. 1989 and *Leiosphaeridia jacutica*

(Timofeev, 1966) emend. Mikhailova & Jankauskas *in* Jankauskas et al. 1989. However, a unimodal size frequency distribution (Fig. 4.2) suggests the population is monospecific, despite a sample of only 73 measured specimens. *Leiosphaeridia* sp. 1 differs from generically from *Tasmanites* Newton 1985 in not possessing observable pores.

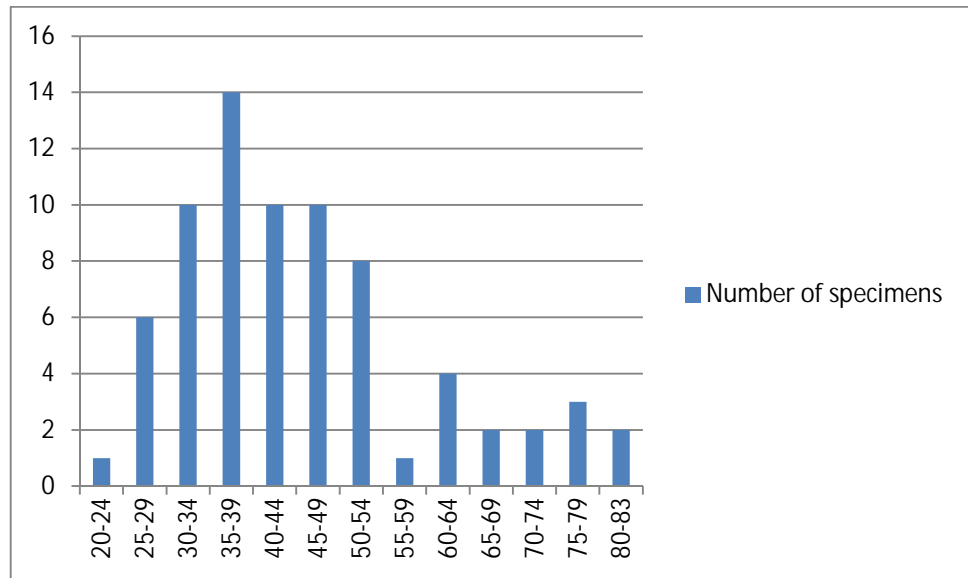


Figure 4.2 Size-frequency distribution of *Leiosphaeridia* sp. 1 at Thorn Hill. Vertical axis: vesicle diameter (μm); Horizontal axis: number of specimens. Number of specimens 108.

Leiosphaeridia sp. 2

Plate 8, Fig 5

Description: Small to large, circular to subcircular in outline, unornamented, moderately thick walled, folds are few to common, vesicle laevigate to shagreenate, pale brown to dark brown. Excystment by median split.

Dimensions: 504 specimens. Vesicle diameter 12-210 μm (av. 61.5 μm)

Occurrence in this study: Rogersville Shale: 08BP-76 Rg; Nolichucky Shale: 08BP-52, 08BP-10; Maynardville Limestone: 08BP-13, 08BP-14.

Remarks: The only discerning characteristic of *Leiosphaeridia* sp. 2 is a moderately thick wall. The lack of other clear and adequate criteria with which to subdivide this group further, were not forthcoming and consequently this group consists of specimens with a wide size range. The Jankauskas subdivisions (1989) based on wall thickness and vesicle size do not apply here, because many Thorn Hill *Leiosphaeridia* populations with similar wall thicknesses have size distributions which straddle the 70 μm size boundary (Fig. 4.3).

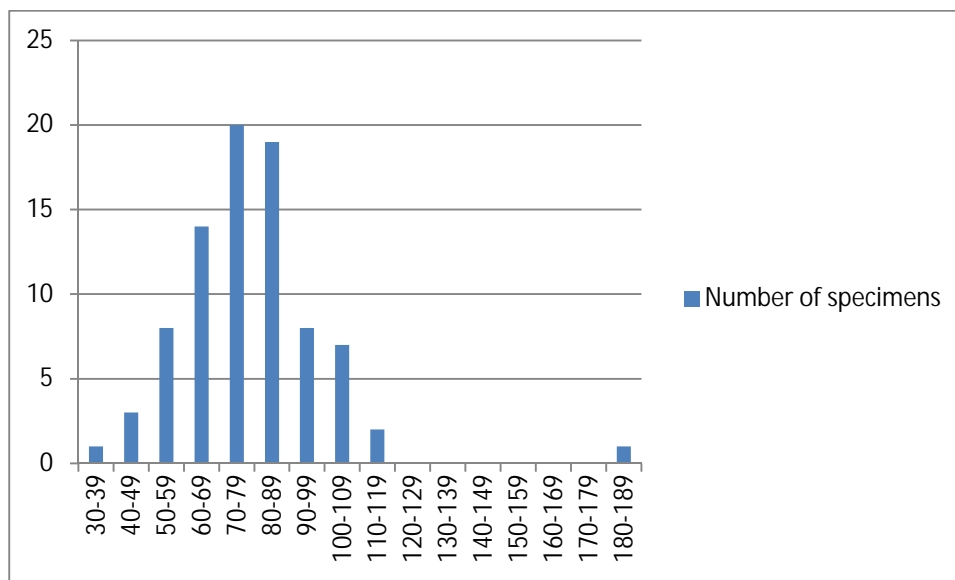


Figure 4.3 Size-frequency distribution of *Leiosphaeridia* sp. 2 from sample 08BP-1 at Thorn Hill. Vertical axis: vesicle diameter (μm); Horizontal axis: number of specimens. Number of specimens 83.

There are some samples where the Jankauskas subdivisions (1989) could be applied to *Leiosphaeridia* sp. 2, but because of the morphological similarity of specimens across all samples, further subdivision would be purely arbitrary. It might be that a more comprehensive study of moderately thick-walled sphaeromorphs at Thorn Hill could reveal certain patterns relating to their size and distribution. However, given

their low stratigraphic value and the inherent difficulties in subdividing such simple forms, this was not undertaken in this study.

Leiosphaeridia sp. 3

Plate 8, Fig 6

Description: Small to large, subcircular to irregularly ellipsoidal in outline, often appearing rolled or crumpled, thin-walled, unornamented, multiple folds and creases, laevigate to shagreenate and always transparent. Irregular ruptures recorded, otherwise no excystment structure observed.

Dimensions: 191 specimens. Maximum vesicle size 15-102 μm , (av. 40.3 μm).

Occurrence in this study: Rogersville Shale: 08BP-76 Rg; throughout the Nolichucky Shale and Maynardville Limestone.

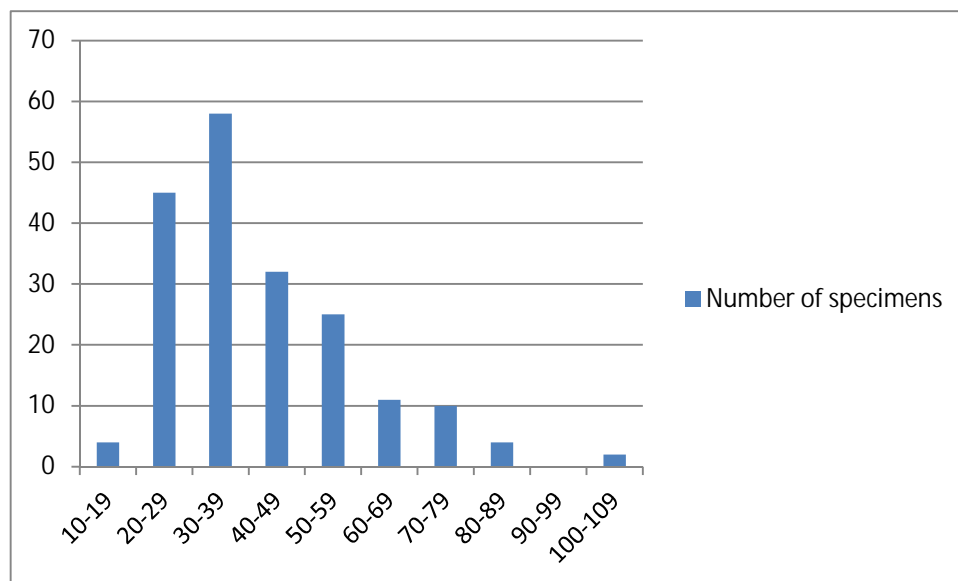


Figure 4.4 Size-frequency distribution of *Leiosphaeridia* sp. 3 throughout the Nolichucky Shale and the lower part of the Maynardville Limestone at Thorn Hill. Vertical axis: vesicle diameter (μm); Horizontal axis: number of specimens. Number of specimens 191.

Remarks: *Leiosphaeridia* sp. 3 occurs throughout the Nolichucky Shale and the lower part of the Maynardville Limestone in varying numbers. It differs from *L.*

minutissima by possessing a thinner wall and multiple folds and creases, though it is accepted here that some specimens might be specimens of *L. minutissima* altered by taphonomic agents.

However, this is a very distinctive form that appears consistently in all samples and shows a unimodal size-frequency distribution (Fig. 4.4) suggesting a monospecific group. The thinness of the vesicle wall is such as to allow easy mechanical disfigurement and numerous specimens are rolled or compressed to form elongate or ellipsoidal shapes with longitudinal structures reminiscent of *Eliasum* Fombella 1977. In such instances, however, seemingly apparent longitudinal ribs were actually longitudinal folds.

Genus *Liepaina* Jankauskas & Volkova, 1979

Type species: *Liepaina plana* Jankauskas & Volkova, 1979, in Volkova et al., p. 28-29, pls. 20: 1-6; 21: 1, 2.

Liepaina plana Jankauskas & Volkova, 1979

Plate 9, Figs 1, 2

- 1979 *Liepaina plana* Jankauskas et Volkova sp. nov., Volkova et al. p. 28-29, pls. 20: 1-6; 21: 1, 2.
- 1989 *Liepaina plana* Jankauskas & Volkova, 1979; Hagenfeldt, pp. 203, 204, pls. 2, 3.
- 1991 *Liepaina plana* Jankauskas & Volkova, 1979; Moczyłowska, p. 61, pl. 10 C-D.

Description: Vesicle laevigate and subpolygonal in outline with approximately twelve to fourteen processes extending outward. Processes are of variable length and width; they consist of a central column or spine supporting a transparent, laevigate membrane which interconnects between processes, either part way or rarely, almost entirely along the length of processes. No excystment structure observed.

Dimensions: 2 specimens. Maximum width of specimens 32-35 μm ; central vesicle diameter 15-18 μm ; process length 5-15 μm ; process basal width 2-4 μm .

Occurrence in this study: Nolichucky Shale: samples 08BP-56, 08BP-57.

Remarks: The two specimens recovered from the Nolichucky Shale are not well preserved and the membranes are poorly preserved distally. They are smaller in overall size than those originally described by Jankauskas & Volkova (*in* Volkova et al., 1979), however, the size of the central vesicle or body of one of the specimens sits within the size range stated in the original description. Equatorial margin difficult to discern. No excystment structure observed.

Previous records: Cambrian Series 1 and 2: East European Platform, Poland, Kaplonosy and Radzy Formations ((Moczyłowska, 1991). Norway, *Holmia* C zone (Moczyłowska & Vidal, 1986). Stansbury Basin, Australia, Lower Minlaton Formation (Zang et al., 2007). Cambrian Series 3: East European Platform, Latvia & Lithuania, middle Cambrian, Kibartai Formation (Volkova et al., 1979).

Genus *Lophosphaeridium* Timofeev, 1959, ex Downie, 1963,
emend. Lister, 1970

Type species: *Lophosphaeridium rarum* Timofeev ex Downie, 1963

Lophosphaeridium tentativum Volkova, 1968

Plate 9, Figs 3, 4

For synonymy see Moczyłowska (1991 p. 62).

Additional synonymy:

2005 *Lophosphaeridium tentativum* Volkova, 1968; Vanguetaine & Leonard, pl. 1 (10, 11).

2008 *Lophosphaeridium tentativum* Volkova, 1968; Vanguetaine & Brück, p. 81, pl. 4 (2, 3).

2009 *Lophosphaeridium tentativum* Volkova, 1968; yli ska & Szczepanik, pls. 6 (30), 7 (14, 15), 9 (20, 40), 10 (28).

Description: Vesicle circular to subcircular in outline, thin- to medium-walled with numerous solid granulae distributed randomly across the vesicle surface. Granulae density upon a specimen is normally relatively uniform but can vary across the vesicle surface, being barely visible in some areas; occasionally specimens have very densely arranged granulae such that the vesicle surface is completely obscured. Occasionally specimens occur in clusters. Excystment by partial rupture.

Dimensions: 140 specimens. Vesicle diameter: 20-49 μm ; width & height of granulae 0.2-0.9 μm .

Occurrence in this study: Occurs intermittently throughout the Nolichucky Shale, Maynardville Limestone and into the Copper Ridge Dolomite.

Remarks: This is a common species occurring throughout the Nolichucky Shale and the lowermost part of the overlying Maynardville Limestone. It has distinctive small granulae and is most similar to that recorded by Moczyłowska (1991).

Selected previous records: *L. tentativum* is widely reported in assemblages world wide ranging from early Cambrian to the Early Ordovician. Occurrence and stratigraphic range is detailed by Moczyłowska (1991, p. 62).

Additional selected previous record.

Cambrian Series 1 and 2: India, early-middle Cambrian, Marwar Supergroup (Prasad et al., 2010); Ireland, Bray Head Formation (Vanguetaine et al., 2002); East European Platform, Poland, Kaplonosy and Radzy Formations (Moczyłowska, 1991 and references therein). Cambrian Series 3: Amadeus Basin, Australia, Tempe Formation (Zang & Walter, 1992a).

Lophosphaeridium truncatum Volkova, 1969

Plate 9, Figs 5, 6

Synonymy: For synonymy see Moczyłowska (1991, p. 62).

Additional synonymy:

2005 *Lophosphaeridium truncatum* Volkova, 1969; yli ska & Szczepanik, pls. 6 (21), 7 (12, 13), 10 (26, 27).

Description: Vesicle circular to rounded rectangular in outline, surface granulate to tuberculate. The larger ornament often clavate and varies in number among specimens from few to numerous. Occasionally they occur in clusters. No excystment structure observed.

Dimensions: 22 specimens. Maximum vesicle diameter 17-48 μm (av. 29 μm); height of sculptural elements <1-3 μm .

Occurrence in this study: Nolichucky Shale: samples 08BP-53, 08BP-55, 08BP-56, 08BP-58.

Remarks: This species is not common at Thorn Hill and only occurs in the lowermost part of the Nolichucky Shale.

Previous records: See Occurrence and stratigraphic range, Moczyłowska (1991).

Selected additional previous records.

Cambrian Series 1 and 2: Holy Cross Mountains, Poland (Szczepanik, 2001).

Cambrian Series 3: India (Prasad et al. 2010); China (Yang & Yin, 2001).

Furongian: India (Prasad et al., 2010).

Lophosphaeridium variabile Volkova, 1974

Plate 10, Figs 1, 2

1974 *Lophosphaeridium variabile* Volkova, 1974, p. 196-197, pl. 28 (4-5)

1979 *Lophosphaeridium variabile* Volkova, 1974, Volkova et al., p. 23, pl. 16 (9-12)

1989 *Lophosphaeridium variabile* Volkova, 1974, Hagenfeldt, p. 207, pl. 2 (8)

Description: Vesicle sub-circular to rounded rectangular in outline, thick-walled and covered in large grana. Occasionally they occur in clusters. Excystment by approximately circular aperture which is not always apparent.

Dimensions: 15 specimens. Maximum vesicle diameter 23-54 μm (av. 41.1 μm); height of sculptural elements <1-3 μm .

Occurrence in this study: Nolichucky Shale: samples 08BP-52, 08BP-56.

Remarks: This species is not common at Thorn Hill and only occurs in the lowermost part of the Nolichucky Shale. It differs from *Lophosphaeridium truncatum* Volkova 1968 in having smaller ornament and possessing a circular excystment structure.

Previous records: Cambrian Series 3: Latvia (Volkova, 1974); Sweden (Hagenfeldt, 1989b); Ireland (Brück & Vanguetaine, 2004); East European Platform, Russia (Raevskaya, 2005).

Lophosphaeridium sp. 1

Plate 10, Figs 3, 4

Description: Vesicle small, circular to subcircular in outline, frequently folded to form a rounded diamond-shaped outline. Vesicle surface covered with granulae. No excystment structure observed.

Dimensions: 34 specimens. Maximum vesicle diameter 5-21 μm (av. 13 μm).

Occurrence in this study: Rogersville Shale: sample 08BP-76; Nolichucky Shale: samples 08BP-54, 08BP-60, 08BP-19, 08BP-28½, 08BP-30, 08BP-39.

Remarks: This differs from other species of *Lophosphaeridium* Timofeev, 1959, ex Downie, 1963, emend. Lister, 1970 in having a small vesicle size. Specimens are frequently folded in such a way as to form a diamond-shaped outline, and appears to be characteristic of this form-species.

Lophosphaeridium sp. 2

Plate 10, Figs 5, 6

Description: Vesicle small, circular to subcircular in outline and moderately thick-walled. The surface is covered in grana which can be quite pronounced and occasionally extend into a short, fine, hair-like process. No excystment structure observed.

Dimensions: Vesicle diameter 10-21 μ m, (av. 18 μ m). Grana height <0.5-1 μ m.

Occurrence in this study: Nolichucky Shale: samples 08BP-52, 08BP-54, 08BP-56, 08BP-19, 08BP-1.

Remarks: This form differs from *Lophosphaeridium* sp. 1 in having more pronounced grana which occasionally possess short, hair-like extensions.

Genus *Micrhystridium* Deflandre 1937, emend. Staplin 1961,
emend Lister, 1970

Type species: *Micrhystridium inconspicuum* Deflandre 1937, by original designation

Micrhystridium spp.

Occurrence in present study: Nolichucky Shale: samples 08BP-58, 08BP-59, 08BP-21, 08BP-24, 08BP-26, 08BP-28½, 08BP-33, 08BP-35, 08BP-36, 08BP-3, 08BP-7, 08BP-9.

Remarks: A number of small (<20 µm) acanthomorphic forms were recorded from the Nolichucky Shale but their small size (many are <10 µm) and poor preservation prevented confident taxonomic assignment. They are necessarily left in open nomenclature.

Genus *Navifusa* Combaz et al. 1967 ex. Eisenack 1976

Type species: *Navifusa navis* (Eisenack 1938) Eisenack, 1976

Navifusa actinomorpha (Maithy) Hofmann & Jackson, 1994

Plate 26, Fig 1

1975 *Leiofusa actinomorpha* sp. nov. Maithy, pl. 5 (43).

1994 *Navifusa actinomorpha* emend. n. comb., Hofmann & Jackson, fig. 15 (5-8).

Description: Vesicle elongate, laevigate, gently tapering to slightly ovate. No excystment structure observed.

Dimensions: 10 complete specimens. Vesicle length 110-265 µm (av. 169 µm); minimum vesicle width 15-43 µm (av. 29µm); maximum vesicle width 22-50 µm (av. 38 µm);

Occurrence in present study: Nolichucky Shale: samples 08BP-22, 08BP-25, 08BP-26, 08BP-29, 08BP-32.

Remarks: Hoffman & Jackson (1994) transferred *Leiofusa actinomorpha* (Maithy, 1975) to *Navifusa* and increased its size range to 57-72 µm wide and 125-207 long.

The key diagnostic feature of *N. actinomorpha* is the tapering nature of the vesicle along its length; the holotype (Maithy, 1975) decreases in width from 38 μm to 25 μm , a difference of 13 μm . The Thorn Hill specimens decrease in widths by 5-12 μm (av. 9 μm); some specimens occur with very slight width variations (1-2 μm) which are interpreted as natural variation occurring within parallel-sided forms, and are not included here.

Previous records: Mesoproterozoic: Zaire (Maithy, 1975); India (Prasad & Asher, 2001; Prasad et al., 2005). Neoproterozoic: Baffin Island, Canada, (Hofmann & Jackson, 1996).

Navifusa sp. 1

Plate 26, Fig 2

Description: Vesicle moderately to thick-walled, elongate, rod-shaped, parallel sided to slightly ellipsoidal with rounded ends; laevigate. Specimens are frequently broken. No excystment structure observed.

Dimensions: 16 complete specimens. Vesicle length 107-361 μm (av. 178 μm); vesicle width 15-40 μm (av. 30 μm).

Occurrence in present study: Nolichucky Shale: samples 08BP-22, 08BP-24, 08BP-30, 08BP-32, 08BP-33, 08BP-35, 08BP-37, 08BP-39.

Remarks: This is a long, narrow form with a vesicle width 9-33% (av. 19%) of the length. It differs from *Navifusa ancepsipuncta* Loeblich 1970 in being thicker-walled and not having punctate ornament. The Ordovician species *Navifusa similis* (Eisenack) Turner, 1984 and the Proterozoic species *Navifusa majensis* Pyatiletov, 1980, tend to have relatively wider vesicles (see remarks at *Navifusa* sp. 2).

Navifusa sp. 2

Plate 26, Figs 3, 4

Description: Vesicle thin to moderately thick-walled, elongate, ends rounded, edges parallel-sided to rounded, laevigate to shagreenate and often slightly thickened at the ends. Specimens frequently broken. No excystment structure observed.

Dimensions: 20 specimens. Vesicle length 54-97 μm (av. 70 μm); vesicle width 16-37 μm (av. 25 μm).

Occurrence in present study: Nolichucky Shale: samples 08BP-60, 08BP-25, 08BP-29, 08BP-32.

Remarks: *Navifusa majensis* Pyatiletov, 1980 is a smooth, elongate Proterozoic form with rounded ends (Hofmann & Jackson, 1994). Jankauskas et al. (1989) stated that *N. majensis* should have a size range of 50-270 μm long and 16-65 μm wide which permits a large variety of forms. At Thorn Hill two clear groups can be discerned based upon occurrence, size and width/length (w/l) ratios. These are *Navifusa* sp. 1, which is large with a relatively small w/l ratio, and *Navifusa* sp. 2 which is smaller and relatively wider. Furthermore, although their occurrences are not strictly mutually exclusive, there is a clear division. *Navifusa* sp. 1 occurs in twelve samples where *Navifusa* sp. 2 is absent; *Navifusa* sp. 2 occurs in one sample where *Navifusa* sp. 1 is absent; samples in which both forms occur tend to be significantly dominated by *Navifusa* sp. 1, e.g. samples 08BP-29 and 08BP-32. Both forms could be included in the taxon *N. majensis* as they both fall within the size range stipulated by Jankauskas et al. (1989). However this would be to deny a clear division within these forms at Thorn Hill and are consequently left in open nomenclature.

Genus *Peteinosphaeridium* Staplin, Jansonius & Pocock 1965
emend. Playford *in* Playford et al., 1995

Type species: *Peteinosphaeridium bergstroemii* Staplin, Jansonius & Pocock 1965
emend. Playford *in* Playford et al., 1995

Peteinosphaeridium? sp. 1

Plate 19, Figs 1-6

Description: Vesicle circular to subcircular in outline, originally spherical to subspherical, single-walled, surface shagreenate to irregularly rugulate and granulate bearing numerous, closely arranged, solid processes. Processes more or less homomorphic, laevigate to shagreenate, generally flat and column-like in outline, parallel sided or slightly tapering before briefly expanding distally into foliate to digitate terminations. Frequently fibrils are located on processes parallel to the process long axis which briefly extend onto the vesicle surface, but attenuate distally along the length of the process. In some instances the fibrils are more developed and form distinct laminae giving the process a trilaminate base. Process length 8-10% of vesicle diameter. The process-vesicle contact is sharply angular. No excystment structure observed.

Dimensions: 15 specimens. Nolichucky Shale: 1 specimen. Vesicle diameter 83 μm ; process length 4-9 μm ; process width $\sim 2 \mu\text{m}$. Gros Ventre Formation: 14 specimens. Vesicle diameter 83-122 μm (av: 101 μm); process length 5-10 μm ; process width $\sim 2 \mu\text{m}$.

Occurrence in this study: Nolichucky Shale: sample 08BP-52; Gros Ventre Formation: samples 09BP-44, 09BP-49.

Remarks: See remarks below for *Peteinosphaeridium?* sp. 1

Peteinosphaeridium? sp. 2

Plate 20, Figs 1-6

Description: Vesicle circular to subcircular in outline, originally spherical to subspherical, single-walled, surface shagreenate to irregularly rugulate and granulate bearing numerous, closely arranged, solid processes. Processes more or less homomorphic, laevigate to shagreenate, generally flat and arch-shaped in outline. Frequently, variably developed fibrils are located on processes parallel to the process

long axis, and can extend along the entire length of the process whilst others often attenuate distally. Process length 5-7% of vesicle diameter. The process-vesicle contact is sharply angular. No excystment structure observed.

Dimensions: Gros Ventre Formation: 12 specimens. Vesicle diameter 104-115 μm ; process length 5-9 μm ; process width \sim 2-3 μm .

Occurrence in this study: Gros Ventre Formation: samples 09BP-44, 09BP-49.

Remarks: *Peteinosphaeridium?* spp. 1 and 2 exhibit the same vesicle size range, vesicle surface and process ornament (including fibrils and laminae) and the number, distribution and relative length of processes. Also, both species are without pylomes. As such they are interpreted as cogenetic species differentiated by the nature of their processes: *Peteinosphaeridium?* sp. 1 having column-like processes with foliate to digitate terminations and *Peteinosphaeridium?* sp. 2 with arch-shaped processes. In SEM the particular nature of the vesicle surface ornament and the process fibrils and laminae becomes apparent and is clearly the same for both species.

In some respects *Peteinosphaeridium?* spp. 1 and 2 generically resemble *Peteinosphaeridium* Staplin, Jansonius & Pocock 1965 emend. Playford *in* Playford et al. 1995 but differ crucially in not possessing a pylome and having less developed laminae. Species of *Peteinosphaeridium* have distinctive laminae which impart a trilaminate and/or a quadrilaminate structure to the process stem and although this is observed in the Chief Joseph Highway specimens, it is much less common, and laminae are relatively underdeveloped in most cases resulting in relatively flat processes. The emended generic diagnosis of *Peteinosphaeridium* by Playford (*in* Playford et al., 1995) states that “distal process termini either (a) attenuate and unbranched, with laminae tapering to a common, evexate or acuminate point, sometimes extending as a spina; or (b) more or less truncate with 3 or 4 ramifications (branches) emanating distally from the process trunk”. *Peteinosphaeridium?* sp. 1 and 2 fall into the first category but do not correspond to any described species.

Peteinosphaeridium? spp. 1 and 2 represent a unique morphological group possibly related to *Peteinosphaeridium*. Given that *Peteinosphaeridium?* spp. 1 and 2 are Cambrian Series 3 in age and *Peteinosphaeridium* is Ordovician, they might be

interpreted as an early form of that taxon. However, because *Peteinosphaeridium?* spp. 1 and 2 are without pylomes and possess underdeveloped laminae they are left in open nomenclature.

Genus *Rhopaliophora* Tappan & Loeblich, 1971 emend.
Playford & Martin, 1984

Type species: *Rhopaliophora foliatis* Tappan & Loeblich, 1971 by original designation

Rhopaliophora? sp. 1

Plate 11, Figs 1, 2

1992 *Rhopaliophora pilata* (Combaz & Peniguel, 1972) emend. Playford & Martin, Martin, 1992.

1984, Martin, p. 28; pl. 8 (1-3).

Description: Vesicle circular to subcircular in outline, psilate and bearing numerous, short, solid, closely arranged processes. Processes are psilate, petaloid and flat or curved and generally arch-shaped, although many processes have an irregular outline. In SEM there appears to be no difference in surface texture between the vesicle and processes which has the effect of masking the vesicle-process contact.

Dimensions: 16 specimens. Vesicle diameter 19-34 μm (av. 25 μm); process length 1-4 μm (av. 2 μm); basal process width 1-3 μm .

Occurrence in present study: Nolichucky Shale: samples 08BP-30 - 08BP-33.

Remarks: This form closely resembles Ordovician specimens of *Rhopaliophora pilata* (Combaz & Peniguel) emend. Playford & Martin 1984 as illustrated by Martin (1992 pl. 8 (1-3)). However, it differs generically from *Rhopaliophora* Tappan & Loeblich, 1971 emend. Playford & Martin, 1984 in having what appear to be solid

processes and also being devoid of a pylome. Consequently the form is left in open nomenclature.

It differs from *Peteinosphaeridium?* sp. 2 in having a much smaller vesicle and lacking fibrils on the processes. Furthermore, there is a clear difference in surface texture/ornament between the vesicle and processes on *Peteinosphaeridium?* sp. 2 which is not apparent on *Rhopaliophora ?* sp.1.

Genus *Symplassosphaeridium* Timofeev, 1959 ex.
Timofeev, 1969 emend.

Type species: *Symplassosphaeridium tumidulum* Timofeev, 1959, p. 27, pl. 1 (11).

Original diagnosis: “Spherical clusters of small, smooth spherical vesicles from 10-60 μm in diameter. The outline of the vesicles is wavy” (trans. Lees, *In*: Potter, 1974); “species differentiated by thickness and dimensions” (trans. Potter, 1974).

Emended diagnosis: Clusters of conjoined, small, smooth to granulate, cells. Clusters circular to subcircular in outline. Cells circular to subcircular in outline, or distorted in shape due to compaction. Clusters have undulating or wavy outlines.

Remarks: At Thorn Hill many specimens have been recorded which clearly conform to the diagnosis of *Symplassosphaeridium* Timofeev, 1969 in all but size and possession of ornament. The emendation removes the arbitrary size limit for clusters and allows for the inclusion of granulate forms. It also removes the stipulations referring to the differentiation of species, as this should be a decision based upon morphological characteristics exhibited by any potentially new species at the time. The stipulation that cells should be conjoined is to permit differentiation from spherical aggregates of cells which would be more appropriately assigned to *Synsphaeridium* Timofeev 1966.

Timofeev (1959) neglected to designate a type species for the generic name *Symplassosphaeridium* thus rendering it invalid. This was rectified when Timofeev (1959) designated *Symplassosphaeridium tumidulum* Timofeev, 1959 as the type species.

Symplassosphaeridium cf. *cambriense* Slavíková, 1968

Plate 17, Figs 1, 2

- 1968 *Symplassosphaeridium cambriense* nov. sp. Slavíková, p. 202, pl. 2 (4, 6)
1991 Coenobial acritarchs, Di Milia, pl. 1 (1-3),
1991 Coenobial acritarchs *sensu* Di Milia 1991, Dean et al., fig. 8 (v)
2009 *Symplassosphaeridium cambriense* Slavíková, 1968, Palacios et al., fig. 5 (A)
2012 *Symplassosphaeridium cambriense* Slavíková, 1968, Palacios et al., fig. 10
(A, B)

Description: Circular to subcircular cluster of approximately 20-50, conjoined cells broadly positioned in one plane. Cells frequently exhibit a spiral arrangement, but not always. Cells circular to subcircular in outline and often distorted due to compaction. Thickening occurs at intercell contacts. The collective form is broadly circular to subcircular in outline with an undulating edge imparted by cells on the periphery. Cells are shagreenate, occasionally granulate. Fragmentary, two dimensional, honeycombed forms sometimes occur and represent broken upper or lower parts of a cluster. These exhibit an hexagonal cell arrangement.

Dimensions: 50 specimens. Cluster diameter 25-135 μm (av. 71 μm); diameter of cells 8-30 μm (av. 20 μm).

Occurrence in present study: Nolichucky Shale: samples 08BP-52, 08BP-56, 08BP-58, 08BP-59, 08BP-25, 08BP-28½, 08BP-34, 08BP-39, 08BP-4, 08BP-11.

Remarks: Slavíková (1968) erected the species *Symplassosphaeridium cambriense* the year before the generic name was validated and was therefore itself invalid. However, the species was finally validated by Fensome et al. (1990).

Taxonomic assignment of *Symplassosphaeridium cambriense* and morphologically related forms is confusing, with very similar forms being either assigned to *S. cambriense* or left in open nomenclature; the divisions being based upon size and the presence of granulate ornament. The original forms described from the middle

Cambrian Jince Formation in the Czech Republic by Slavíková (1968) are small (cluster diameter 30-45 μm ; cell diameter 4-9) with smooth cell walls. Furongian forms from Sardinia, Italy discussed and illustrated by Di Milia (1991, p. 149, pl. 1 (1-3)), were described as being larger (30-50 μm) with reticulate ornament and as such were assigned not to *S. cambriense* but to “Coenobial acritarchs”. This appears to be an overly pedantic approach given that the sizes of clusters are not too dissimilar. The same occurs in Dean et al., (1997, fig. 8, (V, W)) where specimens from the Sosink Formation in Turkey were described as Coenobial acritarchs *sensu* Di Milia, 1991, (size of cluster in fig. 8 (V) is 45 μm) and Erkmen & Bozdogan (1981, p. 56, pl. 2 (6, 7)) assigned similar forms from the same Sosink Formation to *Symplassosphaeridium cf. cambriense*; this was due to the Turkish specimens being larger (40-60 μm) than those described by Slavíková, 1968. However, specimens from Nova Scotia, Canada, illustrated by Palacios et al. (2009a, fig. 5 (A); 2012, fig. 10 (A, B)) have vesicle diameters of ~40-50 μm and were assigned to *S. cambriense*. All specimens illustrated in the above references are clearly very similar, if not exactly the same, and with similar cluster sizes.

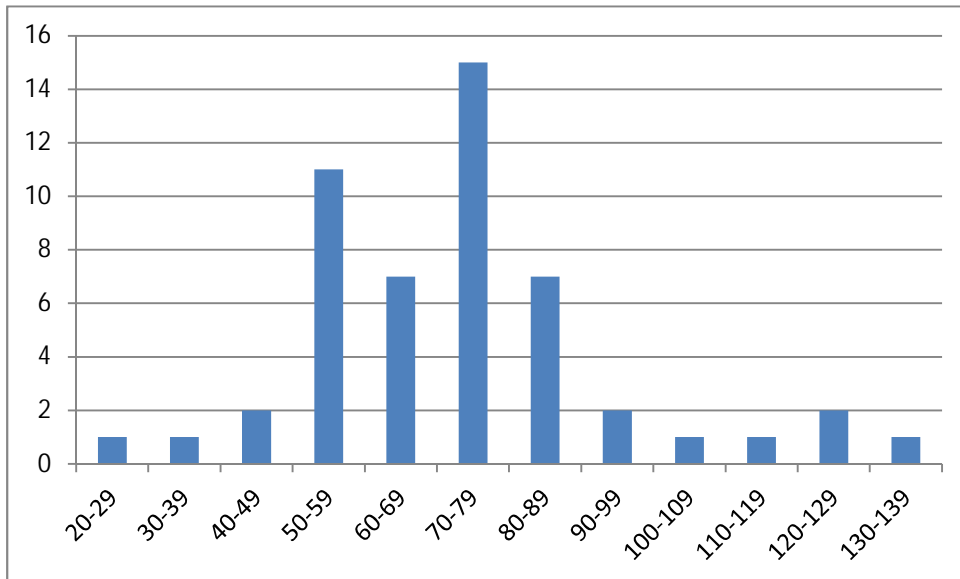


Figure 4.5 Size frequency diagram for *Symplassosphaeridium cf. cambriense* at Thorn Hill. Vertical axis: number of specimens. Horizontal axis: vesicle diameter (μm).

At Thorn Hill the *Symplassosphaeridium* population consists of equivalent forms with a wide spectrum of cluster sizes (25-135 μm), and a broadly unimodal size-frequency distribution (fig. 4.5; N = 50) which straddles the upper cluster size limit (45 μm) set by Slavíková (1968). Also, both smaller and larger specimens occur either with or without granulate ornament. Therefore, given that there are no practicable means of specific division of the Thorn Hill specimens, and that many do not conform to the specific diagnosis of *S. cambriense*, either due to their size or ornament, forms of *Symplassosphaeridium* at Thorn Hill are assigned to *S. cf. cambriense*.

Previous records: Czechoslovakia, middle Cambrian (Slavíková, 1968). Nova Scotia, Canada, Guzhangian Stage, Cambrian (Palacios et al., 2012); Furongian Series, Cambrian (Palacios et al., 2009a).

Genus *Thymadora* Clendening & Wood, 1981

Type species: *Thymadora kerke* Clendening & Wood, 1981

Thymadora kerke Clendening & Wood, 1981

Plate 17, Figs 3, 4

1981 *Thymadora kerke* n. sp. Clendening & Wood 1981, p. 151-156, pl. 1.

Description: Vesicle subcircular to ellipsoidal in outline, single-walled, bearing two to three processes extending from a slight bulge situated at one pole. Processes variable, irregularly furcate and terminate with irregularly rounded tips. Granulae situated on vesicle and processes. Presumed excystment structure (pylome) situated at opposite pole to processes and indicated by a small concave indentation with a slightly thickened rim. No operculum observed.

Dimensions: 12 specimens. Vesicle length 9-17 μm (av. 13.5 μm); vesicle width 7-15 μm (av. 10.9 μm); process length 1.5-8 μm (av. 4 μm); width of excystment structure 1-1.5 μm .

Occurrence in this study: Rogersville Shale: sample 08BP-76.

Remarks: This species was found in a sample collected in the same locality as those by Clendening & Wood (1981) and is the only recorded species of the genus *Thymadora* Clendening & Wood 1981. It is notable for its polarised vesicle, variably formed processes and polar excystment structure. This latter feature was observed on one specimen in SEM and consisted of a simple, approximately circular aperture with a slightly jagged edge. The small concave indentation, as seen in light microscope, is probably the result of the structure being pulled slightly inward toward the vesicle interior; this would also explain the slight thickening observed around the structure, as four folded layers of vesicle wall, rather than two, would be positioned on top of each other.

Also occurring in sample 08BP-76 are *Lophosphaeridium* sp. 1, *Leiosphaeridia minutissima* and *Leiosphaeridia* sp. 2, all in very low abundance.

Previous record: Tennessee, USA, Rogersville Shale, Cambrian Series 3 (Clendening & Wood 1981).

Genus *Timofeevia* Vanguetaine, 1978

Type species: *Timofeevia lancarae* (Cramer & Diez de Cramer, 1972) Vanguetaine, 1978

Timofeevia cf. *pentagonalis* (Vanguetaine, 1974) Vanguetaine, 1978

Plate 11, Fig 6; Plate 12, Fig. 1

Description: Vesicle circular, subcircular to slightly polygonal in outline, laevigate, and divided into polygonal fields delineated by low ridges at the field boundaries. In some instances field boundaries are not apparent, although processes appear to be arranged such as to delineate field areas. Processes are palmate, occasionally bifurcate to the second order and/or digitate, rarely simple and frequently curl back towards the vesicle surface. They occur at the angles and along the edges of the polygonal fields; normally one process is situated between field angles, although occasionally processes were absent from field edges. Processes are of approximately equal length, and appear solid or partially hollow. The number of fields and processes varies between specimens, from 10 to 14 fields and approximately 30-70 processes. No excystment structure observed.

Dimensions: 12 specimens. Vesicle diameter 23-35 μm (av. 29 μm); process length 3-6 μm (av. 4 μm);

Occurrence in present study: Nolichucky Shale: sample 08BP-34.

Remarks: Twelve specimens were observed without pylomes or opercula but with polygonal fields, either delineated by low ridges or rows of processes. Many appear to have processes situated at both the field angles and along the field edges, although in some instances the distribution of processes was difficult to discern and some field edges appeared to be devoid of processes. Also the numbers of fields and processes varied quite significantly between specimens. This morphological variation exhibited within this small sample group precludes confident assignment to *Timofeevia pentagonalis* (Vanguetaine, 1974) Vanguetaine, 1978 and the forms are left in open nomenclature. However, the presence of ramified processes situated at both the angles and in some cases, the edges of fields, supports comparison to it.

This form co-occurs with *Cymatiogalea* cf. *virgulta* and the two forms are very similar. However, *T.* cf. *pentagonalis* differs from *C.* cf. *virgulta* in having larger, more complex processes and being devoid of a pylome/operculum. Their co-occurrence and similarities, and the variation inherent within the *T.* cf. *pentagonalis* group, might suggest they represent transitional forms, perhaps part of a galeate-*Timofeevia* plexus. However, only a few specimens were encountered in this study,

and further analysis of other specimens from the same horizon is necessary to clarify their taxonomic relationships

Genus *Virgatasporites* Combaz, 1967

Type species: *Virgatasporites rudii* Combaz, 1967

Virgatasporites rudii Combaz, 1967

Plate 11, Fig 3

- 1967 *Virgatasporites rudi* Combaz, p.12, pl. 1 (27, 28).
1999 *Virgatasporites rudi* Vecoli, p. 62, pl. 15 (8).
2004 *Virgatasporites rudii* Breuer & Vanguetaine, pl. 3 (14).
2006 *Virgatasporites rudii* Albani et al., pl. 2 (8).

Description: Subcircular in outline, lacking processes, with broad radially arranged grooves or striae. The specimen appears to exhibit two connected valves, one lying flat on top of the other, with the upper valve broken thus revealing the lower. No excystment structure observed.

Dimensions: 1 specimen. Vesicle diameter 33 µm.

Occurrence in present study: Nolichucky Shale: sample 08BP-9.

Remarks: *V. rudii* has only been recorded once in the Cambrian (Furongian), in Spain (Albani et al., 2006).

Selected previous records: Furongian: Spain (Albani et al. 2006). Tremadoc: Algerian Sahara (Combaz, 1967); England (Rasul & Downie, 1974); Saudi Arabia (Jachowicz, 1995); Belgium (Breuer & Vanguetaine, 2004).

Virgatasporites sp. 1

Plate 11, Figs 4, 5

Description: Subcircular in outline, solid and lacking processes with numerous, narrow, sinuous, radially arranged ridges and grooves. Approximately concentrically arranged, discontinuous, step-like ridges underlie the smaller radial grooves. One ridge is particularly noticeable towards the edges of specimens imparting a fringe-like periphery, where radial ridges may extend slightly over the edge. Radial ridges become more irregular and discontinuous towards the centre. One specimen possesses radial ridges which converge on a point close to the edge.

Dimensions: 7 specimens. Vesicle diameter 23-31 μm (av. 26 μm).

Present occurrence: Nolichucky Shale: samples 08BP-28½, 08BP-33 .

Remarks: This form differs from *V. rudii* in having concentrically arranged ridges and narrower, more numerous radial ridges. It bears some resemblance to *Virgatasporites* sp. illustrated by Le Herisse et al. (2007; pl. 2 (6)) which has narrow radial ridges, but concentric ridges appear to be absent.

Unassigned acritarchs

Eleven acritarchs were recovered from Thorn Hill which could not be assigned to known acritarch genera and are considered new forms.

Acritarch sp. 1

Plate 21, Figs 1-6

Description: Vesicle circular to subcircular in outline, originally spherical to subspherical, single-walled, surface psilate to shagreenate and bearing numerous, small, stiff, solid, processes which flare distally. The process-vesicle contact is sharply angular. Transparent membranes run between processes and form a dense, polygonal network perpendicular to the vesicle surface to which they are attached. Membranes are attached along the entire length of each process. Detached

membranes leave a polygonal network of scars upon the vesicle surface. Process length 6-17 % of vesicle diameter. Excystment by median split.

Dimensions: 25 specimens. Vesicle diameter 60-155 μm (av. 95 μm); process length 5-12 μm (av. 6 μm); width of membranes 2-3 μm ; width of polygonal fields 3-5 μm .

Occurrence in this study: Samples 08BP-22, 08BP-23, 08BP-29, 08BP-30, 08BP-32, 08BP-33.

Remarks: This is an anomalously large, Phanerozoic, non-sphaeromorphic form. Large ornamented acritarchs ($>100 \mu\text{m}$) are rare in the Phanerozoic (Vidal & Peel, 1993) and tend to be related morphologically to the genus *Comasphaeridium* (e.g. *Comasphaeridium longispinosum* Vidal n. sp., p. 19-21, fig. 6a, in Vidal & Peel, 1993). In the Proterozoic large forms are the norm but occur without processes interconnected by membranes perpendicular to the vesicle surface; *Trachyhystricosphaera aimika* Hermann 1976 (In: Timofeev et al., 1976) as illustrated in Butterfield et al. (1994) Fig. 18, D, appears to have membranes connected to the processes, but are interpreted as a single, collapsed, outer membrane. Despite the similarities with the genus *Cymatiosphaera* O. Wetzel ex Deflandre, 1954, its sheer size and unique, dense arrangement of relatively small membrane-supporting processes sufficiently distinguish it from that genus.

Acritarch sp. 2

Plate 22, Figs 1-6

Description: Vesicle large, circular to subcircular in outline, originally spherical to subspherical, single-walled, surface laevigate to shagreenate and bearing numerous, closely arranged, simple, small, psilate, stiff, solid, tapering or cylindrical processes. Process termination can be acuminate, evexate and occasionally bulbous. The process-vesicle contact is sharply angular, occasionally process bases expand slightly but remain separate. Process length 2-7 % of vesicle diameter. Excystment by median split or partial rupture.

Dimensions: 30 specimens. Vesicle diameter 82-166 μm (av. 120 μm); process length 2-7 μm ; basal process width <1 μm .

Occurrence in this study: Nolichucky Shale: samples 08BP-53, 08BP-55, 08BP-61, 08BP-22, 08BP-30, 08BP-33.

Remarks: This is a very distinctive and anonymously large Phanerozoic, acanthomorphic acritarch occurring throughout most of the Nolichucky Shale in low numbers. Fragments commonly occur and many complete specimens possess major folds, but otherwise the preservation is excellent. The combination of large vesicle size and numerous, short, solid processes distinguishes this form from any other recorded acritarch taxa. It differs generically from *Appendisphaera* Moczyłowska, Vidal & Rudavskaya, 1993 emend. Moczyłowska, 2005 in possessing consistently solid, relatively short processes. In SEM the underside of the vesicle wall was observed on one well preserved specimen, showing a smooth surface with no communication whatsoever with the process bases. SEM also revealed a submicron, punctate sculpture upon the upper vesicle surface, but absent from the processes. However, whether this is a primary feature is unclear.

Acritarch sp.3

Plate 12, Figs 2-6

1989 Acanthomorph sp. C, Wood & Stephenson, pl. 1, fig. 32.

Description: Vesicle circular to subcircular in outline, originally spherical to subspherical, single-walled, bearing processes of variable length, and a polar excystment structure. Vesicle surface has irregularly distributed granulae which vary in number between specimens. Processes thin, sinuous, occasionally bifurcate, with slightly conical bases and tapering to acuminate or slightly rounded tips. Process-vesicle contact sharply angular. Process length 7-45% of vesicle diameter with longer processes concentrated on one pole where they randomly surround the excystment structure: processes mostly absent from opposite pole and equatorial region, but occasionally a few processes of variable lengths may be present. Excystment

structure consists of an approximately circular opening approximately 30-35 % of the diameter of the vesicle, with processes situated around and on the lip. In SEM an unopened excystment structure was observed consisting of tightly and radially arranged processes, their ends converging towards the centre and forming a plug. During excystment these processes are forced outward.

Dimensions: 30 specimens. Vesicle diameter 14-25 μm (av. 19 μm); process length 1-8 μm ; width of pylome 4-7 μm .

Occurrence in this study: Nolichucky Shale: samples 08BP-54, 08BP-55, 08BP-56.

Remarks: This form possesses a unique excystment structure consisting of a plug formed from radially arranged processes, rather than an operculum. Interestingly, unlike the galeate group of acritarchs which can show a decrease in process size and number towards the excystment structure, *Acritarch* sp. 3 shows the contrary with a decrease in process size and number away from the excystment structure. A specimen recorded as *Acanthomorph* sp. C by Wood & Stephenson (1989; pl.1, fig. 32) from the upper Cambrian Bonnetterre and Davis Formations in Missouri, USA, appears similar to *Acritarch* sp. 3 in being polarised and having a similar distribution of processes. However, the presence of an excystment structure is unclear.

Acritarch sp. 4

Plate 13, Figs 2-4

Description: In lateral view the vesicle outline is elliptical to semi-circular with a broad, unornamented edge on one side (apical pole), either convexly curved, straight or undulating, and twelve to fourteen conical, broad-based, hollow processes located on the antapical pole. The hollow vesicle is broadest at the apical pole and originally would have been dome-shaped; the apical is open to the surrounding environment, The apical edge is either smooth or slightly jagged and regular in overall appearance. The processes are orientated either parallel to or away from the apical pole, and in some cases normal to it. 6-9 large processes, of varied lengths, are quasi-regularly arranged around the vesicle surface and in some cases a larger central process

(antapical process) is apparent; 4-6 smaller processes are irregularly located close to or at the apical edge; many processes have very small thorn-like subsidiary processes located upon their lower regions and around their bases; the processes connect freely with the vesicle interior. In most cases the distal ends of processes have a discreet, fragile terminal element, which represents approximately the last 10% of the process length; otherwise the processes have an acuminate or rounded termination. The terminal element may have the same width as the process or expand slightly before terminating with a rounded or slightly angular tip. The connect between the processes and the terminal elements is unclear but some processes appear to have lost the terminal element and terminate with a straight or concave tip; it is unclear as to whether this is open or closed. No ornament was observed on either the processes or vesicle walls. No operculum was observed.

Dimensions: 4 specimens. Apical basal width of vesicle 47-67 μm ; length of processes 10-50 μm ; basal width of processes 4-24 μm ; length of secondary processes 0.5-2 μm ; basal width of secondary processes 1 μm .

Occurrence in this study: Nolichucky Shale. Sample 08BP-33 .

Remarks: This form bears most similarity to the genus *Corollasphaeridium* Martin in Dean & Martin, 1982 emend. Yin, 1986 in having a vesicle with a wide apical opening and conical, hollow processes situated at the antapical pole. However, the diagnosis for that genus calls for a prominent apical collarete and longitudinal fibrils on the processes, features absent on this species. Additionally *Acritarch* sp. 4 has processes which possess unusual, fragile, terminal elements.

Acritarch sp. 5

Plate 14, Figs 1-6

1995 *Timofeevia* sp. Nowlan et al., Pl. 6, fig. 2.

Description: The vesicle is single-walled, circular to subcircular in outline with a psilate to shagreenate surface. Often a quasi-reticulate surface feature is imparted by

either variably developed radiating ridges around the process bases, compression or both. Few (14) to numerous (>80), hollow, psilate processes emanate from the vesicle surface and connect freely with the vesicle interior; the vesicle-process contact is angular and not confluent. The processes are mostly conical, rarely parallel sided, gently tapering distally before rapidly expanding into a terminal, closed, thickened cap, representing a terminal thickening of the process wall; often the distal end of a process carries a concave indentation. In some instances the cap is not fully developed and only partial thickening is exhibited, indicated by a darkening in the terminal area of the process; occasionally terminal thickening is absent all together and the process terminates with a simple, rounded tip. Process morphology varies from being very short and stout to long and thin, broad-based and quasi-triangular to narrow-based and near-cylindrical, and their distribution across the vesicle surface can be quasi-regular to irregular. However, wide variation in process dimensions is rarely seen on any one specimen and irregular distribution across the vesicle surface is limited to specimens with few processes. Rarely two processes share the same wide base. No excystment structure observed.

Dimensions: 41 specimens. Vesicle diameter 10-32 μm (av. 26 μm); process length 1-8 μm ; basal process width 1-2 μm ; number of processes 14-80

Occurrence in this study: Nolichucky Shale: Intermittingly from samples 08BP-60 - 08BP-33.

Remarks: This form is most similar to the genus *Celtibarium* Fombella, 1977, emend. Sarjeant & Stancliffe, 2000, whose diagnostic criteria it closely matches, but crucially differs in having terminal, cap-like thickenings on the vast majority of its processes. The generic diagnosis of *Celtibarium* Fombella, 1977, emend. Sarjeant & Stancliffe, 2000 stipulates the rounded nature of process terminations and therefore, without further generic emendation, precludes assignment of *Acritarch* sp. 5 to this genus. It should be noted, however, that processes with simple, rounded terminations do occasionally occur on *Acritarch* sp. 5, as do processes with partial terminal thickening. Illustrated specimens of *Celtibarium geminum* Fombella, 1977, (Fombella, 1977, pl. 1, figs. 10, 11) show processes resembling the rounded processes of *Acritarch* sp. 1, some of which appear to exhibit a darkening in the

terminal area. If this is the case *Acritarch* sp. 5 could be assigned to *Celtibarium geminum* Fombella, 1977, with emendations to both the species and generic diagnoses. However, only a re-examination of Fombella's original material can determine the nature of the process terminations and the taxonomic assignment of *Acritarch* sp.5.

Acritarch sp. 5 closely resembles a specimen illustrated in Nowlan et al., (1995, Pl. 6, fig. 2) in the nature of the processes. However, it is assigned as *Timofeevia* sp. which implies the presence of delineated fields on the vesicle surface, a feature not observed in *Acritarch* sp. 5. It might be the case, however, that radiating ridges at the base of processes were interpreted as field boundaries. It differs from *Micrhystridium? mammulatum* Cramer & Diez 1977 in having processes which terminate in a cap-like thickening as opposed to a "distinct nipple". It differs from species belonging to the genus *Adara* Fombella 1977, emend. Martin & Dean 1981 in having longer and less conical processes which terminate in cap-like thickenings; also membranes extending between processes are absent.

Previous records: Alberta, Canada, Furongian?, Finnegan Formation, (Nowlan et al. 1995).

Acritarch sp. 6

Plate 16, Figs 5, 6

Description: Very small sphaeromorphic form, vesicle circular to subcircular in outline, robust, psilate and possessing three to five, very small, irregularly spaced apertures. SEM shows that apertures are mostly open and penetrate the vesicle wall, rarely apertures are closed; many apertures possess a thickened rim with a width approximately 10-50 % of the apertural diameter. No excystment structure observed.

Dimensions: 30 specimens. VD: 10.1-19.7 μ m (av. 14.1 μ m); apertural diameter: 0.5-1.6 μ m; apertural rim: 0.1-0.3 μ m.

Occurrence in this study: Nolichucky Shale: sample 08BP-56.

Remarks: This is a very distinctive, yet very small species, the existence of which only became known through SEM analysis; one specimen has since been found in light microscope. The apertures are so small as to be almost imperceptible in light microscope and all measurements were taken from SEM. In some instances apertures are closed, yet still clearly apparent through the presence of a clearly defined thickened rim; one specimen possesses closed apertures only.

Acritarch sp. 7

Plate 15, Figs 1-8

Description: Subspherical to ellipsoidal vesicle, polarised, hollow and single-walled; one large primary process, rarely two, extends from one pole (apical) whilst two to three, rarely one, smaller, secondary processes are situated irregularly at the opposite, antapical pole. The process-vesicle contact is angular to confluent; in some instances the contact is indiscernible and the overall form is clavate. The processes taper to a pointed, rounded or irregularly-rounded termination, and occasionally furcate or expand distally; they may be solid, hollow or occasionally hollow proximally before becoming solid distally; hollow processes connect freely with the vesicle interior. The vesicle and processes are thin-walled, shagreenate, slightly rugulate with irregularly distributed granulae; processes carry more sculptural elements than vesicles and in SEM the outlines of processes have a slightly jagged appearance. No excystment structure observed.

Dimensions: 18 specimens. Overall length (vesicle length + primary process length) 25-39 μm (av. 30 μm); length of vesicle 12-20 μm (av. 16 μm); width of vesicle 9-16 μm (av. 12 μm); length of primary processes 10-20 μm (av. 14 μm); basal width of primary process 2-4 μm (av. 3 μm); length of secondary processes 2-10 μm (av. 4 μm); basal width of secondary processes 1-3 μm (av. 1.5 μm).

Occurrence in this study: Nolichucky Shale: Sample 08BP-54.

Remarks: This is a very distinctive polarised form showing consistent features; a large apical process (rarely two), one to three smaller, antapical processes, no

excystment structure and exhibiting wrinkled and/or granulate ornament. It differs generically from *Volkovia* Downie, 1982 in not having an operculum or opening. In general appearance and dimensions it closely resembles *Volkovia dentifera* (Volkova, 1969) Downie, 1982 as illustrated by yli ska & Szczepanik (2009) p. 446, pl 6, figs. 31-48, where a significant apical process and granulate ornament are clearly visible. However, the variable occurrence of secondary processes and the consistent presence of a circular opening on the antapical pole differentiate this form from *Acritarch* sp. 7. It differs generically from *Deunffia* Downie, 1960 emend. Thusu, 1973 in normally having two or three antapical process, with lengths equal to, but normally exceeding, 2 μ m. *Deunffia* spp. illustrated in Downie (1960) pl. 1, figs. 1, 2, 4, 6, 8, 9, and Thusu (1973) pl.104, figs. 2, 4, 5, 7, 8, 14, 15, 18, 20, 24, are clearly different forms exhibiting more fusiform vesicles and with no or little apparent surface ornament. It differs generically from *Domasia* Downie 1960, emend. Hill 1974 in normally having more than one reduced process on one pole and only one larger process on the opposite pole. The specimen encountered at Thorn Hill with two larger processes on one pole actually has a single secondary process, and as such conforms to the diagnosis of *Domasia trispinosa* Downie 1960. However, the single process on the Thorn Hill specimen bifurcates and is much smaller than the two larger processes, which are of unequal length. Furthermore, it is unclear as to whether the two larger processes represent one process which bifurcates proximally or two separate elements. This specimen probably represents intraspecific variation. *Acritarch* sp. 7 differs generically from *Pirea* Vavrdová, 1972 and *Alliumella* Vanderflit (*in* Umnova & Vanderflit, 1971) in having more than one process and being without a pylome.

Acritarch sp. 8

Plate 16, Figs 1-4

Description: Vesicle circular, subcircular or suboval in outline, thin- and single-walled, laevigate to shagreenate, without fields and bearing branching processes. Processes hollow, regularly distributed, columnar or narrowing distally and communicate freely with the vesicle interior. Processes branch, bifurcate or trifurcate and/or terminate in sharply digitate ends; furcation can be to the second order, rarely

third, and branching or furcation occurs approximately in the distal half to third of the process. Some specimens possess non-branching processes with digitate terminations only. Rarely processes have a simple, relatively short, triangular form. Process-vesicle contact angular. No excystment structure observed.

Dimensions: 7 specimens. Vesicle diameter 55-102 μm (av. 68 μm); length of processes 6-15 μm (av. 11 μm); process width 1-3 μm ; number of processes ~60-90.

Occurrence in present study: Nolichucky Shale: Samples 08BP-23, 08BP-29, 08BP-30.

Remarks: This is a unique form possessing processes which can branch and/or digitate. It differs from *Multiplicisphaeridium* Staplin 1961, emend. Sarjeant & Vavrdová, 1997 in having more numerous processes (>20), and with lengths less than 50% of the vesicle diameter.

Acritarch sp. 9

Plate 17, Figs 5, 6

Description: Vesicle spherical to subspherical in outline, single-walled and bearing forty or more hollow processes of variable length which communicate freely with the vesicle interior. Vesicle and processes are laevigate to granulate and the vesicle-process contact is sharp and angular. Processes are elongate-conical and acicular, and generally decrease in their lengths from one side of the vesicle to the other suggesting a polarised vesicle. In some instances small processes of equal length occupy most of the vesicle surface, with longer processes occupying the remaining area. No excystment structure observed.

Dimensions: 4 specimens. Vesicle diameter 26-34 μm (av.31 μm); process length 2-18 μm .

Occurrence in present study: Nolichucky Shale: samples 08BP-59, 08BP-32, 08BP-33, 08BP-33 .

Remarks: This is a rare and unusual form, appearing polarised by virtue of the distribution of its conical processes. It differs generically from *Solisphaeridium* Staplin, Jansonius & Pocock, 1965 in having processes of varying lengths. A decrease in process length between vesicular poles is commonly associated with the galeate forms, but the absence of a pylome in *Acritarch* sp. 9, and the morphology of the processes, discounts any association. It is therefore left in open nomenclature.

Acritarch sp. 10

Plate 18, Figs 1-6

Description: Vesicle subspherical to slightly ovate in outline, laevigate and bearing approximately thirty, hollow processes of variable length which communicate freely with the vesicle interior. The vesicle-process contact is sharp and angular. Processes are conical and acicular and increase in size from one vesicular pole to the other, culminating with one distinctly larger, non-acicular apical process. The apical process is columnar to conical and slightly expands distally, terminating in a slight bulge which appears broken; three small acicular processes were observed on one specimen situated at the top of the apical process. No excystment structure observed.

Dimensions: 4 specimens. Vesicle diameter 31-45 μm (av. 38 μm); process length 5-15 μm ; apical process length 12-19 μm (av. 16 μm).

Occurrence in present study: Nolichucky Shale. Samples 08BP-23, 08BP-33 .

Remarks: This is similar to *Acritarch* sp. 9 in appearing polarised and having processes which increase in length from one vesicular pole to the other. However, it differs in possessing a distinct apical process which is larger than other processes and terminates with a slightly expanded bulge.

Acritarch sp. 11

Plate 25, Figs 1-3

Description: Vesicle thin to moderately thick-walled, laevigate to shagreenate and broadly lenticular in outline. One end of the vesicle is acutely pointed and unornamented. The opposite end is slightly rounded with two to three processes or narrow flanges situated upon it; in some instances the closed end of the vesicle extends into a flat, solid flange with an irregular outline. Processes are solid or partially hollow and either parallel-sided with rounded terminations or cone-shaped with acicular terminations. Specimens are frequently broken. No excystment structure observed.

Dimensions: 11 complete specimens. Vesicle length 108-242 μm (av. 160 μm); maximum vesicle width 40-78 μm (av. 55 μm); process length 4-7 μm (av. 5 μm); flange width 5-10 μm .

Occurrence in present study: Nolichucky Shale: sample 08BP-30.

Remarks: This is an unusual and large form found in only one sample from the Nolichucky Shale. Eleven complete specimens were recorded but many broken specimens were also observed. This form differs generically from *Navifusa* Combaz et al. 1967 ex. Eisenack 1976 in having a distinctly lenticular shape and possessing processes or flanges.

Problematica

Problematica 1

Problematica 1 is represented by a diverse assemblage of non-spherical morphotypes which, despite showing variation in general morphology, share a number of key features including wall thickness and colour, circular attachment points or scars (closed apertures), wide subcircular apertures, thickened terminal flanges (collarete) and parallel striations on the cell walls. The forms have been divided into five broad morphotype categories.

Morphotype P1-1: *Subspherical chambers with one or two necks*

Plate 27, Figs 1-4

Description: Spherical to subspherical chamber with one or two column-like necks. Frequently chambers have approximately spherical openings with tear-like edges and occasionally possess either one or two solid, approximately circular features or elements delineated by dark peripheral edges. These latter features are always darker in colour than the surrounding cell wall and in some instances exhibit concentric alternations in tone. Necks are either parallel-sided or tapered, often expanding slightly before terminating. The necks are mainly broken at their ends but occasionally terminate with an aperture consisting of a thickened collarette. One example shows two connecting flasks, with the top of the neck (aperture with collarette) of one flask connected to the base of the chamber of another flask. Where two necks occur on a single chamber they arise from positions situated 90-180° apart. Discrete striations on the necks running parallel to the long axis of the flask are sometimes apparent. Contact between the bowl and necks can either be distinct and angular or gradational.

Dimensions: 6 specimens. Total length 95-176 μm (av. 130 μm); Length of neck 45-86 μm (av. 59 μm); width of neck 19-33 μm (av. 26 μm); width of chamber 40-65 μm (av. 52 μm); maximum diameter of circular elements 17-23 μm (av. 21 μm); width of collarette 22-25 μm ; length of collarette 7-17 μm .

Occurrence in this study: Nolichucky Shale: samples 08BP-24, 08BP-35, 08BP-36, 08BP-7.

Morphotype P1-2: *Vesicles with closed and /or open apertures*

Plate 28, Figs 1-4

Description: Vesicle with two circular to subcircular apertures situated at opposite ends; occasionally a third aperture is situated laterally. Apertures are either open or closed, and bounded by a thickened rim or narrow collarette. Occasionally the apertures appear torn. There is often fragmentary material attached to the peripheries of apertures, suggesting prior attachment to some other, as yet unknown, segment.

Dimensions: 4 specimens. Vesicle length 45-115 μm (av. 76 μm); maximum vesicle width 27-66 μm (av. 45 μm); aperture width 14-35 μm (av. 27 μm).

Occurrence in this study: Nolichucky Shale: samples 08BP-33, 08BP-35, 08BP-36.

Morphotype P1-3: *'Triple-junction' filament*

Plate 29, Fig. 3

Description: Filamentous form consisting of three filamentous sections arising from the same junction. Filaments pinch at the junction and are broken distally. Faint striations are apparent running parallel to the filament long axis.

Dimensions: 1 specimen. Filament lengths 95-113 μm ; maximum filament width 22-34 μm .

Occurrence in this study: Nolichucky Shale: 08BP-35.

Morphotype P1-4: *Disc-like elements*

Plate 29, Figs 1, 2

Description: Disc-like, two dimensional circular to subcircular element surrounded by a discrete rim or fold. Torn fragmentary material is attached to the outside edge of the discs.

Dimensions: 2 specimens. Maximum diameter of disc 22-40 μm .

Occurrence in this study: Nolichucky Shale: sample 08BP-35.

Morphotype P1-5: *Spheroidal cell with filamentous extension*

Plate 30, Figs 1,2

Description: Approximately subspherical cell with filamentous extension. Cell possesses a laterally positioned, open, approximately subspherical aperture bounded by a rim or fold. Aperture diameter approaches that of the cell. Filament ends are either closed and rounded or briefly swell and pinch before terminating with a break. Striations are apparent on the filament running parallel to the filament long axis.

Dimensions: 2 specimens. Filament lengths 182, 230 μm ; maximum filament width 22, 27 μm ; cell width 49, 53 μm ; maximum aperture width 35, 43.

Occurrence in this study: Nolichucky Shale: samples 08BP-37, 08BP-39.

Remarks: Problematica 1 is represented by a diverse assemblage of relatively large, non-spherical morphotypes, which have been identified as the disarticulated elements of a probable, complex, multinucleate algae, as yet undescribed (Butterfield, pers. comm. 2012). Given their irregular forms they are interpreted as being benthic. Although the forms appear to be discrete elements, the presence of torn, fragmentary material at the edges of some forms suggests prior attachments to other elements and supports this hypothesis. This assemblage of morphotypes shows much variation, but distinctive features are shared by some or most of them. The feature common to all morphotypes with the exception of P1-4 (disc-like form) is the occurrence of striations on the filaments and necks, a feature not observed on any other co-occurring palynomorphs. The distinctive closed, circular apertures and the collarettes are present in morphotypes P1-1 and P1-2 and the large subspherical apertures are apparent on morphotypes P1-1 and P1-5. The closed apertures observed on Morphotypes P1-1 and P1-2 may represent septa which were situated at the junctions of conjoining elements; the disc-like morphotypes (P1-4) may represent disarticulated septa and are of a size that may be accommodated by the open apertures.

Some specimens of P1-2 closely resemble the *Osculosphaera*-type morphology of the Neoproterozoic alga *Cheilofilum hysteriopsis* as illustrated by Butterfield (2005b, Fig. 7, F, G). Morphotype P1-5 resembles the spheroidal cells with single filamentous extensions of the alga *Jacutianema solubila*, as described and illustrated from the Neoproterozoic Svanbergfjellet Formation of Spitsbergen (Butterfield,

2004; Fig. 10). However, the Spitsbergen forms are much larger and the spheroidal cells are devoid of openings. It should also be noted that Morphotype P1-1 superficially resembles some flask-like forms of Chitinozoa, and this assignment is not completely ruled out. However, only a few specimens were recovered at Thorn Hill, and given the general absence of Cambrian Chitinozoans in the fossil record, such an assignment would be inappropriate.

Problematica 2

Plate 30, Figs 3, 4

Description: The general form consists of a series of irregularly shaped, hollow chambers interconnected by filaments. Frequently, secondary lobate filaments extend outward from the chambers and connecting filaments, and terminate either with a rounded or irregularly blunt tip or an expanded sphaeromorphic form. The position of the secondary filaments appears random and is not co-planar. Chambers can have multiple filaments and branching can occur up to the third order. It is difficult to discern whether observed specimens are complete or fragmentary. The dimensions of the various components are highly variable. The form is thin-walled and flexible and the surface is psilate to shagreenate.

Dimensions: Maximum length of segments 500 μm ; width of chambers 15-78 μm ; width of connecting filaments 3-40 μm ; width of filamentous extensions 2-13 μm ; width of sphaeromorphic terminals 6-118 μm .

Occurrence in this study: Nolichucky Shale: samples 08BP-56, 08BP-57, 08BP-23, 08BP-24, 08BP-26½, 08BP-27, 08BP-30 - 08BP-33, 08BP-36 - 08BP-12; Maynardville Limestone: samples 08BP-13 - 08BP-15.

Discussion: This form ranges throughout the whole of the Nolichucky Shale and into the lower part of the Maynardville Limestone, and occurs in most samples where it is either rare or highly abundant and dominant. Many examples of the form appear disorganised and random, but numerous specimens have been observed with filamentous extensions terminating with an expanded, sphaeromorphic structure. Its

form essentially consists of a central, elongate body of highly variable width, with laterally branching tubes. This is similar to that seen in some genera of modern, multinucleate, siphonous algae and the Thorn Hill morphotype might represent such a form. Given their irregular form they are interpreted as being benthic.

4.4 Invertebrates

4.4.1 Introduction

A wide and diverse array of spines, plates, mouthparts and cuticular fragments have been recovered from the Nolichucky Shale, and although desirable, a full morphological and taxonomic analysis of all of these forms is beyond the scope of this study. However four significant morphotypes including sclerites, mouthparts and inner leg branches are interpreted as belonging to Cambrian invertebrate forms and are presented here. Terms for the various anatomical components are taken from Harvey et al. (2012).

4.4.2 Descriptions

Branchiopod-type Mandibles (mouthparts)

Plate 31, Figs 1-3

Description: Forms are broadly lenticular to crescent-shaped, occasionally slightly sigmoidal with either broken or narrowing ends. Approximately parallel lineations run across the width of the molar surface between the two edges. The lineations create grooves along one edge and terminate with a fringe along the opposite edge. The fringe is mostly poorly preserved, but in some instances fringe components, such as short setae and protruding elements, are still present. One specimen possesses long setae situated on the fringed edge towards the narrowing end of the mandible.

Dimensions: 5 specimens. Total length 70-113 μm ; maximum width 24-47 μm ; length of setae 3-22 μm .

Occurrence in present study: Nolichucky Shale: samples 08BP-56, 08BP-4, 08BP-9, 08BP-10.

Remarks: See discussion below at copepod-type mandibles.

Branchiopod-type limbs

Plate 33, Figs 1-5

Description: Large and small arrays of various thin, acicular, plumose setae either attached or unattached to cuticle. Setae bear numerous, secondary setae approximately 1 μm apart and are arranged in one to three rows along the length of the primary setae. In some instances plumose setae are accompanied by non-plumose setae. Occasionally small setal arrays occur which are detached from cuticle and possess very fine, hair-like, secondary setae in rows of two. Secondary setae from neighbouring primary setae appear to interlace along the entire length of the primary setae.

Dimensions: Large setal arrays: length of primary setae 40-220 μm ; basal width of primary setae 5-10 μm ; length of secondary setae 3-13 μm ; basal width of secondary setae \sim 1 μm . Small setal arrays: length of primary setae 80-104 μm ; basal width of primary setae $<$ 1 μm ; length of secondary setae 4-7 μm ; μm ; μm ;

Occurrence in present study: Nolichucky Shale: samples 08BP-55, 08BP-56, 08BP-23, 08BP-29, 08BP-32.

Remarks: See discussion below at copepod-type mandibles.

Copepod-type Mandibles (mouthparts)

Plate 32, Figs 1-6

Description: Cuticular fragments bearing a single tooth or rows of up to four teeth. Teeth in rows decrease in size along the length of the row. Teeth are mostly

bicuspidate and bearing a small central cusp, whilst other teeth are bicuspidate without a central cusp or rarely non-bicuspidate and conical. Occasionally a row terminates with a bristly, narrow platform; one tooth array possesses a prominent seta below the bristly platform. In some instances a pair of small, secondary teeth are situated at the base of a tooth. Teeth are either opaque or transparent.

Dimensions: Length of teeth 10-46 μm ; width of bicuspidate teeth 9-42 μm ; length of prominent seta 12 μm .

Occurrence in present study: Nolichucky Shale: samples 08BP-56, 08BP-58, 08BP-60, 08BP-61, 08BP-21 - 08BP-30, 08BP-32, 08BP-33.

Remarks: A number of organic walled microfossils from the Deadwood Formation (Cambrian Series 3 and Furongian) in Canada (Saskatchewan and Alberta) were identified as either branchiopod-type mandibles, limbs or copepod-type mandibles by Harvey et al. (2012); the assignment of the Thorn Hill specimens is based solely upon that study.

The Deadwood branchiopod-type mandibles are characterised by a D-shaped grinding (molar) surface with lineations running across the width of the molar surface, which create grooves along the straight/concave edge. The opposite edge has a fringe along most of its length and long setae situated at the narrowest end of the mandible. Although the preservation of the Thorn Hill specimens is not as good as that of the Canadian specimens, key diagnostic features are still apparent. All the Thorn Hill specimens possess lineations which run across the width of the molar surface, and a number of specimens possess the remnants of grooves, fringed edges and long setae. However, complete well preserved specimens were not recovered and some of the more detailed features of the mandible edges were not observed. Also, the Deadwood specimens are larger. Therefore, despite clear similarities between the Deadwood and Thorn Hill specimens, the latter are only tentatively interpreted as branchiopod-type mandibles.

The branchiopod-type limbs from Deadwood were identified as filter plate components originally attached to the limbs of a branchiopod-like crustacean, and used for filtering food (Harvey et al., 2012). The Thorn Hill and Deadwood

branchiopod-type limbs are clearly comparable, but the Thorn Hill forms lack the detail observed in the Deadwood specimens. In particular the coplanar setal arrangement observed in the Deadwood specimens is not apparent, most likely as a result of poor preservation. However, clear, distinctive arrays of plumose and non-plumose setae attached to cuticle are present, and are of a size comparable to the Deadwood specimens. Also the setae (primary and secondary) morphologies are clearly comparable.

Copepod-type mandibles from the Deadwood Formation (Cambrian Series 3 and Furongian) consist of cuticular fragments bearing up to six teeth and terminating with a bristly platform and a prominent papposerrate seta. Tooth morphology varies from broadly conical to narrow and strongly bicuspidate with some of the latter forms possessing a much smaller, central cusp. Harvey et al. (2012) argued that despite there being many comparable crustacean mandibles, the “combination of fine-scale elaborations (teeth, platform, and protruding seta), their numbers, positions and proportions, and their overall ontogenetic consistency, are shared only with copepods...”

The Thorn Hill specimens occur mainly as single, disarticulated teeth. However, cuticular fragments bearing a number of bicuspidate teeth, a bristly platform and a papposerrate seta have been recovered. These forms are clearly the same as those from the Deadwood Formation and represent the first record of copepod-type mandibles in the USA.

Wiwaxia sclerites

Plate 34, Figs 1, 2

Description: Disarticulated, incomplete (approximately upper half) plate-like forms with a lateral half-lenticular outline. The forms are rigid, appear to be symmetrical and taper to a slightly extended and thickened, pointed tip. They possess closely arranged, longitudinal ridges (microfabric) which extend from the tip-region downwards.

Dimensions: 2 broken specimens. Longitudinal length 42 μm , 90 μm ; maximum width (estimated) 66 μm , 52 μm .

Occurrence in this study: Nolichucky Shale: sample 08BP-29.

Discussion: Two approximately half (upper part) specimens were recovered from one sample in the Nolichucky Shale at Thorn Hill, as well as four fragments. Despite the lack of complete specimens their size, inferred lenticular outline and the longitudinal microfabric identify these forms as *Wiwaxia* sclerites (Harvey et al., 2011). They closely resemble specimens of *Wiwaxia* sclerites illustrated by Butterfield (1990b, Fig. 1, A-F) and Harvey et al. (2011, Fig. 3, D-G). In North America *Wiwaxia* has been recorded in Utah, USA (Conway Morris & Robison, 1988), the Burgess Shale, Canada (Butterfield, 1990b) and the Mount Cap Formation in the Northwest Territories, Canada (Butterfield, 1994). All of these sites represent western Laurentian deposits, and the forms recovered at Thorn Hill represent the first record of *Wiwaxia* in eastern Laurentia.

Chapter 5

Review of Cambrian palynology

5.1 Introduction

Cambrian acritarchs and prasinophytes have been recorded globally with at least 250 form-species so far reported (Mullins et al., 2005), and the literature regarding them is plentiful (see below). The last four decades have seen major developments in the application of acritarchs in biostratigraphy (Volkova et al., 1979, 1983; Moczyłowska 1991; Moczyłowska & Zang 2006; Zang et al. 2007) and a number of acritarch assemblage zonal schemes now exist, either for the Terreneuvian and Cambrian Series 2 (Moczyłowska 1991; Moczyłowska & Zang 2006; Vanguetaine & Van Looy, 1983; Zang et al., 2007) or Cambrian Series 3 and the Furongian (Martin & Dean, 1981, 1988; Parsons & Anderson, 2000). Reviews of Cambrian acritarchs and/or their stratigraphic applications have been discussed by Downie (1984), Vanguetaine (1986), Jago et al., (2006), Martin (1982, 1993), Molyneux et al., (1996) and Rushton & Molyneux (2011).

There have been developments in the use of biochemistry (biomarkers) and transmitting electron microscopy (TEM) in efforts to elucidate the affinities of acritarchs (Talyzina et al., 2000; Talyzina & Moczyłowska, 2000; Moczyłowska & Willman, 2009; Moczyłowska, 2010, 2011) and microscopic, recalcitrant, animal components from Cambrian deposits in North America and China, (otherwise known as Small Carbonaceous Fossils (SCFs)) have been given particular attention for their use in extending our knowledge on the geographical and temporal distribution of invertebrates (Harvey & Butterfield, 2008, 2011; Harvey et al., 2011; Butterfield & Harvey, 2012).

5.2 Terreneuvian and Cambrian Series 2

Acritarchs from the Terreneuvian and Cambrian Series 2 have been reported from Australia (Foster et al., 1985; Gravestock et al., 2001; Zang & Walter, 1992a; Zang et al., 1998, 2001, 2007), the British Isles (Potter 1974a, b; Downie 1982; Gardiner & Vanguetaine, 1971; Brück & Vanguetaine, 2004; Vanguetaine et al., 2002; Young et al., 1994), Canada (Baudet et al., 1989; Downie, 1982; Dean & Martin,

1982), China (Zang & Walter, 1992b; Dong et al. 2009; Leiming & Xunlai, 2007; Naiwen, 1989; Yao et al., 2005; Zang 1992), Czechoslovakia (Fatka & Konzalová, 1995; Konzalová, 1974), Denmark (Moczyłowska & Vidal, 1992; Vidal, 1981b), eastern Newfoundland (Martin & Dean, 1983), East European Platform (Volkova et al., 1979, 1983), Estonia (Moczyłowska, 2011; Volkova, 1968;), Finland (Tynni, 1978, 1982a, b), Greenland (Downie, 1974, 1982; Vidal, 1979; Vidal & Peel, 1984, 1988, 1993), India (Prasad et al., 2010), Poland (Jachowicz-Zdanowska, 2010, 2011; Moczyłowska, 1981, 1988, 1991, 1997; Moczyłowska & Vidal, 1986, 1988; Volkova, 1969), Scandinavia (Downie; 1982; Eklund 1990; Hagenfeldt 1988, 1989a; Moczyłowska, 2001, 2002; Moczyłowska & Vidal, 1986, 1988; Vidal & Nystuen, 1990; Vidal 1981a, b, c), Russia & Siberia (Fridrichsone, 1971; Jankauskas, 1975; Jankauskas & Posti, 1973; 1976; Kirjanov, 1974; Moczyłowska, 1991; Moczyłowska & Vidal, 1988; Moczyłowska et al., 2001; Volkova, 1968, 1969; 1974; Volkova et al., 1979, 1983), Spain (Liñán et al., 1984; Mette, 1989; Palacios & Moczyłowska, 1998; Palacios & Vidal, 1992), Spitsbergen (Knoll & Swett, 1987), USA (Wood & Clendening, 1982).

Acritarch zonation schemes for Terreneuvian and Cambrian Series 2 strata have been proposed for the East European Platform (Volkova 1979, 1983; Moczyłowska 1991), Australia (Zang, 2001; Zang et al. 2001, 2004, 2007) and China (Zang, 1992). Moczyłowska & Zang, (2006) proposed an international zonation scheme for parts of Cambrian Series 1 and 2 based upon correlatable acritarch and faunal zones in the East European Platform, Australia, China and Laurentia.

Moczyłowska (1991) proposed an acritarch zonation scheme for the Terreneuvian Series and Cambrian Series 2 of Baltica, based upon the relative, stratigraphic occurrences of 45 form-species, recovered from the subsurface sequence of the Lublin Slope, East European Platform, Poland. Four assemblage zones were defined and in ascending order are: *Asteridium tornatum* - *Comasphaeridium velvetum*; *Skiagia ornata* - *Fimbriaglomerella membranacea*; *Heliosphaeridium dissimulare* - *Skiagia ciliosa*; and *Volkovia dentifera* - *Liepaina plana*. The base of the lowest assemblage zone, *Asteridium tornatum* - *Comasphaeridium velvetum* is taken as the Proterozoic-Cambrian boundary due of its coincidence with the base of the *Platysolenites antiquissimus* shelly fossil Zone, the latter being equivalent in part to the *Trichophycus pedum* ichnozone (Moczyłowska & Zang, 2006). These zones

Series	ACRITARCHS ZONES			MACROFAUNAL ZONES			
	Baltica	South Australia	South China	Baltica	South Australia	South China	Laurentia
Series 2	<i>Eliasum</i>	Leiospheroids			<i>Redlichia chinensis</i>	<i>Hoffetella</i> - <i>Redlichia</i>	
	<i>Volkovia dentifera</i> - <i>Liepaina plana</i>	Zone 7 <i>Liepaina plana</i>		<i>Protolenus</i>	<i>Pararaia janeae</i>	<i>Mega-palaeolenus</i> <i>Palaeolenus</i> <i>Drepanuroides</i> <i>Yunnanaspis</i> <i>Yiliangella</i> <i>Malungia</i>	<i>Olenellus</i>
	<i>Heliosphaeridium dissimulare</i> - <i>Skiagia ciliosa</i>	Zone 6 <i>Vulcanisphaera pseudofaveolata</i> - <i>Corollasphaeridium opimolum</i>	IV	<i>Holmia kjerulfi</i>	<i>Pararaia bunyerooensis</i>	<i>Eoredlichia</i> - <i>Wutingaspis</i>	
		Zone 5 <i>Skiagia ciliosa</i> - <i>Corollasphaeridium aliquolum</i>			<i>Pararaia tatei</i>		
Terreneuvian	<i>Skiagia ornata</i> - <i>Fimbrigliomerella membranacea</i>	Zone 4 <i>Skiagia ornata</i>	III	<i>Schmidtellus mickwitzi</i>	<i>Abadiella huoi</i>	<i>Parabadiella</i>	<i>Nevadella</i>
		Zone 3 <i>Ceratophyton spinuconum</i> - <i>Veryhachium trisentium</i>	AHC	<i>Platysolenites antiquissinus</i>		<i>Sinosachites</i> - <i>Lapworthella</i>	<i>Fallotaspis</i>
Zone 2 <i>Corollasphaeridium</i> - <i>Comasphaeridium</i>	<i>Paragloborilus</i> - <i>Siphogonuchites</i>	<i>Fritzaspis</i>					
Zone 1 <i>Redkinia</i> - <i>Cymatospaera</i>	<i>Anabarites</i> - <i>Protohertzina</i>						
				<i>Trichophycus pedum</i> ↓			

Figure 5.1 Relative temporal positions of acritarch and macrofauna biozones for the Terreneuvian and Cambrian Series 2 of Baltica, South Australia and South China, and macrofauna biozones of Laurentia. Some uncertainty exists at boundary levels. Grey areas represent absence of biozones. AHC = *Asteridium-Heliosphaeridium-Comasphaeridium* acritarch assemblage (Yao et al., 2005). Sources for Baltica: Moczyłowska (1991); Moczyłowska & Zang (2006); Nielson & Schovsbo (2006). South Australian: Moczyłowska & Zang (2006); Zang et al. (2001, 2004, 2007). South China: Zang (1992); Yao et al. (2005) (in yellow); Moczyłowska & Zang (2006). Laurentia: Moczyłowska & Zang (2006); Taylor et al. (2012).

have since been recorded in other palaeocontinents enabling correlation between Baltica, Laurentia, Gondwana and Barentsia (Palacios and Vidal, 1992; Vidal & Peel, 1993; Vidal & Moczyłowska, 1995, 1996; Moczyłowska, 1998; Palacios & Moczyłowska, 1998; Vanguetaine, 1992; Zang et al., 2007).

In south Australia acritarchs of Terreneuvian and Cambrian Series 2 age have been reported from the Stansbury and Arrowie Basins (Zang & Walter, 1992a; Gravestock et al., 2001; Zang et al. 2001, 2007). Zang et al. (2007) defined seven acritarch assemblage zones (1-7) against an established, comprehensive background of sequence stratigraphic and faunal zonation schemes. The assemblage zones in ascending order are Zone 1: *Redkinia-Cymatiosphaera*; Zone 2: *Corollasphaeridium-Comasphaeridium*; Zone 3: *Ceratophyton spinuconum-Verhachium trisentium*; Zone 4: *Skiagia ornata*; Zone 5: *Skiagia ciliosa-Corollasphaeridium aliquolumum*; Zone 6: *Vulcanisphaera pseudofaveolata-Corollasphaeridium opimolumum*; Zone 7: *Liepaina plana*. These Australian zones correlate well with those from Baltica (Moczyłowska & Zang, 2006; Zang et al., 2007).

Biostratigraphically significant acritarch assemblages have been recorded in the eastern Yunnan Province and the Yangtze gorges of the south China Platform (Luo et al., 1984; Zang, 1992), and the Tarim Block in northwest China (Yao et al., 2005; Dong et al., 2009). Zang (1992) defined four acritarch assemblages (I-IV) for the South China Platform of which only assemblage Zone IV is comparable to assemblage zones elsewhere in the world; in particular it corresponds to the *Heliosphaeridium dissimulare - Skiagia ciliosa* Zone of Baltica (Moczyłowska, 1991; 1999; Zang, 1992; Moczyłowska & Zang, 2006). Zones I and II, and the lower part of Zone III are Ediacaran in age. In the Xinjiang Uygur Autonomous region in northwest China, Yao et al. (2005) defined the *Asteridium-Heliosphaeridium-Comasphaeridium* (ACH) acritarch assemblage which they correlated with the Lower Tal Formation in the Lesser Himalaya and is broadly similar to the basal Cambrian *Asteridium tornatum-Comasphaeridium velvetum* acritarch Zone (Moczyłowska, 1991) of the EEP. Dong et al. (2009) recorded acritarchs characteristic of the ACH in the Yangtze Gorges area of South China and the Aksu area in the Tarim Block in northwest China.

Acritarchs from the Siberia Platform have had relatively little study as compared to other palaeocontinents, and the limited geographical range of faunal groups, and conflicting data between trilobite and archaeocyathid zonations has made local and global correlation difficult (Zang et al. 2007). Further acritarch studies and revisions of pre-existing faunal ranges are required before any meaningful acritarch assemblages zones can be defined.

Terreneuvian and Cambrian Series 2 acritarchs of Laurentia have received even less attention than those of Siberia. Wood & Clendening (1982) recorded a number of spinose forms from the lower Cambrian Murray Shale of the Chilhowee Group in Tennessee, including *Medousapalla choanoklosma* (regarded as a junior synonym of *Skiagia ornata* Downie, 1992 by Zang et al., 2007) and *Comasphaeridium*. Other spinose forms illustrated by Wood & Clendening (1982, p.261, pl. 2) are considered by Zang et al. (2007) as resembling forms in the *Asteridium-Heliosphaeridium* group and suggest the Tennessee, Murray Shale assemblage is probably correlatable with the *Skiagia-Ornata-Fimbriaglomerella membranacea* Zone (Moczydłowska, 1991) of Baltica. Acritarchs characteristic of the *Heliosphaeridium-S. ciliosa* Zone of Moczydłowska (1991) have been recorded by Vidal & Peel (1993) in the Buen Formation in North Greenland and by Vidal (1979) and Downie (1982) in the Ella Island and Bastion Formations on Ella Ø, in East Greenland. These strata are equivalent to the *Bonnia-Olenellus* Zone which was partially correlated to strata of Baltica, Australia and South China (Moczydłowska & Zang, 2006, fig. 4).

With regard to the valid use of individual Terreneuvian and Cambrian Series 2 acritarch species in global biostratigraphy, there are few. However, due to their cosmopolitan distribution and distinct morphologies, *Skiagia ornata* (Volkova, 1968) Downie, 1982 and *Skiagia ciliosa* (Volkova, 1969) Downie, 1982 are considered to be potential, global, biochronological markers (Moczydłowska & Zang, 2006). The first appearance datum (FAD) of *S. ornata* marks the base of the *Skiagia ornata-Fimbriaglomerella membranacea* Zone of Moczydłowska (1991) and is close to the base of the as yet formally undefined Cambrian Series 2/Stage 3. The FAD of *S. ciliosa* is situated within Stage 3 and marks the base of the *Heliosphaeridium dissimulare - Skiagia ciliosa* Zone; it precedes the FAD of the trilobite *Olenellus* (Moczydłowska & Zang, 2006). *S. ciliosa* has been recorded in

Baltica, South China, Australia, Avalonia, Armorica, Laurentia, Siberian and Kazakhstan (Moczyłowska, 1998; Moczyłowska & Zang, 2006).

5.3 Cambrian Series 3 and Furongian

Acritarchs from Cambrian Series 3 and the Furongian have been reported from Australia (Zang & Walter, 1992a), Arctic Russia (Moczyłowska & Stockfors, 2004; Raevskaya & Golubkova, 2006), Argentina (Rubinstein et al., 2003), Belgium (Vanguetaine, 1973; 1974; Ribecai & Vanguetaine, 1993), British Isles (Young et al. 1994; Brück & Vanguetaine, 2004; Vanguetaine & Brück, 2008; Potter et al., 2011), Canada (Martin, 1992; Dean & Martin, 1978; 1982; Martin & Dean, 1981; 1983; 1984; 1988; Nowlan et al., 1995; Binda et al., 1996; Palacios et al., 2009a; b; 2011; 2012), China (Yin, 1986), Czechoslovakia (Fatka, 1989), East European Platform, (Volkova, 1990), Estonia (Paalits, 1992b; 1995), France (Vanguetaine & Léonard, 2005), Germany (Montenari & Servais, 2000), Iran (Ghavidel-syooki, 1996; 2006; Ghavidel-syooki & Vecoli, 2008), Italy (Di Milia, 1991; Vecoli et al., 2008), Jordan (Keegan et al., 1990), North Africa (Vecoli, 1996; 1999; Vecoli & Playford, 1997; Tawadros et al., 2001; Vecoli et al., 2008), Poland (Szczepanik, 2001; yli ska et al., 2006; yli ska & Szczepanik, 2009; Jachowicz-Zdanowska, 2011), Russia (Paalits, 1992a; Volkova, 1990), Spain (Fombella, 1977; 1978; 1979; 1987; Albani et al., 2006; Palacios, 2010), Sweden (Bagnoli et al., 1988; Hagenfeldt, 1989b;), Turkey (Dean et al., 1997) and the USA (Clendening & Wood, 1981; Wood & Stephenson, 1989; Strother, 2008).

Acritarch zonation schemes for Cambrian Series 3 and the Furongian have been developed for the East European Platform (EEP) (Volkova et al., 1979; 1983; Volkova, 1990), northern Norway (Welsch, 1986), Belgium (Vanguetaine, 1974; 1978) and from Avalonian strata in eastern Newfoundland where both acritarchs and trilobites have been comprehensively recorded (Martin & Dean, 1981; 1984; 1988; Parsons & Anderson, 2000) (Fig. 5.1). Also, a composite Cambrian zonation by Vanguetaine and Van Looy (1983) utilised data published by Martin (*in* Martin & Dean, 1981).

Martin & Dean (1981) documented acritarchs and trilobites (with reference to corresponding Scandinavian and Anglo-Welsh trilobite zones) from the upper part of the Manuels River Formation, the Elliot Cove Formation and the overlying

Global standard Series & Stages		Macrofaunal biozones	Eastern Newfoundland		East European Platform. (Volkova et al. 1979, 1983; Volkova 1990)	Finnmark, northern Norway (Welsch 1986)	
L. O.	Tremadocian		Martin & Dean (1981,1988)	Parsons & Anderson (2000)			
Furongian	Stage 10	<i>Acerocare</i>	A6	RA10b	BK5	A V	
				RA10a		A IV	
				RA9			
		<i>Peltura scarabaeoides</i>	Not sampled	RA8	BK4 B BK4 A		
				RA7b			
				MISSING			
				?			
				RA7a			
				A5b ?		RA6b	
				RA6a			
	<i>Peltura minor</i>	Not sampled	A5b	RA5			
			Not sampled				
			A5a				
	<i>Protopeltura praecursor</i>	Not sampled	Not sampled		A III		
	Stage 9	<i>Leptoplastus</i>	A4	MISSING	BK3		
RA4							
<i>Parabolina spinulosa</i>		A3b	A3a	RA3	BK2		
Paibian	<i>Olenus</i>	upper A2					
Series 3	Guzhangian	<i>Agnostus pisiformis</i>		BK1			
				CK2	A II		
	Drumian	<i>Paradoxides paradoxissimus</i>		CK1	A I		
			<i>Adara alea</i> <i>R. terranova</i>				
Stage 5	<i>Eccaparadoxides oelandicus</i>			Kibartai			

Figure 5.2 Correlated acritarch biozones for Cambrian Series 3 and the Furongian in eastern Newfoundland, the East European Platform and Finnmark/northern Norway. Data compiled from Martin & Dean (1981, 1988), Parsons & Anderson (2000), Volkova et al. (1979, 1983), Volkova (1990), Welsch (1986), Molyneux et al. (1996). Grey areas represent sections either not sampled or missing. L. O. = Lower Ordovician.

Formation situated on Random Island in eastern Newfoundland. They proposed six acritarch microfloras, A1-A6, based on the FAD, LAD and/or ranges of various acritarch species. The total range was from the upper part of the *Paradoxides hicksii* trilobite zone (Cambrian Series 3) to the Tremadoc *Parabolina argentina* trilobite zone with microflora A2 straddling the Series 3-Furongian boundary. They mainly recorded acritarchs previously described from the Cambrian of Spain, Belgium and Czechoslovakia (now the Czech Republic & Slovakia) but also from Bell Island in eastern Newfoundland, England, France and north Africa. This work was subsequently augmented (Martin & Dean, 1984) with data from underlying strata in the same area (Random Island): the lower part of the Manuels River Formation and the underlying Chamberlains Brook Formation. The vertical range of microflora A1 introduced by Martin and Dean (1981) was confirmed and two new underlying microfloras, in ascending order A0-1 and A0, were described.

The microflora zones of Martin and Dean (1981; 1984) were then revised by Martin and Dean (1988), supported by a study of new material from Random island and also from Manuels River, situated approximately 100 km SW of the Random Island section. Microfloras A0 and A1 were replaced by the *Rugasphaera terranova* Standard Zone and the *Adara alea* Range Zone respectively. Microfloras A2, A3, and A5 were each split into two subzones: Lower A2, Upper A2; A3a, A3b; and A5a and A5b respectively (Fig. 5.1). The main characteristics of the microfloras are as follows: microflora Lower A2 is characterised by the FAD of *Timofeevia lancarae* and *T. phosphoritica* with *Vulcanisphaera turbata* absent; the base of microflora Upper A2 is defined by the appearance of *Timofeevia pentagonalis* and *Vulcanisphaera turbata* (the Series 3-Furongian boundary is situated in the lower part of Upper A2); microflora A3 is characterised by the appearance of *Cristallinium randomense*, *Ninadiacrodium dumontii* and *Cymatiogalea aspergillum* which occur throughout A3 and beyond, with the appearance of diacrodians dividing A3 into A3a and A3b; A4 is distinguished by the appearance of *Trunculumarium revinium* and A5 by the appearance of *Arbusculidium rommelaerei*. A5 is divided into A5a and A5b by the occurrence (albeit rare) of *Saharidia fragilis* and *Stelliferidium gautieri*. Additionally each of the microfloras is secondarily characterised by the co-occurrence or absence of various acritarch species, e.g. *Stelliferidium pingiculum* is common in A3 but characteristically absent from A4. Importantly the microflora

zones were linked with corresponding trilobite data from the same sections providing direct correlation between trilobite zones and microflora zones, thus producing a mutually supportive stratigraphic framework (see Martin & Dean, 1988; Rushton & Molyneux, 2011 for full discussion).

Parsons and Anderson (2000) reviewed the zonations of Martin and Dean (1981; 1988) and repositioned some of the samples relative to the trilobite stratigraphy. They described seven microfloras, RA4 to RA10 (with microfloras RA6, RA7 and RA10 subdivided) corresponding to trilobite zones. The microfloras ranged from the *Parabolina spinulosa* trilobite zone (lower Furongian) to the *Rhabdinopora flabelliformis* trilobite zone (lower Tremadoc). They paid particular attention to microfloras RA6 to RA10 which represented microfloras not previously described from Random Island and contained new species. There RA3 and RA4 microflora are equivalent to microflora A3 and A4 of Martin and Dean (1988).

The acritarch microfloras and trilobite zones of eastern Newfoundland described by Martin and Dean (1988) and Parsons and Anderson (2000) represent the most comprehensive Avalonian, biostratigraphic schemes for the upper part of Cambrian Series 3 and the Furongian. Correlations have been made with Belgium, England, the Baltic States, the East European Platform, north Africa and Scandinavia (see Parsons & Anderson, (2000) for a full discussion of regional comparisons).

Volkova (1979, 1983) described acritarch assemblages for the East European Platform ranging from Cambrian Series 1 through to the Kibartai “horizon”, which correlates with the *Eccaparadoxides oelandicus* “Stage” (Eklund, 1990) and is situated in the lower part of Cambrian Series 3. Volkova (1990) then proposed eight zones for the East European Platform (CK1, CK2, BK1, BK2, BK3, BK4-A, BK4-B and BK5) ranging from Cambrian Series 3 to the Tremadoc. Volkova correlated assemblage BK3 with microflora A4 of Martin and Dean (1988). However, as pointed out by Molyneux (1996, text-fig. 3), there are numerous acritarchs common to both the East European Platform and eastern Newfoundland, though many appear to have different ranges. This might be the result of insufficient data, erroneous correlation or might perhaps be an accurate account of the ranges (Molyneux, 1996).

Welsch (1986) described four acritarch microfloras for Cambrian Series 3 and the Furongian from the Kistedal Formation of Finnmark, northern Norway, consisting of

many acritarchs recorded in the East European Platform and eastern Newfoundland, as well as a number of new species.

Potter et al. (2012) correlated the Furongian Shoot Rough Road Shales from the Comley area in Shropshire, England to microfloras of eastern Newfoundland (Martin & Dean, 1981; 1988; Parsons & Anderson, 2000). The trilobite *Parabolina spinulosa* (Wahlenberg, 1821) was recovered from the Shoot Rough Shales by Cobbold (1927) and is the diagnostic species for the *Parabolina spinulosa* trilobite zone of Martin & Dean (1988) and Parsons & Anderson (2000). The acritarch *Trunculumarium revinium* is common in assemblage L1 of Potter et al. (2012) permitting correlation with microflora RA4 of Parsons & Anderson (2000) and microflora A4 of Martin in Martin & Dean (1988), both of which correspond to the upper part of the *Parabolina spinulosa* trilobite zone (Martin & Dean, 1988; Parsons & Anderson, 2000). This supports the *P. spinulosa* assignment for the Shoot Rough Road Shales and underlines the importance of recording both acritarchs and trilobites.

There have been few acritarch studies on Cambrian Series 3 and Furongian sections from Laurentia, and consequently acritarch zonation schemes for that palaeocontinent have not been that forthcoming. Those studies that do exist either describe acritarch taxa not recorded elsewhere (e.g., Clendening and Wood, 1981; Strother, 2008) or assemblages that have little in common with other, non-Laurentian, coeval assemblages (e.g. Wood & Stephenson, 1989). Martin (1992) described six microfloras, AU1-AU6, for uppermost Furongian to Lower Ordovician strata from Wilcox Pass in Alberta, Canada. However, only microflora AU1 was taken as being Cambrian, but had little in common with assemblages from eastern Newfoundland and Europe. Other palynological studies on Laurentian material have either focused on the morphology and ultrastructure of cryptospores (Strother et al., 2004; Taylor & Strother, 2008; 2009) or small carbonaceous fossils (SCFs) as described by Butterfield & Harvey (2012).

In China Yin (1986) described five microfloras, A1-A5, with A1-A2 being of Furongian age and A3 straddling the Cambrian-Ordovician boundary. Microfloras A1 and A2 contain some typical Cambrian acritarchs such as *Cristallinium cambriense* and *Dasydiacrodium obsonum*, but no convincing correlation with coeval assemblages from elsewhere was possible.

5.4 Small Carbonaceous Fossils (SCFs)

Small carbonaceous fossils (SCFs) consist primarily of microscopic, recalcitrant animal components such as *Wiwaxia* sclerites, priapulid-like scalids, molluscan radulae and crustacean appendages, as well as arthropod cuticles and various spines (Butterfield & Harvey, 2012). Apart from scolecodonts they have only been recorded in Cambrian strata, most likely because they are routinely ignored in palynological investigations by most workers but actively sought in Cambrian rocks by others. Standard palynological processing has a tendency to break up larger microfossils and therefore SCFs are extracted from rocks using a low manipulation, hydrofluoric acid-extraction procedure, with the aim of enhancing recovery of more complete specimens (Harvey & Butterfield, 2008; 2011; Harvey et al., 2011; Butterfield & Harvey, 2012). They have been reported from: the Mahto Formation (Cambrian Series 2), Alberta, Canada (Butterfield, 2008); the Mount Cap Formation (Cambrian Series 2), Northwest Territories, Canada (Harvey & Butterfield, 2008; 2011); the Kali Formation (Cambrian Series 3), Guizhou Province, China (Harvey et al., 2011); and the Deadwood Formation (Cambrian Series 3 & Furongian), Saskatchewan and Alberta, Canada (Binda et al., 1996; Harvey et al., 2012). See Butterfield & Harvey (2012) for full a discussion.

Due to their relatively recalcitrant nature, SCFs possess a higher preservational potential than their macrofossil equivalents and are often recovered from rocks lacking macrofossils. Their recovery, therefore, has the potential to increase recorded occurrences of animal species and their geographical and temporal distributions: the recovery of *Wiwaxia* sclerites in palynological preparations (SCF-type) has effectively doubled the reported occurrence of *Wiwaxia* (Butterfield & Harvey, 2012). Given their relatively low abundance, the practical use of SCFs as primary markers in biostratigraphy is most likely limited. However, some SCFs do show limited ranges. *Wiwaxia* for example, is conspicuously absent from the Furongian, having been recorded only in older strata (Butterfield & Harvey, 2012), and therefore may show potential as a subordinate, biostratigraphical indicator for strata older than the Furongian.

Chapter 6

Stratigraphy

This chapter discusses the stratigraphy of the Nolichucky Shale. It specifically details the position of the Cambrian Series 3/Furongian boundary (middle/upper boundary) within the Nolichucky Shale at Thorn Hill, based on new results from chemostratigraphic (^{13}C) and trilobite biostratigraphic (trilobites) studies undertaken for this project. The stratigraphic significance of recovered acritarchs/invertebrate components are discussed towards the end. It should be noted that the terms Cambrian Series 3 and Furongian are used as equivalents to the middle and upper Cambrian respectively.

6.1 Introduction

The biostratigraphy of the Nolichucky Shale in northeastern Tennessee based on trilobites has been investigated by Rasetti (1965), Derby (1965) and Sundberg (1989), among others. Sundberg (1989) analysed trilobites from sections at Thorn Hill stratigraphically below the Nolichucky Shale, and identified them as Cambrian Series 3. Rasetti (1965) studied a section close to that at Thorn Hill but failed to find any trilobite evidence for the presence of the Furongian within the Nolichucky Shale, although he did record upper Furongian species at other locations in northeastern Tennessee. Derby (1965) studied the Lee Valley section, an outcrop situated approximately 26 km to the northeast of Thorn Hill, and now poorly exposed. It consisted of the Maryville Limestone, Nolichucky Shale and Maynardville Limestone. He identified the Cambrian Series 3/Furongian boundary within the upper part of the Nolichucky Shale, based on the presence of trilobite species belonging to the genus *Aphelaspis*. This showed that the majority of strata within the Nolichucky Shale is of Cambrian Series 3 age and that only the very uppermost part is of Furongian age.

However, the position of the Cambrian Series 3/Furongian boundary within the Nolichucky Shale at Thorn Hill is unknown. In this study, two independent methods have been used to identify the stratigraphic position of the Cambrian Series 3/Furongian boundary within the Nolichucky Shale at Thorn Hill, providing independent chronostratigraphic controls. The two methods are trilobite biostratigraphy and stable carbon isotope chemostratigraphy.

6.2 Trilobite biostratigraphy

6.2.1 Introduction

Trilobites were systematically collected from Thorn Hill by the present author and Dr. John Beck from the Western Observatory, Boston College, Massachusetts. They were collected from 29 sample points equivalent or very close to palynological sampling points, and ranged throughout the Nolichucky Shale. The trilobite specimens were given initially to Dr. Adrian Rushton at the Natural History Museum, London for taxonomic identification. Following Dr. Rushton's advice the specimens were then sent to Professor John Taylor at the Indiana University of Pennsylvania for a second appraisal, and all the final trilobite identifications and the biostratigraphic zones they represent were supplied by Professor Taylor.

6.2.2 Trilobite biostratigraphy of the Nolichucky Shale

A number of stratigraphically significant trilobite species were identified from the Nolichucky Shale at Thorn Hill. Most notably the species *Aphelaspis camiro*, which was recovered from horizons equivalent to samples 08BP-35 (168 m) and 08BP-36 (169 m), and *Coosia alethes* recovered from an horizon equivalent to sample 08BP-24 No (135 m) (Fig. 6.1). No trilobites were recovered between these two horizons, which represents a stratigraphic thickness of 33 m. The FAD of trilobite species belonging to the genus *Aphelaspis* marks the base of the Furongian in shallow-shelf North American (Laurentian) deposits (Taylor, 2006). Rasetti (1965) recognised three *Aphelaspis* subzones in Tennessee with the FAD of *Aphelaspis camiro* marking the base of the middle subzone. Therefore, the lowermost *Aphelaspis* subzone must occur below the lowest horizon from which *Aphelaspis camiro* was recovered (Palynology sampling point 08BP-35 at 168 m). *Coosia alethes* is one of a number species that define the central subzone of the *Crepicephalus* trilobite zone and occurs in the upper part of that zone (Rasetti, 1965). *Coosia alethes* occurs in one sample (08BP-24) 147 m above the base of the Nolichucky Shale at Thorn Hill. Therefore the upper *Crepicephalus* subzone, the top of which marks the *Crepicephalus/Aphelaspis* boundary (base of Furongian) must occur above the 135 m sampling point. Thus the base of the Furongian in the Nolichucky Shale at Thorn Hill, must occur somewhere

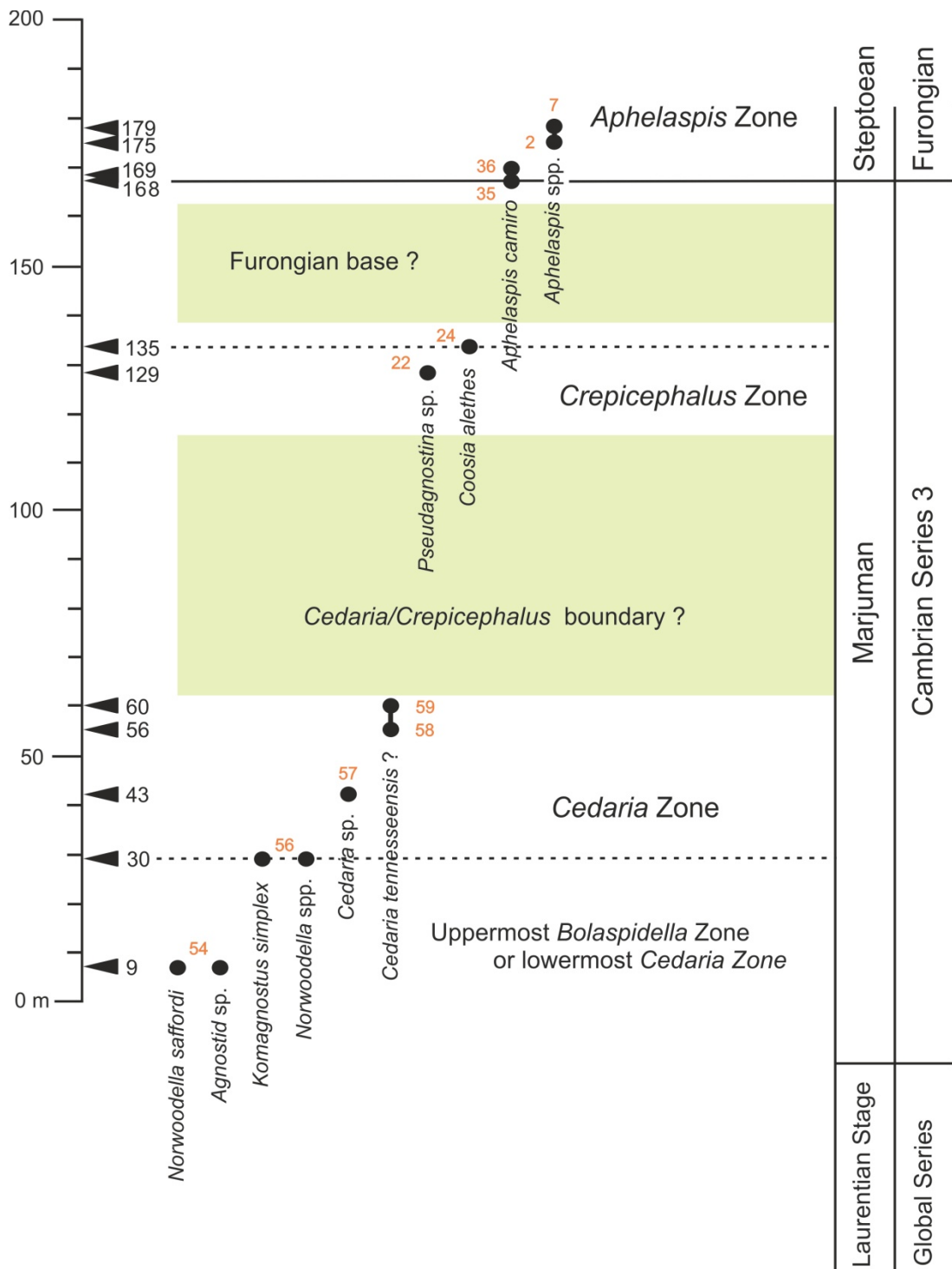


Figure 6.1. Occurrence of stratigraphically significant trilobites within the Nolichucky Shale at Thorn Hill, and accorded trilobite zones. Equivalent palynology sample numbers are in red. Green areas represent possible boundary positions.

between 135 m (sample 08BP-24) and 168 m (sample 08BP-35), (Yellow zone in Fig. 6.4) sandwiched between the uppermost *Crepicephalus* subzone and the lowermost *Aphelaspis* subzone. Furthermore, that the section at and above the 168 m horizon is Furongian. It should be noted that the global chronostratigraphic marker for the base of the Furongian, the trilobite *Glyptagnostus reticulatus*, was not found, and as far the present author is aware has not been recorded in North America.

The oldest significant trilobites recovered were *Norwoodella saffordi* from 9 m above the base of the Nolichucky Shale (sample 08BP-54), and *Kormagnostus simplex* at 30 m (sample 08BP-56). According to Derby (1996), *Kormagnostus simplex* is restricted to the upper part of the *Cedaria* Zone, while *Norwoodella saffordi* ranges through roughly the lower third to quarter of that zone, and into the uppermost strata of the underlying *Bolaspidella* Zone. Consequently, the horizon at 9 m (sample 08BP-54) might be a lower *Cedaria* zone collection, but might also be a bit older, representing uppermost *Bolaspidella*. In either case, it remains a collection from the Marjuman Stage. The section between 9 m and 30 m, therefore, either contains the *Bolaspidella/Cedaria* zones boundary or belongs completely to the *Cedaria* zone.

Trilobite collections from 30 m to 60 m in the section appear to represent the Cambrian Series 3 (Lincolnian Series) *Cedaria* zone, placing that interval in the lower part of the Marjuman Stage. No trilobites were recovered between 60 m and 135 m and therefore no trilobite zones or ranges could be confidently assigned. However, *Coosia alethes* (present at 135 m) is a species characteristic of the upper part of the *Crepicephalus* Zone (Rasetti, 1965), and therefore at least some part of the barren interval belongs to the *Crepicephalus* Zone, which will overly the *Cedaria* zone somewhere in the barren interval. Rasetti (1965) noted.. “At all localities studied, an unfossiliferous interval in the Nolichucky Shale separates the uppermost beds carrying a *Cedaria* fauna from the lowermost beds holding a *Crepicephalus* zone fauna.” So the gap in the Thorn Hill, Nolichucky Shale section is typical of the area.

6.3 Carbon isotope stratigraphy

6.3.1 Introduction

A major carbon isotope excursion (SPICE) in Laurentia, of Furongian (Steptoean) age, was reported by Brasier (1993) and Saltzman et al. (1998) in the Great Basin of the western USA and has subsequently been reported globally (Runnegar & Saltzman 1998; Saltzman et al. 2000; Ahlberg et al., 2008; Kouchinsky et al. 2008). SPICE represents the largest positive carbon isotope excursion in Cambrian Series 3 and Furongian units with a deflection of up to +5‰ (Zhu et al. 2006). Its onset is broadly coincident with the FAD of *Glyptagnostus reticulatus*, the marker for the Global boundary Stratotype Section and Point (GSSP) for the base of the Furongian (Peng et al., 2004). However, determining precisely where ^{13}C values begin to depart from baseline ^{13}C values is difficult (Saltzman et al., 2004) and other stratigraphic controls should be utilised where possible. Even so, the onset of SPICE can give an approximate indication as to the proximity of the base of the Furongian and the Laurentian Steptoean Stage (Saltzman et al., 1998, 2004).

SPICE has been recorded by Brasier (1993), and Saltzman et al. (1998, 2000; 2004) in the western USA and by Glumac & Walker (1998) at Thorn Hill, Tennessee. All of these studies, however, analysed carbonates, and this study is the first to use Cambrian Laurentian organic residues (Total organic content = TOC) for carbon isotope analysis. Forty nine samples from the Nolichucky Shale (43 samples), Maynardville Limestone (5 samples) and Copper Ridge Dolomite (1) were investigated in order to ascertain their stable carbon isotope ratios (^{13}C values). After treatment in HF and HCl an aliquot of organic residue was set aside for carbon isotope analysis (See chapter 3.2.11 for methods).

6.3.2 Results

The results of carbon isotope analysis performed on shales from the Nolichucky Shale, Maynardville Limestone and Copper Ridge Dolomite are given in Table 6.1 and Fig 6.3. The base of the Maynardville Limestone is at 197.10 m and the base of the Copper Ridge Dolomite at 244.60 m.

Table 6.1 Stable isotope data from Thorn Hill, Tennessee, USA.

Sample	Depth (m)	^{13}C (1) (PDB)	^{13}C (2) (PDB)	%C
18 Cr	247.30	-26.3611	-	3.06
17 Md	233.00	-25.5107	-	4.35
16 Md	226.85	-24.8545	-	3.9
15 Md	203.10	-26.9146	-	7.86

14 Md	197.55	-27.0416	-	3.71
13 Md	190.75	-27.4786	-	6.68
12 No	185.00	-27.4552	-	10.14
11 No	184.55	-27.4144	-	5.67
10 No	183.35	-26.9009	-	13.42
9 No	182.30	-27.3414	-	8.29
8 No	180.35	-27.7358	-	5.36
6 No	179.00	-27.43.95	-	10.56
6 No	179.00	-	-27.2432	11.46
5 No	175.75	-27.7381	-	6.63
4 No	177.55	-27.0802	-	9.63
3 No	176.95	-27.2075	-	5.08
1 No	175.15	-27.4662	-	13.74
39 No	172.85	-26.9044	-	10.1
38 No	171.10	-27.3183	-	22.03
37 No	169.40	-27.8067	-	9.6
36 No	168.80	-27.3863	-	15.07
35 No	168.50	-27.8195	-	8.65
34 No	167.90	-28.0742	-	6.33
33 No	165.10	-28.2382	-	11.2
33 No	157.50	-28.8468	-	7.1
31 No	154.70	-28.5277	-	11.09
30 No	153.20	-22.8866	-	10.83
29 No	144.90	-29.4679	-	21.6
28½ No	139.00	-28.5125	-	11.6
28 No	138.10	-29.7007	-	5.23
28 No	138.10	-	-29.6303	3.11
26½ No	137.50	-29.3129	-	10.95
26 No	136.10	-29.1468	-	6.38
25 No	135.85	-28.9956	-	8.94
25 No	135.85	-	-28.9001	9.50
24 No	135.30	-29.3429	-	2.82

23 No	135.10	-28.2024	-	14.94
22 No	129.80	-29.6183	-	3.49
21 No	106.20	-29.3349	-	11.82
20 No	103.45	-28.8861	-	10.77
19 No	103.30	-29.6788	-	13.81
61 No	91.80	-27.7398	-	22.10
60 No	69.50	-28.4598	-	12.91
59 No	60.00	-28.7304	-	17.83
58 No	56.20	-29.1545	-	16.73
57 No	43.20	-29.3666	-	15.72
57 No	43.20	-	-29.4101	14.69
56 No	30.60	-28.5287	-	13.92
55 No	27.80	-28.5429	-	25.42
54 No	8.4	-28.8702	-	14.70
53 No	2.65	-30.6253	-	8.24
53 No	2.65	-30.1053	-	7.06
52 No	0.10	-	-30.0814	5.03

6.3.3 Discussion

Glumac and Walker (1998) recorded SPICE in carbonates from the uppermost Nolichucky Shale, Maynardville Limestone and the Copper Ridge Dolomite from Thorn Hill (Fig. 6.2). Their record of the SPICE event begins in the upper section of the Nolichucky Shale with a ^{13}C value of +0.16 ‰. It increases through the Maynardville Limestone, peaks close to the Maynardville Limestone/Copper Ridge Dolomite boundary (^{13}C +4.78 ‰) and then decreases through the Copper Ridge Dolomite back to pre-SPICE values (^{13}C +1 ‰). This gives an excursion-range of between 4 ‰ and 5 ‰. The base of their carbonate ^{13}C curve appears to represent a time after the onset of SPICE; i.e. the curve does not record SPICE emerging from pre-SPICE values, and therefore the onset of SPICE is not recorded and must occur slightly earlier in the section.

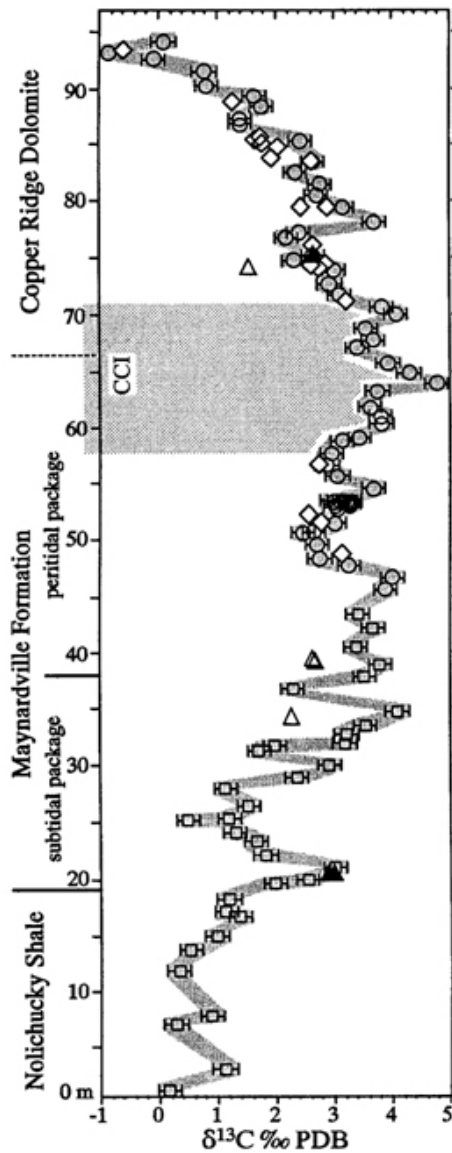


Fig. 6.2 Plot of ^{13}C values (‰) of carbonates as a function of stratigraphic position of the samples, from the Upper Cambrian section at Thorn Hill. (From Glumac and Walker, 1998).

Generally, specific TOC ^{13}C values are different from carbonate ^{13}C values, but relative variations within their respective curves, resulting from the same event, are approximately the same (notwithstanding decoupling as a result of coeval or later diagenetic geochemical processes). The trajectory of the TOC ^{13}C curve as recorded for this report (Fig. 6.3) is similar to that of the carbonate ^{13}C curve recorded by

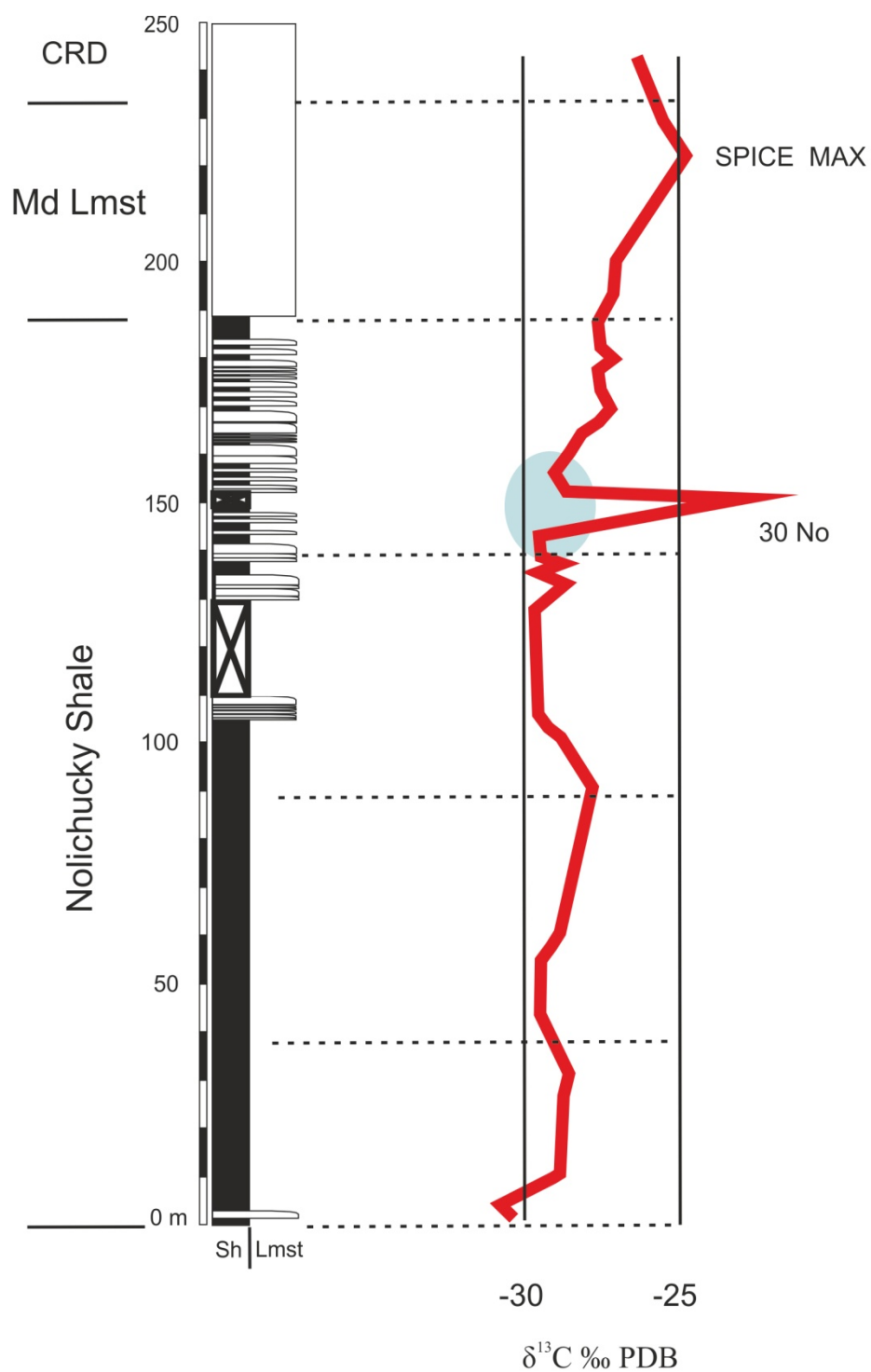


Figure 6.3 Plot of ^{13}C values (‰) of organic residues through the Nolichucky Shale, Maynardville Limestone and lowermost Copper Ridge Dolomite at Thorn Hill. Sh = shale; Lmst = limestones; Md Lmst = Maynardville Limestone; CRD = Copper Ridge Dolomite. The blue circle indicates the approximate position for the onset of SPICE (~140-160 m).

Glumac and Walker (1998) in that they both show a steady increase in ^{13}C values through the upper section of the Nolichucky Shale and the Maynardville Limestone and peaking close to the Maynardville Limestone/Copper Ridge Dolomite boundary. Also, the range of both ^{13}C curves, each between 4 ‰ and 5 ‰, through similar stratigraphic thicknesses, compare favourably. However, a comparison cannot justifiably be made between the two ^{13}C curves in the Copper Ridge Dolomite due to there being only one analysed TOC sample from that formation, despite its seemingly conformable value. It should be noted that one sample, 08BP-30 (Fig 6.3), has an anomalously high TOC ^{13}C value (-22.8866) which cannot be explained nor confirmed due to a lack of material from sample 08BP-30.

The Thorn Hill TOC ^{13}C data set includes the whole of the Nolichucky Shale and shows the onset of SPICE occurring somewhere between 50 m and 30 m (Fig. 6.3: blue circle indicates possible position of SPICE onset) below the base of the Nolichucky Shale/Maynardville Limestone boundary, and 10-30 m below the base of the carbonate ^{13}C curve of Glumac and Walker. It is within this interval that SPICE systematically increases above baseline ^{13}C values (approximately -30.000 to 28.5000). This suggests the base of the Furongian and the Steptoean Stage might be 140-160 m above the base of the Nolichucky Shale which is equivalent to samples 08BP-28½ to 08BP-33.

6.4 Combined trilobite and carbon isotope stratigraphy

The occurrence of the trilobite *Aphelaspis camiro* at 168 m (equivalent to sample 08BP-35) gives a maximum depth for the base of the Furongian, whilst the occurrence of *Coosia alethes* at 135 m (equivalent to sample 08BP-24) gives a minimum depth. This leaves a stratigraphic range of 33 m (135-168 m) within which the base of the Furongian must lie. The carbonate ^{13}C curve of Glumac and Walker (1998) suggests that the SPICE onset occurs somewhere slightly below the base of their sample range situated 20 m below the top of the Nolichucky Shale (~170 m above the base of the Nolichucky Shale). This is confirmed by the TOC ^{13}C curve which suggests the base of the Furongian is somewhere between 140 m and 160 m above the base of the Nolichucky Shale and is stratigraphically equivalent to the position indicated by trilobites (Figs. 6.3, 6.4). Therefore the approximate position

(within a range of 33 m) of the base of the Furongian in the Nolichucky Shale at Thorn Hill is identified and mutually confirmed by two independent means.

6.5 Palynomorphs and biostratigraphy

No known acritarchs were recovered from the Nolichucky Shale, Maynardville Limestone or Copper Ridge Dolomite at Thorn Hill that unequivocally indicate the age of those formations. Many taxa either part-resembled known forms, were newly discovered or extended known ranges. However, the approximate position of the base of the Furongian as identified by trilobite and carbon isotope stratigraphy, means that the acritarchs described from the Thorn Hill section are of either Marjuman (Guzhangian, Cambrian Series 3) or Steptoean age (Paibian, Furongian).

Two forms from the Nolichucky Shale, *Apodastoides* cf. *verobturatus* Grey, 2005 and *Cerebrosphaera* cf. *buickii* Butterfield 1994, very closely resemble Neoproterozoic forms and really only differ in size. Their presence in the Cambrian is therefore surprising and interesting. They might represent relict populations and this could explain their diminutive size (Lilliputism). That they are reworked should not be ruled out, although their size is small compared to their Neoproterozoic counterparts and seems unlikely. Other Neoproterozoic forms encountered at Thorn Hill are *Leiosphaeridia kulgunica* Jankauskas 1980 and *Navifusa actinomorpha* (Maithy) Hoffman & Jackson 1994 which, if truly in situ, would have their ranges extended into uppermost Cambrian Series 3. *Leiosphaeridia minutissima* (Naumova 1949) emend. Jankauskas, in Jankauskas et al., 1989, is mostly restricted to the Neoproterozoic but is occasionally found in Cambrian Series 1 and 2 (e.g., Steiner & Fatka, 1996). Its occurrence at Thorn Hill is the first record of it in the Cambrian Series 3 and Furongian.

Acritarchs recovered from Thorn Hill which have only previously been recorded elsewhere from the early Cambrian (Cambrian Series 1 & 2) include *Comasphaeridium brachyspinosum* and *Comasphaeridium mackenzianum*. *C. brachyspinosum* was recovered from Cambrian Series 3 and Furongian units, whilst *C. mackenzianum* was recovered from Cambrian Series 3 units only.

The presence of a number of Neoproterozoic and Cambrian Series 1 & 2 forms appearing higher in the geological column at Thorn Hill, does prompt the suspicion that they may be reworked. However, the preservation of many of these specimens is

no different from that of co-occurring forms, and so identifying reworked specimens (suspected or otherwise) is difficult if not impossible. Comparisons to other coeval sections and ones older are required to resolve this problem.

Strother (2008) described the range of *Auritusphaera bifurcata* as being from the uppermost part of the *Crepicephalus-Cedaria* trilobite zone to the lowermost part of the *Aphelaspis* trilobite zone, a range of 34 m. He described both these trilobite zones as being Furongian. In fact the base of the Furongian in Laurentia is marked by the base of the *Aphelaspis* trilobite zone, with the *Crepicephalus-Cedaria* trilobite zone representing Cambrian Series 3 deposits. Therefore the range of *A. bifurcata* is actually uppermost Cambrian Series 3 (uppermost Marjuman = uppermost Guzhangian) to lowermost Furongian (lowermost Steptoean = lowermost Paibian). As such, the occurrence of *A. bifurcata* straddles the boundary between Cambrian Series 3 and the Furongian and is confirmed at Thorn Hill. At Thorn Hill *A. bifurcata* is recorded in three samples (08BP-19, 08BP-20 & 08BP-11). Samples 08BP-19 & 08BP-20 occur approximately 60 m below the base of the Furongian and are within Cambrian Series 3. Sample 08BP-11 occurs in the Furongian. Strother (2008) briefly discussed the potential of *A. bifurcata* as a marker for the Marjuman/Steptoean Laurentian Stage boundary (base of Furongian), but given its stratigraphic occurrence at Thorn Hill, it would be more accurate to say it represents Guzhangian to Paibian deposits and not necessarily close proximity to the base of the Furongian.

One specimen of *Corollasphaeridium wilcoxianum* Martin in Dean & Martin, 1982 emend. Martin 1992 was recovered from sample 08BP-33, which most likely represents lowermost Furongian deposits. *C. wilcoxianum* has previously been recorded from uppermost Furongian- Tremadoc(?) units (basal silty member of the Survey Peak Formation) in the Wilcox Pass, Alberta, Canada (Dean & Martin, 1982; Martin, 1992) and the Xiaoyangqiao section, Jilin Province, China (Yin, 1986; Chen et al., 1988). Martin (1992) described six acritarch-based microfloras (AU1-AU6) ranging from uppermost Furongian to Lower Ordovician (Survey Peak, Outram and lowermost Skoki Formations, Wilcox Pass). The second of these (Microflora AU2) was formally proposed as the *Corollasphaeridium wilcoxianum* Zone with the eponymous taxon marking the lower boundary of the zone in the uppermost

Furongian; the upper boundary was not defined. At Thorn Hill *C. wilcoxianum* occurs 3.4 m below the occurrence of the trilobite *Aphelaspis camiro*. Given that another trilobite subzone exists below the horizon containing *Aphelaspis camiro* (Rasetti, 1965), the base of which marks the base of the Furongian, the stratigraphic position of *C. wilcoxianum* at Thorn Hill is most likely lowermost Furongian, just above the Furongian base. This therefore extends the range of *C. wilcoxianum* such that it covers the entire range of the Furongian.

The global occurrence of *Wiwaxia* appears to be restricted to Cambrian Series 3 deposits (Butterfield, 1994) indicating it became extinct at or before the beginning of the Furongian. If this is the case then the occurrence of *Wiwaxia* sclerites in sample 08BP-29 (Horizon 08BP-29: 145 m above the base of the Nolichucky Shale) could be interpreted as representing a minimum depth for the top of Cambrian Series 3 (Fig. 6.4: blue dotted line). Interestingly the ranges of eighteen acritarch taxa terminate at or very close to this horizon (horizon 08BP-29) (See Fig. 6.4: *Leiosphaeridia kulgunica*, *Comasphaeridium mackenzianum*, *Comasphaeridium* sp. 2, *Cymatiosphaera* sp. 1, *Navifusa* sp. 1, *Navifusa* sp. 2, *Navifusa actinomorpha*, *Auritusphaera* cf. *bifurcata*, *Virgatasporites* sp. 1, *Cerebrosphaera* cf. *buickii*, *Rhopaliophora* sp. 1 and *Acritarch* sp. 1, 2, 5, 8, 9, 10, 11). Other taxa either continue through this horizon or, in a few cases, appear briefly just above the horizon (*Corollasphaeridium wilcoxianum*, *Cymatiogalea* cf. *virgulta*, *Timofeevia* cf. *pentagonalis*, *Acritarch* sp. 4). It appears therefore that an extinction of phytoplankton possibly occurred at this horizon, although the disappearance of the eighteen acritarch taxa at or around horizon 08BP-29, may also be interpreted as a change to an offshore facies. In either case, a marked change in the environment in the palaeogeographic vicinity represented at Thorn Hill clearly occurred.

In Laurentia a major extinction of shallow shelf trilobites occurred at the end of Cambrian Series 3 and although the exact causes are unknown, it is related to a major regression (Palmer, 1965, Lochman-Balk, 1971). At Thorn Hill there is clear change up section from predominantly shale units (Nolichucky Lower Shale Member), through interbedded shales and limestones (Middle Limestone Member and Upper Shale Member) and into predominantly limestone units (Maynardville Limestone/Copper Ridge Dolomite). This change from shales to limestones records a drop in sea level from shallow marine, as represented by the Nolichucky Shale, through to subtidal and peritidal deposits in the

upper Maynardville Limestone and Copper Ridge Dolomite (Glumac & Walker, 1998, 2000). The regression maximum occurs at the Maynardville/Copper Ridge transition and marks the Sauk II-Sauk III subsequence boundary (Glumac & Walker, 1998; Lochman-Balk 1971; Osleger & Read, 1993).

Therefore, the change in trilobite fauna (from *Crepicephalus* fauna to *Aphelaspis* fauna) somewhere between samples 08BP-24 (135 m) and 08BP-35 (168 m) (Yellow zone in Fig. 6.4), and which would mark the Furongian base, is generally coincident with a regression, but its exact stratigraphic location is still unknown. It is not unreasonable to imagine that the acritarch extinction at or around horizon 08BP-29 (145 m) is the result of the same environmental changes which promoted the trilobite species turnover, and that the two events were coeval. If this were the case, the acritarch extinction event, which occurs at and around horizon 08BP-29, would indicate the position of the Cambrian Series 3/Furongian boundary. However, it cannot be assumed that the trilobite species turnover and the acritarch extinction event were exactly coincident, and a more thorough investigation of the trilobite stratigraphy at Thorn Hill, specifically around horizon 08BP-29, is required to give a more exact position for the Furongian base.

It should be noted that the acritarch extinction event does represent a significant palynostratigraphic marker for the proximity to the Cambrian Series 3/Furongian boundary in shallow marine facies, and might be a useful correlative tool when compared to other shallow marine, Laurentian systems. Also two acritarchs, Acritarch sp. 1 and Acritarch sp. 2 are very distinctive and large, have short ranges and both terminate at the extinction event. This makes them good candidates for being palynostratigraphic markers for uppermost Cambrian Series 3.

6.6 Conclusion

Using carbon isotope chemostratigraphy and trilobite biostratigraphy, the Cambrian Series 3/Furongian boundary at Thorn Hill is indicated to be within a 33 m stratigraphic range in the uppermost section of the Nolichucky Shale. The 33 m range is between samples 08BP-24 (135 m) and 08BP-35 (168 m). The Furongian trilobite *Aphelaspis camiro* (168 m) marks the maximum depth for the base of the Furongian Series and the Cambrian Series 3 trilobite *Coosia alethes* marks the minimum depth for the top of Cambrian Series 3. This is confirmed by the recorded onset of SPICE within the same stratigraphic section.

Refinement of the position of the base of the Furongian within the 33 m range is speculative. It assumes the occurrence of *Wiwaxia* sclerites marks a minimum position for the top of Cambrian Series 3. Approximately coincident with this is an acritarch extinction event which may or may not be coincident with a trilobite species turnover event which would mark the Cambrian Series 3/Furongian boundary. This would place the base of the Furongian close to sample 08BP-29 (145 m).

Known, stratigraphically significant acritarchs were not recovered from Thorn Hill. However, Acritarch sp.1 and Acritarch sp.2 are potentially useful biostratigraphic markers for uppermost Cambrian Series 3. Also, the extinction event does represent a significant palynostratigraphic marker for proximity to the Cambrian Series 3/Furongian boundary in shallow marine facies, and might be a useful correlative tool when compared to other shallow marine, Laurentian systems.

Chapter 7

Palynofacies and palaeoenvironment

7.1 Sedimentology and palaeoenvironmental interpretation

The Nolichucky Shale consists of three members, the Nolichucky Lower Shale Member, the Nolichucky Middle Limestone Member and the Nolichucky Upper Shale Member. The Shale members represent moderate water depths with the Lower Shale Member representing maximum flooding on the carbonate platform (Weber, 1998). The Nolichucky Lower Shale member represents an increase in water depths on the carbonate platform and the Middle Limestone Member represents a sea level fall (Markello & Read 1982). However, due to part of the section being obscured, the presence of the Nolichucky Middle Limestone Member at Thorn Hill could not be confirmed.

Samples 08BP-52 through to 08BP-61 belong to the Nolichucky Lower Shale Member; samples 08BP-22 through to 08BP-39, and 08BP-1 through to 08BP-12 belong to the Nolichucky Upper Shale Member. Because the presence of the Nolichucky Middle Limestone Member could not be confirmed, samples 08BP-19, 08BP-20 and 08BP-21 are only suspected as belonging to it.

The Maynardville Limestone has been interpreted as representing a period of upward shallowing from subtidal to peritidal deposits and represents deposition on a gently sloping subtidal ramp with localised shoal and lagoonal environments (Glumac & Walker 2000). In the uppermost section there are upward transitions from thrombolites through digitate, columnar and domal stromatolites to microbial laminites (stratiform stromatolites) (Glumac & Walker, 2000) which represent a shoreward transition from subtidal to supratidal environments (Glumac & Walker, 1997). The occasional occurrence of desiccation cracks indicate subaerial exposure, and along with the variety of peritidal settings ranging through the vertical succession, reflect a complex pattern of subtle, laterally shifting microenvironments along a wide restricted tidal flat (Glumac & Walker, 2000).

The Copper Ridge Dolomite lies conformably above the Maynardville Limestone. The transition, however is marked by the occurrence of quartz sand in the carbonate

platform deposits. This has been interpreted as migration towards siliciclastic source areas in response to sea level fall and the subaerial exposure of the craton (Glumac & Walker, 1998). The transition marks the late Steptoean (Dresbachian/Franconian or Sauk II-Sauk III subsequence boundary) unconformity (Lochman-Balk, 1971; Osleger & Read, 1993).

In broad terms the section consisting of the Nolichucky Shale, Maynardville Limestone and Copper Ridge Dolomite represents a period of regression from moderate water depths in the Nolichucky Shale through to peritidal and subaerial deposits in the uppermost Maynardville Limestone and Copper Ridge Dolomite. A brief period of sea level rise occurs in the lower part of the Nolichucky Shale and a period of sea level fall occurs in the middle of the Nolichucky Shale.

7.2 Palynofacies

7.2.1 Classification

For the purpose of palynofacies analysis, palynomorphs were placed into eight categories as defined below. Random counts of 300 specimens were taken for each sample.

7.2.1.1 Acritarchs

This group consists of all acritarchs with the exception of smooth-walled sphaeromorphic forms.

7.2.1.2 Sphaeromorph acritarchs

All smooth-walled sphaeromorphs with a vesicle diameter $\geq 20 \mu\text{m}$ are included in this group. However, some sphaeromorphic forms have a wide range of vesicle diameters which occasionally straddle $20 \mu\text{m}$. In such cases those specimens with a diameter $<20 \mu\text{m}$ but clearly represent the lower end of a size spectrum which straddles $20 \mu\text{m}$, are included in this group.

7.2.1.3 Cells and cryptospores

Numerous small sphaeromorphs or cells ($<20 \mu\text{m}$) were observed, occurring mainly in groups (aggregates) but also singularly. Sphaeromorphs with diameters $<20 \mu\text{m}$ are included in this group unless they represent a form with a size spectrum that straddles $20 \mu\text{m}$. Also, a variety of small dyads and tetrads were observed and are

classed as putative cryptospores. For the purposes of counting an aggregate represents one count.

7.2.1.4 Amorphous organic matter (AOM)

Amorphous organic matter (AOM) is typically structureless, heterogeneous or homogeneous, often fluffy and ranging in colour from yellow through to brown hues. It represents decayed, non-carbonised, biogenic material. For the purposes of counting particles <10 µm were excluded.

7.2.1.5 Inertinite

Inertinite consists of predominantly opaque, black carbonized fragments which range from elongate and shard-like to broadly equidimensional. Edges tend to be smooth, straight to rounded and outlines are irregularly angular. For the purposes of counting particles <10 µm were excluded.

7.2.1.6 Cuticular fragments

A wide variety of cuticular fragments were observed in the Thorn Hill samples. They ranged from very pale to dark brown and smooth to ornamented, occasionally with large spines. The edges are smooth to irregularly angular and frequently appear torn. They most likely represent the cuticle of animals, although they may be derived from complex, multinucleate algae. Also included in this group are branchiopod-type limbs and mandibles and copepod-type mandibles.

7.2.1.7 Plates

This group consists of plate-like forms which commonly occur in some samples. They have regular, circular to arch-shaped morphologies, occasionally elongate and range in size from 20-130 µm. Frequently they regularly decrease in thickness towards their edges to form a thin, peripheral rim. They are solid and range in colour from yellow to dark brown. A variety of forms were observed with distinctive and consistent features including shape, size, texture and peripheral rim dimensions and occurrence. A dedicated study of these forms may well reveal a number of clearly defined morphotypes, but such a study is beyond the scope of this project. However, they are interpreted by the present author as being a unique and distinctive palynomorph group and as such are included in the palynofacies counts. Because they resemble some invertebrate sclerites they are named informally as plates,

although their provenance is as yet unknown. *Wiwaxia* sclerites are included in this group.

7.2.1.8 Spines

A large array of individual disarticulated spines were recovered and are interpreted as being metazoan in origin. They range from 25-150 μm in length.

7.2.1.9 Filaments

Relatively thin, elongate forms are included in this group.

7.2.1.10 Graptolite cuticle

This group consists of graptolite periderm. It is differentiated from other cuticular fragments in possessing distinctive patterning consisting of repeated, overlapping, approximately concentric thickenings.

7.2.1.11 Problematica

This group consists of multinucleate algae (Problematica 1 & 2) and are interpreted as possible mat-forming shallow marine forms.

7.3 Discussion

For this section refer to StrataBugs chart 2.

The abundance of palynomorphs in the Nolichucky Shale is generally low (in many cases <1 specimen per gram) and it is therefore difficult to make any meaningful interpretations with regard changes in the palaeoenvironment. However, some variation does occur which might suggest changes in sea level. The lowermost section of the Nolichucky Shale (20-80 m) is marked by high abundances of small cells, inertinite and AOM and a rise and fall in the abundances of small cells, sphaeromorphs, filaments, graptolite cuticle, cuticular fragments and plates. The decline in the latter might be interpreted as a response to a sea level rise. The abundance of acritarchs increases gradually, peaking at around 90 m before steadily declining over the next 100 m. This trend is coincident with an increase in sea level and gradual flooding of the carbonate bank, followed by a shallowing into the Maynardville Limestone. The acritarch peak is broadly coincident with the decline of small cells, sphaeromorphs, filaments, graptolite cuticle, cuticular fragments and plates and may represent a maximum depth in the Nolichucky Lower Shale Member

where conditions were favourable to phytoplankton, and less favourable to invertebrates. If the acritarchs as a group are interpreted as phytoplankton which prefer deeper waters and are tentatively used as a proxy for water depth, then the maximum depth occurs at their peak at around 90 m, just within the Lower Shale Member of the Nolichucky Shale.

A notable feature is the rapid increase in the abundance of problematica which begins around 160 m in the uppermost Nolichucky Shale and continues into the Maynardville Limestone, where it rapidly declines at around 200 m. The appearance at this point of shallow subtidal to peritidal environments indicates that the Problematica represent forms preferring lagoonal or tidal flat environments. This would support the hypothesis that they are benthic.

7.4 Conclusion

The abundance of palynomorphs is low in the Nolichucky Shale and Maynardville Limestone, precluding any meaningful palaeoenvironmental interpretation. In general terms the sea level fluctuations interpreted by some workers (e.g. Glumac & Walker, 1998; 2000) are not emphatically represented in the palynofacies analysis. However, a transgression appears to be recorded in the first 90 m followed by a regression in the overlying 120 m with the peak in acritarch abundance possibly marking maximum flooding on the carbonate platform.

Chapter 8

Large spinose acritarchs from the Cambrian of the USA: biological affinities

8.1 Introduction

Four large spinose acritarchs (*Acritarch* sp. 1, *Acritarch* sp. 2, *Peteinosphaeridium?* sp. 1 and *Peteinosphaeridium?* sp. 2. See Systematics chapter for descriptions) recovered from the Nolichucky Shale at Thorn Hill, Tennessee and the Gros Ventre Formation, exposed along the Chief Joseph Highway in Wyoming, exhibit anomalously large vesicle dimensions and are therefore considered worthy of further examination with regard to their biological affinities. This chapter includes discussions on the size-controlling factors of phytoplankton and the possible affinities of acritarchs. It also presents evidence for a possible metazoan origin for *Acritarch* sp. 1 using vesicle size and ornament, cell-wall chemistry (acid resistance), wall ultrastructure analysis using transmission electron microscopy (TEM), and crustacean co-occurrence. Evidence for the Chlorophyceae affinities of *Acritarch* sp. 2, *Peteinosphaeridium?* sp. 1 and *Peteinosphaeridium?* sp. 2 is also considered.

Acritarchs were originally described as having unknown affinities (Evitt, 1963a,b) but have subsequently become more regarded as probable precursors either to the dinoflagellates and green microalgae (Downie & Sarjeant, 1963; Evitt, 1963a, 1963b, 1985; Tappan, 1980; Colbath, 1990; Colbath & Grenfell, 1995; Wicander, 2007) or animal egg cases (Van Waveren, 1992; Van Waveren & Marcus, 1993; Cohen et al., 2009). Additionally, Butterfield (2005a) identified the microfossil *Tappania* Yin Lei-ming 1997 as a putative fungi. These informal assignments are based on similarities of size, morphology, environmental distribution, and acid-resistant, sporopollenin cell-wall chemistry. However, these factors alone are not enough for confident assignment of acritarch species to known taxonomic lineages and other approaches are required. Over the past few decades a number of new approaches have been applied to the better understanding of acritarch affinities. These include analysis of cell wall ultrastructure using transmission electron microscopy (TEM) (Oelher, 1976; Arouri et al., 1999, 2000; Talyzina & Moczyłowska, 2000; Javaux et al., 2004; Javaux & Marshal, 2006; Willman &

Moczyłowska, 2007; Moczyłowska & Willman, 2009; Willman, 2009), biomarker (molecular fossils) analysis using energy dispersive spectroscopy (EDS), micro-FTIR, pyrolysis GC-MS and laser Raman microprobe (Arouri et al., 2000; Talyzina et al., 2000), fluorescence microscopy (Talyzina et al., 2000) and synchrotron-radiation X-ray tomographic microscopy (SRXTM) (Donoghue et al., 2006). The results, although not conclusive, are giving useful data, particularly with regard to cell wall ultrastructure-types, and are providing a platform upon which future work may build.

8.2 Algal affinities of acritarchs

A number of studies regarding the algal affinity of Cambrian acritarchs have focused on material from the Cambrian Lükati Formation in Estonia due to its excellent preservation (Talyzina et al., 2000; Talyzina & Moczyłowska, 2000; Moczyłowska & Willman, 2009; Moczyłowska, 2010; 2011). Analysis of Cambrian acritarchs using transmitted electron microscopy (TEM) was undertaken by Talyzina & Moczyłowska (2000) and Moczyłowska & Willman (2009), who recognised four types of vesicle wall ultrastructure (Talyzina & Moczyłowska, 2000, Fig. 1, p. 16): single-layered, electron-tenuous, fibrous (*Archaeodiscina umbonulata*); single-layered, electron-dense, homogeneous (*Globosphaeridium cerinum*, *Comasphaeridium brachyspinosum*, *Skiagia compressa*); single-layered, electron-dense, homogeneous with pores/radial canals (*Tasmanites tenellus*); and composite laminated (*Leiosphaeridia* spp.). This latter ultrastructure consisted of an outer layer which was itself laminated and was recognised as a trilaminar sheath structure (TLS) by Moczyłowska & Willman (2009). Ultrastructures consisting of a composite, multilayered wall with a TLS are characteristic of modern chlorococcales microalgae (Brunner & Honegger, 1985), suggesting a possible phylogenetic affinity with those Cambrian *Leiosphaerids* possessing a similar wall ultrastructure. Moczyłowska (2010, 2011) proposed that the acritarchs studied from the Lükati Formation represent microalgae belonging to the phylum Chlorophyta (green algae) and its two classes, Chlorophyceae and Prasinophyceae. Using her own data and that of other selected references, Moczyłowska (2011 & refs. therein) placed the acritarch genera *Asteridium*, *Heliosphaeridium*, *Lophosphaeridium*, *Archaeodiscina*, *Globosphaeridium*, *Comasphaeridium*, *Skiagia*, *Polygonium*, *Multiplicisphaeridium* and *Stelliferidium* in the Chlorophyceae Class and the genera *Tasmanites*,

Granomarginata, *Pterospermella*, *Pterospermopsimorpha*, *Cymatiosphaera* and *Fimbriaglomerella* in the Prasinophyceae Class. *Leiosphaeridia* was regarded as a convergent form with different species representing Prasinophyceae (asexual resting cysts), Chlorophyceae (zygotic cysts) or vegetative cells. Previous ultrastructural studies on *Leiosphaeridia* spp. have recorded uniform single-layered walls (Kjellström, 1968; Jux, 1969; Arouri et al., 2000). This, along with the observed multi-layered structure with TLS of *Leiosphaeridia* spp. recorded by Talyzina & Moczyłowska (2000) and Moczyłowska & Willman (2009) support the polyphyletic and convergent natures of unornamented, sphaeromorphic forms.

Based on inferred functional morphology, life cycle, palaeoenvironmental distribution and cell wall biochemistry and ultrastructure, Moczyłowska (2010, 2011) also proposed that acritarchs from the *Skiagia*-plexus and the *Leiosphaeridia*-plexus represent developmental stages of alternating generations within a complex life-cycle of the same species.

The informal taxonomic group Acritarcha was erected to accommodate forms lacking key dinoflagellate characteristics, in particular paratabulation and a true archeopyle (Evitt, 1963a), and these features have subsequently not been recorded in acritarchs to date. Dinoflagellate cyst (dinocysts) ultrastructures are two- to four-layered with fibrillar, alveolar, finely laminate or striated textures (Kennaway & Lewis, 2004), and equivalent ultrastructures in acritarchs have not as yet been observed (Willman & Moczyłowska, 2007; Moczyłowska & Willman, 2009). However, a study by Talyzina et al., (2000) suggested that acritarchs from the genera *Globosphaeridium*, *Skiagia*, *Comasphaeridium* and *Lophosphaeridium* do have dinoflagellate affinities. This analysis, again on material from the Lükati Formation, used transmitted light microscopy, fluorescence microscopy and flow cytometry and biomarker analysis. Arouri et al. (2000) observed fibrillar multilayered wall ultrastructures in several Neoproterozoic species (*Tanarium* sp., *Alicesphaeridium medusoidum* and Species C2) from the Australian Centralian Superbasin which they believed corresponded to similar structures recorded in dinoflagellate cysts. However, unequivocal evidence for dinoflagellate affinity for acritarchs remains elusive and existing evidence remains controversial.

In broad terms the net results of all these studies are:

- 1) that acanthomorphic acritarchs and sphaeromorphic forms (*Leiosphaeridia*) can possess single or multiple layers within their cell walls,
- 2) some acanthomorphic acritarchs have possible affinities to the Chlorophyceae (phylum Chlorophyta),
- 3) some non-acanthomorphic acritarchs possessing pores are most likely prasinophytes (Class Prasinophyceae, phylum Chlorophyta),
- 4) affinity to dinoflagellates is unproven.

8.3 Acritarch size in the Ediacaran and Cambrian Periods

Large spinose acritarchs (LSAs) ($>100\ \mu\text{m}$) are very rare in the Cambrian (Vidal & Peel, 1993; Moczyłowska, 2011). Phanerozoic acritarchs have a maximum length or diameter of approximately 5-200 μm (Mendelson & Schopf, 1992; Martin, 1993) with the majority averaging $<100\ \mu\text{m}$ (Vidal & Peel, 1993). Cambrian acritarchs tend to be on average smaller with a range of approximately 5-100 μm (Vidal & Peel, 1993), with the majority of those being 20-60 μm (Moczyłowska, 2011). Larger Cambrian forms ($>100\ \mu\text{m}$) are mostly restricted to unornamented sphaeromorphic or tasmanitid forms (Moczyłowska & Vidal, 1992; Vidal & Peel, 1993), but a few, very rare, large, spinose acritarchs ($>100\ \mu\text{m}$) have been recorded: two species were described from the lower Cambrian Buen Formation in Northern Greenland by Vidal & Peel (1993), with dimensions $>100\ \mu\text{m}$. These were *Comasphaeridium longispinosum* Vidal 1993 (vesicle diameter: 180 μm) and *Comasphaeridium ? densispinosum* Vidal 1993 (vesicle diameter: mean 94.1 μm ; standard deviation 36.9 μm).

Very large spinose acritarchs are confined to the Neoproterozoic, in particular to the Ediacaran period (630-542 Ma), and have a size range of $\sim 200\ \mu\text{m}$ to $>850\ \mu\text{m}$ (Grey, 2005), although many smaller forms (~ 30 -200 μm) do occur (Arouri et al., 2000; Grey, 2005). The Ediacaran microflora appeared just after a period of global glaciation and underwent a rapid diversification through the Ediacaran (Sepkoski & Schopf, 1992; Knoll, 1996; Vidal & Moczyłowska, 1997; Grey, 2005; Butterfield, 2005a; Knoll et al., 2006; Moczyłowska, 2008a; Sergeev et al., 2011) before disappearing around 560 Ma (McFadden et al., 2008). In the period just before the onset of the Cambrian, acritarchs were reduced to much smaller ($>50\ \mu\text{m}$),

sphaeromorphic forms which continued through to the Cambrian and diversified (Knoll et al., 2006; Moczyłowska & Zang, 2006).

Therefore, given the disappearance of the large Ediacaran microflora prior to the Cambrian Period, and the relatively small size of Cambrian acritarchs, the recovery of four Cambrian species of large spinose acritarchs from the USA with dimensions greater than 100 μm is surprising, and prompts questions regarding their biological affinities and the environmental factors which might promote such large vesicle dimensions.

8.4 Large vesicle size and metazoan affinities

Large spinose acritarchs are particularly known from the Ediacaran (Grey, 2005) where they reached sizes $>850 \mu\text{m}$ (Grey, 2005). How they came to be so large is one of the overriding questions in Ediacaran palaeopalynology, and although a definitive answer remains elusive, attempts at resolving the question can be reduced to two, broad, none-mutually exclusive, hypotheses. The first of these relates to predation and that large vesicle size is the result of an evolutionary response to size-selective grazing by metazoans (Peterson & Butterfield, 2005) or protists (Cohen et al., 2009). There are a number of environmental factors which mediate the size of extant phytoplankton cells including cell-sinking rates and water column stability, but in general terms, the two fundamental, environmental controls are nutrient availability and predation (Chisholm, 1992; Kiorboe, 1993; Irwin et al., 2006). Therefore, the argument that the large cell-size acted as a refuge from predation, is a plausible one. However, fossil evidence for the presence of planktonic grazers in the Ediacaran has not been forthcoming. In fact the fossil evidence for Ediacaran metazoans is limited to eumetazoan trace fossils in the Verkhovka Formation ($>558 \text{ Ma}$) of northwest Russia (Martin et al. 2000; Grazhdankin, 2004) and the Ediacaran biota (575-542 Ma) whose affinities, despite bearing some comparison to animals, remain unknown (Narbonne, 2005).

In the absence of direct fossil evidence for predators (metazoan or protist) in the Ediacaran, Peterson & Butterfield (2005) took a different approach and used molecular clock methods, which gave an estimate for the first-appearance-time of motile macrophagous predators of 634-604 Ma. Additionally, they used the record of Neoproterozoic acritarch species diversity as a proxy for eumetazoan presence or

absence. The evolutionary stasis of pre-Ediacaran acritarch populations was interpreted as evidence for eumetazoan absence, whilst the rapidly evolving Ediacaran acanthomorphs as evidence for presence, the latter being coincident with the molecular clock estimate. Even so, predation on Proterozoic acritarchs is difficult to prove, and the hypothesis that Ediacaran acritarchs attained such very large dimensions in response to predation is based on circumstantial evidence and remains no more than a possibility. However, the radiation of acritarchs during the Cambrian is coincident with the onset of biomineralisation and the subsequent radiation of metazoans (Vermeij, 1989), and it is reasonable to assume, given the primary nature of phytoplankton in marine food-chains, that predation has played a major part in controlling phytoplankton cell-size throughout the Phanerozoic (Chisholm, 1992; Kiorboe, 1993; Irwin et al., 2006).

The second broad hypothesis for the occurrence of larger acritarch vesicles relates to possible metazoan affinity, and that some acritarchs are not phytoplanktonic in origin, but the egg cases of animals (Van Waveren, 1992; Van Waveren & Marcus, 1993; Cohen et al., 2009). It has been suggested that Ediacaran acritarch assemblages may comprise benthic or heterotrophic life stages, whereas the smaller Phanerozoic acritarchs are phytoplanktonic (Butterfield, 2005a; b; Knoll et al., 2006), and that this explains the notable difference in size between Proterozoic and Phanerozoic acritarchs. There has recently been a flurry of excitement regarding the discovery of putative animal embryos in the Ediacaran (~570 Ma) Doushantuo Formation in China (Xiao et al., 1998; Xiao, 2002; Yin et al., 2004; 2007; Donoghue et al., 2006; Hagadorn et al., 2006; Cohen et al., 2009; Chen et al., 2009). Some of these microfossils were found inside large acanthomorphic vesicles and presented as evidence for the metazoan affinities of large spinose acritarchs (Yin et al., 2004; 2007; Cohen et al., 2009). However, these microfossils have subsequently been reinterpreted as representing non-metazoan organisms (Huldtgren et al., 2011), and that features they contained, previously accorded to the embryos of bilaterian animals, are in fact the result of late diagenetic mineralization (Cunningham et al., 2012).

Despite this, other studies have produced interesting and compelling results. Harland & Sarjeant (1970) described a new organic-walled microfossil genus, *Cobricosphaeridium*, and two species *C. hebes* and *C. spiniferum* from Quaternary,

freshwater, peat deposits in Victoria, Australia. The forms possessed distinctive processes and an archeopyle, and despite the absence of paratabulation, were described as dinoflagellate cysts. A new, extant species, *Cobricosphaeridium giganteum* McMinn 1991, was described from surface sediments from the coast of New South Wales, Australia (McMinn, 1991) and was subsequently recovered from Lake Macquarie and Sidney Harbour in Australia (McMinn et al., 1992), and Port Esperance in Tasmania (Bolch & Hallengraeff, 1990). The problem was that *C. giganteum* was restricted to waters with relatively high salinities which is unusual for dinoflagellate species. This cast doubt on the taxonomic assignment of *Cobricosphaeridium* as a dinoflagellate and it was decided to incubate viable cysts of *C. giganteum* (McMinn et al., 1992). What emerged was not a dinoflagellate but the nauplius stage of a copepod.

This cautionary tale highlights the similarities that can exist between metazoan (zooplankton) egg cases and acritarchs or dinoflagellates, and it should come as no surprise that some described species of acritarchs or dinoflagellates might be zooplankton egg cases (diapause eggs). There are numerous, extant animal species which produce resting cysts with recalcitrant, acid resistant walls, which are of a size and morphology very similar to that of acanthomorphic acritarchs (Cohen et al., 2009), the most notable of these being the crustacean copepods and branchiopods.

8.5 Crustacean affinities of acritarchs

8.5.1 Copepods, branchiopods and their egg cases

Copepods and branchiopods are small aquatic crustaceans belonging to the phylum Arthropoda (Huys & Boxshall, 1991). Copepods are mostly marine but many species live in fresh water habitats, and there are planktonic, benthic and parasitic forms; planktonic forms are approximately 1-5 mm in length but some of the parasitic forms can be up to 25 cm in length (Boxshall, 1992). Branchiopods are mainly fresh-water and most species are found in ephemeral or permanent freshwater ponds, streams or lakes (Martin, 1992). Some species of both copepods and branchiopods are also found in hypersaline lakes (Moscatello & Belmonte, 2009). They range in size from approximately 0.3 to 100 mm with most being 2-50 mm (Martin, 1992). Between them, Copepods and Branchiopods have managed to colonise a wide array of environments from deep marine to shallow fresh water to hypersaline lakes and are

among the most diverse classes of crustacea (Bradford-Grieve, 2002; Martin, 1992) on the planet. They also have a fossil record going back as far as the Cambrian. Branchiopod-type and copepod-type mandibles and branchiopod-type limb structures have been reported from the Cambrian (Series 3 and Furongian) Deadwood Formation in western Canada (Harvey et al., 2012), and copepod-like maxillopodan crustaceans have been recovered from the Furongian of Sweden (Müller, 1983; Müller & Walossek, 1988; Walossek & Müller, 1998). Branchiopod-like fossils have also been reported from the Devonian Rhynie Chert (Scourfield, 1926) and the Cambrian of Sweden (Walossek, 1993), and Negrea et al. (1999) assigned a hypothetical ancestral branchiopod to Cambrian Series 3 based on cladistic analysis.

A notable characteristic of copepods and branchiopods is their ability to produce diapause eggs. Diapause is an adapted form of dormancy where the metabolism of an organism is reduced in response to the seasonal heterogeneity of environments, and is moderated by a biological predictive mechanism involving environmental signals and an internal biological clock (Alekseev et al., 2007). An organism can enter a diapause period in response to changing environmental conditions, but the period of diapause is ultimately controlled by the biological clock and diapause can persist even after the return of favourable conditions (Elgmork & Nilssen, 1978; Marcus, 1996). Periods of diapause can last weeks, years, decades or even hundreds of years (Alekseev et al., 2007). It consists of three adaptations: 1) the synchronisation by internal biorhythms of an animal's life cycle with environmental seasonal changes, mainly involving photoperiod, food availability and temperature changes; 2) the facility to reduce the metabolic rate of an embryo in response to environmental signals; and 3) the ability to produce protective structures, which have such qualities as to protect the viability of the enclosed embryo for the required period (Alekseev et al., 2007). One of the best examples of a protective structure is the resting egg (diapause egg) produced by many crustacean species, in particular copepods and branchiopods.

Many copepod and branchiopod species can switch from producing subitaneous eggs (eggs that hatch almost immediately) to diapause eggs in response to a variety of environmental changes such as the onset of anoxia or seasonal variations (Uye et al., 1979; Ban, 1992). The copepod species *Acartia josephinae* for example, switches to

diapause egg production with the onset of winter, and the eggs survive in marine bottom sediments (Belmonte & Puce, 1994). For other species, however, diapause egg production is the only form of reproduction (Martin, 1992). The main differences between subitaneous and diapause egg cases lie within their structure and biochemistry. Subitaneous egg cases tend to be single walled structures whereas diapause egg cases possess thicker, more complex walls (Couch et al., 2001), often consisting of three very distinct layers. Also, copepod diapause egg cases have a chitinous component which is absent in subitaneous egg cases (Samchyshyna & Santer, 2010). This latter feature is critical with regard to surviving harsh conditions. Branchiopod diapause egg cases are not chitinous, but consist of a complex lipoprotein with mucopolysaccharides and various other substances, which make the egg case harder than chitinous cuticle (Fryer, 1996). It has been shown that diapause eggs of some branchiopod species can withstand temperatures approaching 100°C (Carlisle, 1968) and temperatures close to absolute zero; in one experiment diapause eggs of the branchiopod *Artemia* were attached to the exterior of space-craft and remained viable after the flight (Planel et al., 1980). The present author has subjected diapause eggs of the branchiopod species *Triops longicaudatus* to palynological processing procedures, including acid (HCl & HF) immersion, and recovered unscathed eggs.

8.5.2 Comparisons between copepod/branchiopod eggs and acritarchs

Copepods and branchiopod eggs can be compared superficially to acritarchs in size, wall chemistry (acid resistance), shape, surface ornament and environmental distribution.

Size: Copepod and Branchiopod eggs have size-ranges of 40-215 μm and 120-385 μm respectively (Kasahara et al., 1974; Koga, 1968). The majority of Cambrian acritarchs are <100 μm although the largest recorded spinose Cambrian acritarch was 180 μm from the Buen Formation in north Greenland (Vidal & Peel, 1993). Therefore, with regard to size, the majority of Cambrian acritarchs compare more favourably to copepod egg cases, although larger acritarchs (>100 μm) might conceivably be compared to both copepod and branchiopod egg cases.

Wall chemistry: Acritarchs and other palynomorphs survive acid treatments in palynological processing procedures, because they possess either a sporopollenous or

chitinous component to their cell walls. Copepod diapause egg cases have a chitinous component (Samchyshyna & Santer, 2010) whilst those of branchiopods possess a mixture of complex compounds which impart a recalcitrant nature to the egg case. This means that ancient diapause eggs might be capable of withstanding both diagenetic processes and palynological processing.

Shape and surface ornament: Many copepod and branchiopod diapause eggs are spherical, (although lenticular and polygonal forms commonly occur in branchiopods), and can occur either with or without ornament (Mura & Thiery, 1986). In fact many diapause egg cases possess ornament (Gilchrist, 1978; Mura & Thiery, 1986; Milicik & Petrov, 2002; Dumont et al., 2002), and the variation between species is such that egg case ornament has been applied to taxonomy (Mura

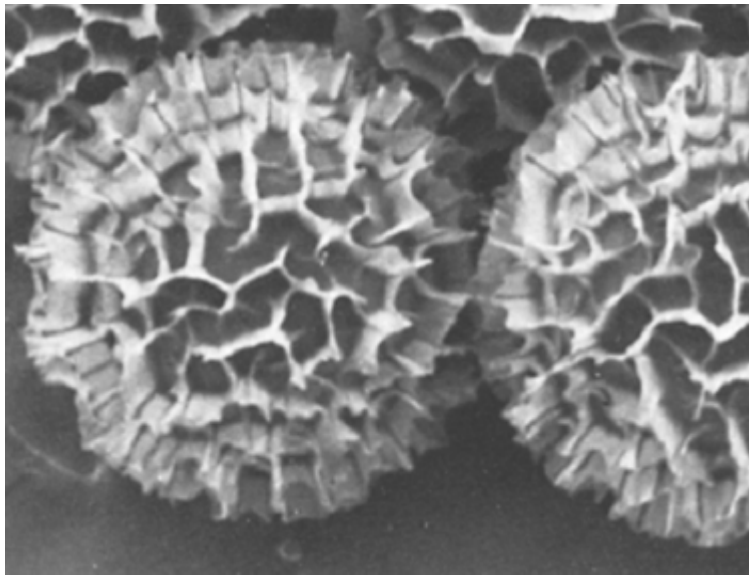


Figure 8.1 Egg cases belonging to the branchiopod *Chirocephalus diaphanus* exhibiting complex surface ornament. Egg cases ~ 240 μm in diameter. After Gilchrist (1978).

& Thiery, 1986; Mili i & Petrov, 2002). Ornament varies widely in copepod and branchiopod diapause eggs, and in many cases the ornament is similar to that observed in acritarchs. Koga (1968) described some copepod eggs as possessing hollow spines which communicate freely with the egg interior. The diapause egg of the branchiopod *Chirocephalus diaphanus* has a surface ornament consisting of spines (or processes) interconnected by veils or flanges. This type of ornament is

very similar to that observed on species belonging to the acritarch genus *Cymatiosphaera* (Fig. 8.1), although much smaller.

Environmental distribution: Acritarchs have been recorded from a wide range of marine environments (Playford, 2003) and have also been reported from deposits interpreted as brackish- and fresh-water (Segroves, 1967; Sarjeant & Strachan, 1968; Tappan, 1980). Given the very wide range of environments inhabited by copepods it is inevitable that their environmental distribution will be coincident with that of acritarchs. However, the majority of extant branchiopods are fresh-water species, many of which are adapted to life in ephemeral fresh water bodies which dry up during certain seasons (Martin, 1992); these are not environments associated with acritarchs. Despite this, it is strongly suggested from the fossil record that branchiopod-like crustaceans did exist in shallow marine environments during the Cambrian Period (Walossek, 1993; Harvey et al., 2012), and that adaptations to fresh-water environments occurred subsequently (Potts & Durning, 1980). Therefore, the assertion that diapause egg cases from a branchiopod-like crustacean might be found in Cambrian marine sediments is reasonable.

Using these criteria Van Waveren (1992) compared microfossils from 300,000 year old pelagic oozes from the Banda Sea (Indonesia), to modern copepod eggs belonging to the species *Pseudocalanus elongatus* and *Temora longicornis*. The morphology of modern copepod eggs and other data suggested that the Banda Sea palynomorphs represent the eggs of planktonic crustaceans. Van Waveren & Marcus (1993) compared sub-recent acritarchs (Schizomorphae) from the Banda Sea (Indonesia) with freshly spawned eggs of a number of copepod species from the Gulf of Mexico. Based on vesicle size, structure, ornamentation, wall colour, aperture types and wall chemistry (the ability to withstand acids), they suggested the Schizomorphae were the egg envelopes of planktonic copepods. These methods, despite being vital in highlighting the possible affinities between acritarchs and crustaceans, are far from unequivocal and other methods are required, such as SEM and TEM analysis of wall ultrastructures.

8.6 Ultrastructure of copepod and branchiopod egg cases

8.6.1 Copepod egg cases

Copepod egg cases have three- or four-layered ultrastructure but the types of layer can vary between different copepod species (Couch et al., 2001). Couch et al. (2001) analysed (TEM) the ultrastructures of both subitaneous and diapause eggs of the calanoid copepod *Boeckella triarticulata* and showed that subitaneous eggs have a thin single-layered shell (0.4 μm) whereas diapause eggs consistently have a relatively thick, solid, three-layered shell (1.8-2.3 μm). The external layer (1.3-1.6 μm) consisted of alternating electron-dense and electron-lucent layers; the intermediate layer (0.3-0.4 μm) had a granular appearance and filled with small white circular features; the interior layer (0.2-0.3 μm) was electron lucent.

8.6.2 Branchiopod egg cases

Branchiopod diapause egg cases have a three-layered wall ultrastructure (Morris & Afzelius, 1967; Mura & Thiery, 1986; Tommasini et al., 1989; Sugumar & Munuswamy, 2006). The typical resting cysts of anostracan and notostracan crustaceans (Branchiopoda) consist of an outer cortex, an alveolar layer, cuticular membranes and cytoplasmic inclusions; the nucleus, yolk droplets, lipid bodies and mitochondria (Sugumar & Munuswamy, 2006). It is the outer three layers (outer cortex, alveolar layer, cuticular membrane) which make up the egg case (Sugumar & Munuswamy, 2006), and it is this recalcitrant, trilaminar structure which protects the enclosed embryo from harsh environmental conditions. Tommasini et al., (1989) looked at the ultrastructure of diapause egg cases of the notostracan branchiopod *Triops cancriformis* (Fig 8.1). The egg case wall was 25 μm thick with external and internal layers 2.5 μm thick and an intermediate alveolar layer 20 μm thick. The alveolar layer is a conspicuous sponge-like or honeycomb structure consisting of numerous voids or pores (alveoli) within a matrix, and is always much wider than the two layers enclosing it (Sugumar & Munuswamy, 2006). The alveolar layer varies in thickness from species to species and can range from <10 μm to 30 μm . Egg cases belonging to the branchiopod species *Streptocephalus torvicornis* have alveolar layers approximately 15 μm thick (De Walsche et al., 1991), those belonging to *Branchius stagnalis* are approximately <10 μm .

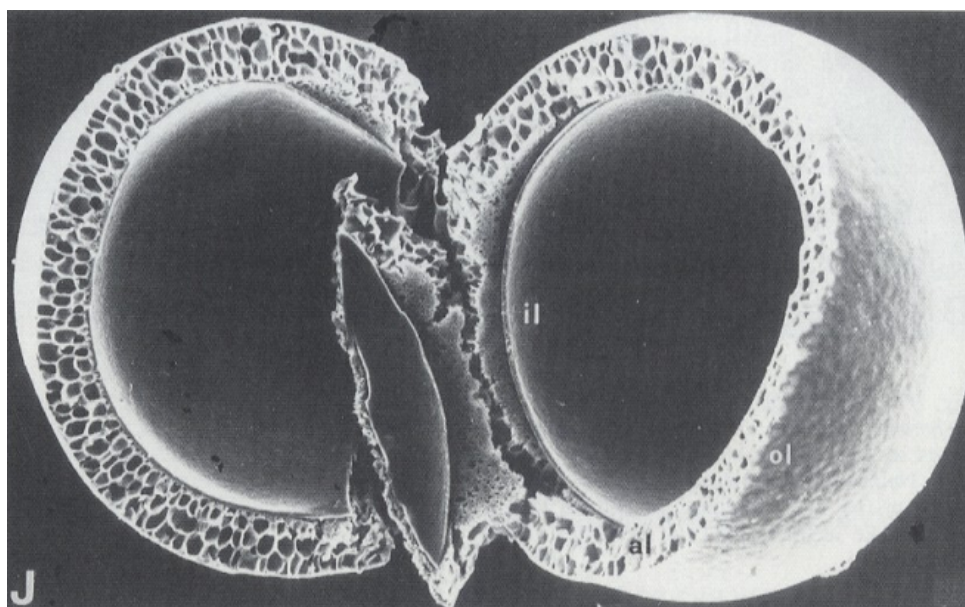


Figure 8.2 View (SEM) of a *Triops cancriformis* egg case after hatching showing the three layers; the sponge-like alveolar layer is sandwiched between two relatively thin, solid layers. Egg case is ~300 μm in diameter. After Tommasini et al. (1989).

8.7 TEM analysis of acritarchs from the USA

8.7.1 Introduction

For methods see chapter 3.

A note on dimensions. Valid, measured, vertical wall thicknesses using SEM images are only available from broken specimens, where a cross sectional area (break surface) of internal cell wall is exposed and orientated at right angles (vertical), both to the plane or direction of view and the cell wall surface. Break surfaces in the cell wall orientated away from the vertical will give dimensions greater than true vertical; break surfaces not perpendicular to the direction of view will give dimensions less than true vertical. Given this, and the lack of correctly orientated break surfaces, total wall thicknesses taken from observed cell wall break surfaces from SEM images were necessarily estimated. Only one of the four species (Acritarch sp. 1) was measured for cell wall thickness using SEM images.

Measured vertical thicknesses of cell wall layers taken from TEM images suffer from similar distortions as a result of variable angles of cut in producing specimen

sections. The dimensions of measured layer thicknesses taken from TEM images are a function of true thickness and the angle of cut, and therefore measured dimensions will either represent true vertical thickness or greater than true vertical thickness. Thus, only minimum measured values were adopted as valid, as these are interpreted as being closer to true vertical distance.

One species (*Acritarch* sp. 1) has alveoli (spherical voids) within its cell walls. Because alveoli were originally three-dimensional and approximately subspherical, it is reasonable to assume that measurements of alveoli taken in any plane would be truly representative of their dimensions and that measurements taken from two-dimensional TEM images are equally valid.

8.7.2 TEM descriptions

***Acritarch* sp. 1 (60-155 μm)**

TEM description.

Plate 24, Figs 1-4.

Total wall thickness as estimated from TEM and SEM images: 200-500 nm.

One specimen examined. Possesses a well preserved complex wall ultrastructure consisting of three layers: two relatively narrow electron dense layers (external and internal), and a relatively wide intermediate, alveolar layer sandwiched between the external and internal layers.

External wall: 30-100 nm. The external wall and its processes are dark, electron dense and homogeneous and the processes emerge directly from the external layer. The external surface of the vesicle and processes is smooth. The contact with the intermediate layer is irregular with pores impinging on the internal region of the external layer.

Intermediate wall - alveolar layer: 300-450 nm. The intermediate wall consists of numerous, closely arranged pores surrounded by thin (10-50 nm) electron dense to electron lucent walls. Pore walls frequently possess smaller pores (<30 nm) and are smooth to irregular in outline. Pores are circular to subcircular to irregular in outline with maximum diameters of <10-700 nm (Most 300-500 nm). Clusters of small (<40 nm) pores frequently occur. The outer regions of the alveolar layer contain smaller voids with larger voids occupying the inner region.

Internal wall: 10-80 nm. The internal wall is dark, electron dense and homogeneous. The contact with the intermediate layer is irregular with pores impinging on the external region of the internal wall.

Acritarch sp. 2 (82-166 μm)

TEM description.

Plate 23, Figs 5, 6.

Wall thickness: 50-110 nm.

Acritarch sp. 2 consists of a single layer from which solid processes directly emerge. The single layer and processes are dark, electron dense and homogeneous. The external surface of the vesicle and processes is smooth, as is the internal surface.

***Peteinosphaeridium?* sp. 1 (83-122 μm)**

TEM description.

Plate 23, Figs 1, 2.

Wall thickness: 60-150 nm.

Peteinosphaeridium? sp. 1 consists of a single layer from which solid processes directly emerge. The single layer and processes are dark, electron dense and homogeneous. The external surface of the vesicle and processes is smooth, as is the internal surface.

***Peteinosphaeridium?* sp. 2 (104-115 μm)**

TEM description.

Plate 23, Figs 3, 4

Wall thickness: 25-120 nm.

The ultrastructure of *Peteinosphaeridium?* sp. 2 is the same as that of *Peteinosphaeridium?* sp. 1.

8.8 Discussion

8.8.1 Acritarch sp. 1.

Comparison of Acritarch sp. 1 to branchiopod diapause egg cases

Positive comparisons:

- 1) The upper vesicle size-range of *Acritarch* sp. 1 is coincident with the lower size-range of extant branchiopod diapause egg cases.
- 2) Branchiopod diapause egg cases are recalcitrant, and could theoretically withstand diagenesis and acid treatment.
- 3) Complex surface ornament similar to that observed on spinose acritarchs is present on many branchiopod diapause egg cases.
- 4) The overall trilaminar wall ultrastructure of *Acritarch* sp. 1 is very similar to that of Branchiopod diapause egg cases, particularly with the presence of a relatively wide alveolar structure. Also the relative proportions of the widths of the three layers are very similar for both, with the alveolar layer taking up the majority of space within the wall structures.
- 5) There is fossil evidence for the presence of potential parent organisms in the form of branchiopod leg structures and mandibles.

Negative comparisons:

- 1) The width of the vesicle wall of *Acritarch* sp. 1 and that of the alveolar layer it contains, are much less than those observed in any diapause egg case from a branchiopod.

Acritarch sp. 1 has a size range of 60-155 μm , was originally spherical and possesses a complex surface ornament. It is associated with shallow marine environments, and fossil evidence proves the existence of branchiopod-like crustaceans in the Cambrian (Harvey et al., 2012); this study has found co-occurrence between *Acritarch* sp. 1 and branchiopod-type microfossils in one sample (23 No). It has a recalcitrant cyst-wall chemistry enabling its survival through diagenesis and palynological processing procedures. Its wall ultrastructure possesses three preserved layers consisting of a relatively wide, intermediate, alveolar layer enclosed by two relatively thin, electron dense layers (external and internal).

These characteristics identify *Acritarch* sp. 1 as a possible diapause egg case of an unknown crustacean, most likely related to present day branchiopods. Affinity to copepod eggs is ruled out due to the lack of an alveolar layer within the egg case wall. Of the key characteristics of *Acritarch* sp. 1, the most notable is the alveolar layer. This is the first record of such a feature in the wall ultrastructure of an acritarch, and differentiates *Acritarch* sp. 1 from all other acritarchs whose

ultrastructures have been previously reported. In fact, as far as the present author is aware, alveolar layers such as those described here, i.e. forming part of a trilaminar wall ultrastructure belonging to an ornamented, organic-walled and recalcitrant, spherical, microscopic form, have only been reported from crustacean egg cases. Another notable feature is the anomalously large vesicle size (60-155 μm). Again, this is a feature which separates *Acritarch* sp. 1 from the vast majority of reported Cambrian acritarchs, but at the same time allows comparisons to branchiopod egg cases.

A major difference in the alveolar layers, however, between *Acritarch* sp. 1 and branchiopod egg cases, is the width of the cyst walls and the individual layers they contain. The widths of the cyst-wall and the alveolar layer of *Acritarch* sp. 1 are estimated to approximately 500 nm and 300-450 nm respectively, whereas branchiopod egg cases have much larger widths of up to 50 μm , with alveolar layer widths of <10-30 μm . This is a huge disparity and difficult to explain. However, in very general terms the ratio of alveolar layer thickness to that of the thin external and internal layers is approximately the same; i.e., within the cyst walls of both *Acritarch* sp. 1 and branchiopod egg cases, the alveolar layer occupies the vast majority of available space, and that despite large differences in cyst-wall dimensions, the ratios of layers are similar. It could be argued that the thin vesicle wall of *Acritarch* sp. 1, if crustacean in origin, might represent an evolutionary step towards thicker cyst walls, but such a supposition is impossible to qualify without understanding the function, or functions, of the alveolar layer.

A number of functions have been accorded to the alveolar layer in diapause egg cases (Dumont & Negrea, 2002), including protection from predation, physical damage, extreme temperatures, ultra-violet light and desiccation (Bishop, 1968; Belk, 1970; Dumont et al., 2002), and also as an aid to flotation and dispersal (Morris & Afzelius, 1967; Thiéry, 1997). Dumont et al., (2002) showed that intact ornamented cysts were less vulnerable to predation than decapsulated cysts belonging to the branchiopod *Chirocephalus diaphanus*. The alveolar layer reduced a predator's access to an egg's interior by enlarging the cyst volume around the embryonic material. This defense was enhanced by the presence of surface ornament such as spines or flanges. Belk (1970) reported that one day's exposure to full sunlight was enough to kill the decapsulated eggs of the branchiopod *Eulimnadia*

antlei (the removal of the egg cases had no impact on hatchability). This, however, proved the protective function of the whole egg case and not just the alveolar layer, although the latter undoubtedly played a major role (Belk, 1970). It has also been shown that the alveolar layer acts as insulation against extreme temperatures (Carlisle, 1968; Planel et al., 1980) and plays a role in preventing desiccation in dry environments (Martin, 1992).

All of these protective functions would clearly be of great benefit to any marine, microscopic, egg-laying organism living in the Cambrian seas. However, an additional, more controversial function has been suggested for the alveolar layer in extant branchiopod egg cases; that of floatation as an aid to dispersal. Morris & Afzelius (1967) pointed out that the consistently spherical shape of the alveoli and their lack of electron-dense material suggested they were formed by gas bubbles, and that if this were the case, the alveolar layer might act as a float. According to De Walsche et al., (1991), as the eggs of some branchiopods are laid, the alveolar chambers within the egg case wall are filled with fluid and they sink to the bottom sediment. During the dry season the alveolar layer dries out enabling the eggs to float and disperse during the next wet season. In such cases the alveolar layer fulfills two functions; one of preventing desiccation and the other as floatation and dispersal mechanism. The production of desiccation-resistant eggs is often considered an adaptation for dispersal and is common with many planktonic branchiopods which free-shed their eggs directly into the water column. (Fryer, 1996; Hairston, 1998; Brendonck & Riddoch, 1999; Bilton et al., 2001). Many of these eggs sink, but are still subject to dispersal. In some cases the alveolar layer imparts buoyancy which will have the effect of increasing dispersion. However, many species of branchiopod attach their diapause eggs to a firm substrate which clearly reduces the chances of dispersal (Fryer, 1996).

The distribution and abundance of branchiopod diapause eggs in bottom, freshwater sediments, were studied by Thiéry (1997) in ephemeral pools and ditches in Morocco and France. He showed that some species physically attached their eggs, using an excreted sticky adhesive, to substrates at the peripheries of pools. Other species in the same pool, freely released their eggs into the water column which either sank or floated, depending on the species. Furthermore, that the density of diapause eggs varied between species, resulting in different sinking rates. Those eggs

which sank accumulated at the pool bottom with their distribution moderated by sinking-rate and the floor topography. Those eggs which immediately floated (these have gases within the alveolar layer) to or near the surface, were dispersed by currents and winds and accumulated along the downwind edge of a pool. These eggs were then further dispersed by wind and animals. It was also noted that the floating period can vary from hours to days, depending on species, and that this would influence their distribution. This research clearly showed that different species within the same branchiopod community were able to develop various dispersal strategies in order to maximise survival. Hajirostamloo (2008) noted that the alveolar layer in egg cases belonging to the branchiopod *Artemia urmiana* from Urmia Lake in Iran, varied in thickness to such an extent that some eggs floated whilst others sank. He argued that the variation in alveolar volume was an evolutionary response to varying salinities within the lake, brought about by seasonal fluctuations. The attained buoyancy resulting from a combination of salinity and alveolar volume ultimately moderated the vertical and lateral distribution of eggs and increased dispersal. Thus, patterns of egg distribution are influenced by egg-laying strategy (substrate-attached or water column), floor topography (orientation and degree of slope), salinity, floating and sinking rates, floating/buoyancy period and current and wind dynamics. With the exceptions of egg-laying strategy and floor topography, all the other factors relate to the volume of the alveolar layer. Given this, and the protective nature of the egg case, it is clear that the alveolar layer has multiple functions and plays a major role in the dispersal and survival of branchiopod species. This research highlights a key aspect to the successful survival of branchiopods: that diapause eggs, being resistant to desiccation and other environmental dangers, and subject to wide geographical dispersal through a number of factors, not least the presence and volume of an alveolar layer, enable a species to survive fluctuating environmental conditions and continually extend its habitat and colonise new ones. It should be noted that these studies (Thiéry, 1997; Hajirostamloo, 2008) were undertaken in either freshwater or hypersaline habitats that are subject to environmental fluctuations, and that *Acritarch* sp. 1 was marine. It should also be noted that the volume of the alveolar layer in *Acritarch* sp. 1 is much less than that observed in branchiopod eggs. However, an alveolar layer is present in *Acritarch* species 1 and forms part of a trilaminar structure. The formation of the voids

(alveoli) within the alveolar layer, were most likely formed by either gases or low density liquids in order to attain the observed structures. If gases remained in the alveolar layer after laying, it would have increased buoyancy, not enough to float perhaps, but enough to promote ease of movement by currents or waves. It might be that some became stranded on the shore, possibly in small pools or on to dry land. In either situation the egg case might have protected the embryo from ultra-violet radiation and other dangers such as desiccation. Also, these kinds of scenarios could be seen as evolutionary drivers that initiated the development of both complex crustacean egg case structures and diapause in the first place. The point is that if *Acritarch* sp. 1 is in fact an egg case from a marine habitat, the presence of an enveloped alveolar layer might be explained, albeit qualitatively. However, if *Acritarch* sp. 1 is algal in origin then it was most likely a phytoplanktonic resting cyst, the function being to sink and carry its algal cargo to the safety of bottom sediments. Given the necessity for a cyst to sink, and that a gas-filled cell wall might increase buoyancy, it is hard to imagine what the possible function of an alveolar layer might be within an algal cyst, other than protection.

It would be almost impossible to prove unequivocally that *Acritarch* sp. 1, or indeed any egg-like palynomorph, is an actual crustacean egg case. The analysis of acritarch ultrastructures is really just beginning and as yet only a few ultrastructure types have been described from a few acritarchs. If *Acritarch* sp. 1 is an egg case it would probably represent the earliest evidence of diapause in the fossil record. This would be a significant discovery given that many workers are convinced that diapause was a major agent for the colonisation of terrestrial fresh water systems. It might be that future work will resolve the puzzle of *Acritarch* sp. 1 and its alveolar layer, but until then we are left with only circumstantial evidence which, although not conclusive, is nothing less than compelling.

8.8.2 *Acritarch* sp. 2, *Peteinosphaeridium?* sp. 1 and *Peteinosphaeridium?* sp. 2.

The form-species *Acritarch* sp. 2, *Peteinosphaeridium?* sp. 1 and *Peteinosphaeridium?* sp. 2 from this study, all possess single-layered, electron-dense, homogeneous cell wall ultrastructures. These ultrastructural features correspond to those observed in the species *Globosphaeridium cerinum*, *Comasphaeridium brachyspinosum* and *Skiagia compressa* as described by Moczyłowska & Willman (2009) and classified as belonging to the Class

Chlorophyceae (Moczyłowska, 2011). Despite similarities between *Acritarch* sp. 2, *Peteinosphaeridium?* sp. 1 and *Peteinosphaeridium?* sp. 2 and branchiopod/copepod egg cases in vesicle size and shape, surface ornament and recalcitrant wall chemistry, there is no comparison to be made with regard to wall ultrastructure. Consequently *Acritarch* sp. 2, *Peteinosphaeridium?* sp. 1 and *Peteinosphaeridium?* sp. 2 are tentatively assigned to the Class Chlorophyceae.

The fact remains, however, that *Acritarch* sp. 2, *Peteinosphaeridium?* sp. 1 and *Peteinosphaeridium?* sp. 2 have unusually large vesicles (>100 μm). Cambrian acanthomorphs tend to be <80 μm and therefore *Acritarch* sp. 2, *Peteinosphaeridium?* sp. 1 and *Peteinosphaeridium?* sp. 2 might simply represent algal species that have evolved to occupy an ecological niche, favourable to forms with large vesicle dimensions. As such they would represent species situated at one end of an algal community size-spectrum, and although relatively rare in the fossil record, their presence is part of a natural order. In other words, the occurrence of large Cambrian acritarchs, albeit rare, should be expected.

It may be that these forms were benthic. The Nalichucky Basin has been interpreted as being relatively shallow (Weber, 1988) with depths ranging from 5-50 m. As such, light would most likely have penetrated to the basin floor, allowing photosynthesizing organisms to survive without being planktonic. This would be advantageous to larger forms which would quickly sink to the basin floor in such shallow waters. Whether these forms were benthic or planktonic is debatable, but their large size and shallow water palaeoenvironment does support the idea that they were benthic.

8.9 Conclusion

Based on vesicle size, shape and ornament, recalcitrant cyst-wall chemistry, facies, co-occurrence with branchiopod-type crustaceans and the presence of a trilaminar wall ultrastructure with an alveolar layer, *Acritarch* sp. 1 is interpreted as a diapause egg case of a Cambrian branchiopod-type crustacean. As such it represents the earliest evidence for diapause-type dormancy in the fossil record and suggests crustaceans were utilising complex reproductive strategies during the Cambrian.

Acritarch sp. 2, *Peteinosphaeridium?* sp. 1 and *Peteinosphaeridium?* sp. 2 possess single-layered, electron-dense, homogeneous cell wall ultrastructures and are

comparable with the cell wall ultrastructures of *Globosphaeridium cerinum*, *Comasphaeridium brachyspinosum* and *Skiagia compressa* as described by Moczyłowska & Willman (2009). They are interpreted as belonging to the Class Chlorophyceae.

Chapter 9

Conclusion

- Recovered palynomorphs from the Rogersville Shale, Nolichucky Shale, Maynardville Limestone and Copper Ridge Dolomite and at Thorn Hill, Tennessee, USA showed low abundances and palynomorph assemblages showed low diversity.
- 52 acritarchs were described of which 15 were identified to species level, 26 were left in open nomenclature and 11 represent new undescribed forms. Additionally, 2 Problematica and four invertebrate components were described including branchiopod-type mandibles and limbs, copepod-type mandibles and *Wiwaxia* sclerites.
- No acritarch species were recovered that unequivocally indicated the age of the units sampled. However, trilobites indicated that the position of the base of the Furongian series (Marjuman/Steptoean boundary) lies within a 30 m section of the uppermost Nolichucky Shale. This was confirmed by stable carbon isotope analysis (^{13}C) which placed the onset of SPICE in the same stratigraphic section, and is the first record of SPICE in Laurentia using stable carbon isotope analysis on organic residues. Trilobites indicated that, in ascending order, the *Cedaria*, *Crepicephalus* and *Aphelaspis* Zones are present in the Nolichucky Shale. Using the given stratigraphic framework, Acritarch sp. 1 and Acritarch sp. 2 show potential as markers for uppermost Cambrian Series 3 (uppermost Marjuman/upper *Crepicephalus* Zone) units in Laurentian, shallow marine facies.
- Palynofacies analysis suggests a transgressive/regressive cycle through the Nolichucky Shale and Maynardville Limestone. Assuming that relative acritarch abundance can be used as a proxy for water depth, the acritarch abundance peak stratigraphically places maximum water depth at approximately 90 m above the base of the Nolichucky Shale.
- The ultrastructure of four large spinose acritarchs, Acritarch sp. 1, Acritarch sp. 2, *Peteinosphaeridium?* sp. 1 and *Peteinosphaeridium?* sp. 2 were analysed using TEM. Acritarch sp. 2, *Peteinosphaeridium?* sp. 1 and *Peteinosphaeridium?* sp. 2 have a single-layered wall ultrastructure and are interpreted as belonging to the Class *Chlorophyceae*. Acritarch sp. 1 has a trilaminar wall ultrastructure consisting of an alveolar layer sandwiched between two relatively thin electron dense layers. Principally based on similarities with the wall ultrastructure of branchiopod diapause egg cases, Acritarch sp. 1 is interpreted as the egg case of an unknown Cambrian

crustacean. This is supported by comparisons in size, surface ornament, the recalcitrant nature of the vesicle/egg case and co-occurrence of potential parent organisms.

PLATES

Plate 1

Fig. 1 *Apodastoides cf. verobturatus*

Nolichucky Shale Sample 08BP-57 BEP-0250 (M27/0)

Fig. 2 *Apodastoides cf. verobturatus*

Nolichucky Shale Sample 08BP-57 BEP-0250 (K37/0)

Fig. 3 *Auritusphaera bifurcata*

Nolichucky Shale Sample 08BP-19 BEP-0108 (H26/2)

Arrow indicates bifurcate process

Fig. 4 *Auritusphaera bifurcata*

Nolichucky Shale Sample 08BP-20 BEP-0112 (N25/0).

Arrow indicates bifurcate process.

Fig. 5 *Auritusphaera bifurcata* cluster

Nolichucky Shale Sample 08BP-19 BEP-0108 (G34/4).

Arrow indicates bifurcate process

Fig. 6 *Auritusphaera bifurcata*

Nolichucky Shale Sample 08BP-19 SEM-10.

Arrow indicates bifurcate process.

Plate 1

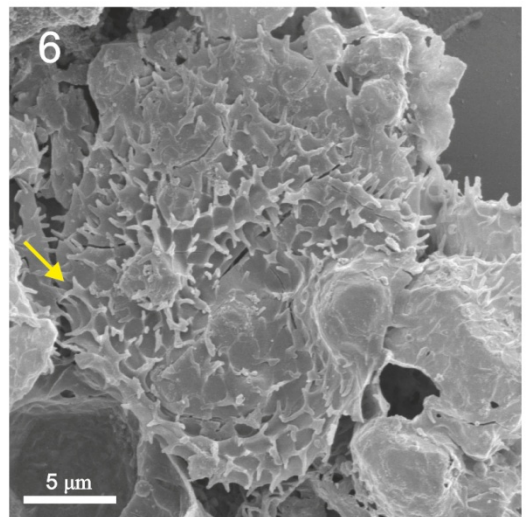
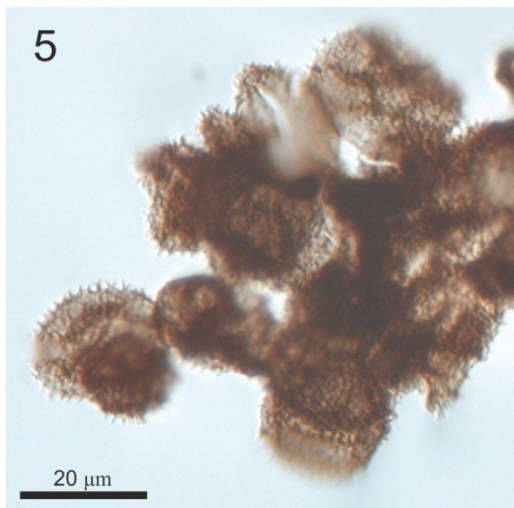
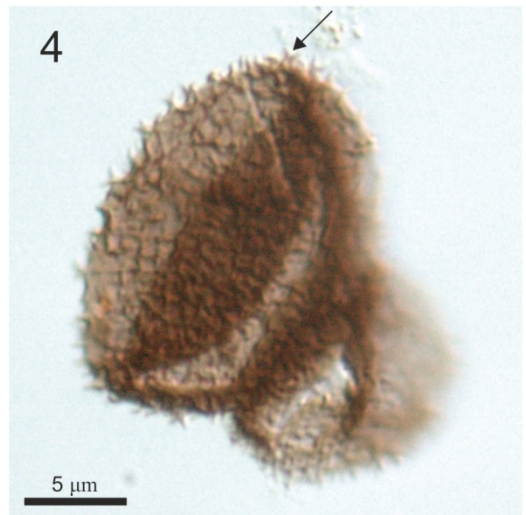
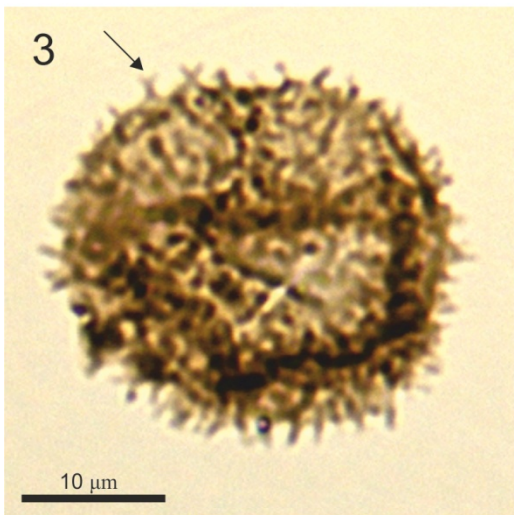
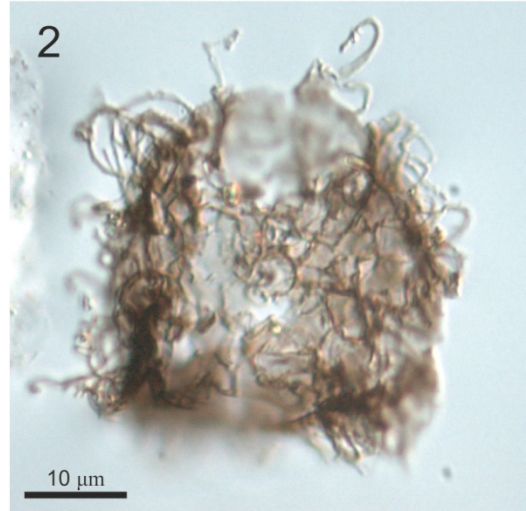
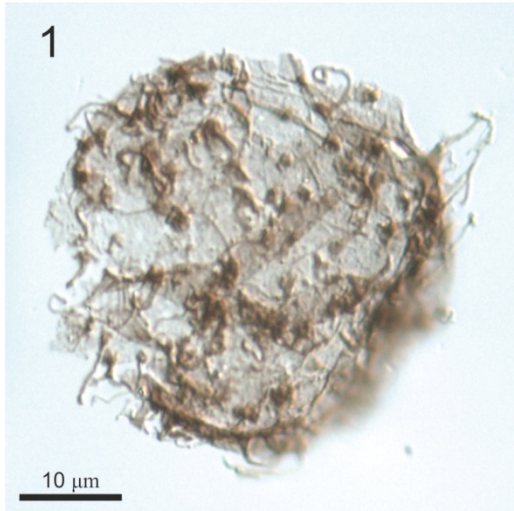


Plate 2

Fig. 1 *Auritusphaera* cf. *bifurcata*

Nolichucky Shale Sample 08BP-24 BEP-0127 (H46/2)

Fig. 2 *Auritusphaera* cf. *bifurcata*

Nolichucky Shale Sample 08BP-61 SEM-68

Fig. 3 *Auritusphaera* sp. 1

Nolichucky Shale Sample 08BP-24 BEP-0127 (N25/2)

Fig. 4 *Auritusphaera* sp. 1

Nolichucky Shale Sample 08BP-24 SEM-Z4

Fig. 5 *Auritusphaera* sp. 2

Nolichucky Shale Sample 08BP-57 BEP-0250 (E41/3)

Fig. 6 *Auritusphaera* sp. 2

Nolichucky Shale Sample 08BP-57 BEP-0250 (J28/1)

Plate 2

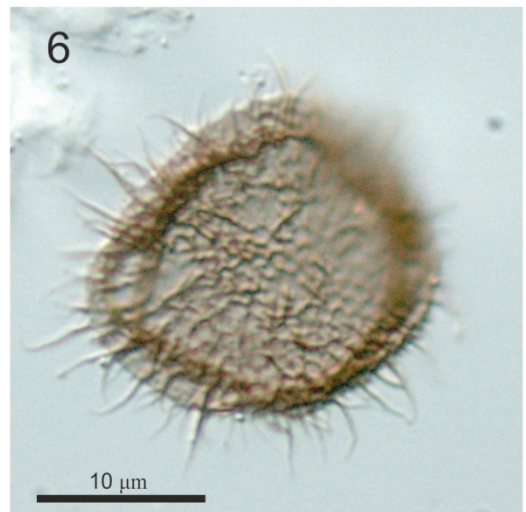
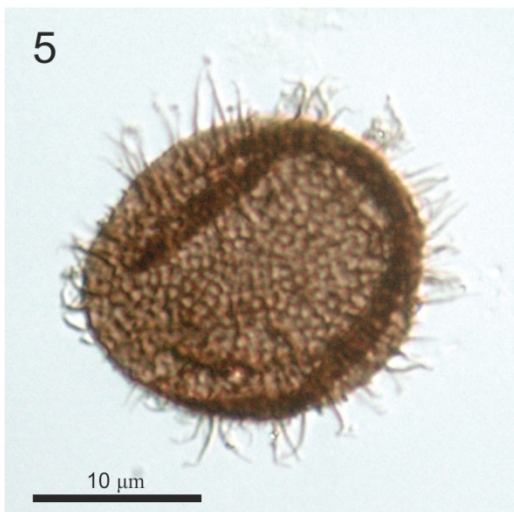
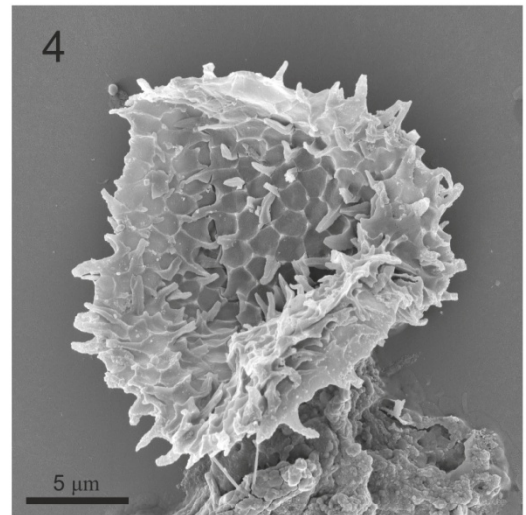
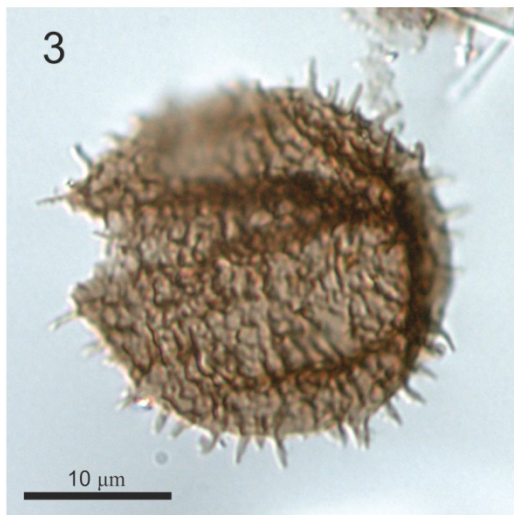
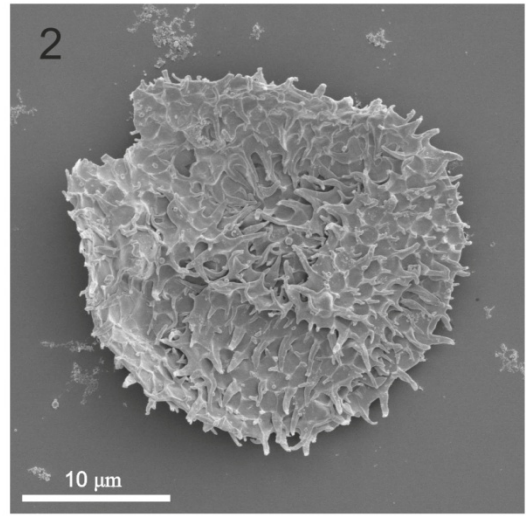
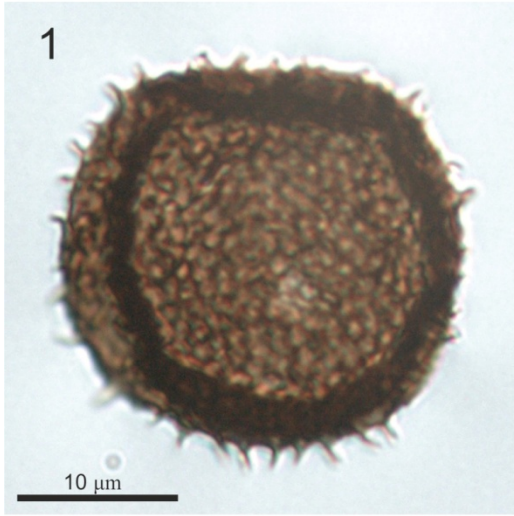


Plate 3

Fig. 1 *Auritusphaera* sp. 2

Nolichucky Shale Sample 08BP-57 SEM-65

Fig. 2 *Auritusphaera* sp. 3

Nolichucky Shale Sample 08BP-19 BEP-0108 (J23/4)

Fig. 3 *Auritusphaera* sp. 3

Nolichucky Shale Sample 08BP-19 BEP-0108 (U42/3)

Fig. 4 *Auritusphaera* sp. 3

Nolichucky Shale Sample 08BP-19 SEM-10

Fig. 5 *Caldariola* sp.1

Nolichucky Shale Sample 08BP-52 BEP-0242 (J53/3)

Fig. 6 *Caldariola* sp.1

Nolichucky Shale Sample 08BP-53 BEP-0243 (W48/0)

Plate 3

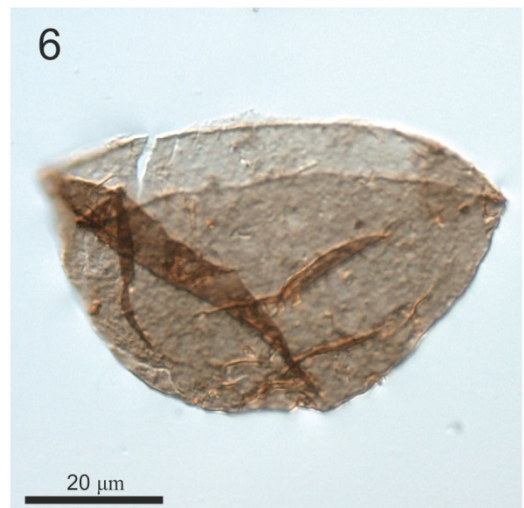
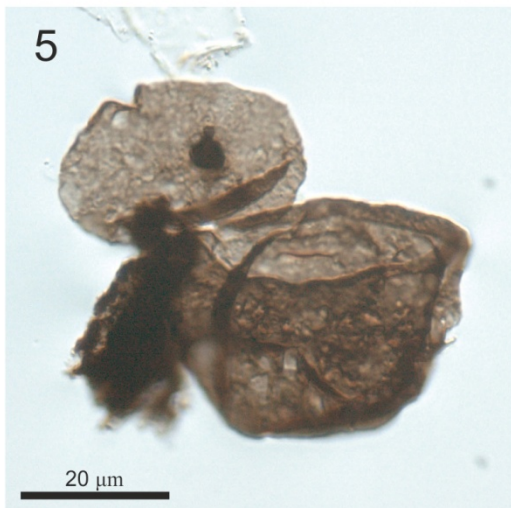
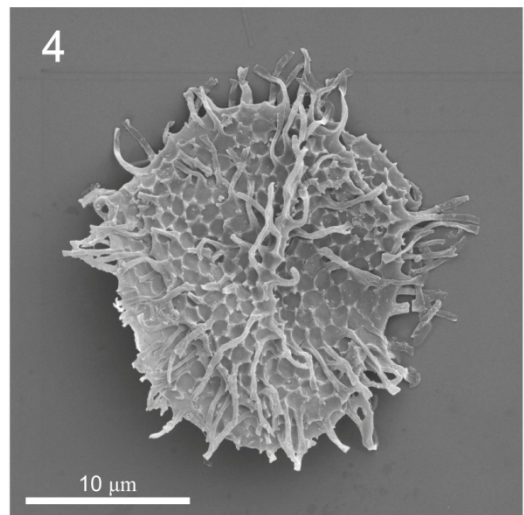
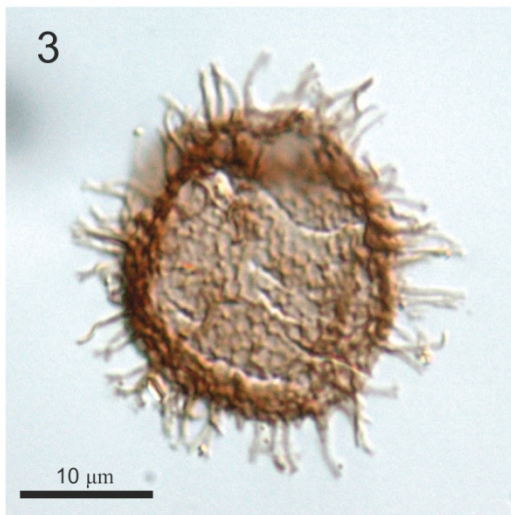
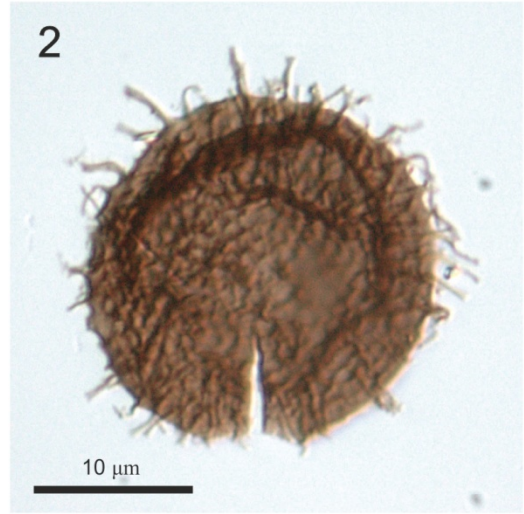
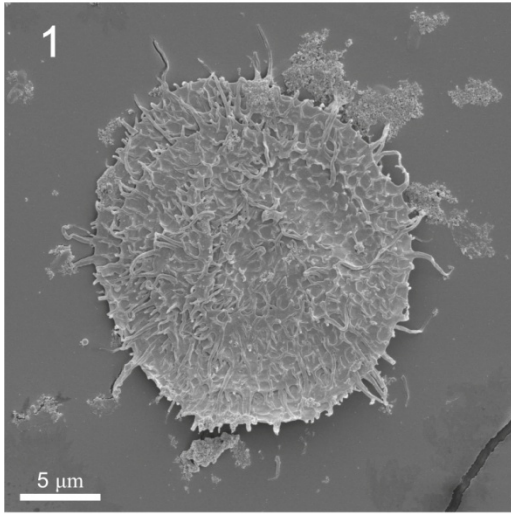


Plate 4

Fig. 1 *Caldariola* sp.1

Nolichucky Shale Sample 08BP-36 BEP-0202 (K40/3)

Fig. 2 *Caldariola* sp.1

Nolichucky Shale Sample 08BP-32 BEP-0168 (T/32/2)

Fig. 3 *Cerebrosphaera* cf. *buickii*

Nolichucky Shale Sample 08BP-29 BEP-0155 (H39/2)

Fig. 4 *Comasphaeridium* *brachyspinosum*

Nolichucky Shale Sample 08BP-26 BEP-0135 (V52/1)

Fig. 5 *Comasphaeridium* *brachyspinosum*

Nolichucky Shale Sample 08BP-26 BEP-0135 (O23/2)

Fig. 6 *Comasphaeridium* *mackenzianum*

Nolichucky Shale Sample 08BP-26 BEP-0135 (V52/1)

Plate 4

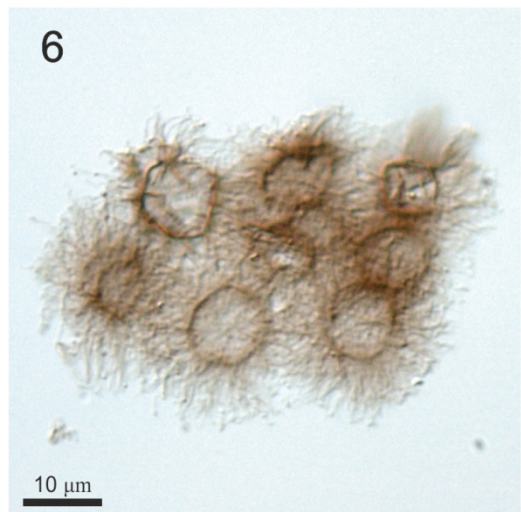
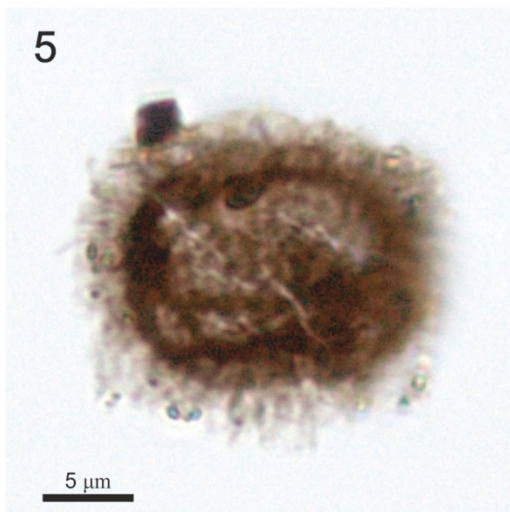
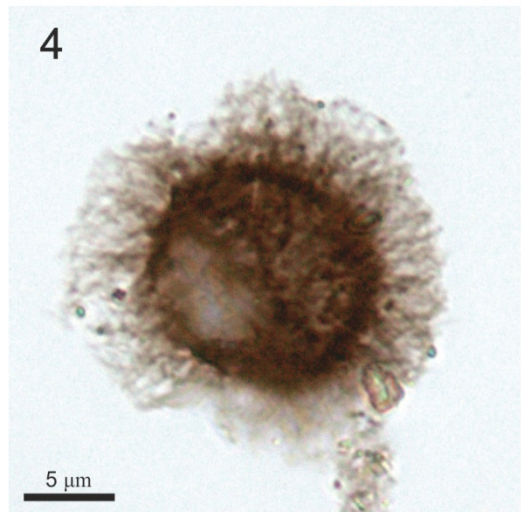
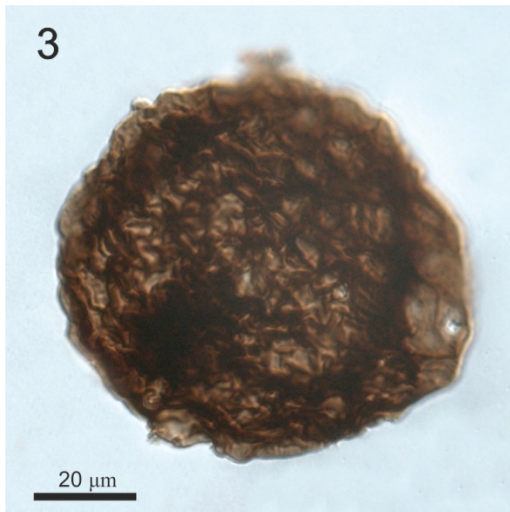
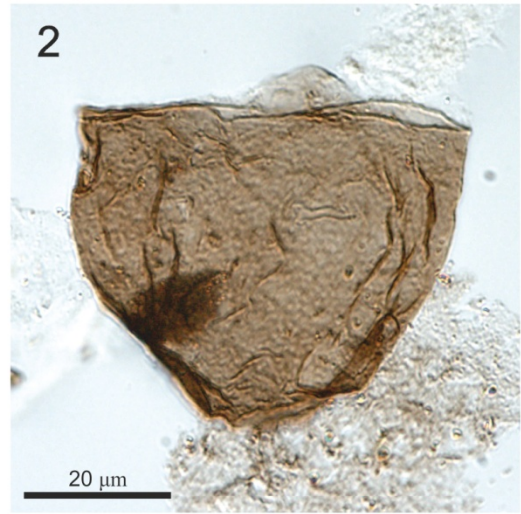
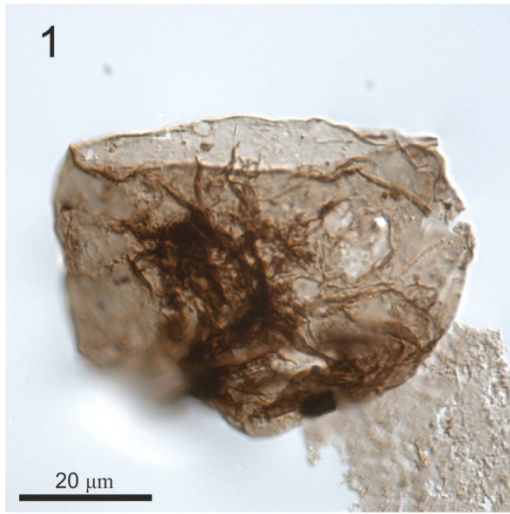


Plate 5

Fig. 1 *Comasphaeridium mackenzianum*

Nolichucky Shale Sample 08BP-59 BEP-0245 (R50/2)

Fig. 2 *Comasphaeridium mackenzianum*

Nolichucky Shale Sample 08BP-61 BEP-0260 (G50/2)

Fig. 3 *Comasphaeridium* sp. 1

Nolichucky Shale Sample 08BP-59 BEP-0256 (R36/4)

Fig. 4 *Comasphaeridium* sp. 2

Nolichucky Shale Sample 08BP-22 BEP-0121 (K35/0)

Fig. 5 *Comasphaeridium* sp. 2

Nolichucky Shale Sample 08BP-28½ BEP-0150 (T54/3)

Plate 5

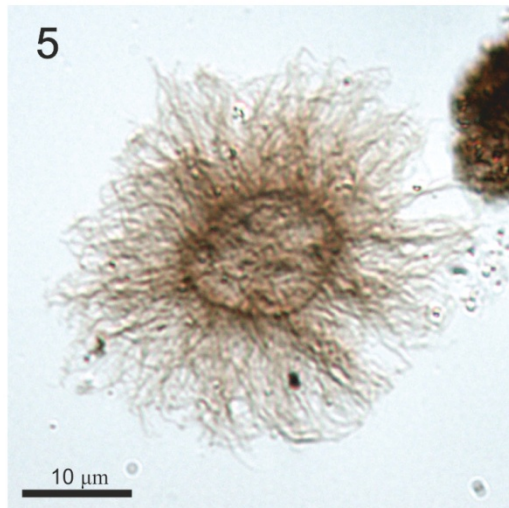
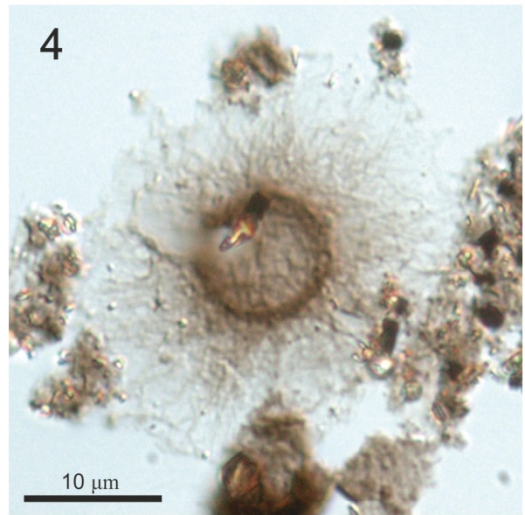
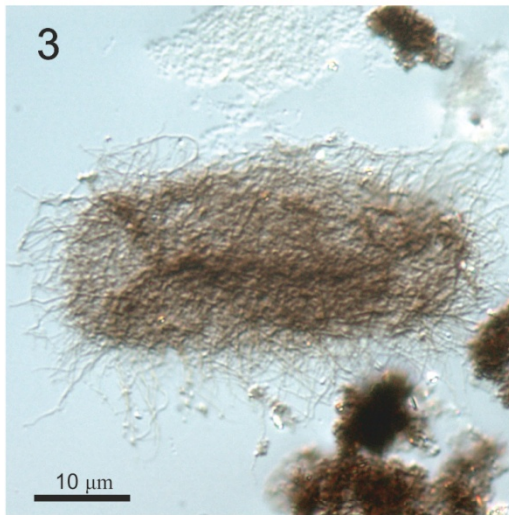
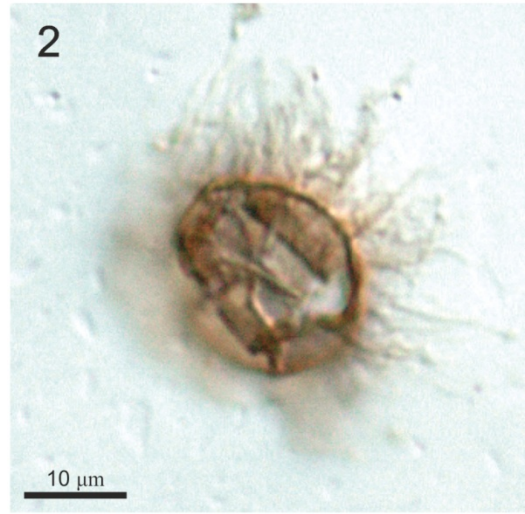
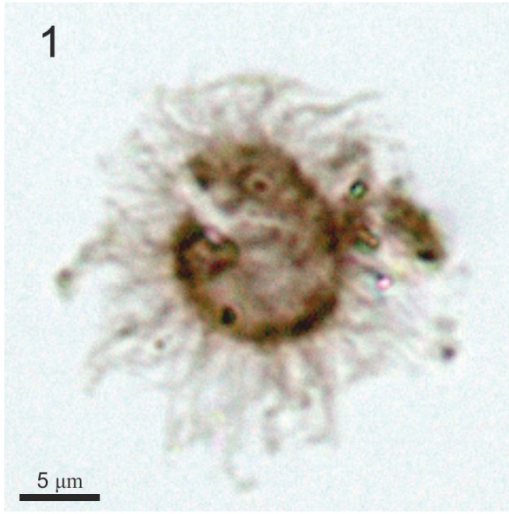


Plate 6

Fig. 1 *Cymatiogalea* cf. *virgulta*

Nolichucky Shale Sample 08BP-34 SEM-75

Suspected operculum is enclosed by white square and is enlarged in Fig. 2. Part of the operculum has fallen within the vesicle and is obscured.

Fig. 2 *Cymatiogalea* cf. *virgulta*. Detail of specimen in Fig. 1. Yellow arrows indicate plate angles which are devoid of processes.

Fig. 3 *Cymatiosphaera* sp. 1

Nolichucky Shale Sample 08BP-32 BEP-0168 (Q33/0)

Fig. 4 *Cymatiosphaera* sp. 1

Nolichucky Shale Sample 08BP-26 BEP-0135 (M35/1)

Fig. 5 *Cymatiosphaera?* sp.

Nolichucky Shale Sample 08BP-54 BEP-0244 (C24/2)

Fig. 6 *Fimbriaglomerella membranacea* cluster

Nolichucky Shale Sample 08BP-24 BEP-0127 (E26/1)

Plate 6

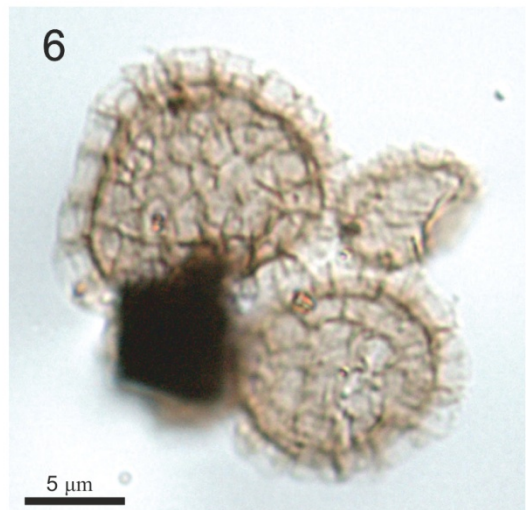
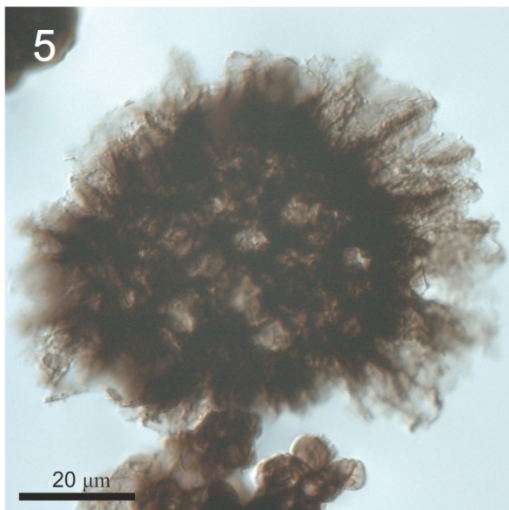
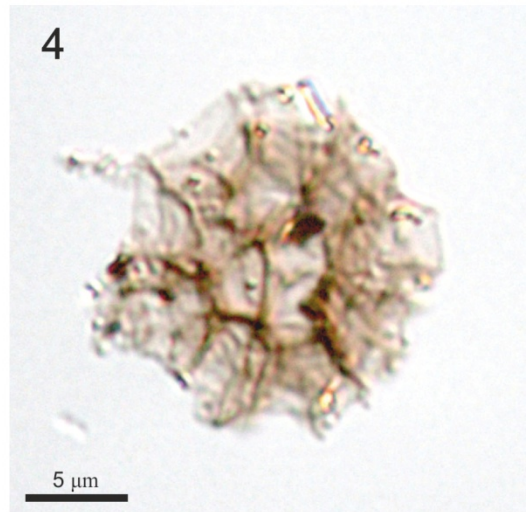
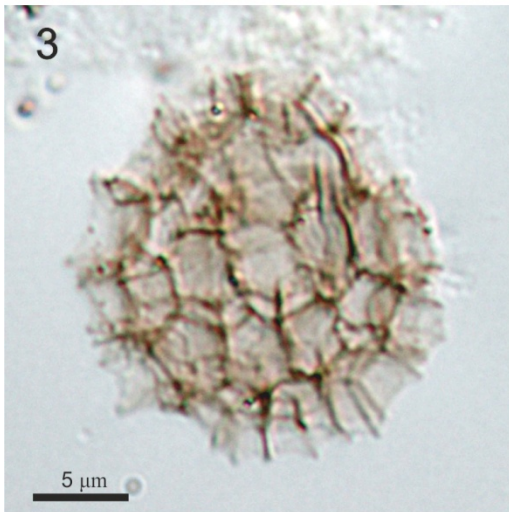
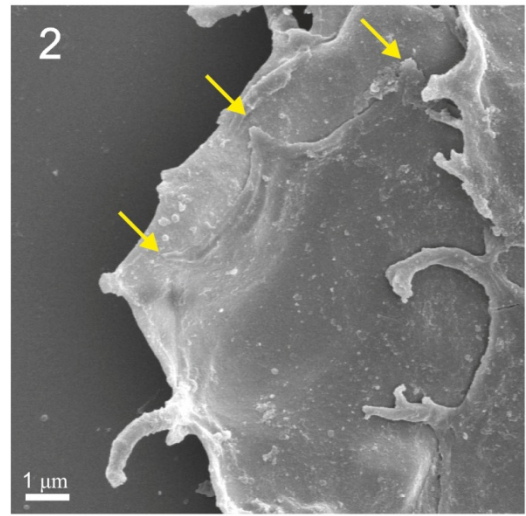
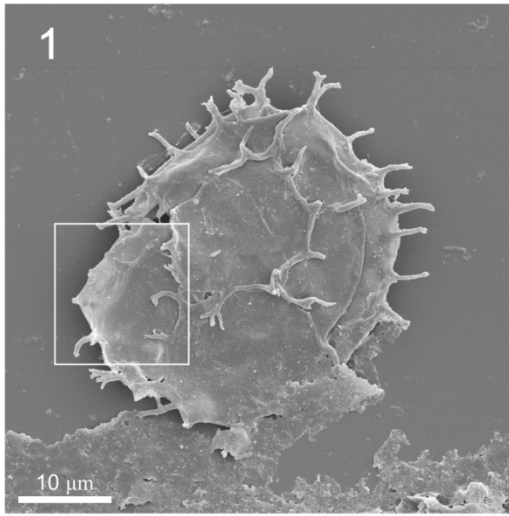


Plate 7

Fig. 1 *Fimbriaglomerella membranacea*

Nolichucky Shale Sample 08BP-24 BEP-0127 (P47/2)

Fig. 2 *Fimbriaglomerella membranacea*

Nolichucky Shale Sample 08BP-24 BEP-0127 (C44/4)

Fig. 3 *Granomarginata squamacea*

Nolichucky Shale Sample 08BP-03 BEP-0012 (E39/4)

Fig. 4 *Granomarginata squamacea*

Nolichucky Shale Sample 08BP-22 BEP-0121 (F23/2)

Fig. 5 *Leiosphaeridia kulgunica*

Nolichucky Shale Sample 08BP-52 BEP-0242 (L29/0)

Fig. 6 *Leiosphaeridia kulgunica*

Nolichucky Shale Sample 08BP-53 BEP-0243 (H44/0)

Plate 7

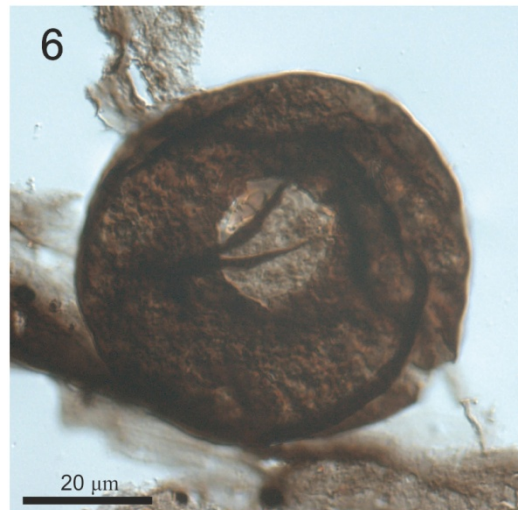
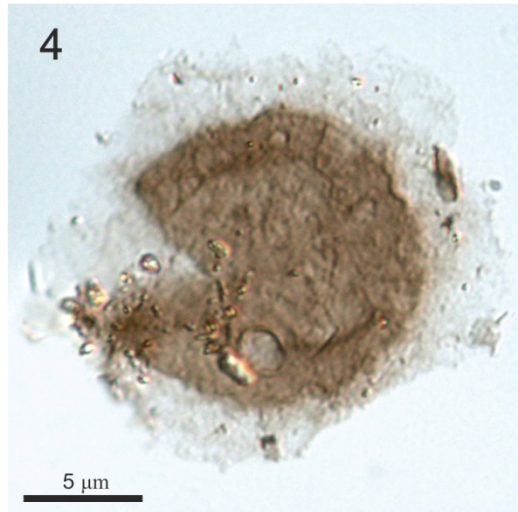
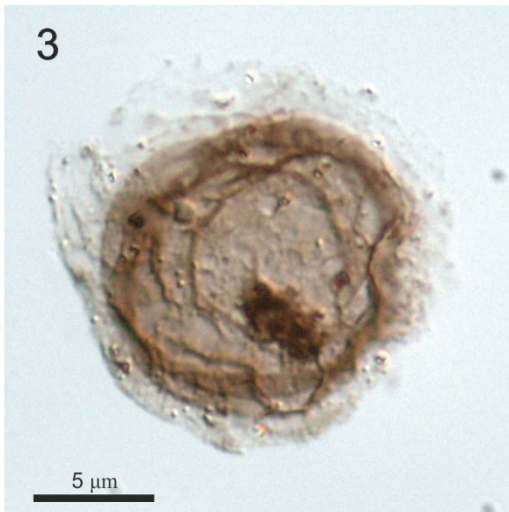
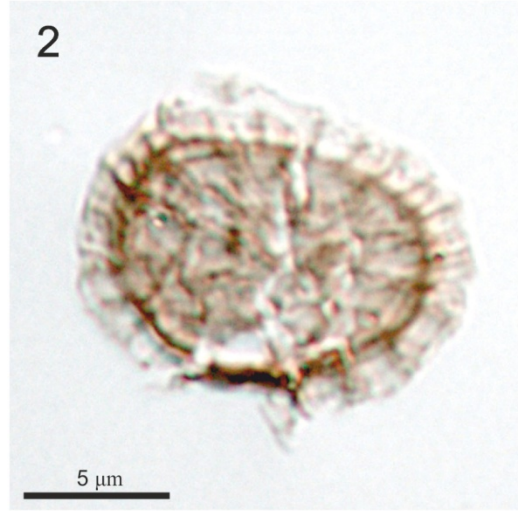
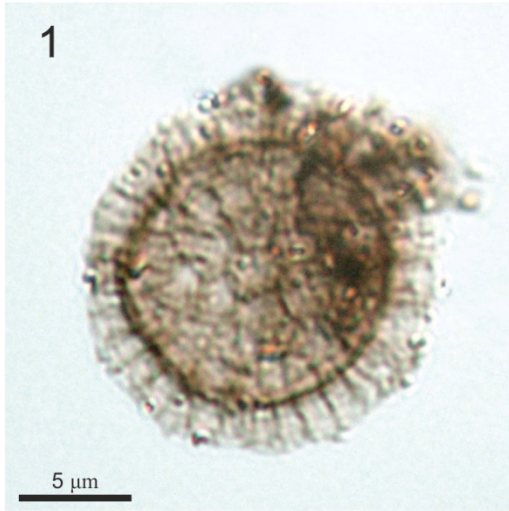


Plate 8

Fig. 1 *Leiosphaeridia minutissima*

Nolichucky Shale Sample 08BP-24 BEP-0127 (W30/0)

Fig. 2 *Leiosphaeridia minutissima*

Nolichucky Shale Sample 08BP-33 BEP-0183 (S33/0)

Fig. 3 *Leiosphaeridia* sp. 1

Nolichucky Shale Sample 08BP-52 BEP-0242 (F40/2)

Fig. 4 *Leiosphaeridia* sp. 1

Nolichucky Shale Sample 08BP-52 BEP-0242 (D40/0)

Fig. 5 *Leiosphaeridia* sp. 2

Nolichucky Shale Sample 08BP-01 BEP-0003 (C44/4)

Fig. 6 *Leiosphaeridia* sp. 3

Nolichucky Shale Sample 08BP-60 BEP-0258 (Z40/0)

Plate 8

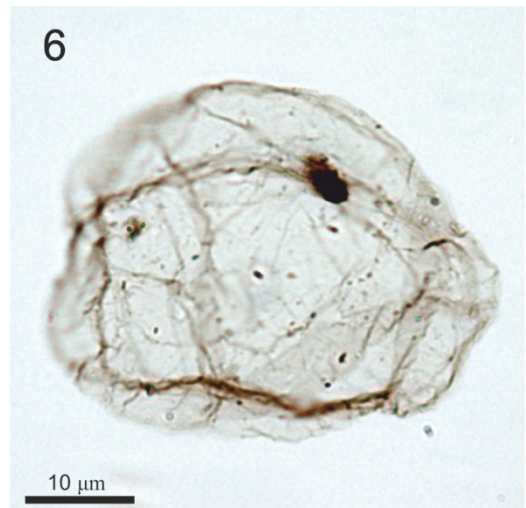
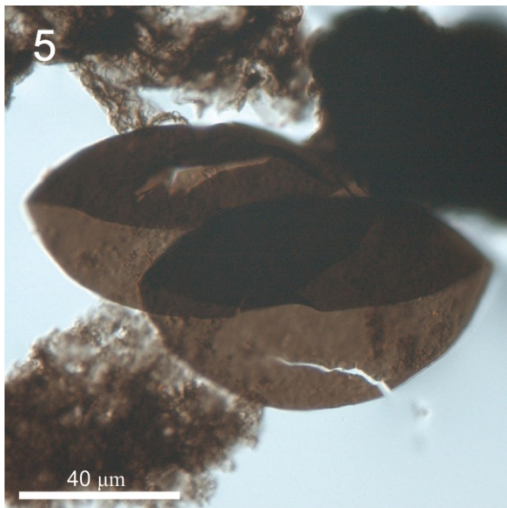
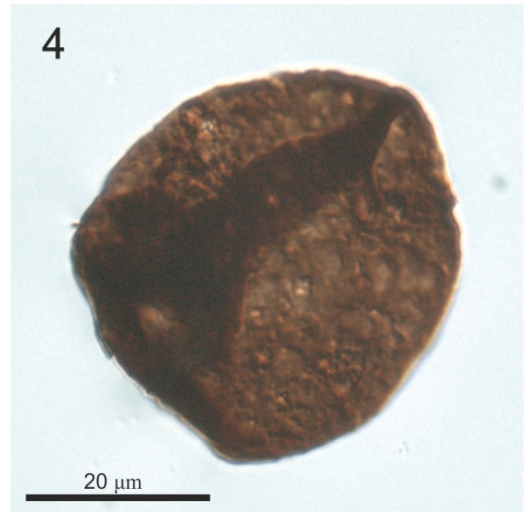
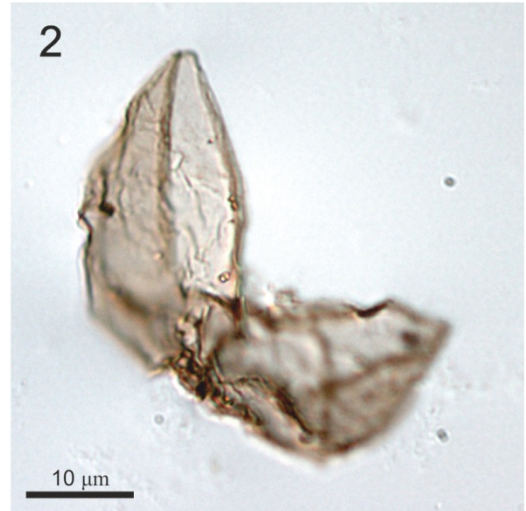
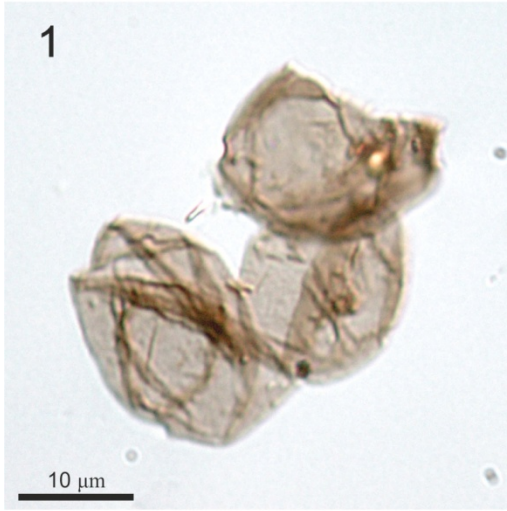


Plate 9

Fig. 1 *Liepaina plana*

Nolichucky Shale Sample 08BP-56 BEP-0248 (L46/4)

Fig. 2 *Liepaina plana*

Nolichucky Shale Sample 08BP-57 BEP-0250 (O34/1)

Fig. 3 *Lophosphaeridium tentativum*

Nolichucky Shale Sample 08BP-54 BEP-0244 (E38/1)

Fig. 4 *Lophosphaeridium tentativum*

Nolichucky Shale Sample 08BP-28½ BEP-0150 (Q50/1)

Fig. 5 *Lophosphaeridium truncatum*

Nolichucky Shale Sample 08BP-53 BEP-0243 (M36/1)

Fig. 6 *Lophosphaeridium truncatum*

Nolichucky Shale Sample 08BP-58 SEM-66

Plate 9

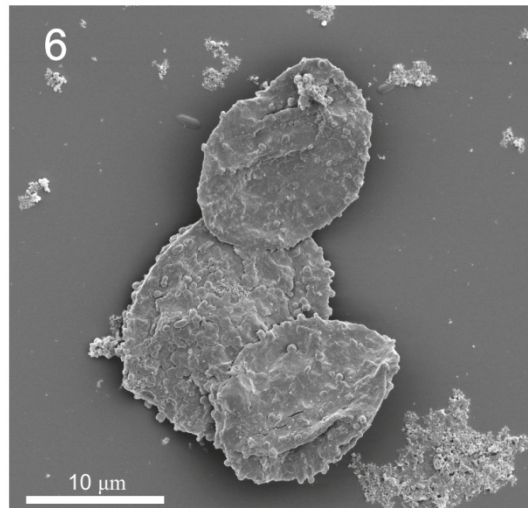
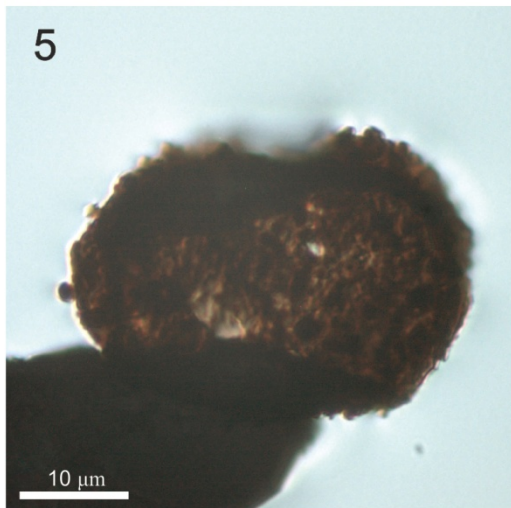
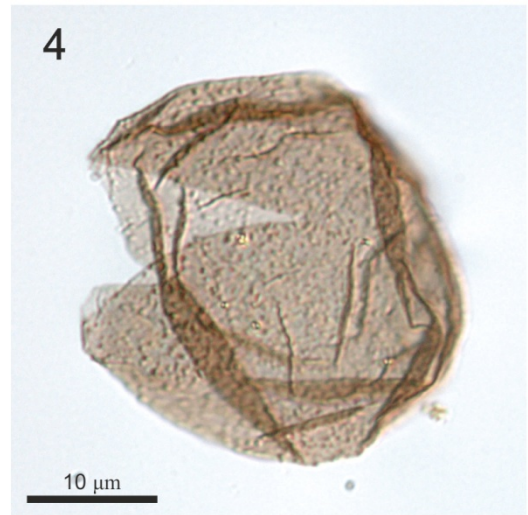
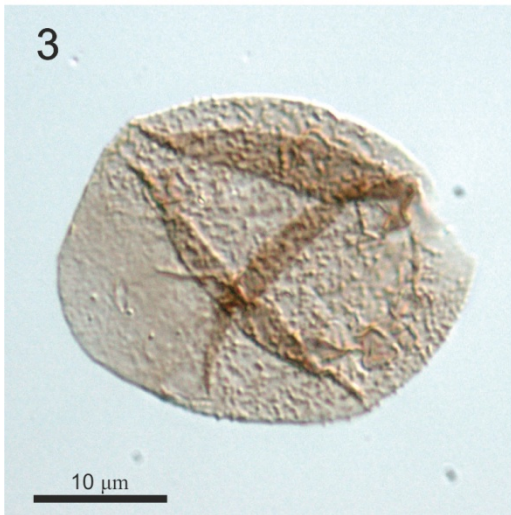
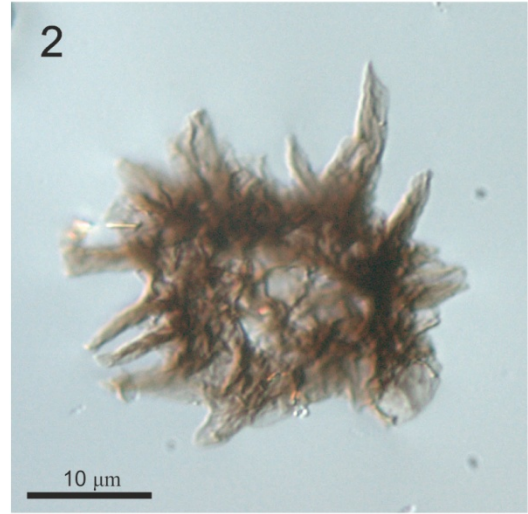
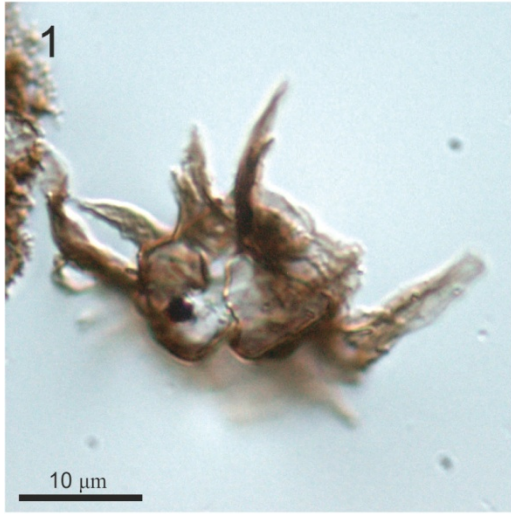


Plate 10

Fig. 1 *Lophosphaeridium variabile*

Nolichucky Shale Sample 08BP-53 BEP-0243 (F35/4)

Fig. 2 *Lophosphaeridium variabile* cluster

Nolichucky Shale Sample 08BP-56 BEP-0248 (G50/0)

Fig. 3 *Lophosphaeridium* sp. 1

Nolichucky Shale Sample 08BP-58 BEP-0254 (K49/4)

Fig. 4 *Lophosphaeridium* sp. 1

Nolichucky Shale Sample 08BP-60 BEP-0258 (T25/2)

Fig. 5 *Lophosphaeridium* sp. 2

Nolichucky Shale Sample 08BP-52 BEP-0242 (G45/3)

Fig. 6 *Lophosphaeridium* sp. 2

Nolichucky Shale Sample 08BP-52 BEP-0242 (U23/0)

Plate 10

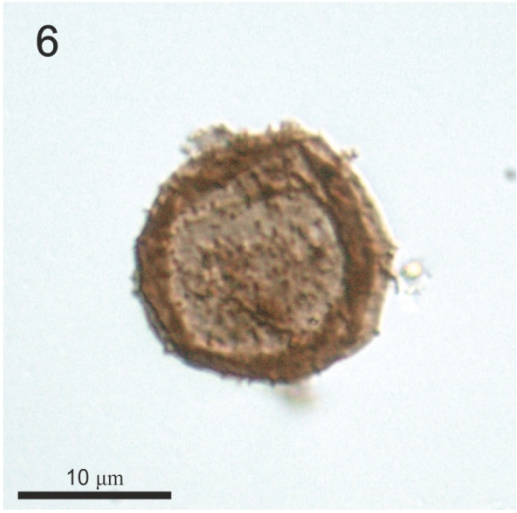
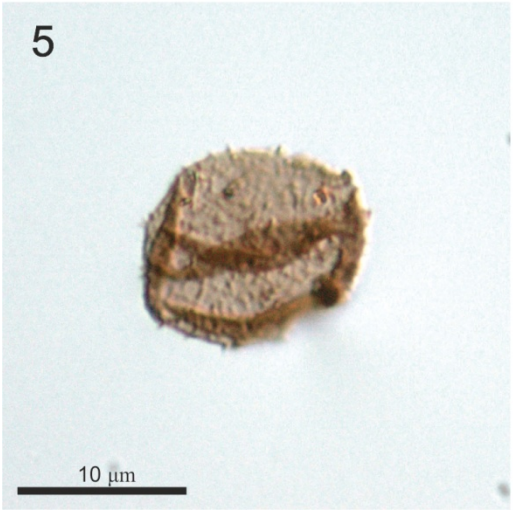
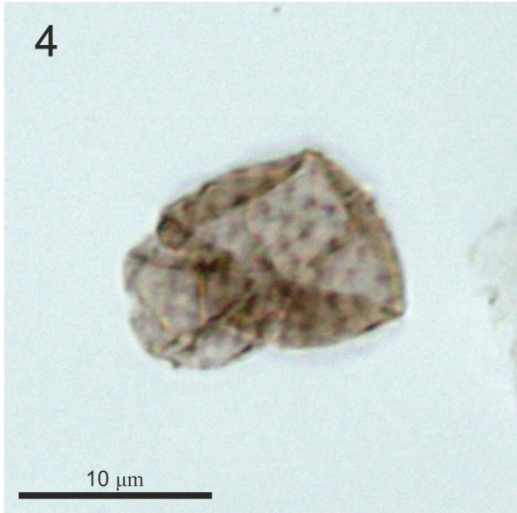
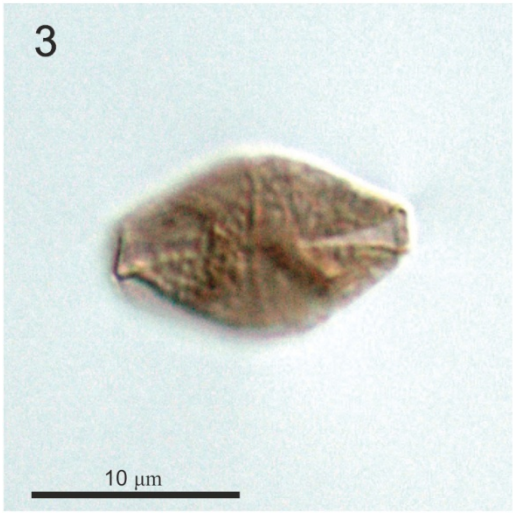
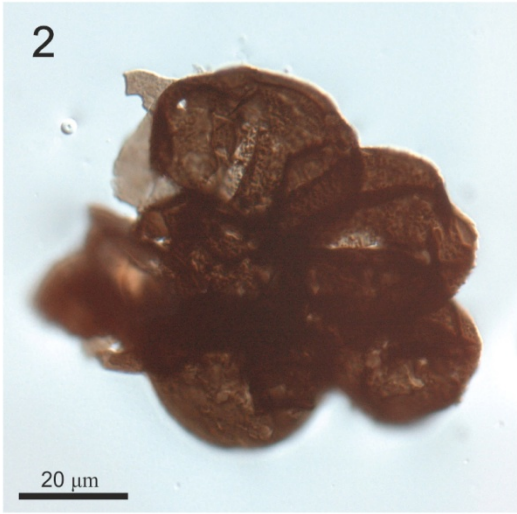
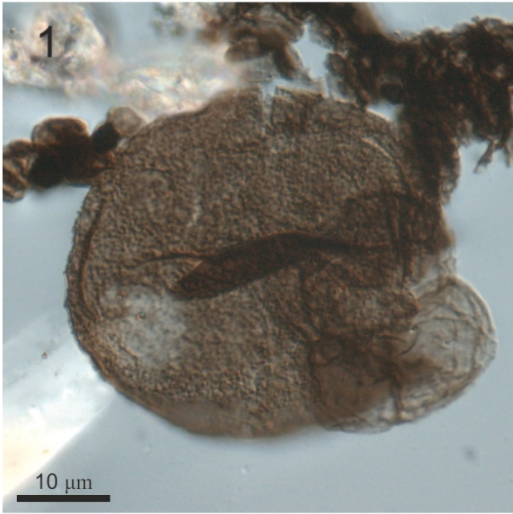


Plate 11

Fig. 1 *Rhopaliophora?* sp. 1

Nolichucky Shale Sample 08BP-30 BEP-0162 (K46/4)

Fig. 2 *Rhopaliophora?* sp. 1

Nolichucky Shale Sample 08BP-32 SEM-36

Fig. 3 *Virgatasporites rudii*

Nolichucky Shale Sample 08BP-09 BEP-0060 (H25/4)

Fig. 4 *Virgatasporites* sp. 1

Nolichucky Shale Sample 08BP-33 BEP-0195 (N48/0)

Fig. 5 *Virgatasporites* sp. 1

Nolichucky Shale Sample 08BP-33 BEP-0196 (G45/4)

Fig. 6 *Timofeevia* cf. *pentagonalis*

Nolichucky Shale Sample 08BP-34 BEP-0197 (C28/0)

Plate 11

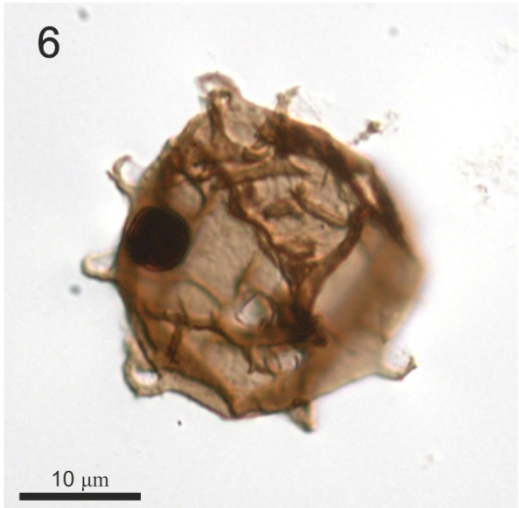
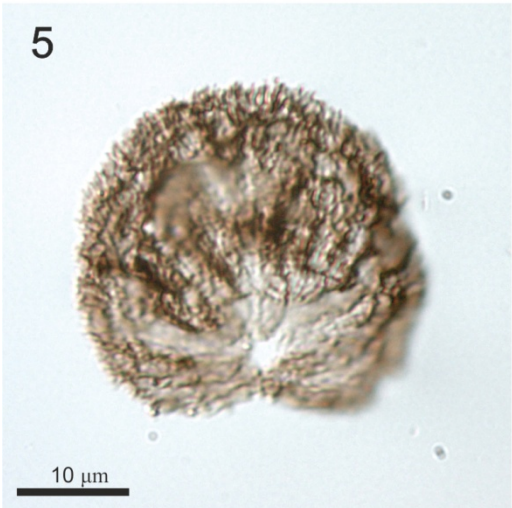
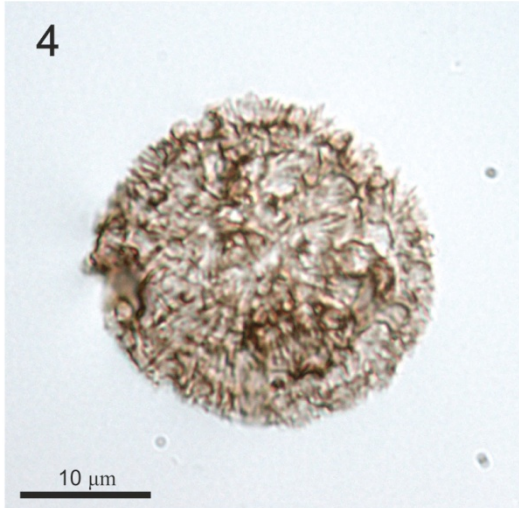
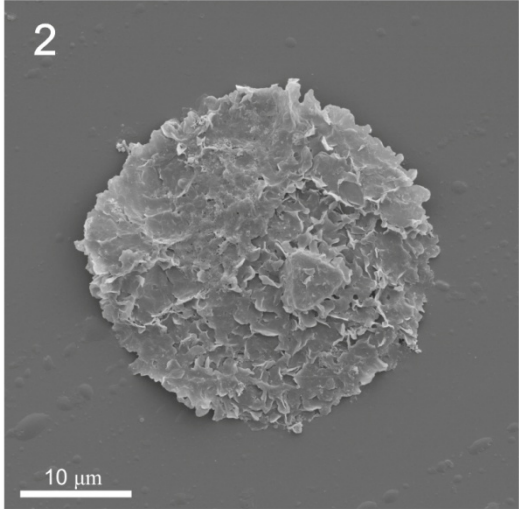
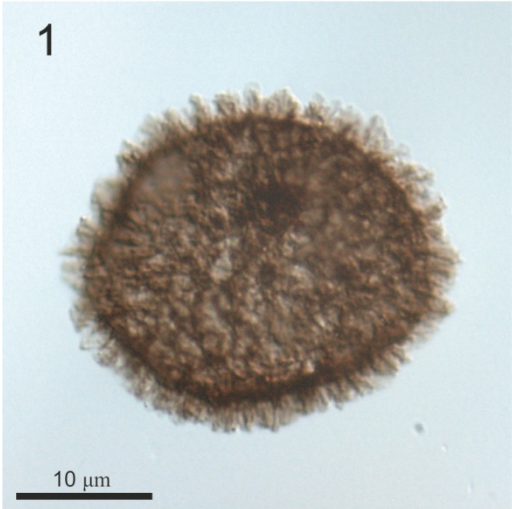


Plate 12

Fig. 1 *Timofeevia cf. pentagonalis*

Nolichucky Shale Sample 08BP-34 BEP-0197 (T48/2)

Fig. 2 Acritarch sp. 3

Nolichucky Shale Sample 08BP-54 BEP-0244 (F37/0)

Fig. 3 Acritarch sp. 3

Nolichucky Shale Sample 08BP-54 BEP-0244 (E52/3)

Fig. 4 Acritarch sp. 3

Nolichucky Shale Sample 08BP-54 BEP-0244 (J26/2)

Fig. 5 Acritarch sp. 3

Nolichucky Shale Sample 08BP-54 SEM-60

Excystment structure is enclosed by white square and is enlarged in Fig. 6.

Fig. 6 Acritarch sp. 3. Detail of specimen in Fig. 5.

Plate 12

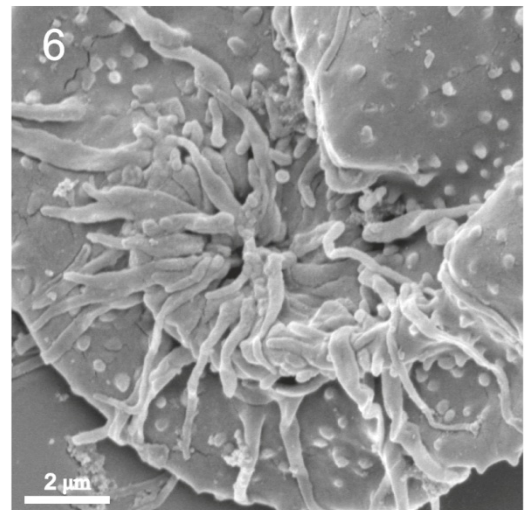
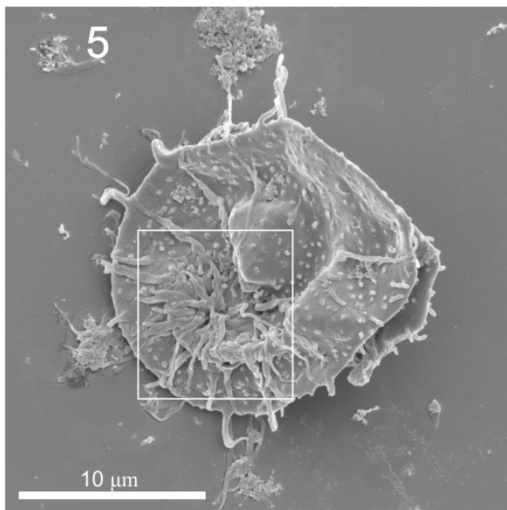
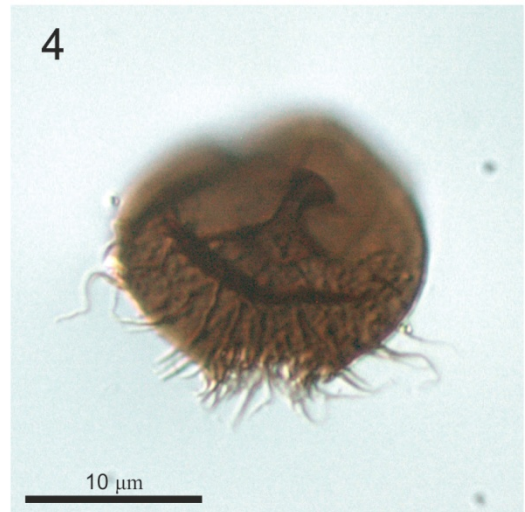
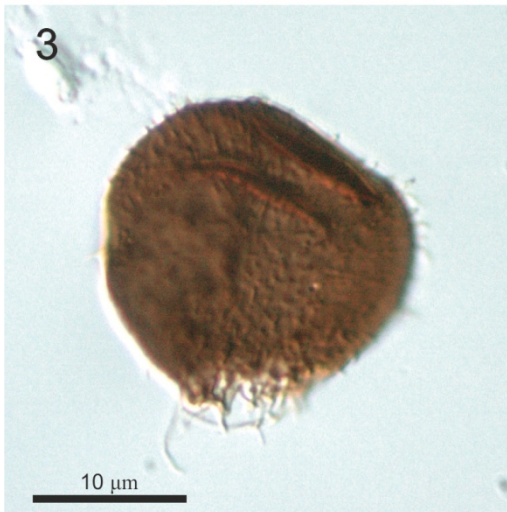
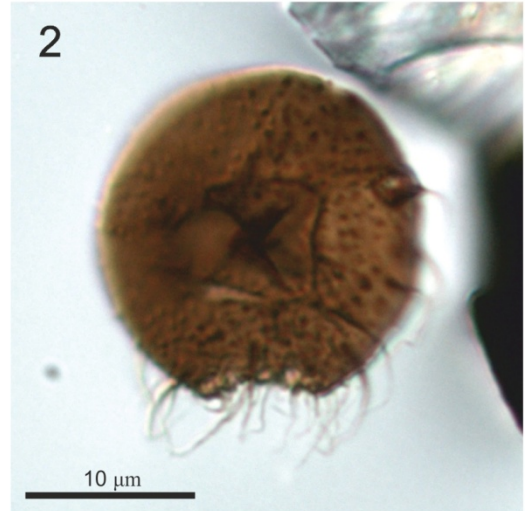
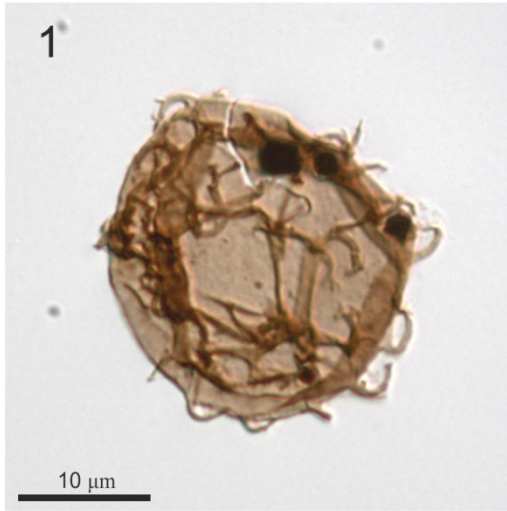


Plate 13

Fig. 1 *Corollasphaeridium wilcoxianum*

Nolichucky Shale Sample 08BP-33 BEP-0195 (K35/0)

Note the fibrils running down the lengths of processes and onto the vestigial collarete.

Fig. 2 Acritarch sp. 4

Nolichucky Shale Sample 08BP-33 SEM-83

Fig. 3 Acritarch sp. 4

Nolichucky Shale Sample 08BP-34 SEM-75

Fig. 4 Acritarch sp. 4

Nolichucky Shale Sample 08BP-33 SEM-82

Plate 13

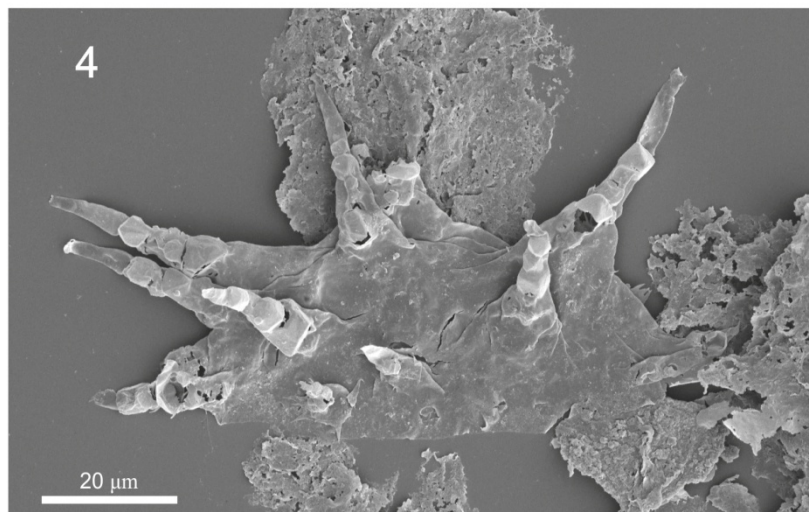
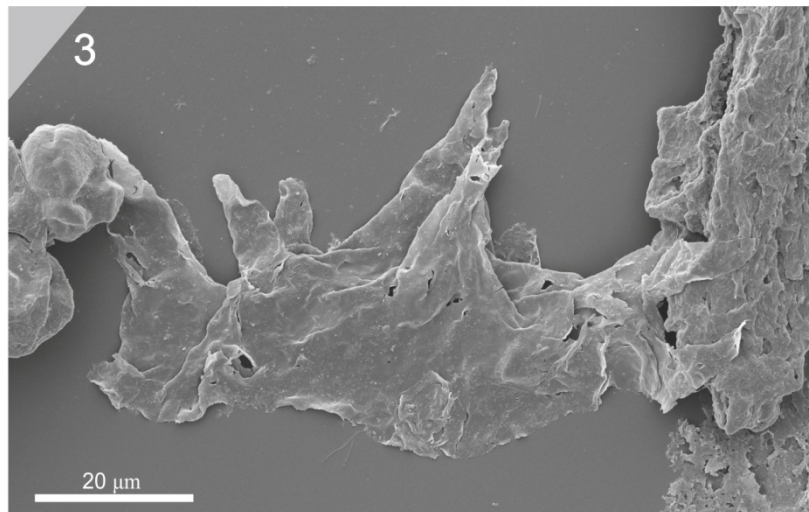
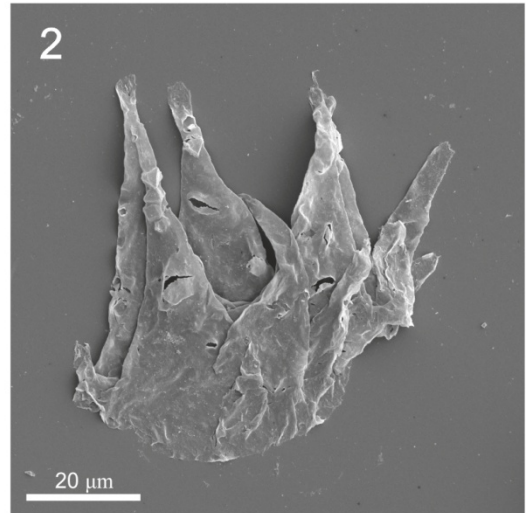
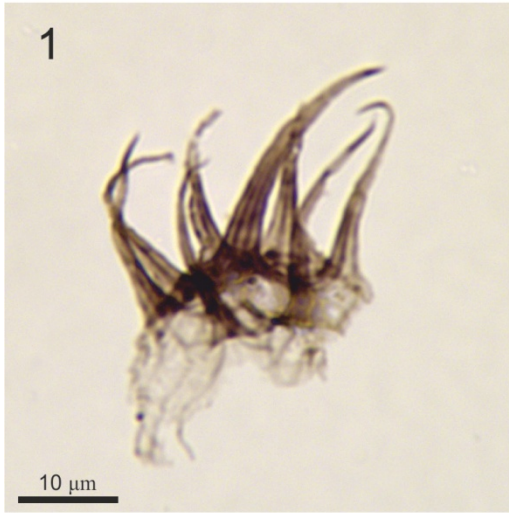


Plate 14

Fig. 1 Acritarch sp. 5

Nolichucky Shale Sample 08BP-30 BEP-0162 (G40/3)

Fig. 2 Acritarch sp. 5

Nolichucky Shale Sample 08BP-29 BEP-0155 (X44/0)

Fig. 3 Acritarch sp. 5

Nolichucky Shale Sample 08BP-32 BEP-0167 (T34/0)

Fig. 4 Acritarch sp. 5

Nolichucky Shale Sample 08BP-30 BEP-0162 (G40/3)

Fig. 5 Acritarch sp. 5

Nolichucky Shale Sample 08BP-30 SEM-23

Fig. 6 Acritarch sp. 5

Nolichucky Shale Sample 08BP-19 SEM-24

Plate 14

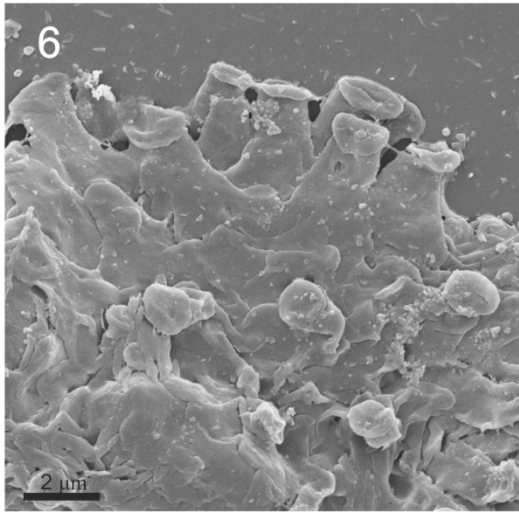
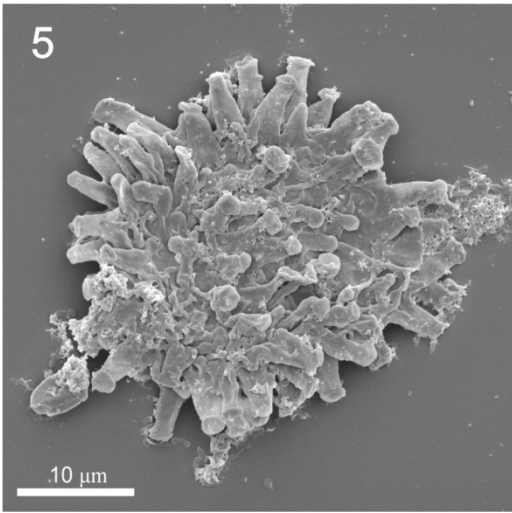
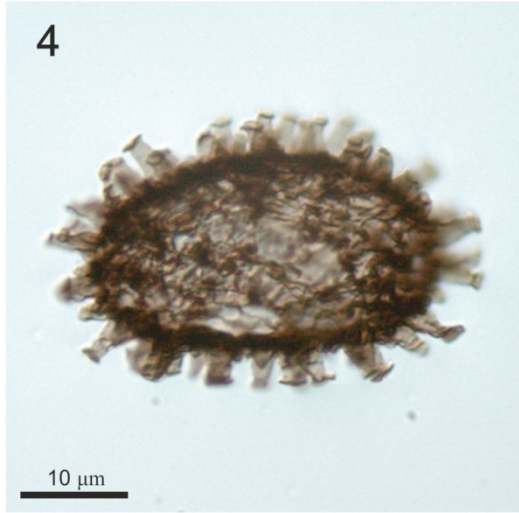
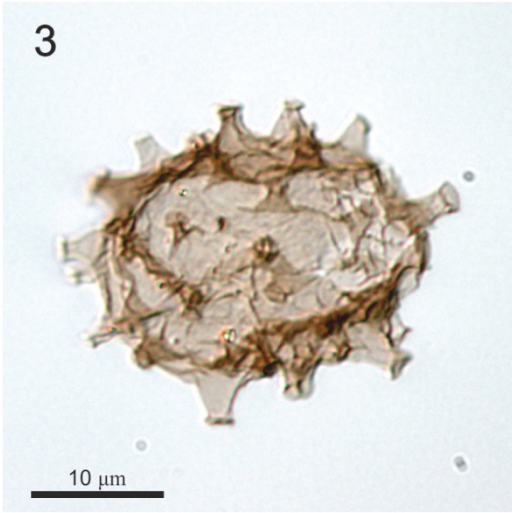
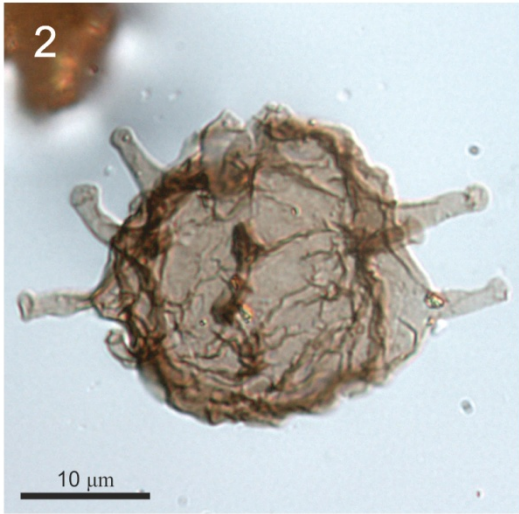
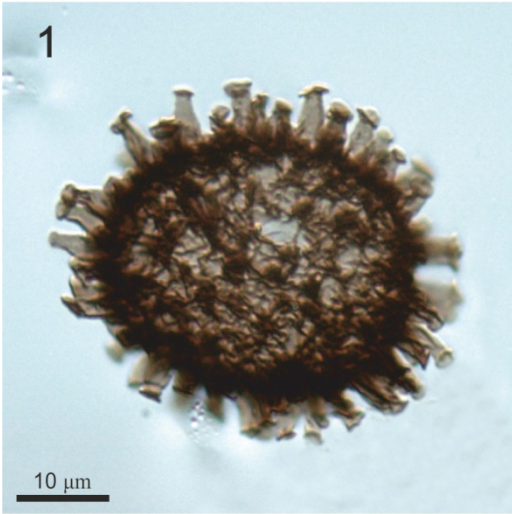


Plate 15

Fig. 1 Acritarch sp. 7

Nolichucky Shale Sample 08BP-54 BEP-0244 (H23/4)

Fig. 2 Acritarch sp. 7

Nolichucky Shale Sample 08BP-54 BEP-0244 (G50/4)

Fig. 3 Acritarch sp. 7

Nolichucky Shale Sample 08BP-54 BEP-0244 (G50/2)

Fig. 4 Acritarch sp. 7

Nolichucky Shale Sample 08BP-54 BEP-0244 (C42/3)

Fig. 5 Acritarch sp. 7

Nolichucky Shale Sample 08BP-54 BEP-0244 (E30/3)

Fig. 6 Acritarch sp. 7

Nolichucky Shale Sample 08BP-54 BEP-0244 (L23/4)

Fig. 7 Acritarch sp. 7

Nolichucky Shale Sample 08BP-54 SEM-60

Fig. 8 Acritarch sp. 7

Nolichucky Shale Sample 08BP-54 SEM-65

Plate 15



10 μ m

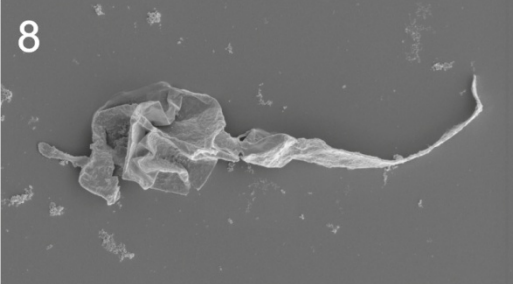
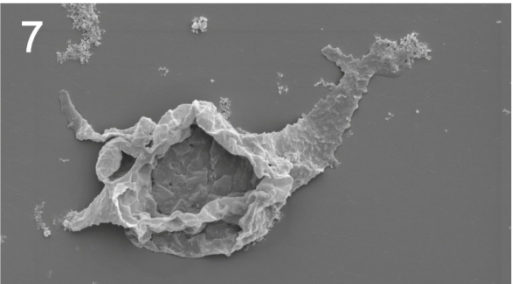
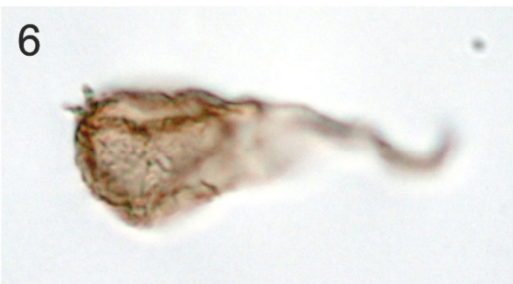


Plate 16

Fig. 1 Acritarch sp. 8

Nolichucky Shale Sample 08BP-29 BEP-0157 (1614)

Area within black square is enlarged in Fig 2.

Fig. 2 Acritarch sp. 8. Detail of processes from specimen in Fig. 1

Fig. 3 Acritarch sp. 8

Nolichucky Shale Sample 08BP-29 BEP-0154 (T50/3)

Fig. 4 Acritarch sp. 8

Nolichucky Shale Sample 08BP-30 BEP-0162 (Q30/1)

Fig. 5 Acritarch sp. 6

Nolichucky Shale Sample 08BP-56 SEM-62

Fig. 6 Acritarch sp. 6

Nolichucky Shale Sample 08BP-56 SEM-62

Plate 16

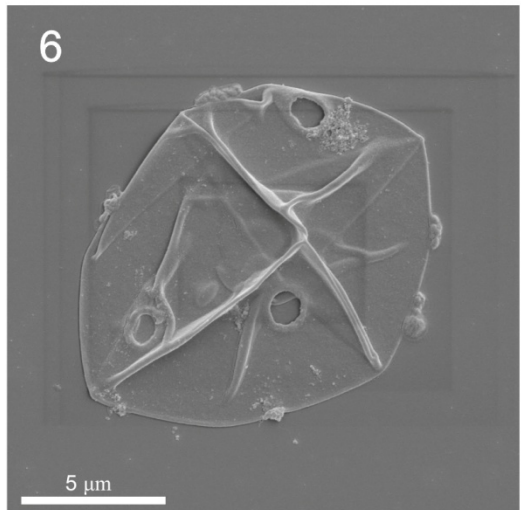
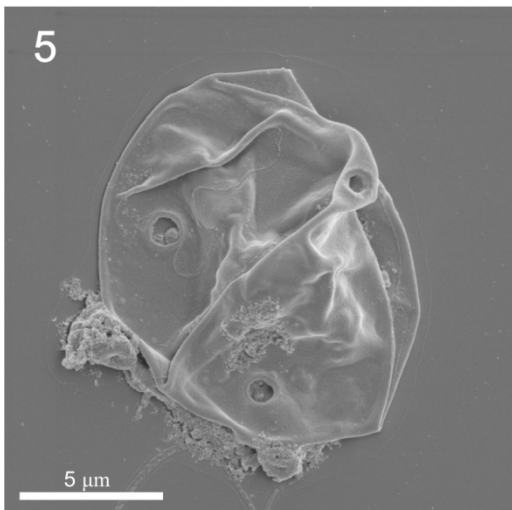
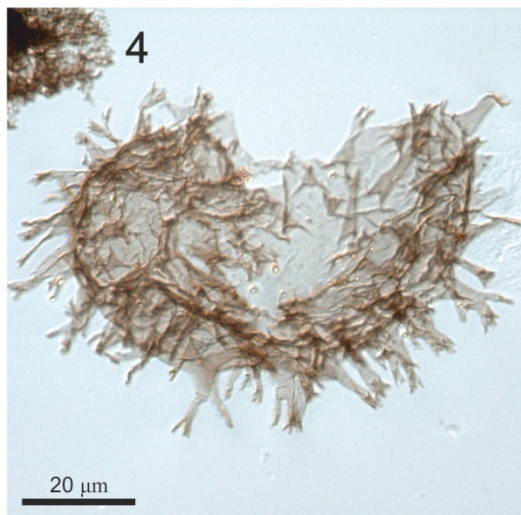
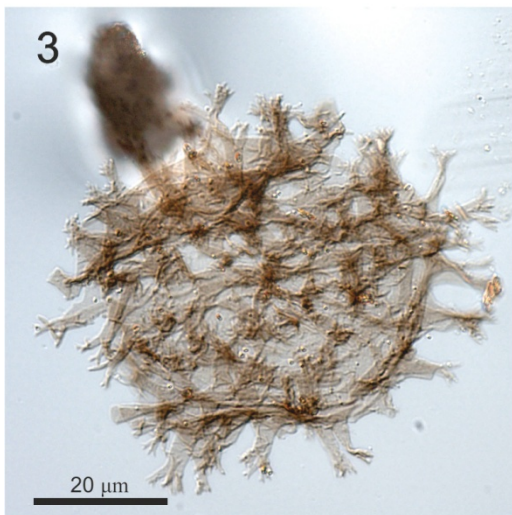
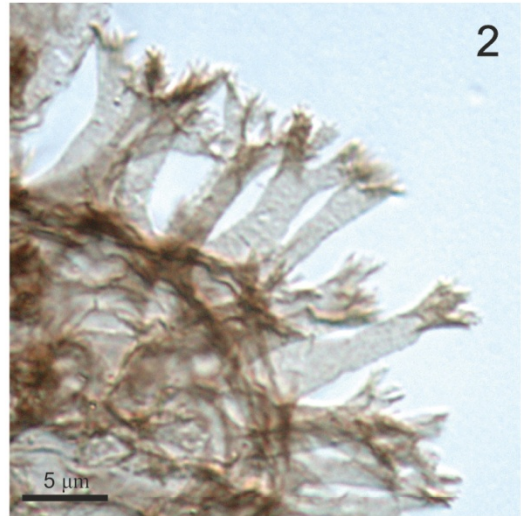
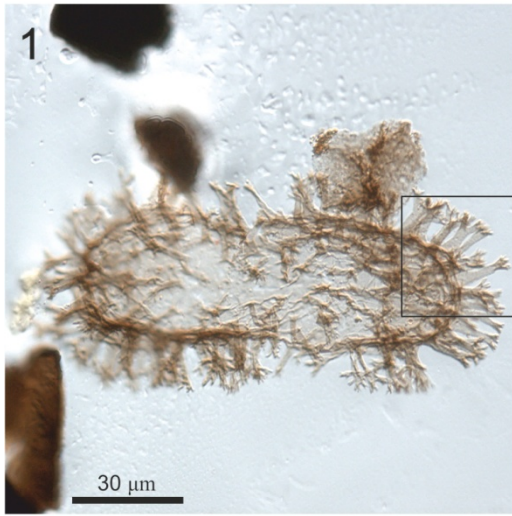


Plate 17

Fig. 1 *Symplassosphaeridium cf. cambriense*

Nolichucky Shale Sample 08BP-54 BEP-0244 (K35/0)

Fig. 2 *Symplassosphaeridium cf. cambriense*

Nolichucky Shale Sample 08BP-04 BEP-0018 (L30/1)

Fig. 3 *Thymadora kerke*

Rogersville Shale Sample 08BP-76 SEM-88

Fig. 4 *Thymadora kerke*

Rogersville Shale Sample 08BP-76 SEM-88

Fig. 5 *Acritarch sp. 9*

Nolichucky Shale Sample 08BP-32 BEP-0167 (L33/2)

Fig. 6 *Acritarch sp. 9*

Nolichucky Shale Sample 08BP-59 BEP-0256 (X31/3)

Plate 17

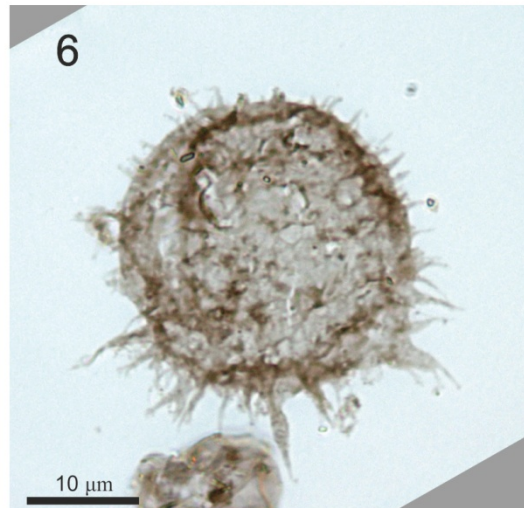
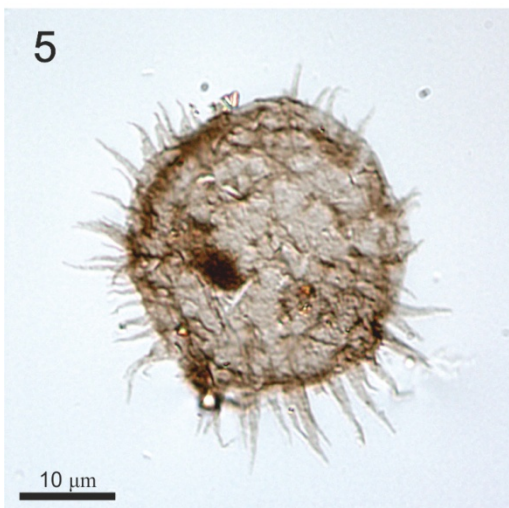
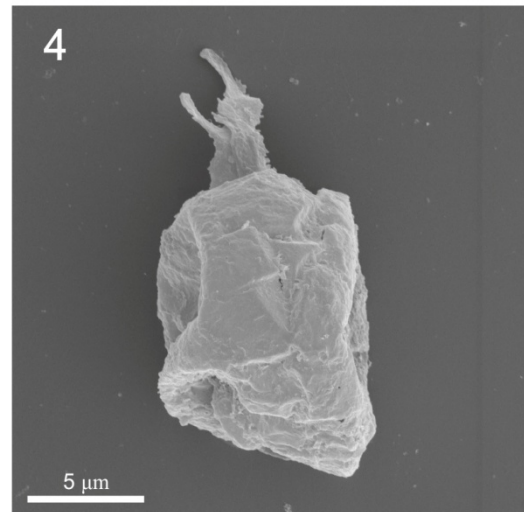
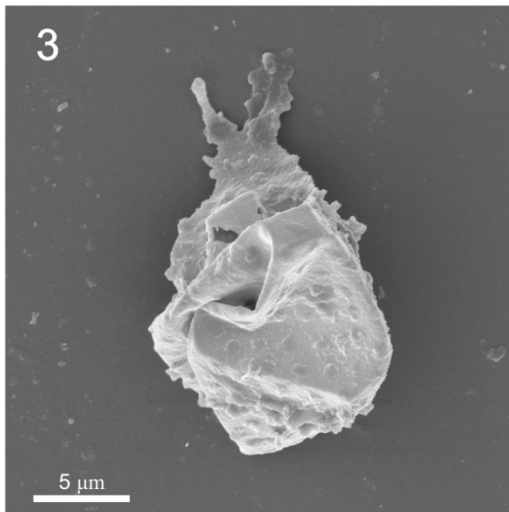
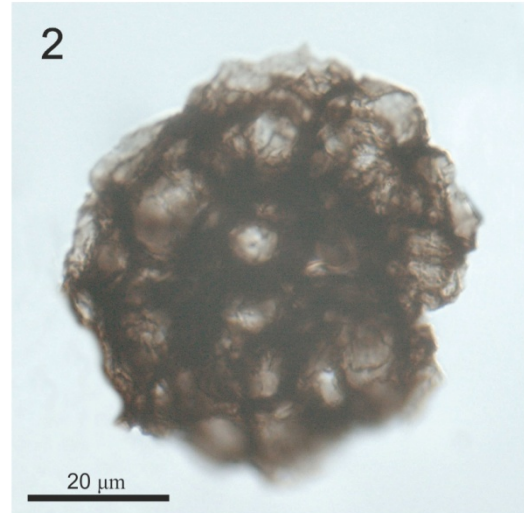
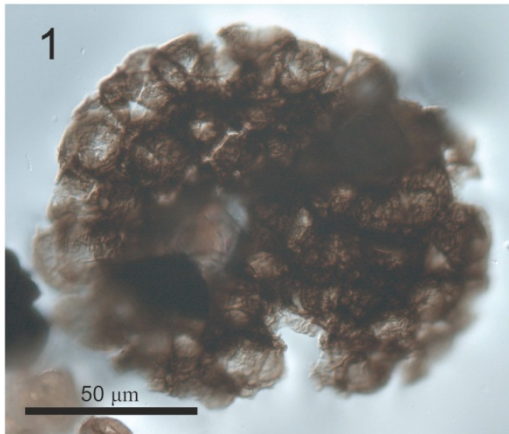


Plate 18

Fig. 1 Acritarch sp. 10

Nolichucky Shale Sample 08BP-23 BEP-0126 (M29/4)

Fig. 2 Acritarch sp. 10

Nolichucky Shale Sample 08BP-33 BEP-0196 (U44/1)

Fig. 3 Acritarch sp. 10

Nolichucky Shale Sample 08BP-33 SEM-83

Fig. 4 Acritarch sp. 10. Enlarged apical process of specimen in Fig. 3.

Fig. 5 Acritarch sp. 10

Nolichucky Shale Sample 08BP-33 SEM-83

Fig. 6 Acritarch sp. 10. Enlarged apical process of specimen in Fig. 5.

Plate 18

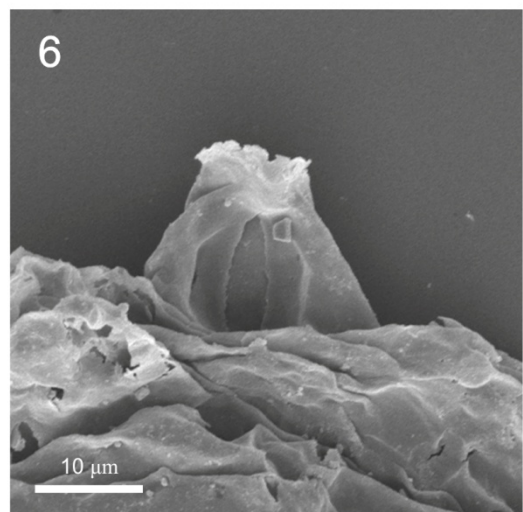
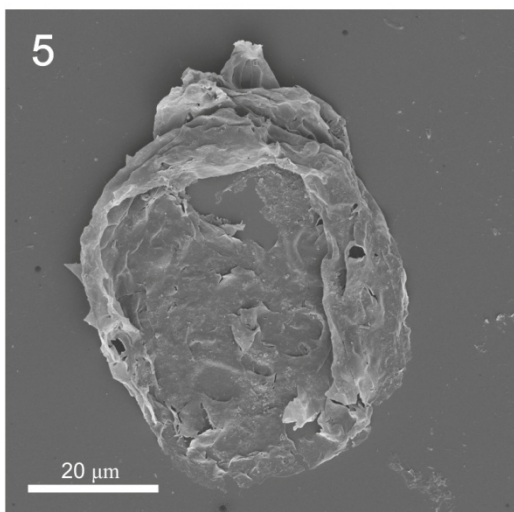
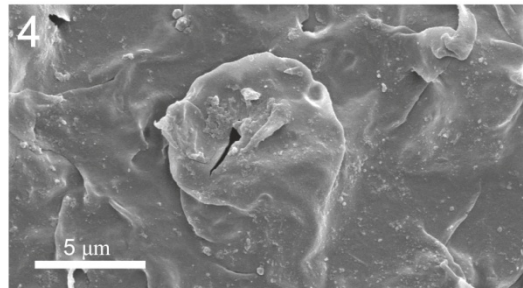
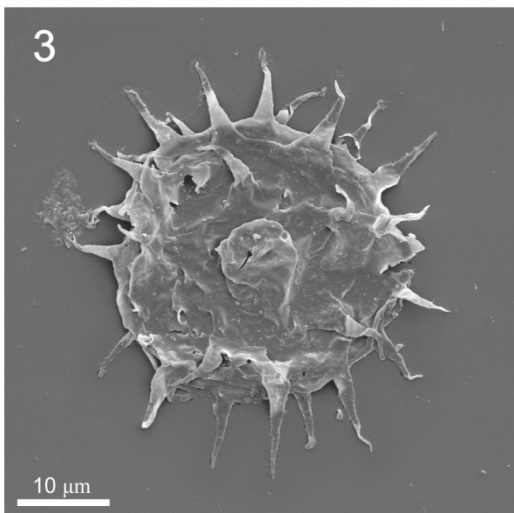
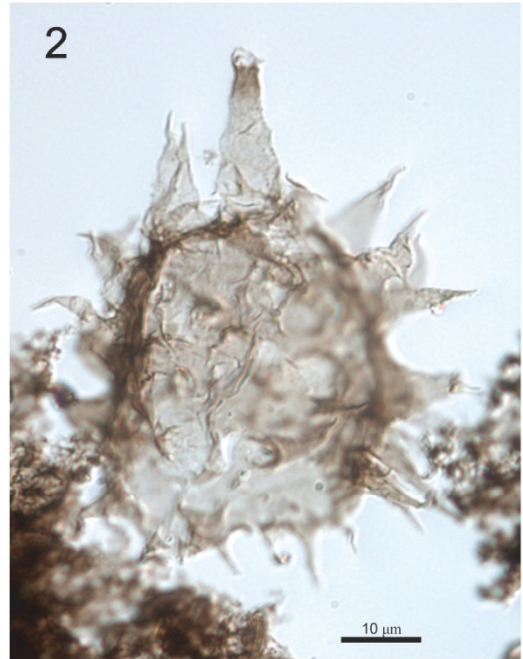
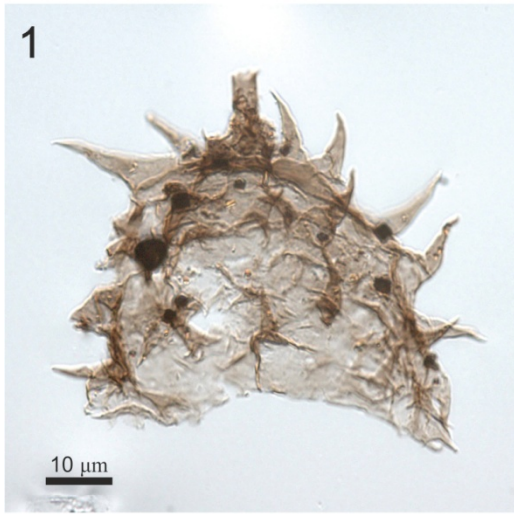


Plate 19

Fig. 1 *Peteinosphaeridium?* sp. 1

Gros Ventre Formation Sample 09BP-49 BEP-0308 (P44/4)

Fig. 2 *Peteinosphaeridium?* sp. 1. Enlargement of processes from specimen in Fig. 1.

Fig. 3 *Peteinosphaeridium?* sp. 1

Nolichucky Shale Sample 08BP-52 BEP-0242 (R36/4)

Fig. 4 *Peteinosphaeridium?* sp. 1. Details of processes.

Gros Ventre Formation Sample 09BP-49 SEM-54

Fig. 5 *Peteinosphaeridium?* sp. 1. Details of processes.

Gros Ventre Formation Sample 09BP-49 SEM-54

Fig. 6 *Peteinosphaeridium?* sp. 1. Showing smooth, internal surface of vesicle.

Gros Ventre Formation Sample 08BP-49 SEM-55

Plate 19

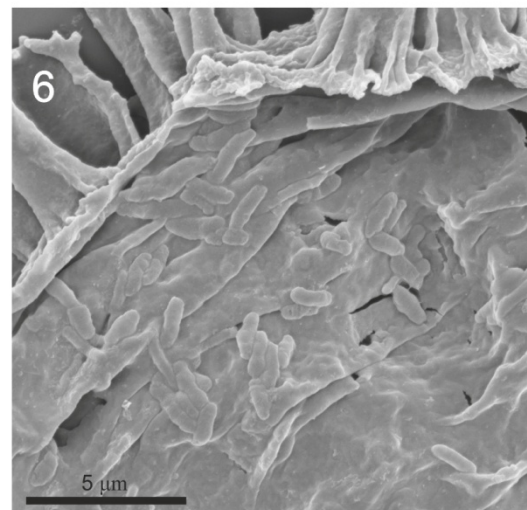
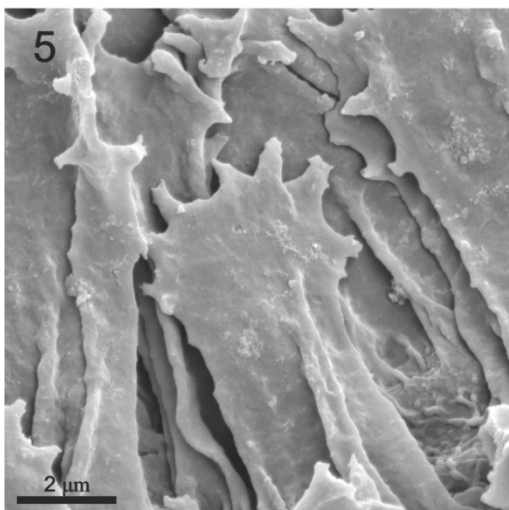
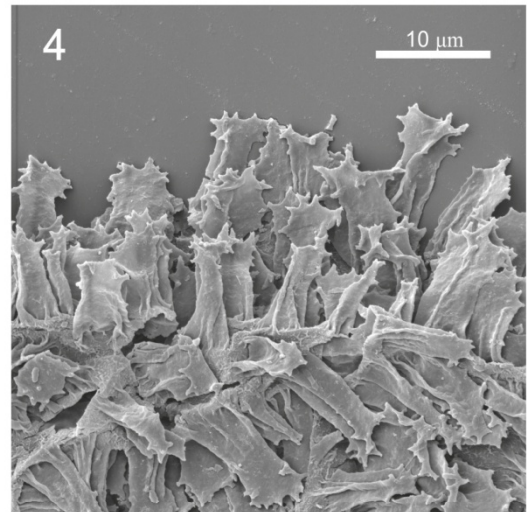
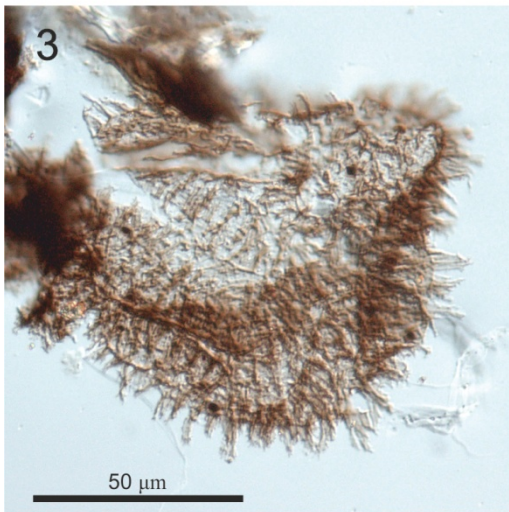
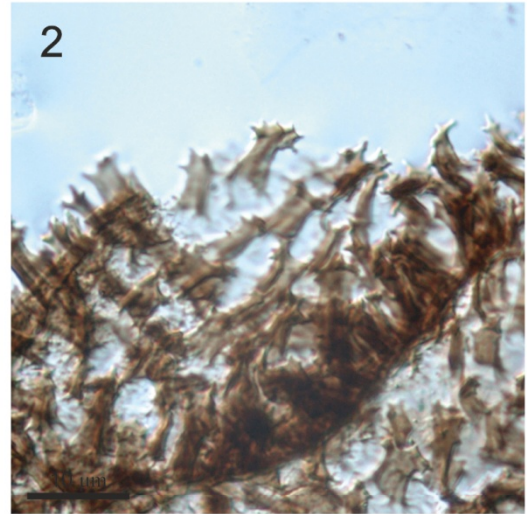
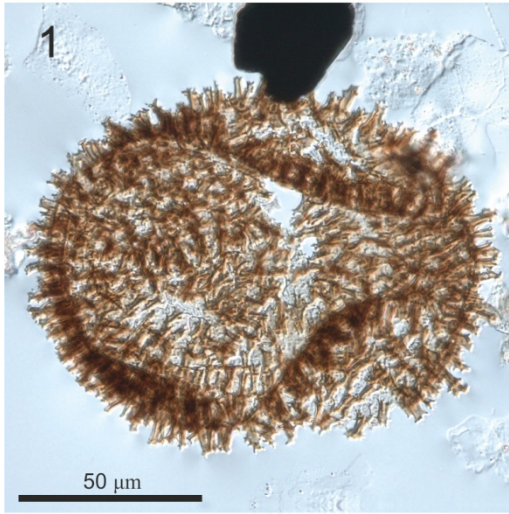


Plate 20

Fig. 1 *Peteinosphaeridium?* sp. 2

Gros Ventre Formation Sample 09BP-49 BEP-0308 (O29/0).

Fig. 2 *Peteinosphaeridium?* sp. 2. Detail of processes from specimen in Fig. 1.

Fig. 3 *Peteinosphaeridium?* sp. 2

Gros Ventre Formation Sample 09BP-49 BEP-0309 (V26/0)

Fig. 4 *Peteinosphaeridium?* sp. 2

Gros Ventre Formation Sample 09BP-49 SEM-51

Fig. 5 *Peteinosphaeridium?* sp. 2

Gros Ventre Formation Sample 09BP-49 SEM-50

Fig. 6 *Peteinosphaeridium?* sp. 2. Showing rugulate vesicle surface.

Gros Ventre Formation Sample 09BP-49 SEM-49

Plate 20

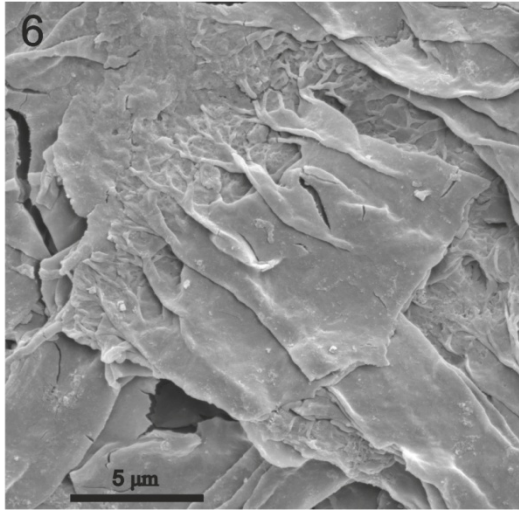
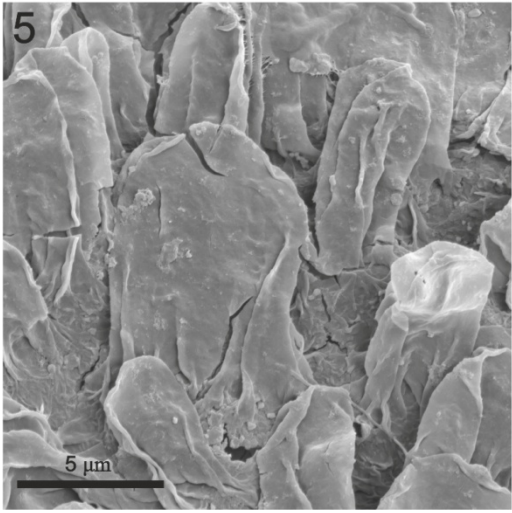
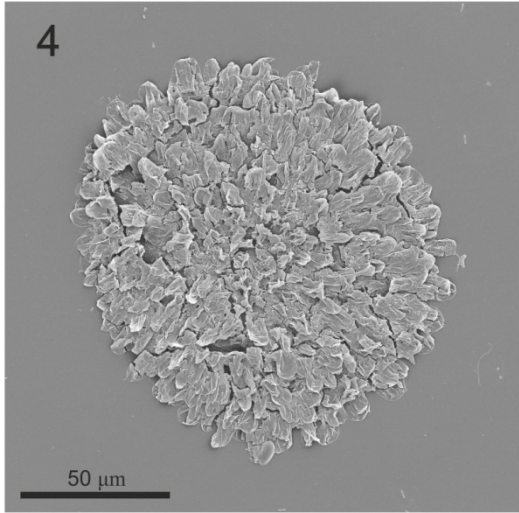
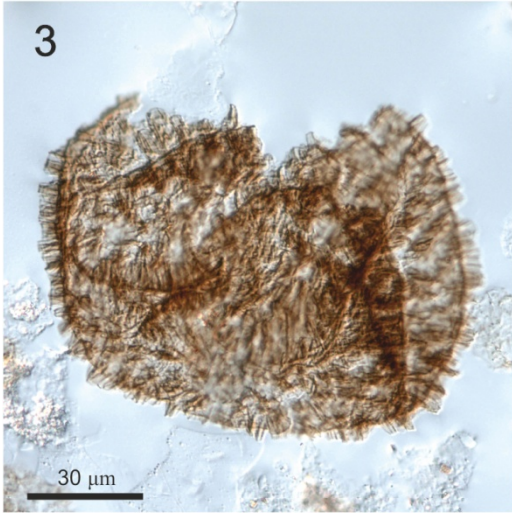
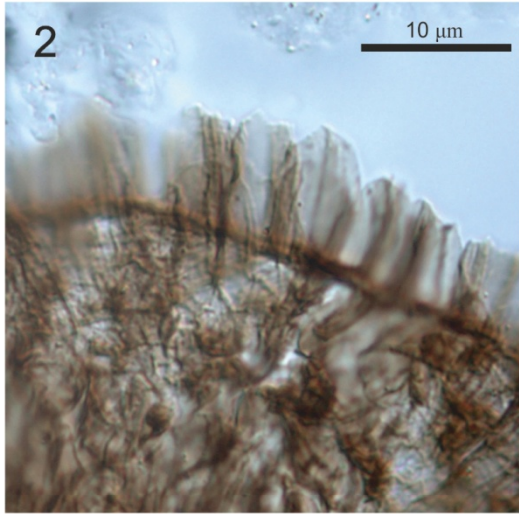
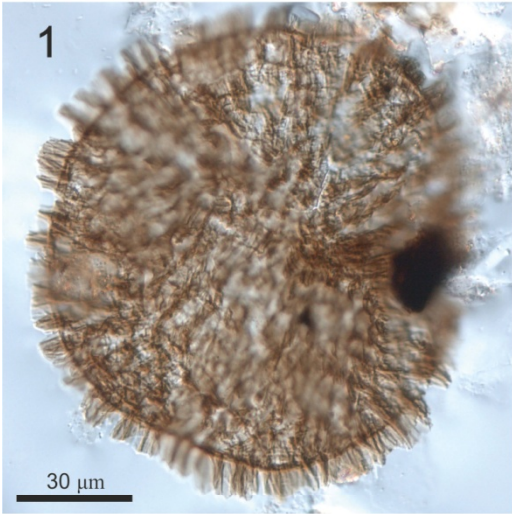


Plate 21

Fig. 1 Acritarch sp. 1

Nolichucky Shale Sample 08BP-32 BEP-0175 (P30/3)

Fig. 2 Acritarch sp. 1. Detail of processes from specimen in Fig. 1.

Fig. 3 Acritarch sp. 1

Nolichucky Shale Sample 08BP-32 SEM-Y6

Fig. 4 Acritarch sp. 1. Detail of processes and connecting membranes.

Nolichucky Shale Sample 08BP-32 SEM-Y6

Fig. 5 Acritarch sp. 1. Detail showing process/membrane attachment scars on vesicle surface.

Nolichucky Shale Sample 08BP-33 SEM-70

Fig. 6 Acritarch sp. 1

Nolichucky Shale Sample 08BP-29 BEP-0156 (F32/0)

Plate 21

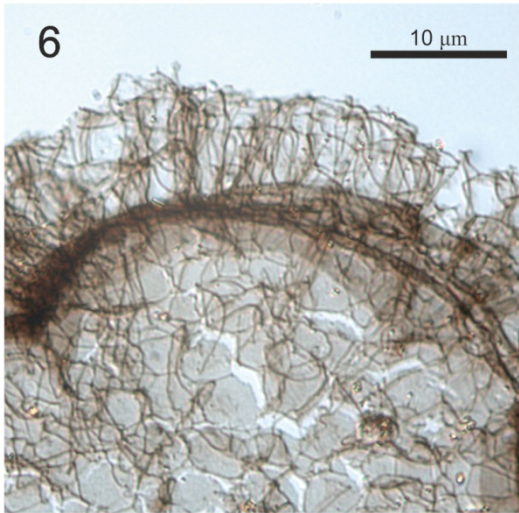
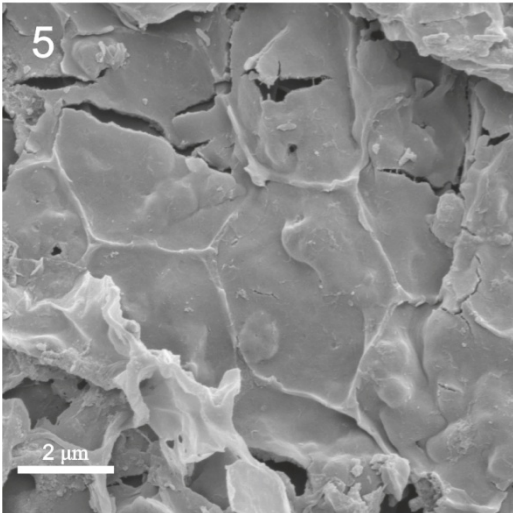
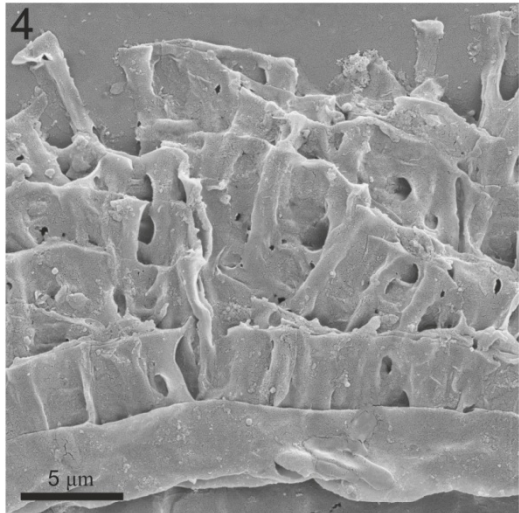
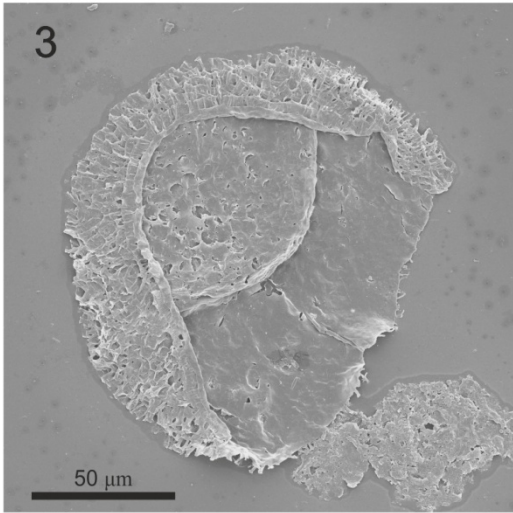
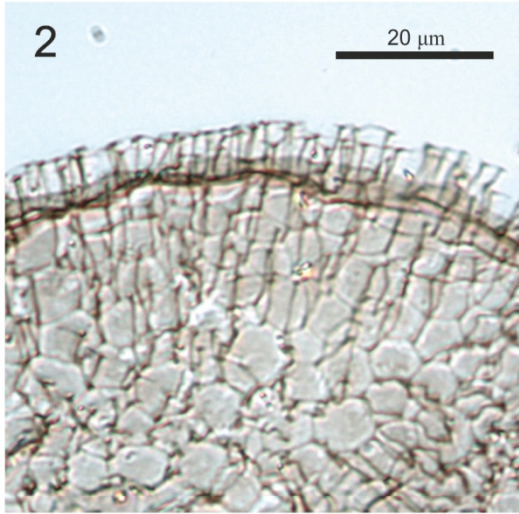


Plate 22

Fig. 1 Acritarch sp. 2

Nolichucky Shale Sample 08BP-29 BEP-0154 (S28/0)

Fig. 2 Acritarch sp. 2

Nolichucky Shale Sample 08BP-29 BEP-0154 (H17/0)

Fig. 3 Acritarch sp. 2

Nolichucky Shale Sample 08BP-32 SEM-37

Fig. 4 Acritarch sp. 2. Showing processes from specimen in Fig. 3.

Fig. 5 Acritarch sp. 2. Showing processes from specimen in Fig. 3.

Fig. 6 Acritarch sp. 2. Showing smooth internal vesicle surface from specimen in Fig. 3.

Plate 22

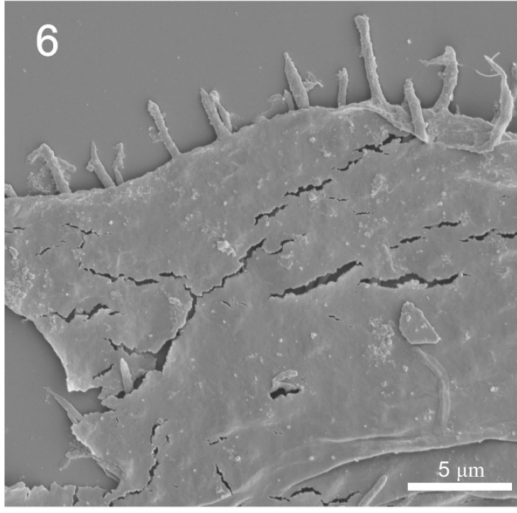
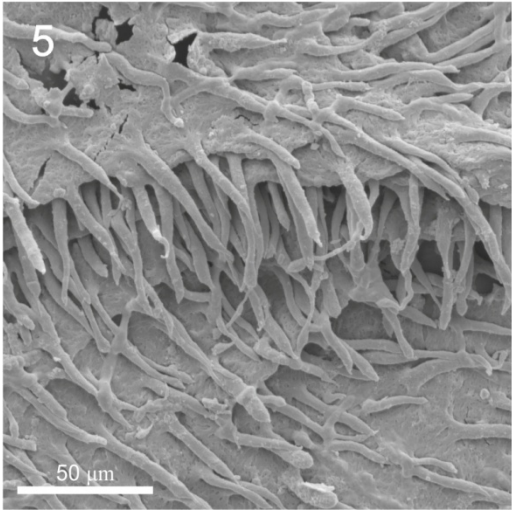
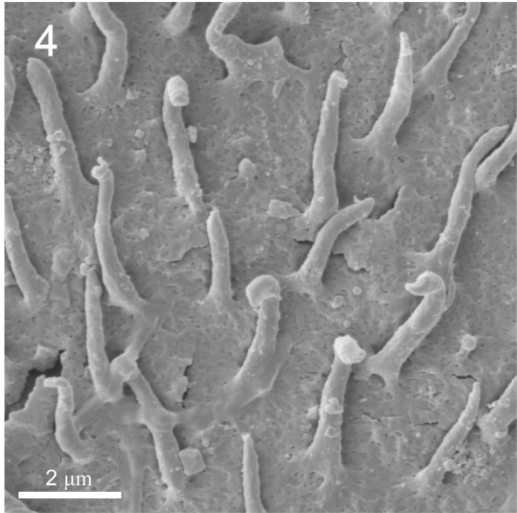
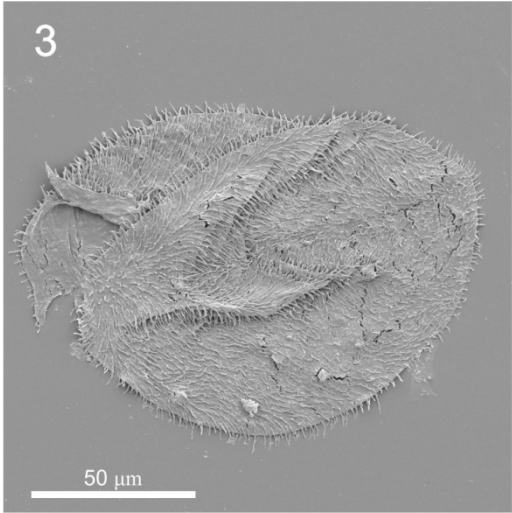
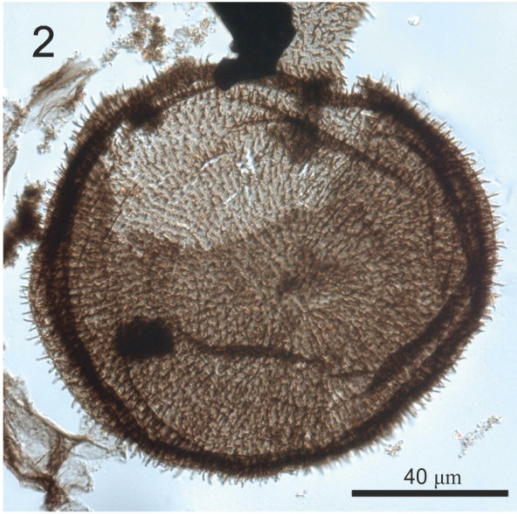
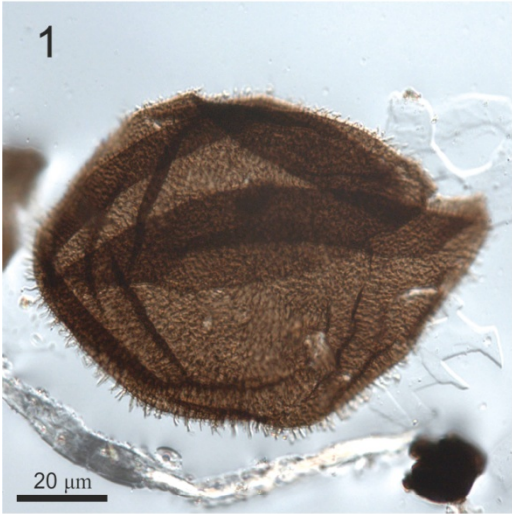


Plate 23

Fig. 1 *Peteinosphaeridium?* sp. 1. Ultrastructure of vesicle wall and large process.

Gros Ventre Formation Sample 09BP-49

TEM micrograph: LAS3c BP_0053.

Fig. 2 *Peteinosphaeridium?* sp. 1. Ultrastructure of vesicle wall and processes. Two strands of vesicle wall are present. Each strand has bases of severed processes emanating from one side (external). The smooth surface represents the internal vesicle surface.

Gros Ventre Formation Sample 09BP-49

TEM micrograph: LSA3c BP_0017

Fig. 3 *Peteinosphaeridium?* sp. 2. Ultrastructure of vesicle wall and processes. Processes lie collapsed on each other.

Gros Ventre Formation Sample 09BP-49

TEM micrograph: LSA4a BP_0058

Fig. 4 *Peteinosphaeridium?* sp. 2. Ultrastructure of vesicle wall and processes.

Gros Ventre Formation. Sample 09BP-49

TEM micrograph: LSA4a BP_0025

Fig. 5 *Acritarch* sp. 2. Ultrastructure of vesicle wall and processes. Processes appear to be detaching.

Gros Ventre Formation Sample 09BP-49

TEM micrograph: LSA1A S24_0001

Fig. 6 *Acritarch* sp. 2. Ultrastructure of vesicle wall with single processes.

Gros Ventre Formation. Sample 09BP-49

TEM micrograph: LSA1B S24-0009

Plate 23

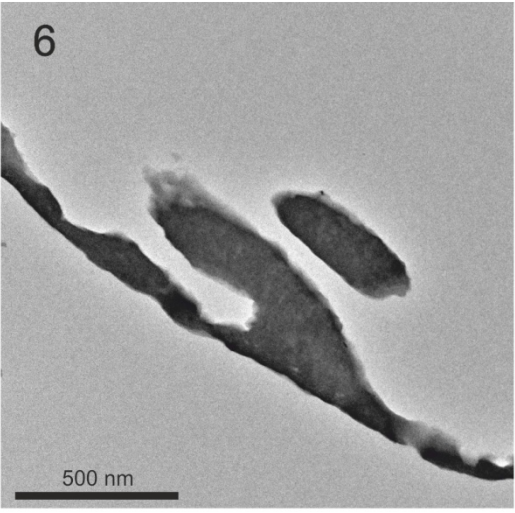
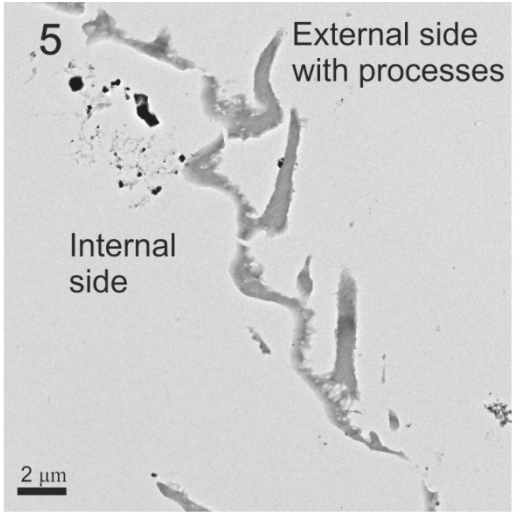
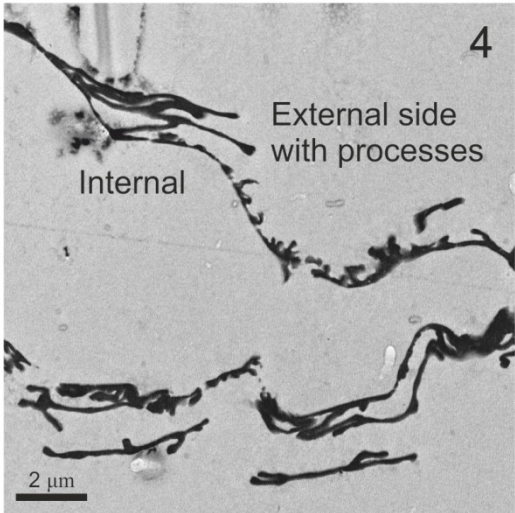
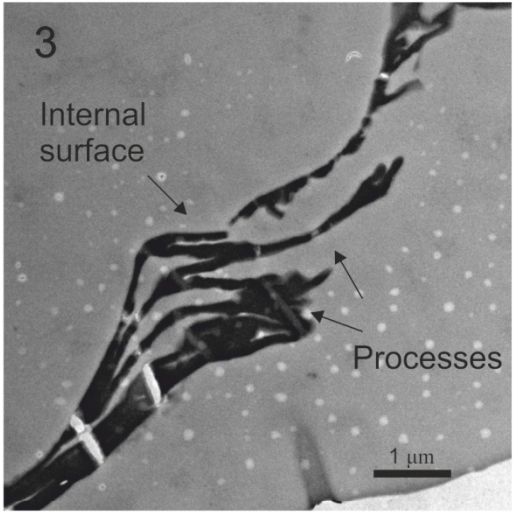
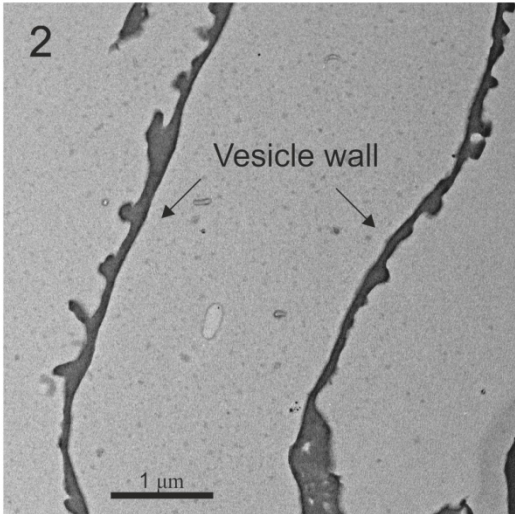
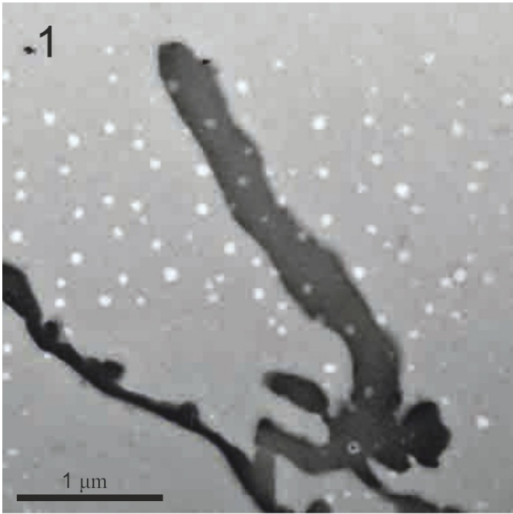


Plate 24

Fig. 1 Acritarch sp. 1. Ultrastructure of vesicle wall with alveolar layer. EL = external electron dense layer; IL = internal electron dense layer; AL = alveolar layer.

Nolichucky Shale Sample 08BP-32

TEM micrograph: LSA2.b-0006

Fig. 2 Acritarch sp. 1. Ultrastructure of vesicle wall with processes. Processes are bent over so as to lie flat on the vesicle surface.

Nolichucky Shale Sample 08BP-32

TEM micrograph: LSA2.b-BP_0048

Fig. 3 Acritarch sp. 1. Ultrastructure of vesicle wall with processes. AL = alveolar layer.

Nolichucky Shale Sample 08BP-32

TEM micrograph: LSA2.b 0002

Fig. 4 Acritarch sp. 1. Ultrastructure of vesicle wall. AL = alveolar layer; EDL = electron dense layer.

Nolichucky Shale Sample 08BP-32

TEM micrograph: LSA2.b 0005

Plate 24

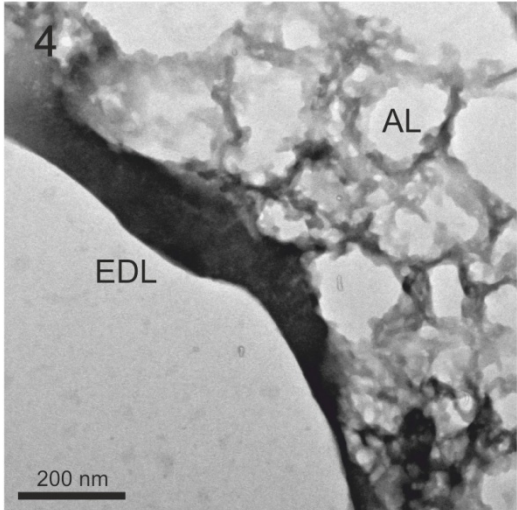
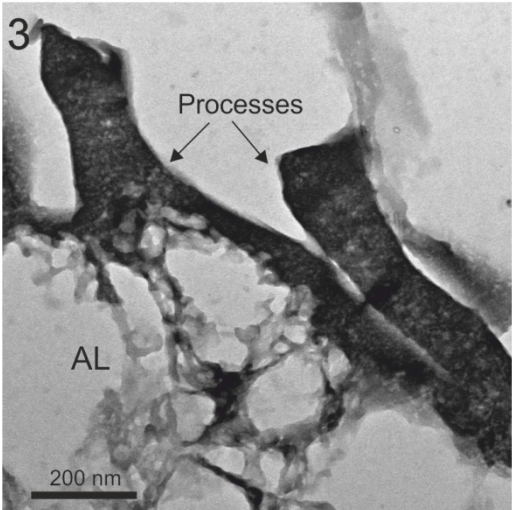
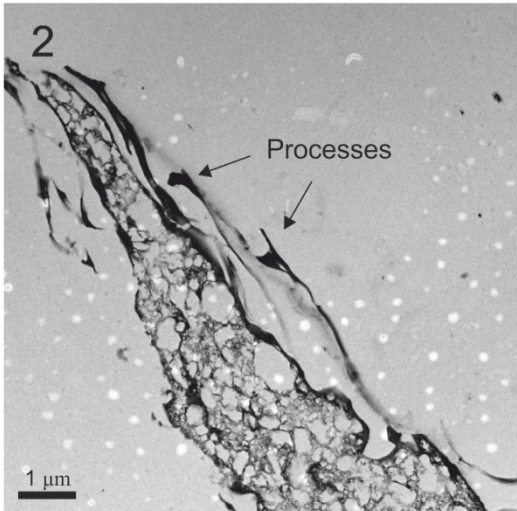
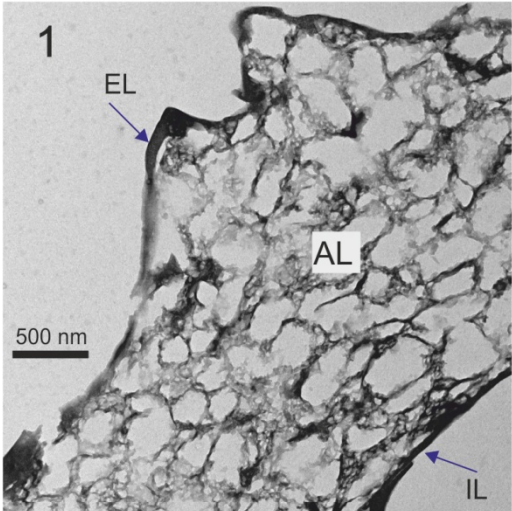


Plate 25

Scale bar is 20 μm for each figure.

Fig. 1 Acritarch sp. 11

Nolichucky Shale Sample 08BP-30 BEP-0163 (C32/0)

Arrow indicates terminal flange.

Fig. 2 Acritarch sp. 11

Nolichucky Shale Sample 08BP-30 BEP-0163 (K39/4)

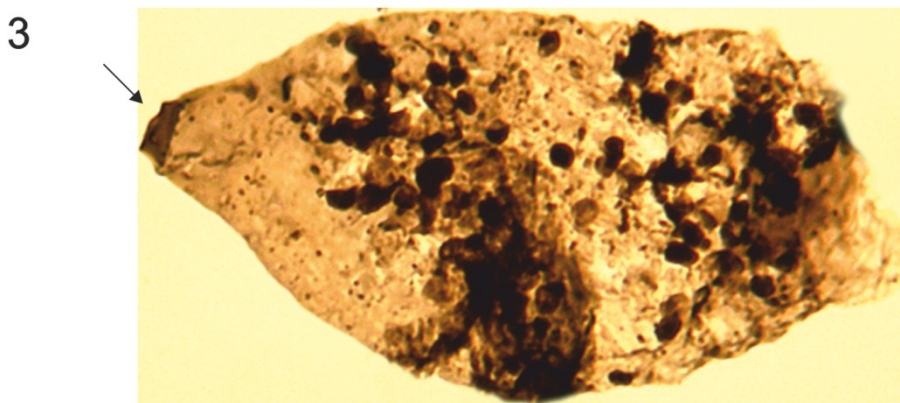
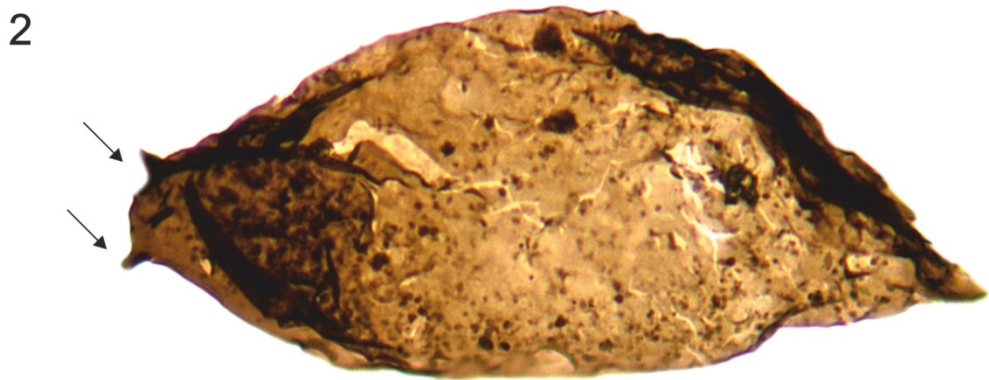
Arrows indicate terminal processes.

Fig. 3 Acritarch sp. 11

Nolichucky Shale Sample 08BP-30 BEP-0163 (F50/2)

Arrow indicates terminal flange.

Plate 25



20 μm



Plate 26

Fig. 1 *Navifusa actinomorpha*

Nolichucky Shale Sample 08BP-35 BEP-0199 (J45/0)

Fig. 2 *Navifusa* sp. 1

Nolichucky Shale Sample 08BP-22 BEP-0121 (P47/2)

Fig. 3 *Navifusa* sp. 2

Nolichucky Shale Sample 08BP-33 BEP-0180 (V25/3)

Fig. 4 *Navifusa* sp. 2

Nolichucky Shale Sample 08BP-32 SEM-36

Plate 26

1



2

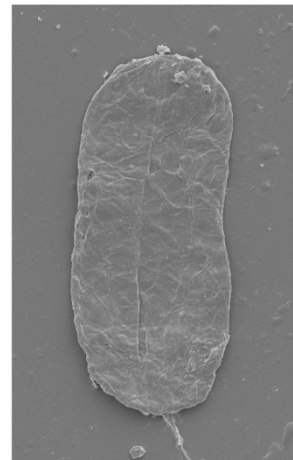


20 μ m

3



4



20 μ m

Plate 27

Fig. 1 Problematica 1: *Morphotype P1-1*

Nolichucky Shale Sample 08BP-36 BEP-0202 (G37/0)

Arrows indicate closed apertures.

Fig. 2 Problematica 1: *Morphotype P1-1*

Nolichucky Shale Sample 08BP-36 BEP-0203 (W32/1)

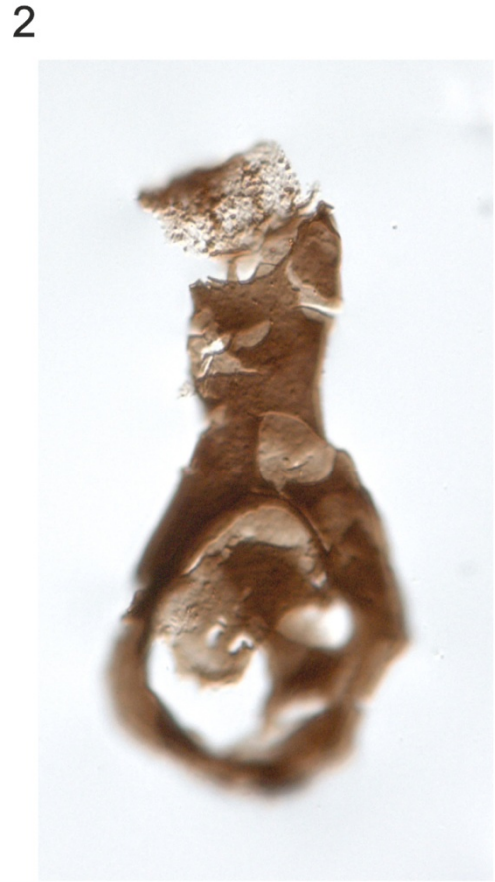
Fig. 3 Problematica 1: *Morphotype P1-1*

Nolichucky Shale Sample 08BP-35 BEP-0201 (Y37/2)

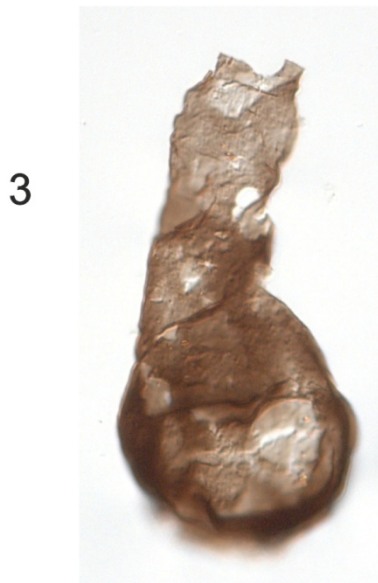
Fig. 4 Problematica 1: *Morphotype P1-1*

Nolichucky Shale. Sample 36 No. BEP-0202 (Q50/1).

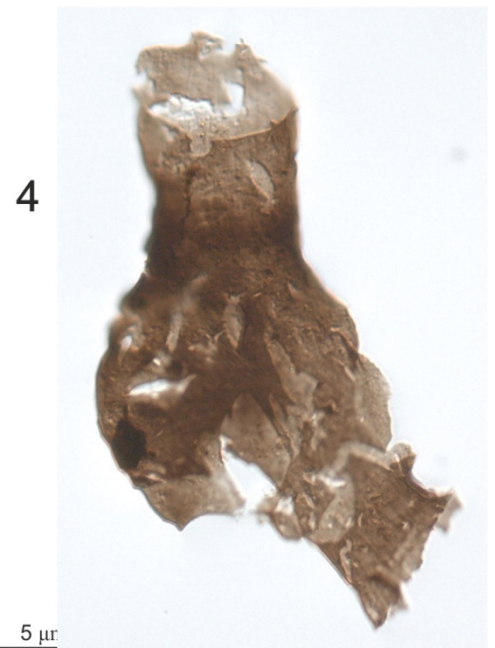
Plate 27



50 μm



20 μm



5 μm

Plate 28

Scale bar is 20 μm for each figure.

Fig. 1 Problematica 1: *Morphotype P1-2*

Nolichucky Shale Sample 08BP-33 BEP-0187 (D28/0)

Fig. 2 Problematica 1: *Morphotype P1-2*

Nolichucky Shale Sample 08BP-35 BEP-0199 (V43/0)

Fig. 3 Problematica 1: *Morphotype P1-2*

Nolichucky Shale Sample 08BP-36 BEP-0202 (G40/3)

Fig. 4 Problematica 1: *Morphotype P1-2*

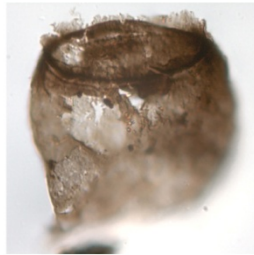
Nolichucky Shale Sample 08BP-35 BEP-0200 (Y38/0)

Plate 28

1



2



20 μ m



3



4

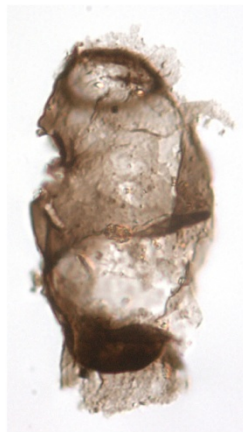


Plate 29

Fig. 1 Problematica 1: *Morphotype P1-4*

Nolichucky Shale Sample 08BP-35 BEP-0201 (L43/0)

Fig. 2 Problematica 1: *Morphotype P1-4*

Nolichucky Shale Sample 08BP-35 BEP-0199 (H33/1)

Fig. 3 Problematica 1: *Morphotype P1-3*

Nolichucky Shale Sample 08BP-35 BEP-0201 (P40/0)

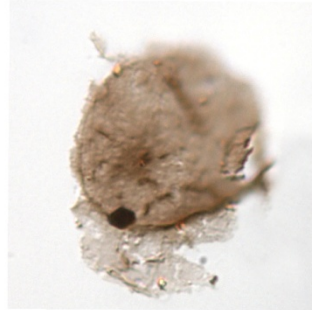
Plate 29

1

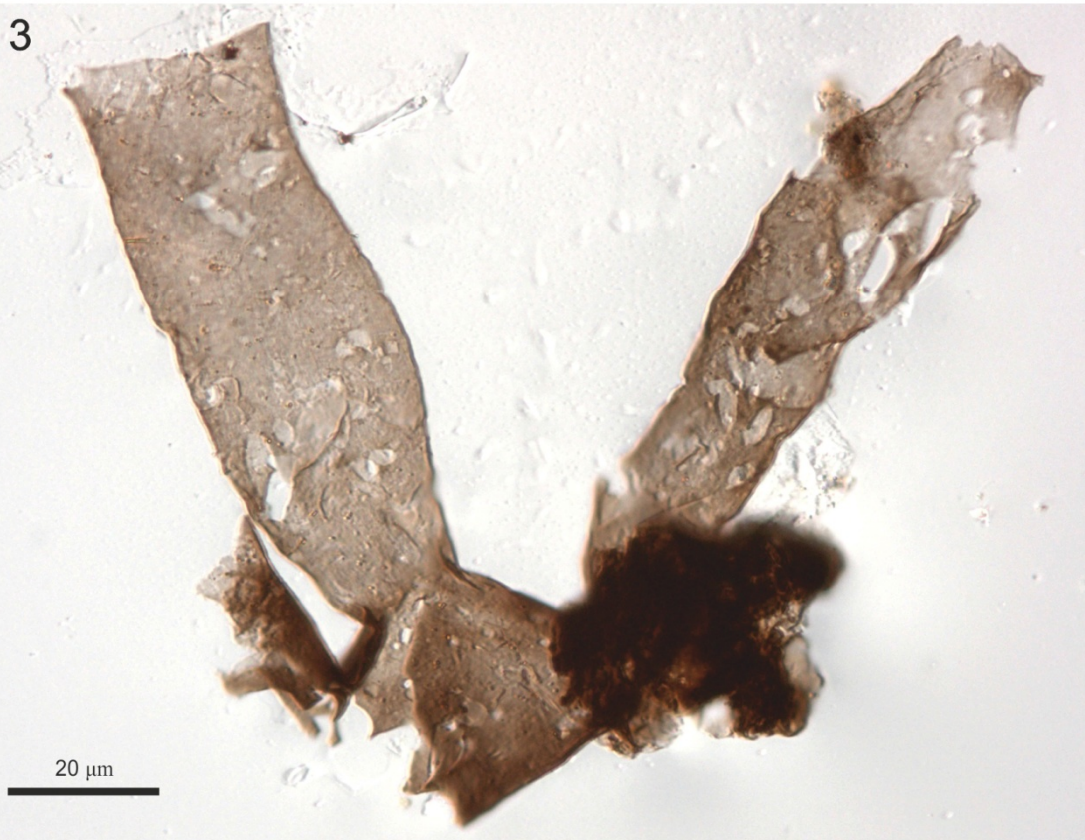


20 μ m

2



20 μ m



20 μ m

Plate 30

Fig. 1 Problematica 1: *Morphotype P1-5*

Nolichucky Shale Sample 08BP-39 BEP-0209 (T33/3)

Fig. 2 Problematica 1: *Morphotype P1-5*

Nolichucky Shale Sample 08BP-37 BEP-0207 (E27/2)

Fig. 3 Problematica 2

Nolichucky Shale Sample 08BP-37 SEM-93

Fig. 4 Problematica 2

Nolichucky Shale Sample 08BP-37 SEM-93

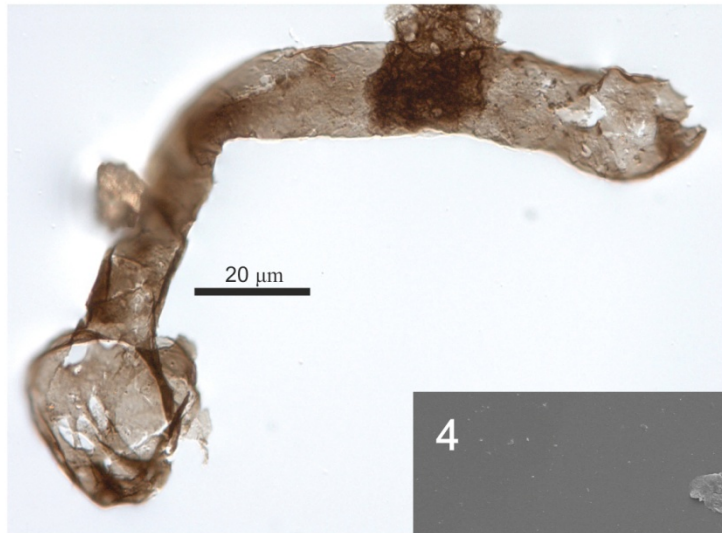
Plate 30

1



20 μ m

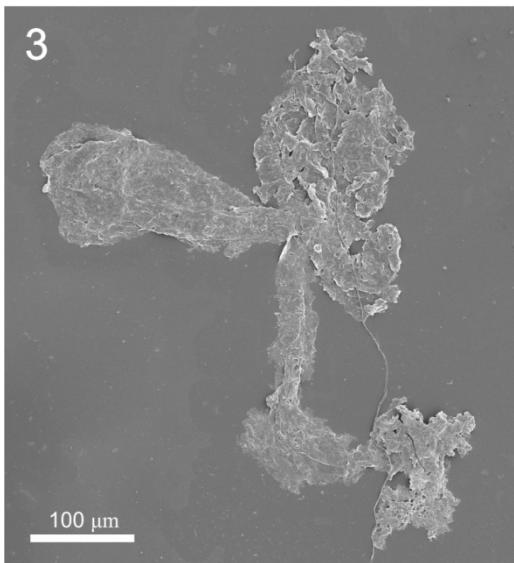
2



20 μ m

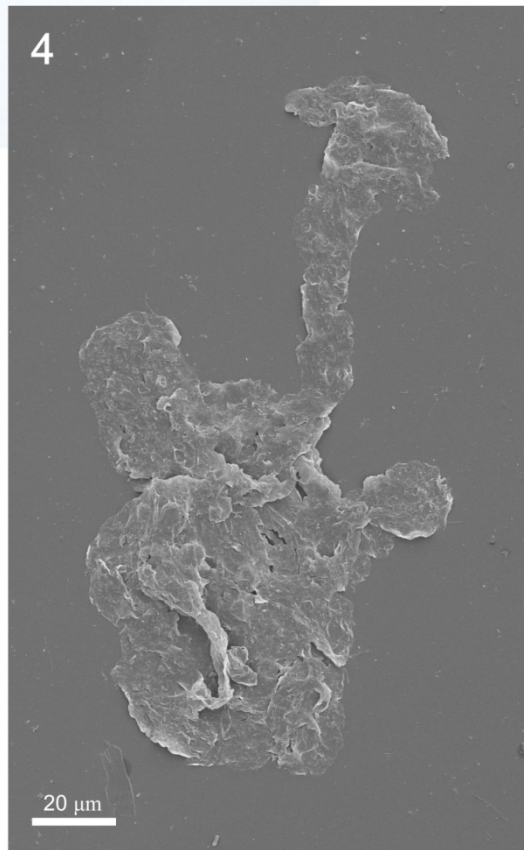
5 μ m

3



100 μ m

4



20 μ m

Plate 31

Fig. 1 Branchiopod-type Mandibles (mouthparts)

Nolichucky Shale Sample 08BP-56 BEP-0248 (K37/3)

Fig. 2 Branchiopod-type Mandibles (mouthparts)

Nolichucky Shale. Sample 08BP-09 BEP-0061 (J35/3)

Fig. 3 Branchiopod-type Mandibles (mouthparts)

Nolichucky Shale. Sample 08BP-09 BEP-0061 (R23/3)

Plate 31

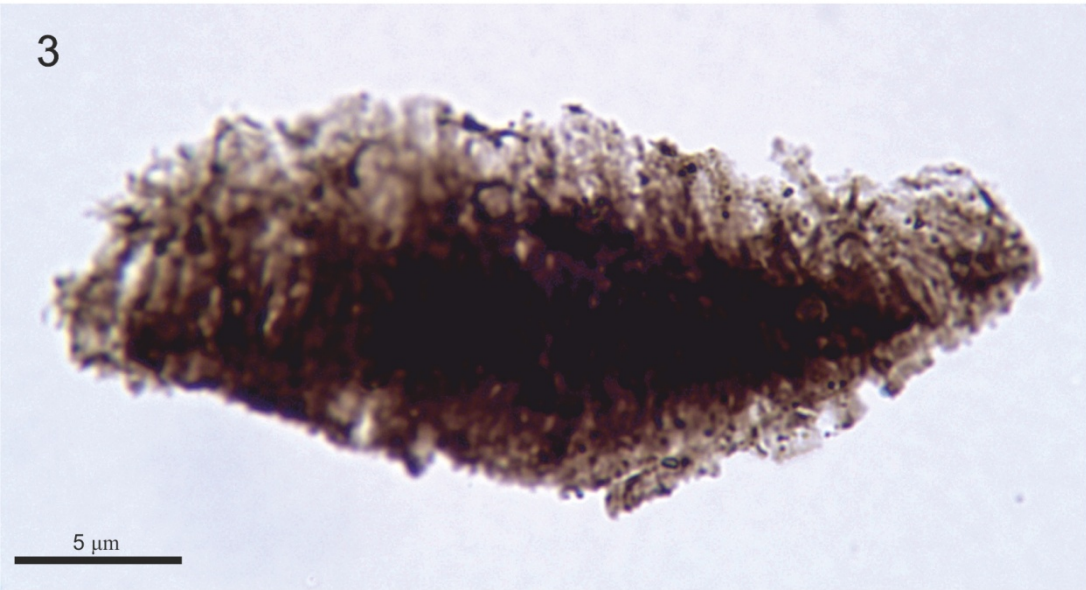
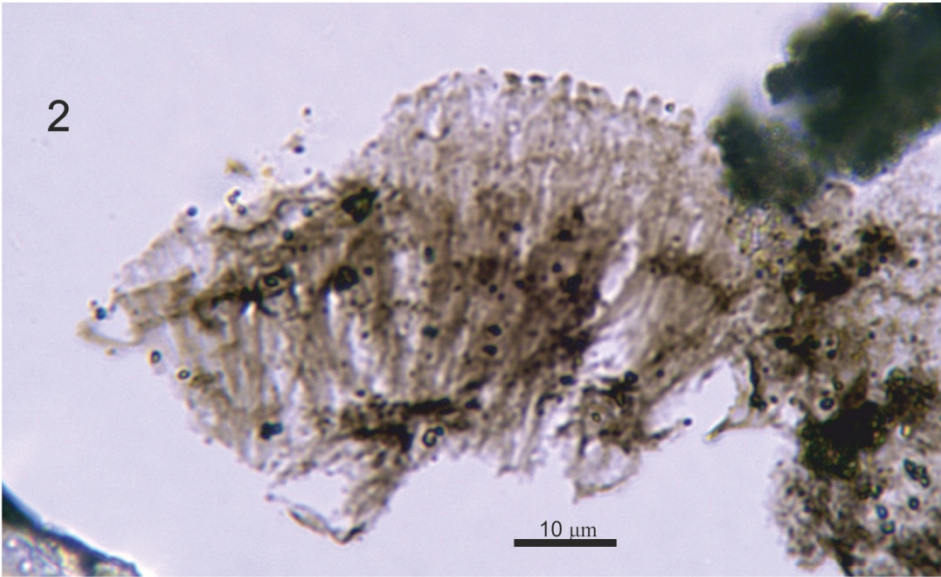
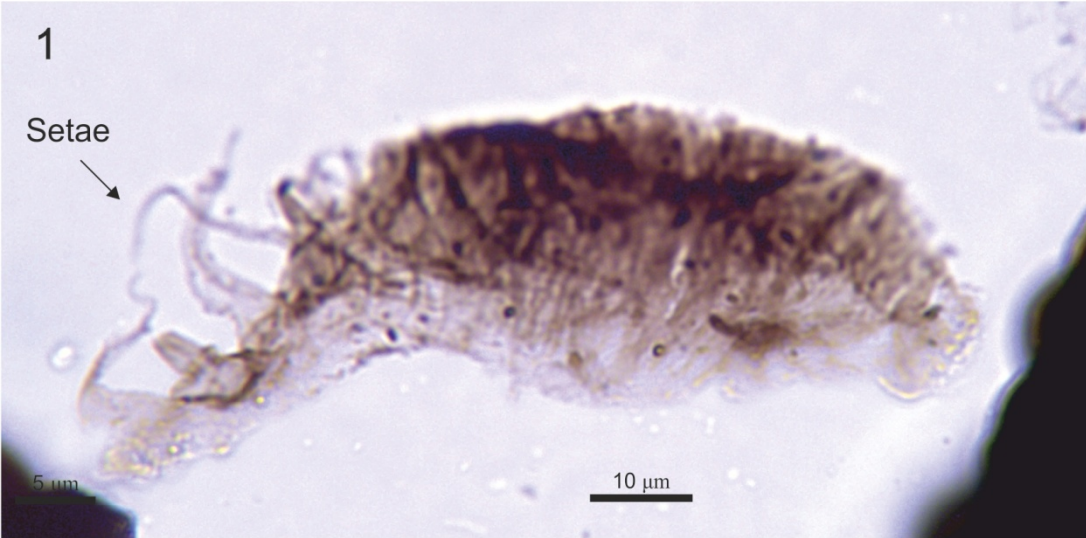


Plate 32

Fig. 1 Copepod-type mandibles

Nolichucky Shale.0 Sample 08BP-29 BEP-0157 (F25/0)

Arrow indicates prominent seta below the bristly platform.

Fig. 2 Copepod-type mandibles

Nolichucky Shale Sample 08BP-29 BEP-0154 (D50/0)

Fig. 3 Copepod-type mandibles

Nolichucky Shale Sample 08BP-29 BEP-0154 (F23/0)

Fig. 4 Copepod-type mandibles

Nolichucky Shale Sample 08BP-28½ BEP-0150 (C48/2)

Fig. 5 Copepod-type mandibles

Nolichucky Shale Sample 08BP-29 BEP-0154 (F25/4)

Fig. 6 Copepod-type mandibles

Nolichucky Shale. Sample 28½ No. BEP-0150 (G49/1)

Plate 32

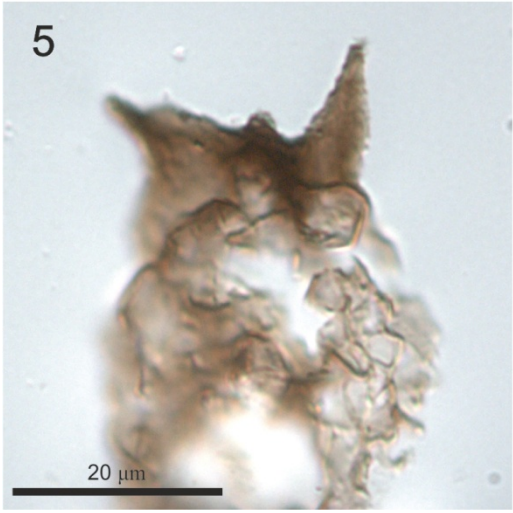
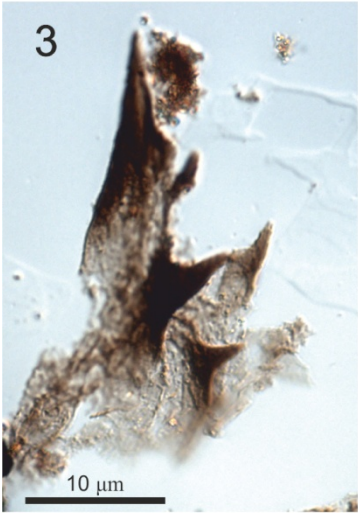
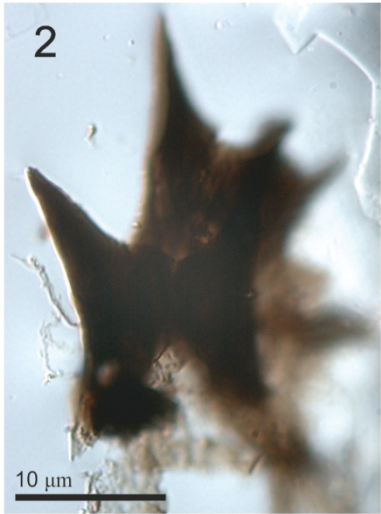
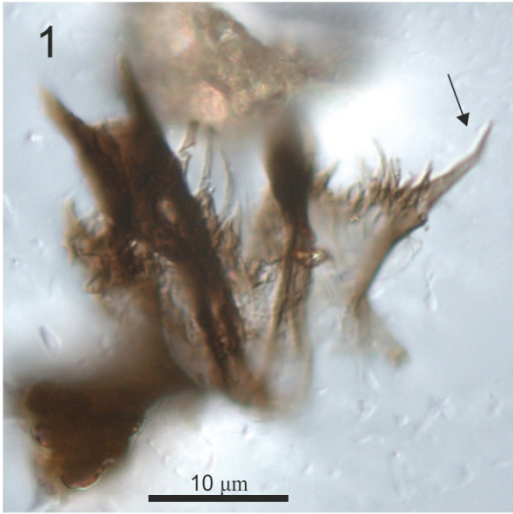


Plate 33

Fig. 1 Branchiopod-type limbs

Nolichucky Shale Sample 08BP-56 BEP-0248 (L34/1)

Fig. 2 Branchiopod-type limbs

Nolichucky Shale Sample 08BP-23 BEP-0126 (C23/0)

Fig. 3 Branchiopod-type limbs

Nolichucky Shale Sample 08BP-55 BEP-0246 (V42/0)

Fig. 4 Branchiopod-type limbs

Nolichucky Shale Sample 08BP-23 BEP-0126 (S34/2)

Fig. 5 Branchiopod-type limbs

Nolichucky Shale Sample 08BP-56 BEP-0248 (O33/0)

Plate 33

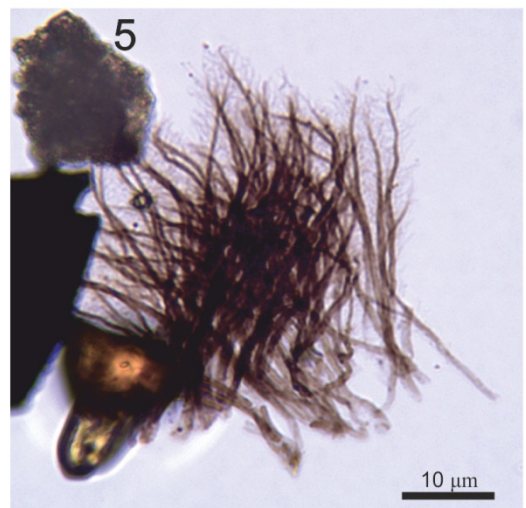
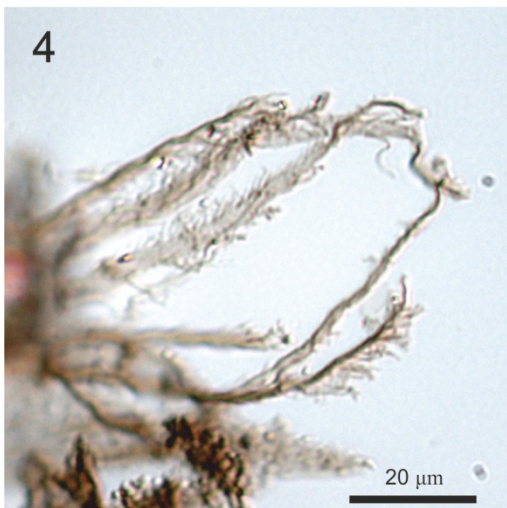
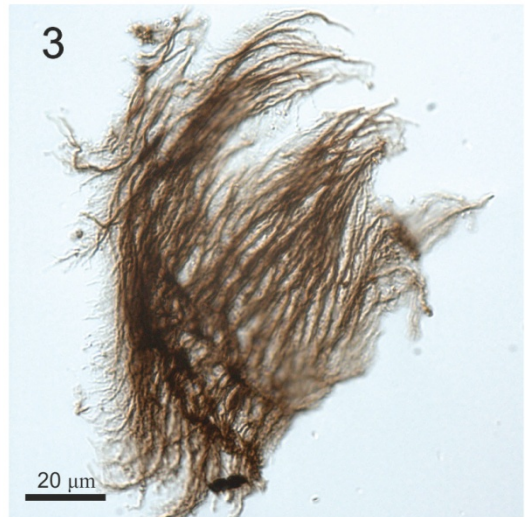
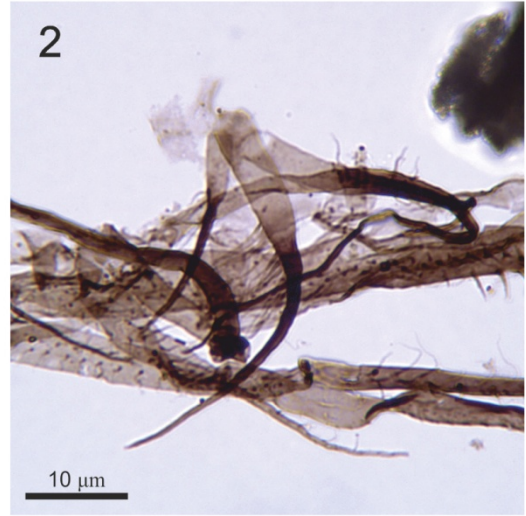


Plate 34

Fig. 1 *Wiwaxia* sclerites

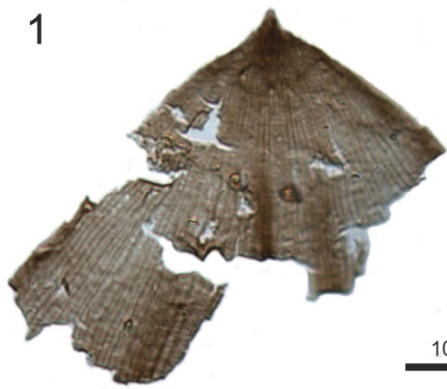
Nolichucky Shale Sample 08BP-29 BEP-0154 (F25/0)

Fig. 2 *Wiwaxia* sclerites

Nolichucky Shale Sample 08BP-29 BEP-0154 (Y51/1)

Plate 34

1



2



10 μ m

REFERENCES

- Ahlberg, P., Axheimer, N., Babcock, L. E., Eriksson, M. E., Schmitz, B. & Terfelt, F. 2008. Cambrian high-resolution biostratigraphy and carbon isotope chemostratigraphy in Scania, Sweden: first record of SPICE and DICE excursions in Scandinavia. *Lethaia*, **42**: 2-16.
- Aitken, J. D. 1966. Middle Cambrian to Middle Ordovician Cyclic Sedimentation, Southern Rocky Mountains of Alberta. *Bulletin of Canadian Petroleum Geology*, **14** (4): 405-441.
- Aitken, J.D. 1978. Revised models for depositional Grand Cycles, Cambrian of the southern Rocky Mountains, Canada. *Canadian petroleum Geology Bulletin*, **26**: 515–542.
- Aitken, J. D. 1981. Generalizations about grand cycles. *In*: Taylor, M. E. (Ed.), Short Papers for the Second International Symposium on the Cambrian System. U.S. Geological Survey Open-File Report 81-743, 8-14.
- Albani, R., Bagnoli, G., Bernárdez, E., Gutiérrez-Marco, J. C. & Ribecai, C. 2006. Late Cambrian acritarchs from the “Túnel Ordovícico del Fabar”, Cantabrian Zone, N. Spain. *Review of Palaeobotany and Palynology*, **139**: 41-52.
- Albani, R., Di Milia, A., Minzoni, N. & Tongiorgi, M. 1985. Nuovi dati palinologici e considerazioni geologiche sull’eta delle Arenarie di Solanas (Cambro-Ordoviciano–Sardegna Centrale). *Atti della Società Toscana di Scienze Naturali, Memorie, Serie A*, **92**: 1-33.
- Albani, R., Massa, D. & Tongiorgi, M. 1991. Palynostratigraphy (acritarchs) of some Cambrian beds from the Rhadames (Ghadamis) Basin (western Libya–southern Tunisia). *Bollettino della Società Paleontologica Italiana*, **30** (3): 255-280.
- Alekseev, V. R., Ravera, O. & De Stasio, B. T. 2007. Introduction to diapause. *In* Alekseev, V. R., Ravera, O. & De Stasio, B. T. (eds.), Diapause in Aquatic Invertebrates. Theory and Human Use. *Monographiae biologicae* **84**: 257 pp.
- Anderson, E., Lochhead, J. H., Lochhead, M. S. & Huebner, E. 1970. The origin and structure of the tertiary envelope in thick-shelled eggs of the brine shrimp, *Artemia*. *Journal of Ultrastructure Research*, **32**: 497-525.
- Aráoz, L. & Vergel, M. M. 2006. Palinología de la transición Cambro-Ordovícica en Quebrada de Moya, Cordillera Oriental, Argentina. *Revista Brasileira de Paleontologia*, **9**(1): 1-8.
- Arouri, K., Greenwood, P. F. & Walter, M. R. 1999. A possible chlorophycean affinity of some Neoproterozoic acritarchs. *Organic Chemistry*, **30**: 1323-1337.

- Arouri, K., Greenwood, P. F. & Walter, M. R. 2000. Biological affinities of Neoproterozoic acritarchs from Australia: microscopic and chemical characterisation. *Organic Geochemistry*, **31**: 75-89.
- Baars, D. L., 1988. Triassic and older stratigraphy; Southern Rocky mountains and Colorado Plateau. *In*: Sloss, L. L., (ed.), *Sedimentary Cover-North American Craton*. US Geological Society of America, the Geology of North America, v. D-2: 53-64.
- Babcock, L. E. & Peng, S. C. 2007. Cambrian chronostratigraphy: current state and future plans. *Palaeogeography, Palaeoclimatology, Palaeoecology*, **254**: 62-66.
- Babcock, L. E. & Peng, S. C. Geyer, G. & Shergold, J. H. 2005. Changing perspectives on Cambrian chronostratigraphy and progress toward subdivision of the Cambrian System. *Geosciences Journal*, **9**: 101-106.
- Babcock, L. E., Rees, M. N. Robison, R. A., Langenburg, E. S. & Peng, S. C. 2004. Potential Global Stratotype-section and Point (GSSP) for a Cambrian stage boundary defined by the first appearance of the trilobite *Ptychagnostus atavus* Drum Mountains, Utah, USA. *Geobios*, **37**: 149-158.
- Babcock, L. E., Robison, R. A., Rees, M. N., Peng, S. C. & Saltzman, M. R. 2007. The Global boundary Stratotype Section and Point (GSSP) of the Drumian Stage (Cambrian) in the Drum Mountains, Utah, USA. *Episodes* **30**: 85-95.
- Bagnoli, G., Qi, Y. P., and Wang, Z. H. 2008. Conodonts from the global stratotype section for the base of the Guzhangian Stage (Cambrian) at Luoyixi, Hunan, South China. *Palaeoworld* **17**: 108-114.
- Bagnoli, G., Stouge, S. & Tongiorgi, M. 1988. Acritarchs and conodonts from the Cambro-Ordovician Furuhäll (Köpingsklint) section (Öland, Sweden). *Rivista Italiana di Paleontologia e Stratigrafia*, **94 (2)**: 163-248.
- Ban, S. 1992. Effects of photoperiod, temperature and population density on induction of diapause egg production in *Eurytemora affinis* (Copepoda: Calanoida) in Lake Ohnuma, Hokkaido, Japan. *Journal of Crustacean biology*, **12 (3)**: 147-153.
- Baudet, D., Aitken, J. D. & Vanguetaine, M. 1989. Palynology of uppermost Proterozoic and lowermost Cambrian formations, central Mackenzie Mountains, northwestern Canada, *Canadian Journal of Earth Sciences*, **26**: 129-148.
- Beardall, J. 2009. Allometry and stoichiometry of unicellular, colonial, and multicellular phytoplankton. *New phytologist*, **181**: 295-309.
- Belk, D. 1970. Functions of the conchostracan egg shell. *Crustaceana*, **19**: 105-106.
- Belmonte, G. & Puce, M. 1994. Morphological aspects of subitaneous and resting eggs from *Acartia josephinae* (Calanoida). *Hydrobiologia*, **292/293**: 131-135.
- Belmonte, G., Miglietta, A., Rubino, F. & Boero, F. 1997. Morphological convergence of resting stages of planktonic organisms: A review. *Hydrobiologia*, **335**: 159-165.

- Bergman, N. M., Lenton, T. & Watson. 2004. COPSE: A new model of biogeochemical cycling over Phanerozoic time. *American Journal of Science*, **304**: 397-437.
- Berner, R. A. 1991. A model for atmospheric CO₂ over Phanerozoic time. *American Journal of Science*, **291**: 339-376.
- Berner, R. A. 1998. The carbon cycle and CO₂ over Phanerozoic time: the role of land plants. *Philosophical Transactions of the Royal Society, Series B*, **353**: 75-82.
- Berner, R. A. 2001. Modelling atmospheric O₂ over Phanerozoic time. *Geochimica et Cosmochimica Acta*, **65 (5)**: 685-694.
- Berner, R. A. 2006a. Geological nitrogen cycle and atmosphere N₂ over Phanerozoic time. *Geological*, **34 (5)**: 413-415.
- Berner, R. A. 2006b. GEOCARBSULF: A combined model for Phanerozoic atmospheric O₂ and CO₂. *Geochimica et Cosmochimica Acta*, **70 (23)**: 5653-5664.
- Berner, R. A., Beerling, D. J., Dudley, R., Robinson, J. M. & Wildman, R. A. Jr. 2003. Phanerozoic atmospheric oxygen. *Annual Review of Earth and Planetary Science*, **31**: 105-134.
- Berner, R. A. & Canfield, D. E. 1989. A new model of atmospheric oxygen over Phanerozoic time. *American Journal of Science*, **289**: 333-361.
- Berner, R. A. & Kothavala, Z. 2001. "GEOCARB III: A revised model of atmospheric CO₂ over Phanerozoic time". *American Journal of Science*, **304**: 397-437.
- Bhat, G. M., Ram, G. & Koul, S. 2009. Potential for oil and gas in the Proterozoic carbonates (Sirban Limestone) of Jammu, northern India. In: Craig, J., Thurow, J., Thusu, B., Whitham, A. & Abutar-Ruma, Y. (Eds.), *Global Neoproterozoic Petroleum Systems: The Emerging Potential in North Africa*. Geological Society, London, Special Publications, **326**: 245-254.
- Bilton, D. T., Freeland, J. R. & Okamura, B. 2001. Dispersal in freshwater invertebrates. *Annual Review of Ecology and systematics*, **32**: 159-181.
- Binda, P. L., Sparks, D. E., Beaudoin, N. C., Stasiuk, L. D., Bend, S. L. & Buchanan, A. A. 1996. Preliminary observations on the Acid-resistant Microfossils from the Lower Paleozoic of Southern Saskatchewan. *Summary of investigations 1996, Saskatchewan Geological Survey, Saskatchewan Energy Mines, Miscellaneous Report*, **96-4**.
- Bishop, J. A. 1968. Resistance of *Limmadia stanleyana* King (Branchiopoda, Conchostraca) to desiccation. *Crustaceana*, **14**: 35-38.
- Bolch, C. J. & Hallegraeff, G. 1990. Dinoflagellate cysts in Recent marine sediments from Tasmania, Australia. *Botanica Marina*, **33**: 173-192.
- Bond, G. C. Kominz, M. A. & Grotzinger, J. P. 1988. Cambro-Ordovician eustasy: evidence from geophysical modelling of subsidence in Cordilleran and Appalachian passive margins. In: Paola, C., Kleinspehn, K. (Eds.), *New perspectives in Basin Analysis*: New York, Springer-Verlag, 129-161.

- Bond, G. C. Kominz, M. A. Steckler, M. S. & Grotzinger, J. P. 1989. Role of thermal subsidence, flexure, and eustasy in the evolution of early Paleozoic passive-margin carbonate platforms. *In: Crevello, P. D., Wilson, J. L., Sarg, J. F., Read, J. F., (Eds.), Society of Economic Paleontologists and Mineralogists, Special Publication, 44: 39-62.*
- Boxshall, G. A. 1992. Copepoda. *In: F. R. Harrison and A. G. Humes, (Eds.), Microscopic anatomy of Invertebrates, Vol. 9. Crustacea. P. 347-384. Wiley-Liss Publishers, New York, New York.*
- Bradford-Grieve, J. M. 2002. Colonization of the pelagic realm by calanoid copepods. *Hydrobiologia, 485: 223-244.*
- Brasier, M. D. 1992. Background to the Cambrian explosion. *Journal of the Geological Society, 149: 585-587.*
- Brasier, M. D. 1993. Towards a carbon isotope stratigraphy of the Cambrian System; potential of the Great Basin succession. *Geological Society, London, Special Publications, 70: 341-350.*
- Brasier, M. D., Cowie, J. & Taylor, M. 1994. Decision on the Precambrian-Cambrian boundary. *Episodes, 17: 95-100.*
- Brasier, M. D., Khomentovsky, V. V. & Corfield, R. M. 1993. Stable isotopic calibration of the earliest skeletal fossil assemblages in eastern Siberia (Precambrian-Cambrian boundary). *Terra Nova, 5: 225-232.*
- Brasier, M. D., Shields, G., Kuleshov, V. N. & Zhegallo, E. A. 1996. Integrated chemo- and biostratigraphic calibration of early animal evolution: Neoproterozoic–early Cambrian of southwest Mongolia. *Geological magazine, 133 (4): 445-485.*
- Brendonck, L. & Riddoch, B. J. 1999. Wind-borne short-range egg dispersal in anostracans (Crustacea: Branchiopoda). *Zoological journal of the Linnean Society, 67: 87-95.*
- Breuer, P. & Vanguestaine, M. 2004. The latest Tremadocian *messauoudensis-trifidum* acritarch assemblage from the upper part of the Lierneux Member (Salm Group, Stavelot Inlier, Belgium). *Review of Palaeobotany and Palynology, 130: 41-58.*
- Bridge, J. 1956. Stratigraphy of the Mascot-Jefferson City Zinc District, Tennessee. U.S. Geological Survey Professional Paper, 277, 74 pp.
- Bridge, D. McC., Carney, J. N., Lawley, R. S. & Rushton, A. W. A. 1998. The geology of the country around Coventry and Nuneaton. *Memoir of the Geological Survey of Great Britain, Sheet 169 (England and Wales). 185 pp., HMSO, London.*
- Briggs, D. E. G., Erwin, D. H. & Collier, F. J. 1994. The fossils of the Burgess Shale Smithsonian Institution Press: Washington, p. 1-238.
- Brocke, R., Fatka, O. 1999. Acritarch assemblages at the “Tremadocian” - “Arenigian” boundary. *In: Quo Vadis Ordovician? Short papers of the 8th International Symposium on the Ordovician System. Acta Universitatis Carolinae - Geologica, 43: 245-248.*

- Brück P. M., & Vanguetaine, M. 2004; Acritarchs from the Lower Palaeozoic succession on the south County Wexford coast, Ireland: new age constraints for the Cullenstown Formation and the Cahore and Ribband Groups. *Geological Journal* **39**: 199-224.
- Brunner, U., Honegger, R. 1985. Chemical and ultrastructural studies on the distribution of sporopollenin-like biopolymers in six genera of lichen phycobionts. *Canadian Journal of Biology*, **63**: 2221-2230.
- Bunker, B. J., Witzke, B. J., Watney, W. L. & Ludvigson, G. A. 1988. Phanerozoic history of the central midcontinent, United States. *In*: Sloss, L. L., (Ed.), Sedimentary cover-North American craton, United States: Boulder, Colorado, Geological Society of America, Geology of North America, **D-2**: 243-260.
- Butterfield, N. J. 1990a. Organic preservation of non-mineralizing organisms and the taphonomy of the Burgess Shale. *Paleobiology*, **16**: 272-286.
- Butterfield, N. J. 1990b. A reassessment of the enigmatic Burgess Shale fossil *Wiwaxia corrugata* (Matthew) and its relationship to the polychaete *Canadia spinosa* Walcott. *Paleobiology*, **16**: 287-303.
- Butterfield, N. J. 1994. Burgess Shale-type fossils from a Lower Cambrian shallow-shelf sequence in northwestern Canada. *Nature*, **369**: 477-479.
- Butterfield, N. J. 2004. A Vaucheriacean alga from the middle Neoproterozoic of Spitsbergen: implications for the evolution of Proterozoic eukaryotes and the Cambrian explosion. *Paleobiology*, **30** (2): 231-252.
- Butterfield, N. J. 2005a. Probable Proterozoic fungi. *Palaeobiology*, **31**: 165-182.
- Butterfield, N. J. 2005b. Reconstructing a complex early Neoproterozoic eukaryote, Wynniatt Formation, arctic Canada. *Lethaia*, **38**: 155-169.
- Butterfield, N. J. 2007. Macroevolution and macroecology through deep time. *Palaeontology*, **50**: 41-55.
- Butterfield, N. J. 2008. An Early Cambrian Radula. *Journal of Paleontology*, **82**: 543-554.
- Butterfield, N. J. & Chandler, F. W. 1992. Palaeoenvironmental distribution of Proterozoic microfossils, with an example from the Agu Bay Formation, Baffin Island. *Palaeontology*, **35**: 943-957.
- Butterfield, N. J. & Harvey, T. H. P. 2012. Small carbonaceous fossils (SCFs): A new measure of early Paleozoic paleobiology. *Geology*, **40** (1): 71-74.
- Butterfield, N. J., Knoll, A. H. & Swett, K. 1994. Paleobiology of the Neoproterozoic Svanbergfjellet Formation, Spitsbergen. *Fossils and Strata*, **34**: 1-84.
- Byerly, D. W., Walker, K. R., Diehl, W. W., Ghazizadeh, D. M., Johnson, R. E., Lutz, C. T. & Schoner, A. A. K. 1986. Thorn Hill: a classic Paleozoic stratigraphic section in Tennessee. *In* Neathery, T. L. (Ed). Centennial field guide: southeastern section. *Geol. Soc. Am.* **6**: 131-136.
- Carlisle, D. B. 1968. *Triops* (Entomostraca) eggs killed by boiling. *Science*, **161**: 279.

- Chen Jun-Yuan, Qian Yi-Yuan, Zhang Jun-Ming, Lin Yao-Kun, Yin Lei-Ming, Wang Zong-Zhe, Yang Jie-Dong & Wang Ying-Xi. 1988. The recommended Cambrian-Ordovician global Boundary stratotype of the Xiaoyangqiao section (Dayangcha, Jilin Province), China. *Geological magazine*, **25**: 415-444.
- Chen, J. Y., Bottjer, D. J., Li., G., Hadfield, M. G., Gao, F., Cameron, A. R., Zhang, C. Y., Xian. D. C., Tafforeau, P. & Liao, X. 2009. Complex embryos displaying bilaterian characters from Precambrian Doushantuo phosphate deposits, Weng'an, Guizhou, China. *Proc Natl Acad Sci*, **106**: 19056–19060.
- Chisholm, S. W. 1992. Phytoplankton size. In: Falkowski, P. G. & Woodhead, A. D. (Eds.), *Primary Productivity and Biogeochemical Cycles in the Sea*. Plenum Press, New York. 213-237.
- Chow, N. & James, N. P. 1992. Synsedimentary Diagenesis of Cambrian Peritidal Carbonates: Evidence from Hardgrounds and Surface Paleokarst in the Port au Port Group, Western Newfoundland. *Bulletin of Canadian Petroleum Geology*, **40** (2): 115-127
- Clendening, J. A. & Wood, G. D. 1981. Thymadora, a new Acritarch Genus from the Middle Cambrian Rogersville Shale of Tennessee, U.S.A. *Palynology*, **5**: 153-158.
- Cobbold, E.S. 1927. The stratigraphy and geological structure of the Cambrian area of Comley (Shropshire). *Quarterly Journal of the Geological Society of London*. **83**: 551-573.
- Cocks, L. R. M., Fortey, R. A. & Rushton, A. W. A. 2010. Correlation for the Lower Palaeozoic. *Geological Magazine*, **147**: 171-180.
- Cocks, L.R.M. & Torsvik, T.H. 2002. Earth geography from 500 to 400 million years ago: a faunal and palaeomagnetic review. *Journal of the Geological Society, London*, **159**: 631-644.
- Cocks, L.R.M. & Torsvik, T.H. 2006. European geography in a global context from the Vendian to the end of the Palaeozoic. In: Gee, D. G. & Stephenson, R. A. (eds), *European Lithosphere Dynamics. Geological Society, London, Memoirs*, **32**: 83-95.
- Cohen, P. A., Knoll. A. H. & Kodner, R. B. 2009. Large spinose microfossils in Ediacaran rocks as resting stages of early animals. *proc. Natl. Acad. Sci. U.S.A.* **106**: 6519-6524.
- Colbath, G. K. 1990. Devonian (Givetian-Frasnian) organic-walled phytoplankton from the Limestone Billy Hills reef complex, Canning Basin, Western Australia. *Palaeontographica B*, **217**: 87-145.
- Colbath, G. K. & Grenfell, H. R. 1995. Review of biological affinities of Paleozoic acid-resistant, organic-walled eukaryotic algal microfossils (including “acritarch”). *Review of Palaeobotany and Palynology*, **86**: 287-314.
- Combaz, A. 1967. Un microbios du trémadocien dans un sondage d’Hassi-Messaoud. *Actes Soc. Linn. Bordeaux, Ser. B* **104** (29): 1-26.

- Combaz, A., Lange, F. W. & Pansart, J. 1967. Les "Leiofusidae" Eisenack, 1938. *Review of Palaeobotany and Palynology*, **1**: 291-307.
- Combaz, A. & Peniguel, G. 1972. Étude palynostratigraphique de l'Ordovicien dans quelques sondages du Bassin de Cannig (Australie Occidentale). *Bull. Cent. Rech. Pau SNPA*, **6**: 121-167.
- Conway Morris, S. 1998. *The Crucible of Creation*. Oxford University Press, Oxford, England, p. 242.
- Conway Morris, S. & Robison, R. A. 1988. More soft-bodied animals and algae from the Middle Cambrian of Utah and British Columbia. *Univ. Kansas Paleont. Contr.* **122**.
- Cooper, R. A., Nowlan, G. S. & Williams, S. H. 2001. Global Stratotype Section and Point for base of the Ordovician System. *Episodes*, **24** (1): 19-28.
- Cotter, K. L. 1999. Microfossils from Neoproterozoic Supersequence 1 of the Officer Basin, Western Australia. *Alcheringa*, **23**: 63-86.
- Couch, K. M., Downes, M. & Burns, C. W. 2001. Morphological differences between subitaneous and diapause eggs of *Boekella triarticulata* (Copepoda: Calanoida). **46**: 925-933.
- Cowie, J. W., Rushton, A. W. A. & Stubblefield, C. J. 1972. A correlation of Cambrian rocks in the British Isles. *Geological Society, Special Report*, **2**: 1-42.
- Cramer, F. H., & Diez de Cramer, M. C. R. 1972. Acritarchs from the upper Middle Cambrian Oville Formation of Le n, northwestern Spain. *Revista española de Micropaleontología, número extraordinario*, **30**: 39-50.
- Cramer, F. H., & Diez de Cramer, M. C. R. 1977. Late Arenigian (Ordovician) acritarchs from Cis-Saharan Morocco. *Micropalaeontology*, **23** (3): 339-360.
- Cressey, R. F. & Boxshall, G. A. 1989. *Kabatarina pattersoni*, a fossil parasitic copepod from a Lower Cretaceous fish, *Cladocycclus gardneri* Agassiz. *Micropaleontology*, **35**: 150-167.
- Cressey, R. F. & Patterson, C. 1973. Fossil parasitic copepods from a Lower Cretaceous fish. *Science, N. Y.* **180**: 1283-1285.
- Cunningham, J. A., Thomas, C., Bengtson, S., Kearns, S. L., Xiao, S., Marone, F., Stampanoni, M. & Donoghue, P. C. J. 2012. Distinguishing geology from biology in the Ediacaran Doushantuo biota relaxes constraints on the timing of the origin of bilaterians. *Proceedings of the Royal Society B*, **279**: 2369-2376.
- Curtis, M. L., Leat, P. T., Riley, T. R., Storey, B. C., Millar, I. L. & Randall, D. E. 1999. Middle Cambrian rift-related volcanism in the Ellsworth Mountains, Antarctica: tectonic implications for the palaeo-Pacific margin of Gondwana. *Tectonophysics*, **304** (4): 275-299.
- Curtis, M. L. & Storey, B. C. 1996. A review of the geological constraints on the pre-break-up position of the Ellsworth Mountains within Gondwana: implications for Weddell

- Sea evolution. In: storey, B. C., king, E. C., Livermore, R. A. (Editors), Weddell sea tectonics and Gondwana Break-up. *Geological Society of London Special Publication*, **108**: 11-30.
- Dalziel, I. W. D. 1992. On the organization of America plates in the Neoproterozoic and the breakout of Laurentia. *GSA Today*, **2** (11): 237-241
- Dalziel, I. W. D., Dalla Salda, L. H. & Gahagan, L. M. 1994. Paleozoic Laurentia-Gondwana interaction and the origin of the Appalachian-Andean mountain system. *Geological Society of America Bulletin*, **106**: 243-352.
- Dean, W. T. & Martin, F. 1978. Lower Ordovician acritarchs and trilobites from Bell Island, eastern Newfoundland. *Geological Survey of Canada, Bulletin*, **284**: 35p.
- Dean, W. T. & Martin, F. 1982. The sequence of trilobite faunas and acritarch microfloras at the Cambrian-Ordovician boundary, Wilcox Pass, Alberta, Canada. In: Bassett, M. G., Dean, W. T. (Eds.), The Cambrian-Ordovician Boundary: sections, fossil distributions and correlations. *Geological Series (National Museum of Wales)*, **3**: 131-140.
- Dean, W. T., Martin, F., Monod, O., Gunay, Y., Kozlu, H. & Bozdog, N. 1997. Precambrian? and Cambrian stratigraphy of the Penbeg [Caron] Li-Tut inlier, southeastern Turkey. *Geological Magazine*, **134** (1): 37-53.
- Deflandre, G. 1937. Micr fossiles des silex crétacés. Deuxième partie. Flagellés *incertae sedis*. Hystrichosphaeridés. Sarcodinés. Organismes divers. *Annales de Paléontologie*, **26**: 51-103.
- Deflandre, G. 1954. Systématique des Hystrichosphaeridés: sur l'acceptation du genre *Cymatioshaera* O. Wetzel. *C. R. Soc. Géol. Fr.*, **12**: 257-8.
- Derby, J. R. 1965. Paleontology and stratigraphy of the Nolichucky Formation in southwestern Virginia and northeastern Tennessee. Unpublished Ph.D. Dissertation, Virginia Polytechnic Institute, Blacksburg. 468 p.
- Deunff, J. 1961. Un micropaléonton à Hystrichosphères dans le Tremadoc du Sahara. *Revue Micropaléont*, **4**: 37-52
- Deunff, J., Gorka, H. & Rauscher, R. 1974. Observations nouvelles et précisions sur les Acritarchs à large ouverture polaire du Paléozoïque inférieur. *Geobios*, **7**: 5-18.
- De Walsche, C., Munuswamy, N. & Dumont, H. J. 1991. structural differences between the cyst walls of *Streptocephalus dichotomus* (Baird), *S. torvicornis* (Waga) and *Thamnocephalus platyurus* (Packard) (Crustacea: Anostraca), and comparison with other genera and species. *Hydrobiologia*, **212**: 195-212.
- Di Milia, A. 1991. Upper Cambrian acritarchs from the Solanas Sandstone Formation, Central Sardinia, Italy. *Bollettino della Società Paleontologica Italiana*, **30** (2): 127-152.
- Di Milia, A., Ribecai, C. & Tongiorgi, M. 1989. Late Cambrian acritarchs from the *Peltura scarabaeoides* Trilobite Zone at Degerhamn (Öland, Sweden). *Palaeontographia Italica*, **76**: 1-56.

- Di Milia, A. & Tongiorgi, M. 1993. Tremadocian acritarch assemblages from the Solanas Sandstone Formation (Nappe Zone of central Sardinia). *Memorie della Società Geologica Italiana*, 49: 193-204.
- Dong, L., Xiao, S., Shen, B., Zhou, C., Li, G. & Yao, J. 2009. Basal Cambrian microfossils from the Yangtze Gorges area (South China) and the Aksu area (Tarim Block, northwestern China). *Journal of Paleontology*, **83** (1): 30-44.
- Donnelly, T. H., Shergold, J. H., & Southgate, P. N. 1988. Anomalous geochemical signals from phosphatic Middle Cambrian rocks in the southern Georgina Basin, Australia. *Sedimentology*, **35**: 549-570.
- Donoghue, C. J., Bengtson, S., Dong, X., Gostling, N. J., Huldtgren, T., Cunningham, J. A., Yin, C., Yue, Z., Peng, F. & Stambanoni, M. 2006. Synchrotron X-ray tomographic microscopy of fossil embryos. *Nature*, **442**: 680-683.
- Downie, C. 1958. An assemblage of microplankton from the Shineton Shales (Tremadocian). *Proceedings of the Yorkshire Geological Society*, **31** (12): 331-349.
- Downie, C. 1960. Deunffia and Domasia, New Genera of Hystrichospheres. *Micropaleontology*, **6** (2): 197-202.
- Downie, C. 1963. "Hystrichospheres" (acritarchs) and spores of the Wenlock Shales (Silurian) of Wenlock, England. *Palaeontology*, **6** (4): 625-652.
- Downie, C. 1973. Observations on the nature of the acritarchs. *Palaeontology*, **6**: 625-652.
- Downie, C. 1974. Acritarchs from near the Precambrian-Cambrian boundary. *Review of Palaeobotany and Palynology* **18**: 57-60.
- Downie, C. 1982. Lower Cambrian acritarchs from Scotland, Norway, Greenland and Canada. *Transactions of the Royal Society, Edinburgh: Earth Sciences*, **72**: 257-282.
- Downie, C. 1984. Acritarchs in British stratigraphy. *Geological Society of London, Special Report*, **17**: 26 pp.
- Downie, C. & Sarjeant, W. A. S. 1963. On the interpretation and status of some Hystrichosphere genera. *Palaeontology*, **6**: 83-96.
- Dumont, H. J., Negrea, S. 2002. Introduction to the Class Branchiopoda. Guides to the Microinvertebrates of the Continental Waters of the World. Backhuys, Leiden, 398 pp.
- Dumont, H. J., Nandini, S. & Sarma, S. S. S. 2002. Cyst ornamentation in aquatic invertebrates: a defence against egg-production. *Hydrobiologia*, **86**: 161-167.
- Ebner, S., Shields, G. A., Veizer, J. F. Miller, & J. H. Shergold. 2001. High resolution strontium isotope stratigraphy across the Cambrian-Ordovician transition. *Geochimica, Cosmochimica Acta*, **65**: 2273-2292.
- Eisenack, A. 1938. Hystrichosphaerideen und verwandte Formen im baltischen Silur. *Z. Geschiebek. Flachlandgeol.*, **14**: 1-30.

- Eisenack, A. 1958. *Tasmanites* Newton und *Leiosphaeridia* n. g. als Gattungen der Hystrichosphaeridea. *Palaeontographica*, (A) **110**: 1-19.
- Eisenack, A. 1976. Mikrofossilien aus dem Vaginatenkalk von Hälludden, Öland. *Palaeontographica A*, **154** (4/6): 181–203.
- Eklund, C. 1990. Lower Cambrian acritarch stratigraphy of the Bårstad 2 core. Östergötland, Sweden. *Geol. Fören, Stockholm, Förhandl.*, **112**: 19-44.
- Elgmork, K. & Nilssen, J. P. 1978. Equivalence of copepod and insect diapause. *Verhandlungen der Internationalen Vereinigung für Theoretische und Angewandte Limnologie*, **20**: 2511-2517.
- Erkmen, U. & Bozdoğan, N. 1981. Cambrian acritarchs from the Sosink Formation in southeast Turkey. *Revista Española de Micropaleontología*, **13**: 47-60.
- Evitt, W. R. 1963a. A discussion and proposals concerning fossil Dinoflagellates, Hystrichospheres and Acritarchs, I. *National Academy of Sciences Proceedings*, **49**: 158-164.
- Evitt, W. R. 1963b. A discussion and proposals concerning fossil Dinoflagellates, Hystrichospheres and Acritarchs, II. *National Academy of Sciences Proceedings*, **49**: 298-302.
- Evitt, W. R. 1985. Sporopollenin Dinoflagellate Cysts. Their Morphology and Interpretation. *American Association of Stratigraphic Palynologists Foundation, Texas*, 333 pp.
- Eyles, C. H., Eyles, N. & Grey, K. 2007. Palaeoclimate implications from deep drilling of Neoproterozoic strata in the Officer Basin and Adelaide Rift Complex of Australia; a marine record of wet-based glaciers. *Palaeogeography, Palaeoclimatology, Palaeoecology*, **248**: 291-312.
- Fatka, O. 1989. Acritarch assemblage in the *Onymagnostus hybridus* Zone (Jince Formation, Middle Cambrian, Czechoslovakia). *Vest. Ustr. Ust. geol., Praha*, **64** (6): 363-367.
- Fatka, O. & Konzalová, M. 1995. Mikrofosílie paseckých vrstev (spodní Kambrium, eská republika). [Microfossils of the Paseky Shale (Lower Cambrian, Czech republic)]. *Journal of the Czech Geological Society*, **40** (4): 55-66.
- Fensome, R. A., Williams, G. L., Barss, S. M., Freeman, J. M. & Hill, J. M. 1990. Acritarchs and fossil prasinophytes: An index to genera, species and infraspecific taxa. *American Association of Stratigraphic Palynologists, Contribution Series*, **25**: 771 pp.
- Finkel, Z., Sebbo, J., Feist-Burkhardt, S. & Irwin, A. 2007. A universal driver of macroevolutionary change in the size of marine phytoplankton over the Cenozoic. *Proc. Natl Acad. Sci. USA*, **104**: 20416-20420..
- Fombella, M. A. 1977. Acritarcos de Edad Cámbrico Medio-Inferior de la Provincia de León, España. *Revista española de Micropaleontología*, **9**: 115-124.
- Fombella, M. A. 1978. Acritarchs de la Formación Oville, Edad Cámbrico Medio-Tremadoc, Provincia de León, España. *Palinología, Numero Extraord.*, **1**: 245-261.

- Fombella, M. A. 1979. Palinologia de la Formación Oville al Norte y Sur de la Cordillera Cantábrica, España. *Palinologia*, **1**: 1-15.
- Fombella, M. A. 1987. Resemblances and differences between the palynological associations of Upper Cambrian age in the NW of Spain (Vozmediano) and North Africa. *Revista española de Micropaleontología*, **30** (2): 111-116.
- Foster, C. B., Cednovskis, A. & O'Brien, G. W., 1985. Organic-walled microfossils from the Early Cambrian of South Australia. *Alcheringa*, **9**: 259-268.
- Frakes, L. A., Francis, J. E. & Syktus, J. I. 1992. climatic models of the Phanerozoic. Cambridge, United Kingdom, Cambridge University press. 274 pp.
- Fridrichsone, A. I. 1971. Akritarchi *Baltisphaeridium* i gistrikhosfery (?) iz kembriyskikh otlozhenij Latvii (Acritarchs *Baltisphaeridium* and hystrichosphaers (?) from the Cambrian deposits of Latvia). *Paleontologiya i Stratigrafiya Pribaltiki i Belorusi 3* (*Palaeontology and Stratigraphy of Peribaltic and Belorussia*), **3**: 5-22.
- Fryer, G. 1996. Diapause, a potent force in the evolution of freshwater crustaceans. *Hydrobiologia*, **320**: 1-14.
- Gardiner, P. R. R. & Vanguetaine, M. 1971. Cambrian and Ordovician microfossils from south-east Ireland and their implications. *Geological Survey of Ireland, Bulletin* **1**(2), 163-210.
- Geyer, G. & Palmer, A. R. 1995. Neltneriidae and Holmiidae (Trilobita) from Morocco and the problem of Early Cambrian intercontinental correlation. *Journal of Paleontology*, **69** (3): 459-474.
- Gehling, J. G., Jensen, S., Droser, M. L., Myrow, P. M., & Narbonne, G. M. 2001. Burrowing below the basal Cambrian GSSP, Fortune Head, Newfoundland. *Geological Magazine*, **138**: 213-218.
- Ghavidel-syooki, M. 1996. Acritarch biostratigraphy of the Palaeozoic rock units in the Zagros Basin, Southern Iran. In: Fatka, O. & Servais, T. (Eds.), *Acritarcha in Praha*, Acta Universitatis Carolinae. Geologica, **40**: 385-411.
- Ghavidel-syooki, M. 2006. Palynostratigraphy and palaeogeography of the Cambro-Ordovician strata in southwest of Shahrud City (Kuh-e-Kharbash, near Deh-Molla), Central Alborz Range, northern Iran. *Review of Palaeobotany and Palynology*, **139** (1-4): 81-95.
- Ghavidel-syooki, M. & Vecoli, M. 2008. Palynostratigraphy of Middle Cambrian to lowermost Ordovician stratal sequences in the High Zagros Mountains, southern Iran: Regional stratigraphic implications, and palaeobiogeographic significance. *Review of Palaeobotany and Palynology*, **150** (1-4): 97-114.
- Gilchrist, B. 1978. Scanning electron microscope studies of the egg shell in some Anostraca (Crustacea, Branchiopoda). *Cell and Tissue Research*, **193**: 337-351.
- Glumac, B. 1997. Cessation of grand cycle deposition in the framework of passive margin evolution: Controlling mechanisms and effects on carbonate deposition and

- diagenesis, Cambrian Maynardville Formation, southern Appalachians [unpublished Ph.D. Thesis]: The University of Tennessee, Knoxville, 380 pp.
- Glumac, B. & Spivak-Birndorf, M. L. 2002. Stable isotopes of carbon as an invaluable stratigraphic tool: an example from the Cambrian of the northern Appalachians, USA. *Geology*, **30**, 563-566.
- Glumac, B. & Walker, K. R. 1997. Selective dolomitization of Cambrian microbial carbonate deposits: A key to mechanisms and environments of origin. *Palaios*, **12**: 98-110.
- Glumac, B. & Walker, K. R. 1998. A late Cambrian positive carbon-isotope excursion in the southern Appalachians: relation to biostratigraphy, sequence stratigraphy, environments of deposition, and diagenesis. *Journal of Sedimentary Research*, **68**, 1212-1222.
- Glumac, B. and Walker, K. R. 2000. Carbonate deposition and sequence stratigraphy of the terminal Cambrian grand cycle in the southern Appalachians. *Journal of Sedimentary Research*, **70**: 952-963.
- Gradstein, F., Ogg, J., & Smith, A. 2004, A geological Time Scale 2004. Cambridge University Press, 589 p.
- Gravestock, D. I., Alexander, E. M., Demidenko, Yu. E., Esakova, N. V., Holmer, L. E., Jago, J. B., Lin, T. R., Melnikova, L. M., Parkhaev, P. Yu., Rozanov, A. Yu., Ushatinskaya, G. T., Zang, W. L., Zhegallo, E. A. & Zhuravlev, A. Yu., 2001. The Cambrian biostratigraphy of the Stansbury Basin, South Australia. *Palaeontological Institute of the Russian Academy of Sciences, Transactions*, **282**: 344 pp.
- Grazhdankin, D. 2004. Patterns of distribution in the Ediacaran biotas: Facies versus Biogeography and Evolution. *Paleobiology*, **30**: 203-221.
- Greig, D. C., Wright, J. E., Hains, B. A. & Mitchell, G. H. 1968. Geology of the Country around Church Stretton, Craven Arms, Wenlock Edge and Brown Clee. *Memoir of the Geological Survey of Great Britain, sheet 116 (England and Wales)*. HMSO, London. 379p.
- Grey, K. 2005. Ediacaran palynology of Australia. *Memoir of the Association of Australian Palaeontologists*, **31**: 439 pp.
- Grey, K. & Cotter, K. L. 1996. Palynology in the search for Proterozoic hydrocarbons. *Western Australia Geological Survey Annual Review for 1995-96*, 70-80.
- Grey, K., Walter, M. R. & Calver, C. R. 2003. Neoproterozoic biotic diversification: Snowball Earth or aftermath of the Acraman impact? *Geology*, **31** (5): 459-462.
- Hajirostamloo, M. 2008. Differences of shell structure in cysts of *Artemia* from various depth of Urmia Lake (Iran). *Research Journal of Biological Sciences*, **3** (6): 648-653.
- Hagadorn, J. W., Xiao, S., Donoghue, P. C. J., Bengtson, S., Gostling, N. J., Pawlowska, M., Raff, E. C., Raff, R. A., Turner, F. R., Chongyu, Y., Zhou, C., Yuan, X., McFeely, M.

- B., Stampanoni, M. & Nealson, K. H. 2006. Cellular and Subcellular Structure of Neoproterozoic Animal Embryos. *Science*, **314**: 291-294.
- Hagenfeldt, S. E. 1988. Acritarch assemblages of Early and Middle Cambrian age in the Baltic Depression and South-central Sweden. In: Winterhalter, B. (Ed.), *Geological Survey of Finland Special Paper, The Baltic Sea*, **6**: 153-163.
- Hagenfeldt, S. E. 1989a. Lower Cambrian acritarchs from the Baltic Depression and south-central Sweden, taxonomy and biostratigraphy. *Stockholm Contributions in Geology*, **41**: 1-176.
- Hagenfeldt, S. E. 1989b. Middle Cambrian acritarchs from the Baltic Depression and south-central Sweden, taxonomy and biostratigraphy. *Stockholm Contributions in Geology*, **41**: 177-250.
- Hairston, N. G., Jr. 1998. Time travellers: What's timely in diapause research? *Archiv für Hydrobiologie Special Issues Advances in Limnology*, **52**: 1-15.
- Hajirostamloo, M. 2008. Differences in shell structure in Cysts of *Artemia* from Various Depth of Urmia Lake (Iran). *Research Journal of Biological Sciences*, **3 (6)**: 648-653.
- Ham, W. E., Denison, R. E. & Merritt, C. A. 1964. Basement rocks and structural evolution of southern Oklahoma. *Oklahoma Geological Survey Bulletin*, **95**: 302 pp.
- Haq, B. U. & Schutter, S. R. 2010 A chronology of Paleozoic sea-level changes. *Science*, **322**: 64-68.
- Harland, R. & Sarjeant, W. A. S. 1970. Fossil freshwater microplankton (dinoflagellates and acritarchs) from Flandrian (Holocene) sediments of Victorian and Western Australia. *Royal Society of Victoria, Proceedings*, **83**: 211-234.
- Harris, L. D. 1964. Facies relations of exposed Rome Formation and Conasauga Group of northeastern Tennessee with equivalent rocks in the subsurface of Kentucky and Virginia. *Professional Paper of the U.S. Geological Survey*, **501-B**: 25-29.
- Harvey, T. H. P. & Butterfield, N. J. 2008. Sophisticated particle-feeding in a large Early Cambrian crustacean. *Nature*, **452**: 868-871.
- Harvey, T. H. P. & Butterfield, N. J. 2011. Macro- and Microfossils of the Mount Cap Formation (Early and Middle Cambrian, Northwest Territories). *Geoscience Canada*, **38**: 165-173.
- Harvey, T. H. P., Ortega-Hernández, J., Lin, J.-P., Zhao, Y. & Butterfield, N. J. 2011. Burgess Shale-type microfossils from the middle Cambrian Kaili Formation, Guizhou Province, China. *Acta Palaeontologica Polonica*, **57 (2)**: 423-436.
- Harvey, T. H. P., Vélez, M. L. & Butterfield, N. J. 2012. Exceptionally preserved crustaceans from western Canada reveal a cryptic Cambrian radiation. *PNAS*, **109**: 1589-1594.

- Hasson, K. O. & Haase, C. S. 1988. Lithofacies and paleogeography of the Conasauga Group, (Middle and Late Cambrian) in the Valley and Ridge province of east Tennessee *Geological Society of America Bulletin*, **100**: 234-246
- Henningsmoen, G. 1957. The trilobite family Olenidae. *Skrifter utgitt av Det Norske Videnskaps-Akademi i Oslo. 1. Matematisk-Naturvidenskapelig Klasse for 1957*, No. **1**, 1-303.
- Hill, J. H. 1974. Stratigraphic palynology of acritarchs from the type area of the Llandovery and the Welsh Borderland. *Review of Palaeobotany and Palynology*, **18 (1-2)**: 11-23.
- Hinz, I. 1987. The Lower Cambrian microfauna of Comley and Rushton, Shropshire/England. *Palaeontographica Abteilung A*, **198**: 41-100.
- Hinze, W. J. & Braille, R. S. 1988. Geophysical aspects of the craton: US. In: Sloss, L. L. (ed.), *Sedimentary cover-North American craton: US: Boulder, Colorado, Geological Society of America, The geology of North America*, v. D-2: 5-24.
- Hoefs, J. 1987. *Stable Isotope geochemistry*, 3rd Edition. Springer-Verlag, Heidelberg. 241 pp.
- Hofmann, H. J. & Jackson, G. D. 1994. Shale-Facies Microfossils from the Proterozoic Bylot Supergroup, Baffin Island, Canada. *Paleontological Society Memoir*, **37**: 39 pp.
- Hou, X. G., Bergström, J., Wang, H. F., Feng, X. H. & Chen, A. L. 1999. The Chengjiang Fauna-exceptionally well-preserved animals from 530 million years ago. *Yunnan Science and Technology Press, Kunming*. P. 1-170.
- Howell, B. F., Bridge, J., Deiss, C. F. Edwards, I. R. A., Lochman, C., Raasch, G. O. & Resser, C. E. 1944. Correlation of the Cambrian formations of North America. *Bulletin of the Geological Society of America*, **55**: 993-1004.
- Huldtgren, T., Cunningham, J. A., Yin, C., Stampanoni, M., Marone, F., Donoghue, P. C. J. & Bengtson, S. 2011. Fossilized Nuclei and Germination Structures Identify Ediacaran “Animal Embryos” as Encysting Protists. *Science*, **334**: 1696-1699.
- Huys, R. & Boxshall, G. A. 1991. Copepod Evolution. *The Ray Society, London*, 468 pp.
- Irwin, A. J., Finkel, Z. V., Schofield, O. M. E. & Falkowski, P. G. 2006. Scaling-up from nutrient physiology to the size-structure of phytoplankton communities. *Journal of Plankton Research*, **28 (5)**: 459-471.
- Jachowicz, M. 1995. Ordovician acritarch assemblages from central and northwestern Saudi Arabia. *review of Palaeobotany and Palynology*, **89**: 19-25.
- Jachowicz-Zdanowska, M. 2010. Palinologia Kambru Dolnego Bloku G rno l skiego w Regionie Krakowskim. (Palynology of the lower Cambrian in the Upper Silesian Block, Krak w Region). *Biuletyn Pa stwowego Instytutu Geologicznego*, **443**: 1-32.
- Jachowicz-Zdanowska, M. 2011. Cambrian organic microfossils at the border area of the East- and West-European Platforms (SE Poland and western Ukraine). *Annales Societatis Geologorum Poloniae*, **81**: 241-267.

- Jago, J. B., Zang, W., Sun, X., Brock, G. A., Patterson, J. R. & Skovsted, C. B. 2006. A review of the Cambrian biostratigraphy of South Australia. *Palaeoworld*, **15**, 406-423.
- Jankauskas, T. V. 1979. Srednerifeiskie mikrobioty yuzuogo Urala I ashkirskogo Priuralya (Middle Riphean microbiota from the southern Urals and the Bashkirian Urals). *Akad. Nauk SSSR (Dokl. Earth Sci.)*, **248 (1)**: 190-193 (in Russian).
- Jankauskas, T. V. 1975. New Lower Cambrian acritarchs of the Baltic region. *Paleontol. Zh. Akad. Nauk S.S.S.R.*, **1**: 94–104 (in Russian).
- Jankauskas, T. V. 1980. Shishenyakskaya mikrobiota verkhnego rifeya Yuzhnogo Yurala. *Doklady Akademiyi Nauk SSSR*, **251**: 190-192 (In Russian).
- Jankauskas, T. V. Mikhailova, N. S. & German, T. N. 1989. (Eds.), *Mikrofossilii Dokembriya SSSR (Precambrian microfossils of the USSR)*. Nauka, Leningrad, 190 pp.
- Jankauskas & Posti, 1973. Micropalaeontological characteristic of the stratotype sections of the Estonian Lower Cambrian. *Izv. Akad. Nauk Estonskoy SSR 22, Kimiya Geol.*, **2**: 143-148.
- Jankauskas & Posti, 1976. New Cambrian acritarchs from the East Baltic area. *Izv. Akad. Nauk Estonskoy SSR 22, Kimiya Geol.*, **2**: 145-151.
- Javaux, E. J., Knoll, A. H. & Walter, M. R. 2004. TEM evidence for eukaryotic diversity in mid-Proterozoic oceans. *Geobiology*, **2**: 121-132.
- Javaux, E. J. & Marshal, C. P. 2006. A new approach in deciphering early protist palaeobiology and evolution: combined microscopy and microchemistry of single Proterozoic acritarchs. *Review of Palaeobotany and Palynology*, **139**: 1-15.
- Jux, U. 1969. Über den Feinbau der Zystenwandung von *Hlaosphaera* Schmitz, 1878. *Palaeontographica, Abt. B*, **128**: 48-55.
- Kasahara, S., Uye, S. & Onbe, T. 1974. Calanoid copepod eggs in sea-bottom muds. *Marine Biology*, **26**: 167-171.
- Kaufman, A. J., Jacobsen, S. B. & Knoll, A. H. 1993. The Vendian record of $\delta^{13}C$ and $\delta^{18}O$ isotopic variations in seawater: Implications for tectonics and palaeoclimate. *Earth and Planetary Science Letters*, **120**: 409-430.
- Keegan, J.B., Rasul, S. M. & Shaheen, Y. 1990. Palynostratigraphy of the lower Paleozoic, Cambrian to Silurian of the Hashemite Kingdom of Jordan. *Revue of Palaeobotany and Palynology*, **66**: 167–180.
- Kennaway, G. M., Lewis, J. M. 2004. An ultrastructural study of hypnozygotes of *Alexandrium* species (Dinophyceae). *Phycologia*, **43**: 353-363.
- Kjørboe, T. 1993. Turbulence, Phytoplankton Cell Size, and the Structure of Pelagic Food Webs. *Advances in Marine Biology*, **29**: 1-72.

- Kirjanov, V. V. 1974. New Acritarchs from the Cambrian of Volynia. *Paleontologitsheskii Zhurnal*, **2**: 117-129 (in Russian).
- Kirjanov, V. V. 1979. Kembrij (The Cambrian). In: Keller, B. M., Rozanov, Y. A., (Eds.). Stratigrafiya verkhnedokembrijskikh i kembrijskikh otlozhenij Vostochno-vropejskoj platformy (Upper Precambrian and Cambrian stratigraphy of the western part of the East European Platform). Moscow: Nauka. p. 151-177.
- Kjellström, G. 1968. Remarks on the chemistry and ultrastructure of the cell wall of some Palaeozoic leiospheres. *Geologiska Föreningens i Stockholm Förhandlingar* **90**: 118-221.
- Knoll, A. H. 1996. Archean and Proterozoic paleontology. In: Jansonius, J., McGregor, D. C. (Eds.). *Palynology: Principles and Applications*, American Association of Stratigraphic Palynologists Foundation, Salt Lake City, Utah. 51-80.
- Knoll, A. H., Javaux, E. J., Hewitt, D. & Cohen, P. 2006. Eukaryotic organisms in Proterozoic oceans. *Philosophical Transactions of the Royal Society B*, **361**: 1023-1038.
- Knoll, A. H. & Swett, K. 1987. Micropaleontology across the Precambrian-Cambrian boundary in Spitsbergen. *Journal of Paleontology*, **61**: 898-926.
- Knoll, A. H., Swett, K. & Mark, J. 1991. Paleobiology of a Neoproterozoic tidal flat/lagoonal complex: the Draken Conglomerate Formation, Spitsbergen. *Journal of paleontology*, **65**: 531-570.
- Koga, F. 1968. On the pelagic eggs of Copepoda. *Journal of the Oceanographical Society of Japan*, **24** (1): 16-20.
- Konzalová, M. 1974. Acritarchs from the Bohemian Precambrian (Upper Proterozoic) and Lower-Middle Cambrian. *Review of Palaeobotany and Palynology* **18**: 41-56.
- Kouchinsky, A., Bengtson, S., Gallet, Y., Korovnikov, I., Pavlov, V., Runnegar, B., Shields, G., Veizer, J., Young, E. & Ziegler, K. 2008. The spike carbon isotope excursion in Siberia: a combined study of the upper middle Cambrian-lowermost Ordovician Kulyumbe river section, northwestern Siberian platform. *Geological magazine*, **145**: 609-622.
- Landing, E. 1994. Precambrian-Cambrian boundary global Stratotype ratified and a new perspective of Cambrian time. *Geology*, **22**: 179-182.
- Landing, E. & MacGabhann, B. A. 2010. First evidence for Cambrian glaciation provided by sections in Avalonian New Brunswick and Ireland-Additional data for Avalon-Gondwana separation by the earliest Palaeozoic: *Palaeogeography, Palaeoclimatology, Palaeoecology*, **295**: 174-185.
- Landing, E., Peng, S., Babcock, L. E., Geyer, G. & Moczydłowska-Vidal, M. 2007. Global standard names for the Lowermost Cambrian Series and Stage. *Episodes*, **30** (4): 287-289.

- Landing, E., Bowring, S. A., Davidek, L. Westrop, S. R., Geyer, G. & Heldmaier, W. 1998. Duration of the early Cambrian: U-Pb ages of volcanic ashes from Avalon and Gondwana. *Canadian Journal of Earth Sciences*, **35** (4): 329-338.
- Lapworth, C. 1888. On the discovery of the *Olenellus* fauna in the Lower Cambrian rocks of Britain. *Nature*, **39**: 212-213.
- Le Herisse, A., Al-Ruwaili, M., Miller, M. & Vecoli, M. 2007. Environmental changes reflected by palynomorphs in the early Middle Ordovician Hanadir Member of the Qasim Formation, Saudi Arabia. *Revue de micropaléontologie*, **50**: 3-16.
- Liñán, E., Gámez Vintaned, J. A., Gozalo, R., Dies, M. E. & Mayoral, E. 2006. Events and biostratigraphy in the Lower Cambrian of Iberia. *Zeitschrift der Deutschen Gesellschaft für Geowissenschaften*, **157** (4): 597-609.
- Liñán, E., Palacios, T. & Perejón, A. 1984. Precambrian-Cambrian boundary and correlation from Southwestern and Central part of Spain. *Geological Magazine*, **121**: 221-8.
- Lindley, J. A. 1986. Dormant eggs of calanoid copepods in sea bed sediments of the English Channel and southern North sea. *Journal of Plankton Research*, **8**: 399-400.
- Lister T. R. 1970. A monograph of the acritarchs and chitinozoa from the Wenlock and Ludlow Series and Millichope areas, Shropshire. Part 1. *Palaeontographical Society Monographs*, **124**: 100 pp.
- Lochman-Balk, C. 1971. The Cambrian of the craton of the United States. In: Holland, C. H. (ed.), *Cambrian of the New World*. Wiley-Interscience, London, 79-167.
- Loeblich, A. R. Jr. 1970. Morphology, ultrastructure and distribution of Paleozoic acritarchs. *Proceedings of the North American Paleontological Convention, Chicago, 1969, part G*, **2**: 705-788.
- Loeblich, A. R. & Drugg, W. S. 1968. New acritarchs from the Early Devonian (Late Gedinnian) Haragan of Oklahoma, USA. *Tulane Studies in Geology*, **6** (4): 129-137.
- Longwell, C. R. (ed.). 1949. Sedimentary facies in geologic history. *Geological Society of America, Memoir*, **39**: 171 pp.
- Ludvigsen, R. & Westrop, S. R. 1985. Three new Upper Cambrian stages for North America. *Geology*, **13**: 139-143.
- Ludvigsen, R., Westrop, S. R. & Kindle, C. H. 1989. Sunwaptan (Upper Cambrian) trilobites of the Cow Head Group, western Newfoundland, Canada. *Palaeontographica Canadiana*, **6**: 175 pp.
- Maithy, P. K. 1975. Micro-organisms from the Bushimay System (Late Precambrian) of Kanshi, Zaire. *The Palaeobotanist*, **22**: 133-149.
- Marcus, N. H. 1984. Recruitment of copepod nauplii into the plankton: importance of diapause eggs and benthic processes. *Mar. Ecol. Prog. Ser.* **15**: 47-54.

- Marcus, N. H. 1990. Calanoid Copepod, Cladoceran, and Rotifer eggs in sea-bottom sediments of Northern California coastal waters: identification, occurrence and hatching. *Marine Biology*, **105**: 413-418.
- Marcus, N. H. 1996. Ecological and evolutionary significance of resting eggs in marine copepods: past, present and future studies, *Hydrobiologia*, **320**: 141-152.
- Marcus, N. H. & Fuller, C. M. 1986. Subitaneous and diapause eggs of *Labidocera aestiva* Wheeler (Copepoda: Calanoida): Differences in fall velocity and density. *Journal of Experimental Marine Biology and Ecology*, **99**: 247-256.
- Marcus, N. H. 1989. Abundance in bottom sediments and hatching requirements of eggs of *Centropages hamatus* (Copepoda: Calanoida) from the Alligator Harbor region, Florida. *Biological Bulletin of the Marine Biological Laboratory, Woods Hole (Massachusetts)*, **176**: 142-146.
- Marcus, N. H. & Fuller, C. M. 1989. Distribution and abundance of eggs of *Labidocera aestiva* (Copepoda: Calanoida) in the bottom sediments of Buzzards Bay, Massachusetts, USA. *Marine Biology*, **100**: 319-326.
- Markello, J. R. & Read, J. F. 1981. Carbonate ramp-to-deeper shale shelf transitions of an Upper Cambrian intrashelf basin, Nolichucky Formation, southwest Virginia Appalachians. *Sedimentology*, **28**: 573-597.
- Markello, J. R. & Read, J. F. 1982. Upper Cambrian intrashelf basin, Nolichucky Formation, southwest Virginia Appalachians. *American Association of Petroleum Geologists Bulletin*, **66**: 860-878.
- Martin, F. 1973. Les Acritarches de l'Ordovicien inférieur de la Montagne Noire (Hérault, France). *Bulletin, Institut Royal des Sciences Naturelles de Belgique*, **48**: 1-61.
- Martin, F. 1982. Some aspects of late Cambrian and early Ordovician acritarchs. In: Bassett, M. G., Dean, W. T. (editors), *The Cambrian-Ordovician Boundary: sections, fossil distributions and correlations. National Museum of Wales, Geological Series no. 3*: 29-40.
- Martin, F. 1992. Uppermost Cambrian and Lower Ordovician acritarchs and Lower Ordovician chitinozoans from Wilcox Pass, Alberta. *Geological Survey of Canada, Bulletin*, **420**: 57 pp.
- Martin, F. 1993. Acritarchs: a review. *Biological Reviews*, **68**: 475-538.
- Martin, F. & Dean, W. T. 1981. Middle and Upper Cambrian and Lower Ordovician acritarchs from Random Island, eastern Newfoundland. *Geological Survey of Canada, Bulletin*, **343**: 43 p.
- Martin, F. & Dean, W. T. 1983. Late Early Cambrian and Early Middle Cambrian acritarchs from Manuels River, eastern Newfoundland, In: *Current Research, Part B, Geological survey of Canada, paper 83-1B*: 353-363.

- Martin, F. & Dean, W. T. 1984. Middle Cambrian acritarchs from the Chamberlains Brook and Manuels River Formations at Random Island, Eastern Newfoundland. *In: Current Research, part A, Geological Survey of Canada, Paper 84-1A*: 429-440.
- Martin, F. & Dean, W. T. 1988. Middle and Upper Cambrian acritarch and trilobite zonation at Manuels River and Random Island, eastern Newfoundland. *Geological Survey of Canada, Bulletin*, **381**: 91p.
- Martin, J. W. 1992. Branchiopoda. *In: F. R. Harrison and A. G. Humes, (Eds.), Microscopic Anatomy of Invertebrates, Vol. 9. Crustacea. P. 25-224. Wiley-Liss Publishers, New York, New York.*
- Martin, M. W., Grazhdankin, D. V. Bowring, S. A., Evans, D. A. D., Fedonkin, M. A. & Kirschvink, J. L. 2000. *Science*, **288**: 841-845.
- McFadden, K. A., Xiao, S., Zhou, C. & Kowalewski, M. 2008. Quantitative evaluation of the biostratigraphic distribution of acanthomorphic acritarchs in the Ediacaran Doushantuo Formation in the Yangtze Gorges area, South China. 2008. *Precambrian Research*, **173 (1-4)**: 170-190.
- McKerrow, W. S., Scotese, C. R. & Brasier, M. D. 1992. Early Cambrian continental reconstructions. *Journal of the Geological Society, London*, **149**: 599-606.
- Meert, J. G. & Lieberman, B. S. 2004. A palaeomagnetic and palaeobiogeographic perspective on latest Neoproterozoic and early Cambrian tectonic events, *Journal of the Geological Society of London*, **161**: 1-11.
- McMinn, A. 1991. Recent dinoflagellate cysts from estuaries on the central coast of New South Wales, Australia. *Micropaleontology*, **37**: 269-287.
- McMinn, A., Bolch, C. & Hallegraeff, G. 1992. *Cobricosphaeridium* Harland and Sarjeant: Dinoflagellate cyst or copepod egg? *Micropaleontology*, **38 (3)**: 315-316.
- Mendelson, C. V. & Schopf, J. W. 1992. Proterozoic and Early Cambrian microfossils and microfossil-like objects. 865-951, *in Schopf, J. W. & Klein, C. (editors), Evolution of the Proterozoic biosphere - a multidisciplinary study. Cambridge University Press, New York.*
- Mens, K., Paalits, I. & Puura, I. 1997. Upper Cambrian acritarchs from the basal conglomerate of the Kallavere Formation on the Pakri Peninsula, NW Estonia. *In: Fatka, O. & Servais, T. (Editors), Acritarcha in Praha 1996. Acta Universitatis Carolinae Geologica*, **40**: 531-543.
- Mette, W. 1989. Acritarchs from Lower Paleozoic rocks of the western Sierra Morena, SW-Spain and biostratigraphic results. *Geol. Palaentol.*, **23**: 1-19.
- Middleton, L. T., Steidtmann, J. R. & DeBour, D. A. 1980. Stratigraphy and Depositional Setting of Some Middle and Upper Cambrian Rocks, Wyoming. *Stratigraphy of Wyoming: 31st Annual Field Conference Guidebook*. 23-35.

- Milici, R. C. & De Witt, W. Jr., 1988. The Appalachian basin. *In*: Sloss, L. L. (ed.), Sedimentary cover-North American craton: US: Geological Society of America, The Geology of North America, v. D-2: 427-469.
- Mili i , D. & Petrov, B. 2002. SEM morphological analysis of fertilized cysts in the genus *Branchipus* (Branchiopoda, Anostraca) - can cyst morphology be used as a reliable taxonomic criterion? *Arch. Biol. Sci.*, Belgrade, **61** (3): 563-569.
- Miller, M. A. & Al-Ruwaili, M. H. 2007. Preliminary palynological investigation of Saudi Arabian Upper Ordovician glacial sediments. *Revue de Micropaléontologie*, **50** (1): 17-26.
- Moczyłowska, M. 1981. Lower and Middle Cambrian acritarchs from northeastern Poland. *Precambrian Research*, **15**: 63-74.
- Moczyłowska, M. 1988. New Lower Cambrian acritarchs from Poland. *Review of Palaeobotany and Palynology*, **54**: 1-10.
- Moczyłowska, M. 1997. Proterozoic and Cambrian successions in Upper Silesia: an Avalonian terrane in southern Poland. *Geological Magazine*, **133**: 679-689.
- Moczyłowska, M. 1991. Acritarch biostratigraphy of the Lower Cambrian and the Precambrian-Cambrian boundary in southeastern Poland. *Fossils and Strata*, **29**: 127p.
- Moczyłowska, M. 2001. Early Cambrian phytoplankton radiations and appearance of metazoans. *In*: Shanchi Peng, Babcock, L.E., Zhu Maoyan, (Eds.), Cambrian System of South China. Press of University of Science and Technology of China, 293-296.
- Moczyłowska, M. 2002. Early Cambrian phytoplankton diversification and appearance of trilobites in the Swedish Caledonides with implications for coupled evolutionary events between primary producers and consumers. *Lethaia* **35**: 191-214.
- Moczyłowska, M. 2005. Taxonomic review of some Ediacaran acritarchs from the Siberian Platform. *Precambrian Research*, **136**: 283-307.
- Moczyłowska, M. 2008a. The Ediacaran microbiota and the survival of Snowball Earth conditions. *Precambrian Research*, **167**: 1-15.
- Moczyłowska, M. 2008b. New records of late Ediacaran microbiota from Poland. *Precambrian Research*, **167**: 71-92.
- Moczyłowska, M. 2010. Life cycle of early Cambrian microalgae from the Skiagia-plexus acritarchs. *Journal of Paleontology*, **84** (2): 216-230.
- Moczyłowska, M. 2011. The early Cambrian phytoplankton radiation: acritarch evidence from the Lükati Formation, Estonia. *palynology*, **35** (1): 103-145.
- Moczyłowska, M., Jensen, S., Ebbestad, J., Budd, G. & Marti-Mus, M., 2001. Biochronology of the autochthonous Lower Cambrian in the Laisvall-Storuman area, Swedish Caledonides. *Geological Magazine*, **138**: 435-453.

- Moczyłowska, M. & Stockfors, M. 2004. Acritarchs from the Cambrian-Ordovician boundary interval on Kolguev Island, Arctic Russia. *Palynology*, **28**: 15-73.
- Moczyłowska, M. & Vidal, G. 1986. Lower Cambrian acritarchs zonation in southern Scandinavia and southeastern Poland. *Geologiska Föreningens i Stockholm Förhandlingar*, **108**: 201-223.
- Moczyłowska, M. & Vidal, G. 1988. Early Cambrian acritarchs from Scandinavia and Poland. *Palynology*, **12**: 1-10.
- Moczyłowska, M. & Vidal, G. 1992. Phytoplankton from the Lower Cambrian L så Formation on Bornholm, Denmark: biostratigraphy and palaeoenvironmental constraints. *Geological magazine*, **129**: 17-40.
- Moczyłowska, M., Vidal, G. & Rudavskaya, V. A. 1993. Neoproterozoic (Vendian) Phytoplankton from the Siberian Platform, Yakutia. *Palaeontology*, **36 (3)**: 495-521.
- Moczyłowska, M. & Willman, S. 2009. Ultrastructure of cell walls in ancient microfossils as a proxy to their biological affinities. *Precambrian Research* **173**: 27-38.
- Moczyłowska, M. & Zang, W. 2006. The Early Cambrian acritarch *Skiagia* and its significance for global correlation. *Palaeoworld*, **15**: 328-347.
- Moczyłowska, M., Schopf, J. W. & Willman, S. 2010. Micro- and nano-scale ultrastructure of cell walls in Cryogenian microfossils: revealing their biological affinity. *Lethaia*, **43**: 129-136.
- Moldowan, J. M. & Talyzina, M. N. 1998. Biogeochemical evidence for dinoflagellates ancestors in the early Cambrian. *Science*, **281**: 1168-1170.
- Molyneux, S. G., Le Hérisse, A., Wicander, R. 1996. Chapter 16: Paleozoic phytoplankton. *In*: Jansonius, J., McGregor, D. C., (editors), *Palynology: principles and applications*, Volume 2. American Association of Stratigraphic Palynologists Foundation 1. Salt Lake City: Publishers Press. p. 493-530.
- Molyneux, S. G. & Rushton, A. W. A. 1988. The age of the Watch Hill Grits (Ordovician), English Lake District: structural and palaeogeographical implications. *Transactions of the Royal Society of Edinburgh: Earth Sciences*, **79**: 43-69.
- Montañez, I. P., banner, J. L., Osleger, D. A., Borg, L. E & Bosserman, P. J. 1996. Integrated Sr isotope variations and sea-level history of Middle to Upper Cambrian platform carbonates: Implications for the evolution of Cambrian seawater. *Geology*, **24**: 917-920.
- Montañez, I. P., Osleger, D. A., banner, J. L., Mack, L.E. & Musgrove, M. 2000. Evolution of the Sr and C isotope composition of Cambrian oceans. *GSA Today*, **10 (5)**: 1-10.
- Montenari, M. & Servais, T. 2000. Early Palaeozoic (Late Cambrian-Early Ordovician) acritarchs from the metasedimentary Baden-Baden - Gaggenau zone (Schwarzwald, SW, Germany). *Review of Palaeobotany and Palynology*, **113**: 73-85.

- Morris, J. E. & Afzelius, B. A. 1967. The structure of the Shell and Outer Membranes in Encysted *Artemia salina* Embryos during Cryptobiosis and Development. *Journal of Ultrastructure Research*, **20**: 244-259.
- Moscatello, S. & Belmonte, G. 2009. Egg banks in hypersaline lakes of South-East Europe. *Saline systems*, **5** (3): 1-7.
- Müller, K. J. 1983. Crustacea with preserved soft parts from the upper Cambrian of Sweden. *Lethaia*, **16**: 93-109.
- Müller, K. & Walossek, D. 1988. External morphology and larval development of the Upper Cambrian maxillopod *Bredocaris admirabilis*. *Fossils and Strata*, **23**: 1-20.
- Mullins, G. L., Aldridge, R. J., Dorning, K. J., Le Hérisse, A., Moczyłowska-Vidal, M., Molyneux, S., Servais, T., Wicander, R. 2005. The diversity of the lower Palaeozoic phytoplankton: The PhytoPal Project. 38th Annual Meeting of the AASP, St Louis, Missouri, Program and abstracts, **43**.
- Mura, G. & Thiery, A. 1986. Taxonomical significance of scanning electron microscope morphology of the euphilopod's resting eggs from Morocco. Part 1. Anostraca. *Vie Milieu*, **36**: 125-131.
- Myrow, P. M., Tice, L., Archuleta, B., Clark, B., Taylor, J. F. & Ripperdan, R. L. 2004. Flat-pebble conglomerate: its multiple origins and relationship to metre-scale depositional cycles. *Sedimentology*, **51**: 973-996.
- Naumova, S. N. 1949. Spory nizhnego kembriya. *Izvestiya Akademiyi Nauk SSSR, Seriya Geologicheskaya*, 49-56.
- Naumova, S. N. 1961. Spore-pollen complexes of the Riphean and Lower Cambrian (in USSR). *Intn. geol. Congr., XXI Sess., Copenhagen 1960, Dokl. Sov. Geol.* 109-117.
- Negrea, S., Botnariuc, N. & Dumont, H. J. 1999. Phylogeny, evolution and classification of the Branchiopoda (Crustacea). *Hydrobiologia*, **412**: 191-212.
- Naiwen, W. 1989. Micropaleontological study of lower Palaeozoic siliceous sequences of the Yangtze Platform and Eastern Quiling Range. *Journal of Southeast Asian Earth Sciences*, **3** (1-4): 141-161.
- Narbonne, G. M. 2005. The Ediacaran Biota: Neoproterozoic Origin of Animals and Their Ecosystems. *Annual Review of Earth Planet Sciences*, **33**: 421-442.
- Newton, E. T. 1885. On "Tasmanite" and Australian "white coal". *Geol. Mag.*, **12**: 337-342.
- Nowlan, G. S., McGregor, D. C., Norford, B. S. & Wicander, R. 1995. Paleontology and Biostratigraphy; *In*: Nowlan G. S., (editor), the Lower Paleozoic: A New Frontier in the Western Canada Sedimentary Basin, Report to Partners 1994-1995, Internal Report by the Geological Survey of Canada, section 6: 17 pp.
- Oelher, D. Z. 1976. Transmission electron microscopy of organic microfossils from the late Precambrian Bitter Springs Formation in Australia: techniques and survey of preserved ultrastructure. *Journal of Paleontology*, **50**: 90-106.

- Osleger, D. A. & Read, J. F. 1991. Relation of eustasy to stacking patterns of meter-scale carbonate cycles, Late Cambrian, U.S.A. *Journal of Sedimentary Petrology*, **61** (7): 1225-1252.
- Osleger, D. A. & Read, J. F. 1993. Comparative analysis of methods used to define eustatic variations in outcrop: Late Cambrian interbasinal sequence development. *American Journal of Science*, **293**: 157-216.
- Paalits, I. 1992a. Upper Cambrian acritarchs from the Petseri Formation (East European Platform). *Acta et Commentationes Universitatis Tartuensis*, **956**: 44-55.
- Paalits, I. 1992b. Upper Cambrian acritarchs from boring core M-72 of North Estonia. *Proceedings of the Estonian Academy of Sciences, Geology*, **41** (1): 29-37.
- Paalits, I. 1995. Acritarchs from the Cambrian-Ordovician boundary beds.. at Tõnismägi, Tallinn, North Estonia. *Proceedings of the Estonian Academy of Sciences, Geology*, **44** (2): 87-96.
- Paalits, I. & Heuse, T. 2000. Taxonomic review of the acritarch genera *Acanthodiacrodium* Timofeev, 1958 and *Diornatosphaera* Downie, 1958. *Bollettino della Società Paleontologica Italiana*, **39** (2): 311-317.
- Palacios, T. 2010. Middle-Upper Cambrian acritarchs from the Oville and Barrios Formations, Cantabrian Mountains, Northern Spain. *CIMP, Abstracts*, Warsaw, 50-53.
- Palacios, T., Jensen, S., Barr, S. M. & White, C. E. 2009a. Acritarchs from the MacLean Brook Formation, southeastern Cape Breton Island, Nova Scotia, Canada: New data on Middle Cambrian-Lower Furongian acritarch zonation. *Palaeogeography, Palaeoclimatology, Palaeoecology*, **273** (1-2): 123-141.
- Palacios, T., Jensen, S., Barr, S. M., White, C. E. & Miller, R. F. 2009b. Preliminary Results from an Ongoing Study of Acritarchs in Cambrian and Lower Ordovician Rocks of Nova Scotia and New Brunswick. In: *Atlantic Geoscience Society 35th Colloquium and Annual General Meeting, Program and Abstracts*, p. 25.
- Palacios, T., Jensen, S., Barr, S. M., White, C. E. & Miller, R. F. 2011. New biostratigraphical constraints on the lower Cambrian Ratcliffe Brook Formation, southern New Brunswick, Canada, from organic-walled microfossils. *Stratigraphy*, **8** (1): 45-60.
- Palacios, T., Jensen, S., White, C. E. & Barr, S. M. 2012. Cambrian acritarchs from the Bourinot belt, Cape Breton Island, Nova Scotia: age and stratigraphic implications. *Canadian Journal of Earth Sciences*, **49**: 289-307.
- Palacios, T., & Moczyłowska, M. 1998. Acritarch biostratigraphy of the Lower-Middle Cambrian boundary in the Iberian Chains, Province of Soria, northeastern Spain. *Revista Española de Paleontología, no extr. Homenaje al Prof. Gonzalo Vidal*, 65-82.

- Palacios, T. & Vidal, G. 1992. Lower Cambrian acritarchs from northern Spain: the Precambrian-Cambrian boundary and biostratigraphic implications. *Geological Magazine*, **129**: 421-436.
- Palmer, A. R. 1960. Trilobites of the Upper Cambrian Dunderberg Shale, Eureka District, Nevada. *US Geological Survey, Professional Paper*, **334C**: 1-109.
- Palmer, A. R. 1962. *Glyptagnostus* and associated trilobites in the United States. *Professional Paper U. S. Geological Survey*, **374-F**.
- Palmer, A. R. 1965. Trilobites of the Late Cambrian *Pterocephaliid* Biomere in the Great Basin, United States. *U. S. Geological Survey Professional Paper*, **493**: 105 p.
- Palmer, A. R. 1971. The Cambrian of the Great Basin and adjacent areas, western United States. *In*: Holland, H. C., (Ed.), *Cambrian of the New World*: London, Wiley-Interscience, 1-79.
- Palmer, A. R. 1979. Biomere boundaries re-examined. *Alcheringa*, **3**: 33-41.
- Palmer, A. R. 1981. Subdivision of the Sauk Sequence. *In*: Taylor, M. E. (Ed.), *Short Papers for the Second International Symposium on the Cambrian System*. U.S. Geological Survey Open-File Report, 81-743, 160-162.
- Palmer, A. R. 1984. The biomere problem: evolution of an idea. *Journal of Paleontology*, **58**: 599-611.
- Palmer, A. R. 1998. A proposed nomenclature for stages and series for the Cambrian of Laurentia. *Canadian Journal of Earth Sciences*, **35 (4)**: 323-328.
- Parsons, M. G. & Anderson, M. M. 2000. Acritarch microfloral succession from the Late Cambrian and Ordovician (Early Tremadoc) of Random Island, eastern Newfoundland, and its comparison to coeval microflora, particularly to those of the East European Platform. *American Association of Stratigraphic Palynologists Foundation Contribution Series*, **38**: 123p.
- Peng, S. C. & Babcock, L. E. 2001. Cambrian of the Hunan-Guizhou region, South China. *In*: Peng Shanchi, Babcock, L. E. & Zhu Maoyan (Eds.), *Cambrian System of China*, University of Science and Technology of China Press, Hefei, pp. 3-51.
- Peng, S. C., Babcock, L. E., Geyer, M. & Moczyłowska, M. 2006a. Nomenclature of Cambrian epochs and series based on GSSPs-comments on an alternative proposal by Rowland and Hicks. *Episodes*, **29**: 130-132.
- Peng, S. C., Babcock, L. E., Robison, R. A., Lin, H. L., Rees, M. N. & Saltzman, M. R. 2004. Global Standard Stratotype-section and Point (GSSP) of the Furongian Series and Paibian Stage (Cambrian). *Lethaia* **37**: 365-379.
- Peng, S. C., Babcock, L. E., Zuo, J. X., Lin, H. L., Zhu, X. J., Yang, X. F., Robison, R. A., Qi, Y. P., Bagnoli, G. & Chen, Y. A. 2006b. Proposed GSSP for the base of Cambrian Stage 7, coinciding with the first appearance of *Lejopyge laevigata*, Hunan, China. *Palaeoworld*, **15 (3-4)**: 367-383.

- Peterson, K. J. & Butterfield, N. J. 2005. Origin of the Eumetazoa: Testing ecological predictions of molecular clocks against the Proterozoic fossil record. *Proc. Natl. Acad. Sci. U.S.A.*, **102**: 9547-9552.
- Pisarevsky, S. A., Komissarova, R. A. & Khramov, A. N. 2000. New palaeomagnetic result from Vendian red sediments in Cisbaikalia and the problem, of the relationship of Siberia and Laurentia in the Vendian. *Geophysical Journal International*, **140**: 598-610.
- Pittau, P. 1985. Tremadocian (Early Ordovician) acritarchs of the Arburese Unit, southwest Sardinia (Italy). *Bollettino della Società Paleontologica Italiana*, **23** (2): 161-204.
- Planel, H., Gaubin, Y., Kaiser, R. & Pianezzi, B. 1980. Effects of space environment on *Artemia* eggs. In: *The Brine Shrimp Artemia*, Vol. 1 (G. Personne, P. Sargeloos, O. Roels & E. Jaspers). *Wetteren Universa Press*, 189-198.
- Playford, G. 2003. Acritarchs and prasinophyte phycmata: a short course. AASP Contribution Series, **41**: 47 pp.
- Playford, G. & Martin, F. 1984. Ordovician acritarchs from the Canning Basin, Western Australia. *Alcheringa*, **10** (2): 187-223.
- Playford, G., Ribecai, C. & Tongiorgi, M. 1995. Ordovician genera *Peteinosphaeridium*, *Liliosphaeridium*, and *Cycloposphaeridium*: morphology, taxonomy, biostratigraphy, and palaeogeographic significance. *Bollettino della Società Paleontologica Italiana*, **34**: 3-54.
- Potts, W. T. W. & Durning, C. T. 1980. Physiological evolution in the branchiopods. *Comp. Biochem. Physiol.*, **67B**: 475-484.
- Potter, T. L. 1974a. The stratigraphic palynology of some Cambrian successions in North Wales, England and north-west Spain. Unpublished PhD Thesis, University of Sheffield.
- Potter, T. L. 1974b. British Cambrian acritarchs - a preliminary account. *Review of Palaeobotany and Palynology*, **18**: 61-62.
- Potter, T. L., Pedder, B. E., Feist-Burkhardt, S. 2012. Cambrian Furongian Series acritarchs from the Comley area, Shropshire, England. *Journal of Micropalaeontology*, **31**, 1-28.
- Prasad, B., Asher, R. & Borgohai, B. 2010. Late Neoproterozoic (Ediacaran)-Early Paleozoic (Cambrian) Acritarchs from the Marwar Supergroup, Bikaner-Nagaur Basin, Rajasthan. *Journal Geological Society of India*, **75**: 415-431.
- Prasad, B., Asher, R. 2001. Acritarch biostratigraphy and lithostratigraphic classification of Proterozoic and Lower Paleozoic sediments (Pre-Unconformity Sequence) of Ganga Basin, India. *Paleontographica Indica*, **5**: 1-151.
- Pyatiletov, V. G. 1980. Yudomskii kompleks microfossili Yuxhnoi Yakutii (Yudoma complex microfossils from southern Yakutia). *Geologiya i Geofizika*, **7**: 8-20.

- Quintavalle, M. & Playford, G. 2006. Palynostratigraphy of Ordovician strata, Canning Basin, Western Australia. Part Two: chitinozoans and biostratigraphy. *Palaeontographica. Abt. B: Palaeophytologie*, **275 (4-6)**: 89-131.
- Raevskaya, E. 2005. Diversity and distribution of Cambrian acritarchs from the Siberian and East-European platforms - a generalized scheme. In: Steemans, P. & Javaux, E (Eds.), Pre-Cambrian to Palaeozoic Palaeopalynology and Palaeobotany, *Carnets de Géologie / Notebooks on Geology, Brest, Memoir 2005/02*, Abstract 07.
- Raevskaya, E. & Golubkova, E. 2006. Biostratigraphical implication of Middle-Upper Cambrian acritarchs from Severnaya Zemlya (high Arctic of Russia). *Review of Palaeobotany and Palynology*, **139 (1-4)**: 53-69.
- Raevskaya, E. G. & Servais, T. 2009. *Ninadiacrodium*: A new Late Cambrian acritarch genus and index fossil. *Palynology*, **33**, 219-239.
- Rasetti, F. 1965. Upper Cambrian trilobite faunas of northeastern Tennessee. *Smithsonian Miscellaneous Collections*, **148**: 127 p.
- Rasul, S. M. 1974. The Lower Palaeozoic acritarchs *Priscogalea* and *Cymatiogalea*. *Palaeontology*, **17 (1)**: 41-63.
- Rasul, S. M. 1979. Acritarch zonation of the Tremadoc Series of the Shineton Shales, Shropshire, England. *Palynology*, **3**: 53-72.
- Rasul, S. M. & Downie, C. 1974. The stratigraphic distribution of Tremadoc acritarchs in the Shineton Shales succession, Shropshire, England. *Review of Palaeobotany and Palynology*, **18**: 1-9.
- Read, J. F. 1989. Controls on evolution of Cambrian Ordovician passive margin. U.S. Appalachians. In: Crevello, P. D., Wilson J. L., Sarg, J. F., Read, J. F. (Eds.), Control on Carbonate Platform and Basin Development. Society of Economic Paleontologists and Mineralogists, Special Publication, **44**: 147-165.
- Resser. C. E. 1938. Cambrian System (restricted) of the southern Appalachians. *Geological Society of America Special Paper*, **15**: 140 p.
- Retallack, G. J. 2011. Problematic megafossils in Cambrian palaeosols of South Australia. *Palaeontology*, **54**: 1223-1242.
- Ribbert, K.-H., Servais, T. & Vanguetstaine, M. 2001. 4.28 Stavelot-Venn-Antiklinale (28). In: *Stratigraphie von Deutschland II, Teil III*. Courier Forschungsinstitut Senckenberg, **235**, 68-89.
- Ribecai, C & Vanguetstaine, M. 1993. Latest Middle - Late Cambrian acritarchs from Belgium and northern France. *Special Papers in Palaeontology*, **48**: 45-55.
- Ribecai, C., Bagnoli, G., Mazzarini, F. & Musumeci, G. 2005. Paleontological evidence for Late Cambrian in the Arburese area, SW Sardinia. *Carnets de Géologie-Memoir 2005/02, Abstract 8*: 45-50.

- Richter, F. M., Rowley, D. B. & DePaolo, D. J. 1992. Sr isotope evolution of seawater: the role of tectonics. *Earth and Planetary Science Letters*, **109** (1-2): 11-23.
- Robison, R. A. 1988. Trilobites of the Holm Dal Formation (late Middle Cambrian), central North Greenland. *In*: Peel, J. S. (Ed.), Stratigraphy and paleontology of the Holm Dal Formation (late Middle Cambrian), central North Greenland. *Meddelelser om Grønland, Geoscience*, **20**: 23-103.
- Ross, R. J. Jr., Hintze, L. F., Ethington, R. L., Miller, J. F., Taylor, M. E. & Repetski, J. E. 1997. The Ibexian, lowermost series in the North American Ordovician. *Professional Paper of the U.S. Geological Survey*, **1579**: 1-50.
- Royer, D. L. 2006. CO₂-forced climate thresholds during the Phanerozoic. *Geochimica Cosmochimica Acta*, **70**: 5665-5675.
- Royer, D. L., Berner, R. A. & Beerling, D. J. 2001. Phanerozoic atmospheric CO₂ change: evaluating geochemical and paleobiological approaches. *Earth-Science Reviews*, **54**: 349-392.
- Rubenstein, C. V., Mángano, M. G. & Buatois, L. A. 2003. Late Cambrian acritarchs from the Santa Rosita Formation: implications for the Cambrian-Ordovician boundary in the Eastern Cordillera of northwest Argentina. *Revista Brasileira de Paleontologia*, **6**: 43-48.
- Rudavskaya, V. A. & Vassileva, N. J. 1984. The first finds of Lükati acritarchs in the Lower Cambrian Tshukorovsk section of eastern Siberia. *Doklady Akademii Nauk SSSR*, **274** (6): 1454-1456 (in Russian).
- Runnegar, B. & Saltzman, M. R. 1998. Global significance of the Late Cambrian Steptoean positive carbon isotope excursion (SPICE). *In* Landing, E. & Westrop, S. R. (Editors): *Avalon 1997: the Cambrian Standard*. *New York State Museum, Bulletin* **492**, 89.
- Rushton, A. W. A., & Molyneux, S. G., 2011. Chapter 3: Biostratigraphical divisions. *In*: Rushton, A. W. A., Brück, P.M. Molyneux, S. G., Williams, M. & Woodcock, N. H. A Revised Correlation of the Cambrian rocks in the British Isles. *Geological Society, London, Special Report*, **25**: 6-12.
- Rushton, A. W. A., Owen, A. W., Owens, R. M. & Prigmore, J.K. 1999. British Cambrian to Ordovician Stratigraphy. *Geological conservation review series* **18**. Joint Nature Conservation Committee, Peterborough, England, xxi+435 pp.
- Saltzman, M. R. Brasier, M. D., Ripperdan, R. L., Regaliev, G. K., Lohmann, K. C., Robison, R. A., Chang, W. T., Peng, S. & Runnegar, B. 2000. A global carbon isotope excursion during the Late Cambrian: Relation to trilobite extinctions, organic-matter burial and sea level. *Palaeogeography, Palaeoceanography, Palaeoclimatology*, **162**: 211-223.
- Saltzman, M. R., Cowan, A. C., Runkel, A. C., Runnegar, B., Stewart, M. C. and Palmer, A. R. 2004. The Late Cambrian SPICE event and the SAUK II-SAUK III regression:

- new evidence from Laurentian basins in Utah, Iowa and Newfoundland. *Journal of Sedimentary Research*, **74**, 366-377.
- Saltzman, M. R., Runnegar, B. & Lohmann, K. C. 1998. Carbon-isotope stratigraphy of the *Pterocephaliid* Biomere in the eastern Great basin: Record of a global oceanographic event during the Late Cambrian. *Geological Society of America, Bulletin*, **110**: 285-297.
- Samchyshyna, L. & Santer, B. 2010. Chorion structure of diapause and subitaneous eggs of four diaptomid copepods (calanoida, diaptomidae): SEM observations. *Vestnik zoologii*, **44** (3): 26-32.
- Sarjeant, W. A. S. & Stancliffe, R. P. W. 1994. The *Micrhystridium* and *Veryhachium* complexes (Acritarcha: Acanthomorphytae and Polygonomorphytae): a taxonomic reconsideration. *Micropaleontology*, **40** (1): 1-77.
- Sarjeant, W. A. S. & Stancliffe, R. P. W. 2000. Acritarch taxonomy: certain controverted questions. *Modern Geology*, **24**: 159-176.
- Sarjeant, W. A. S. & Strachan, I. 1968. Freshwater acritarchs in Pleistocene peats from Staffordshire, England. *Grana Palynologica*, **8**: 204-209.
- Sarjeant, W. A. S. & Vavrlová, M. 1997. Taxonomic reconsideration of *Multiplicisphaeridium* Staplin, 1961 and other acritarch genera with branching processes. *Geolines (Praha)*, **5**: 1-52.
- Schram, F. R. 1982. The Fossil record and evolution of Crustacea. In: Abele, L. G. (ed.). *The Biology of Crustacea Volume 1. Systematics, the Fossil Record and Biogeography*. Academic Press, New York: 93-147.
- Scotese, C. R. 2002. www.scotese.com (Paleomap project)
- Scourfield, D. J. 1926. On a new type of crustacean from the Old Red Sandstone (Rhynie Chert Bed, Aberdeenshire) - *Lepidocaris rhyiensis* gen. et. sp. nov. - Philosophical Transactions of the Royal Society, London, **214**: 153-187.
- Segroves, K. L. 1967. Cutinized microfossils of probably nonvascular origin from the Permian of Western Australia. *Micropaleontology*, **13**: 289-305.
- Sepkoski Jr., J. J. & Schopf, J. W. 1992. Biotic diversity and rates of evolution during Proterozoic and earliest Phanerozoic time. In: Schopf, J. W., Klein, C. (Editors), *The Proterozoic Biosphere: A Multidisciplinary Study*. Cambridge University Press, pp. 521-566.
- Sergeev, V. N., Knoll, H. K. & Vorob'eva, N. G. 2011. Ediacaran Microfossils from the Ura Formation, Baikal-Patom Uplift, Siberia: Taxonomy and Biostratigraphic Significance. *Journal of Paleontology*, **85** (5): 987-1011.
- Servais, T. & Eiserhardt, K. H. 1995. A discussion and proposals concerning the Lower Paleozoic "galeate" acritarch plexus. *Palynology*, **19**: 191-210.

- Servais, T., Vecoli, M., Jun Li, Molyneux, S. G., Raevskaya, E.G. & Rubinstein, C. V. 2007. The acritarch genus *Veryhachium* Deunff 1954: taxonomic evaluation and first appearance. *Palynology*, **31**: 191-203.
- Shaw, A. B. & DeLand, C. R. 1955. Cambrian of Southwestern Wyoming. Green River Basin: 10th Annual Field Conference Guidebook. 38-42.
- Siveter, D. J., Williams, M. & Waloszek, D. 2001. A phosphatocopid crustacean with appendages from the Lower Cambrian. *Science*, **293**: 479-481.
- Slavíková, K. 1968. New finds of acritarchs in the Middle Cambrian of the Barrandian (Czechoslovakia). *Věstník Ústr dneho ústavu geologického*, **43**: 199-205.
- Sloss, L. L. 1963. Sequences in the Cratonic Interior of North America. *Geological Society of America Bulletin*, **74**: 93-114.
- Sloss, L. L. 1964. Tectonic cycles of the North American Craton. In: Merriam, D. F., (ed.), *Symposium on cyclic sedimentation: Kansas Geological Survey, Bulletin*, **169**: 449-459.
- Sloss, L. L. (ed.) 1988. Sedimentary Cover – North American Craton, U.S.: The Geology of North America. Geological Society of America, Boulder Colorado, D-2, 506 pp.
- Sloss, L. L., Krumbein, W. C. & Dapples, E. C. 1949. Integrated facies analysis. *Geological Society of America, Memoir*, **39**: 91-124.
- Stanevich, A. M., Nemerov, V. K., Sovetov, Y. K., Chatta, E. N., Mazukabzov, A. M., Perelyaev, V. I & Kornilova, T. A. 2005. Precambrian microfossil-characterized biotopes from the southern margin of the Siberian craton. *Russ. J. Earth Sci*, **7**.
- Staplin, F. L. 1961. Reef-controlled distribution of Devonian microplankton in Alberta. *Paleontology*, **4**: 392–424.
- Staplin, F. L., Jansonius, J. & Pocock, S. A. J. 1965. Evaluation of some acritarchous hystrichosphere genera. *Neues Jarbuch für Geologie und Paläontologie*, **123**: 167-201.
- Steiner, M. & Fatka, O. 1996. Lower Cambrian tubular micro- to macrofossils from the Paseky Shale of the Barrandian area (Czech Republic). *Paläontologische Zeitschrift*, **70**: 275–299.
- Stitt, J. H. 1975. Adaptive radiation, trilobite paleoecology and extinction, Ptychaspid Biome, Late Cambrian of Oklahoma. *Fossils and Strata*, **4**: 381-390.
- Strother, P. K. 2008. A new Cambrian Acritarch from the Nolichucky Shale, eastern Tennessee, USA. *Palynology*, **32**: 205-212.
- Strother, P. K. & Beck, J. H. 2000. Spore-like microfossils from Middle Cambrian strata: expanding the meaning of the term cryptospore. In: Harley, M. M., Morton, C. M. &

- Blackmore, S. (Eds.), *Pollen and spores: Morphology and Biology*. Royal Botanic Gardens, Kew. 413-424.
- Strother, P. K., Wood, G. D., Taylor, W. A. & Beck, J. H. 2004. Middle Cambrian cryptospores and the origin of land plants. *Memoirs of the Association of Australian Palaeontologists*, **29**: 99-113.
- Stubblefield, C. J. 1930. A new Upper Cambrian Section in South Shropshire. *Summary of Progress of the Geological Survey of Great Britain*. for 1929, part 2: 54-62.
- Sugumar, V. & Munuswamy, N. 2006. Ultrastructure of Cyst Shell and Underlying Membranes of Three Strains of the Brine Shrimp *Artemia* (Branchiopoda: Anostraca) From South India. *Microscopy Research and Technique*, **69**: 957-963.
- Summons, R. E. & Walter, M. R. 1990. Molecular fossils and microfossils of prokaryotes and protists from Proterozoic sediments. *American Journal of Science*, **290-A**: 212-244.
- Sundberg, F. A. 1989. Biostratigraphy of the lower Conasauga Group. A preliminary report. In: Shumaker, R. C. (ed.). *Appalachian Basin Associates Spring Program*, **15**: 166-176.
- Symons, D. T. A. & Chiasson A. D. 1991. Paleomagnetism of the Callender Complex and the Cambrian apparent polar wander path for North America. *Canadian Journal of Earth Sciences*, **28**: 355-363.
- Szczepanik, Z. 1997. Preliminary results of thermal alteration investigations of the Cambrian acritarchs in the Holy Cross Mts. *Geological Quarterly*, **41 (3)**: 257-264.
- Szczepanik, Z. 2001. Acritarchs from Cambrian deposits of the southern part of the Łysogóry unit in the Holy Cross Mountains, Poland. *Geological Quarterly*, **45 (2)**: 117-130.
- Talyzina, N. M. & Moczyłowska, M., 2000. Morphology and ultrastructural studies of some acritarchs from the Lower Cambrian Lükati Formation, Estonia. *Review of Palaeobotany and Palynology*, **112**: 1-21.
- Talyzina, N. M., Moldowan, J. M., Johannisson, A. & Fago, F. J. 2000. Affinities of Early Cambrian acritarchs studied by using microscopy, Fluorescence flow cytometry and biomarkers. *Review of Palaeobotany and Palynology*, **108**: 37-53.
- Tappan, H. 1980. *The Paleobiology of Plant Protists*. W. H. Freeman & Co., San Francisco, 1028 pp.
- Tappan, H. & Loeblich, A. R. 1971. Surface sculpture of the wall in Lower Paleozoic acritarchs. *Micropaleontology*, **17 (4)**: 305-410.
- Tawadros, E., Rasul, S. M. & Elzaroug, R. 2001. Petrography and palynology of quartzites in the Sirte Basin, central Libya. *Journal of African Earth Sciences*, **32 (3)**: 373-390.
- Taylor, J. F. 1997. Upper Cambrian biomerer and stages, two distinctly different and equally vital stratigraphic units. 2nd International Conference on Trilobites, Abstracts with program.

- Taylor, J. F. 2006. History and status of the biomere concept. *Memoirs of the Association of Australasian Palaeontologists*, **32**: 247-265.
- Taylor, K. & Rushton, A. W. A. 1972. *The pre-Westphalian geology of the Warwickshire Coalfield with a description of three boreholes in the Merevale area*. Bulletin of the Geological Survey of Great Britain, **35**: 1-152. [dated 1971].
- Taylor, W. A. & Strother, P. K. 2008. Ultrastructure of some Cambrian Palynomorphs from the Bright Angel Shale, Arizona, USA. *Review of Palaeobotany and Palynology*, **151**: 41-50.
- Taylor, W. A. & Strother, P. K. 2009. Ultrastructure, morphology and topology of Cambrian palynomorphs from the Lone Rock Formation, Wisconsin, USA. *Review of Palaeobotany and Palynology*, **153**: 296-309.
- Thiéry, A. 1997. Horizontal distribution and abundance of cysts of several large branchiopods in temporary pool and ditch sediments. *Hydrobiologia*, **359**: 177-189.
- Thusu, B. 1973. Acritarchs of the Middle Silurian Rochester Formation of southern Ontario. *Palaeontology*, **16 (4)**: 799-826.
- Timofeev, B.V. 1959. *Drevnejshaya flora Pribaltiki* [The oldest flora of the Baltic area]. *Trudy VNIGRI* **129**. 320p. Leningrad.
- Timofeev, B.V. 1966. Microphytological investigations of ancient formations. *Acad. Sci. USSR Laboratory Precambrian Geol. Geochronol.* Nauka, Leningrad, 145 pp. (in Russian).
- Timofeev, B.V. 1969. Proterozoic sphaeromorphs. *Acad. Sci. USSR Inst. Precambrian Geol. Geochronol.* Nauka, Leningrad. 146 pp. (in Russian).
- Timofeev, B. V., Hermann, T. N. & Mikhailova, N. S. 1976. *Microfitofossilii Dokembriya Kembriya i Ordovika*, (Microphytofossils of the Precambrian, Cambrian and Ordovician), Nauka, Leningrad, 106 pp.
- Tommasini, S., Scanabissi Sabelli, F. & Trentini, M. 1989. Scanning electron microscope study of eggshell development in *Triops cancriformis* (BOSC) (Crustacea, Notostraca). *Vie Milieu*, **39 (1)**: 29-32.
- Tongiorgi, M. & Ribecai, C. 1990. Late Cambrian and Tremadocian phytoplankton (acritarchs) communities from Öland (Sweden). *Bollettino della Societa Paleontologica Italiana*, **29 (1)**: 77-88.
- Torsvik, T. H. & Rehnström, E. F. 2001. Cambrian palaeomagnetic data from Baltica: implications for true polar wander and Cambrian palaeogeography. *Journal of the Geological Society, London*, **158**: 321-329.
- Torsvik, T. H., Smethurst, M. A., Meert, J. G., Van der Voo, R., Mckerrow, W. S., Brasier, M. D., Sturt, B. A. & Walderhaug, H. J. 1996. Continental break up and collision in the Neoproterozoic and Paleozoic-A tale of Baltica and Laurentia. *Earth-Science Reviews*, **40**: 229-258.

- Turner, R. E. 1984. Acritarchs from the type area of the Ordovician Caradoc Series, Shropshire, England. *Palaeontographica, Abt. B.*, **190**: 87-157.
- Tynni, R. 1978. Lower Cambrian fossils and acritarchs in the sedimentary rocks of Söderfjärden, western Finland. *Geological Survey of Finland, Bulletin* **297**: 39-81
- Tynni, R. 1982a. New results of studies on the fossils in the Lower Cambrian sediment deposit of the Söderfjärden Basin. *Bulletin of the Geological Society of Finland* **54**: 57-68.
- Tynni, R. 1982b. On Paleozoic microfossils in clastic dykes on the Åland Islands and in the core samples of Lumparn. *Geological Survey of Finland, Bulletin*, **317**: 35-114.
- Umnova, N. I. & Vanderflit, E. K. 1971. Acritarch complexes from the Cambrian and Lower Ordovician sediments of the western and north-western Russian platform. *In*: Golubzov, V. K. (Ed.), *Palynological Research in Byelorussia and Other Regions of the U.S.S.R.* Uprav. Geol. Nauka i Teknika, Soviet. Minist. B.S.S.R., Beloruss, Nauchno-Issledovatelskogo Geologorazvegochnogo Instituta (BeINIGRI), Minsk (1971), pp. 45–72 (in Russian).
- Uye, S. 1985. Resting egg production as a life history strategy of marine planktonic copepod. *Bulletin of Marine Science*, **37**: 440-449.
- Uye, S., Kasahara, S. & Onbé, T. 1979. Calanoid Copepod Eggs in Sea-Bottom Muds. IV. Effects of Some Environmental Factors on the Hatching of Resting Eggs. *Marine Biology*, **51**: 151-156.
- Valensi, L. 1949. Sur quelques microorganismes planctoniques de silex du Jurassique moyen du Poitou et de Normandie Bulletin de la Société géologique de France, 5^e série, **18** (5): 537–550.
- Vanguetaine, M. 1973. New acritarchs from the Upper Cambrian of Belgium. *Microfossils of the oldest deposits, Proceedings of the Third International Palynological Conference, Novosibirsk, 1971.* Akademiya Nauk S.S.S.R., Siberskoe Otdelenie, Institut Geologii I Geofizikii, Izdatelstvo “Nauka”, Moskva: 28-30.
- Vanguetaine, M. 1974. Espèces zonales d’acritarches du Cambro-Trémadocien de Belgique et de l’Ardenne française. (Zone species of acritarchs from the Cambro-Tremadocian of Belgium and the French Ardennes). *Review of Palaeobotany and Palynology*, **18** (1-4): 63-82.
- Vanguetaine, M. 1978. Critères palynostratigraphiques conduisant à la reconnaissance d’un pli couché Revinien dans le Sondage de Grand-Halleux. *Annales de la Société Géologique de Belgique*, **100**: 249-276.
- Vanguetaine, M. 1986. Progrès récents de la stratigraphie par Acritarches du Cambro-Ordovicien d’Ardenne, d’Irlande, d’Angleterre, du Pays de Galles et de Terre-Neuve orientale. (Advances in Cambro-Ordovician stratigraphy using Acritarchs in Ardennes, Ireland, England, Wales and eastern Newfoundland). *Annales de la Société géologique du Nord*, **55**: 65-76.

- Vanguetaine, M. 2002. The Late Cambrian acritarch *Cristallinium randomense*: morphology, taxonomy and stratigraphical extension. *Review of Palaeobotany and Palynology*, **118** (1-4): 269-285.
- Vanguetaine, M. & Brück, P. M. 2008. A Middle and Late Cambrian age for the Booley Bay Formation, County Wexford, Ireland: New acritarch data and its implications. *Revue de Micropaléontologie*, **51** (1): 67-95.
- Vanguetaine, M., Brück, P. M., Maziane-Serraj, N., Higgs, K. T. 2002. Cambrian palynology of the Bray Group in County Wicklow and South County Dublin, Ireland. *Review of Palaeobotany and palynology*, **120**: 53-72.
- Vanguetaine, M. & Leonard, R. 2005. New biostratigraphic and chronostratigraphic data from the Sautou Formation and adjacent strata (Cambrian, Givonne Inlier, Revin group, northern France) and some lithostratigraphic and tectonic implications. In: T. Debacker, T., Sintubin, M., & Verniers, J. (Eds.), Avalonia–Moesia: Early Palaeozoic orogens in the Trans-European Suture Zone, *Geologica Belgica*, **8**(4): 131–144.
- Vanguetaine, M. & Van Looy, J. 1983. Acritarches du Cambrien Moyen de la vallée de Tacheddirt (Haut-Atlas, Maroc) dans le cadre d'une nouvelle zonation du Cambrien. *Annales de la Société Géologique de Belgique*, **106**: 69-85.
- Van Waveren, I. M. 1992. Morphology of probable planktonic crustacean eggs from the Holocene of the Banda Sea (Indonesia). In Head, M. J. & Wrenn, J. H. (editors), 1992, Neogene and Quaternary Dinoflagellate Cysts and Acritarchs: *American Association of Stratigraphic Palynologists Foundation, Dallas*, 89-120.
- Van Waveren, I. M. & Marcus, N. H. 1993. Morphology of recent copepod egg envelopes from Turkey Point, Gulf of Mexico, and their implications for acritarch affinity. *special Papers in Palaeontology*, **48**: 111-124.
- Vavrdová, M. 1972. Acritarchs from Klabava Shales (Arenig). *Vest. ustred. Ust. geol.*, **47**: 79-86.
- Vavrdová, M. & Bek, J. 2001. Further palynomorphs of Early Cambrian age from clastic sediments underlying the Moravian Devonian (borehole N m i ky-3). *Bulletin of Geosciences*, **76** (2): 113 - 125.
- Vecoli, M. 1996. Stratigraphic significance of acritarchs in Cambro-Ordovician boundary strata, Hassi-Rmel area, Algerian Sahara. *Bollettino della Società Paleontologica Italiana*, **35** (1): 3-58.
- Vecoli, M. 1999. Cambro-Ordovician palynostratigraphy (acritarchs and prasinophytes) of the Hassi-R'Mel area and northern Rhadames Basin, North Africa. *Palaeontographia Italica*, **86**: 1-112.
- Vecoli, M. & G. Playford, G. 1997. Stratigraphically significant acritarchs in uppermost Cambrian to basal Ordovician strata of northwestern Algeria. *Grana*, **36**: 17–28.
- Vecoli, M., Videt, B. & Paris, F. 2008. First biostratigraphic (palynological) dating of Middle and Cambrian strata in the subsurface of northwestern Algeria, North Africa:

- implications for regional stratigraphy. *Review of Palaeobotany and Palynology*, **149**: 57–62.
- Veis, A. F., Kozlov, V. I., Sergeeva N. D. & Vorob'eva, N. G. 2003. "Microfossils from the Riphean Type Section (the Karatau Group of Southern Urals)". *Stratigr. Geol. Korrelyatsiya*, **11 (6)**: 29-45.
- Vermeij, G. J. 1989. The origin of skeletons. *Palaios*, **4**: 585-589.
- Vidal, G. 1979. Acritarchs from the Upper Proterozoic and Lower Cambrian of East Greenland. *Grønland Geol. Unders Bull.* **134**: 55 p.
- Vidal, G. 1981a. Micropalaeontology and biostratigraphy of the Upper Proterozoic and Lower Cambrian sequence in east Finnmark, northern Norway. *Norges geol. Unders.*, **362**: 53 pp.
- Vidal, G. 1981b. Micropalaeontology and biostratigraphy of the Upper Proterozoic and Lower Cambrian sequence in Scandinavia. In: Taylor, M. E. (ed.), Short papers for the Second International Symposium on the Cambrian System. *U.S. Geological Survey Open-File report*, **81-743**: 232-235.
- Vidal, G. 1981c. Lower Cambrian acritarch stratigraphy in Scandinavia. *Geol. Foren. Stock. Forhandl.*, **102**: 183-192.
- Vidal, G. & Moczyłowska, M. 1997. Biodiversity, speciation and extinction trends of Proterozoic and Cambrian phytoplankton. *Paleobiology*, **23**: 230-246.
- Vidal, G. & Nystuen 1990. Micropaleontology, depositional environment and biostratigraphy of the upper Proterozoic Hedmark Group, southern Norway. *American Journal of Science*, **290-A**: 170-211.
- Vidal, G. & Peel, J. S. 1984. Acritarch biostratigraphy of the Lower Cambrian of Greenland. In: Armands, G. & Schager, S. (editors): *Abstracts of the 16th Nordiska Geologiska Vintermötet, Stockholm. Meddelanden, Stockholms Universitets Geologiska Institution* **225**: 234.
- Vidal, G. & Peel, J. S. 1988. Acritarchs from the Buen Formation (Lower Cambrian), North Greenland. *Grønlands Geologiske Undersøgelse, Rapport*, **137**: 54 pp.
- Vidal, G. & Peel, J. S. 1993. Acritarchs from the Lower Cambrian Buen Formation in North Greenland. *Grønlands Geologiske Undersøgelse, Bulletin* **164**: 35 pp.
- Volkova, N. A. 1968. Akritarkhi dokembrijskikh i nizhnekembrijskikh otlozhenij Estonii [Acritarchs from the Precambrian and Cambrian deposits of Estonia]. In Volkova, N. A. Zhuravleva, Z. A., Zabrodin, V. E. & Klinger, B. S.: *Problematiki pogranychnykh sloev rifeya i kembriya Russkoj platformy, Urala i Kazakhstana* [Problematics of Riphean and Cambrian layers of the Russian Platform, Urals and Kazakhstan], Nauka, Moscow, 8-36.
- Volkova, N. A. 1969a. Raspredelenie akritarch v razrezkh severovostochnoj Polshi [Distribution of acritarchs in the north-eastern Poland]. In Rozanov, A. Yu. et al.:

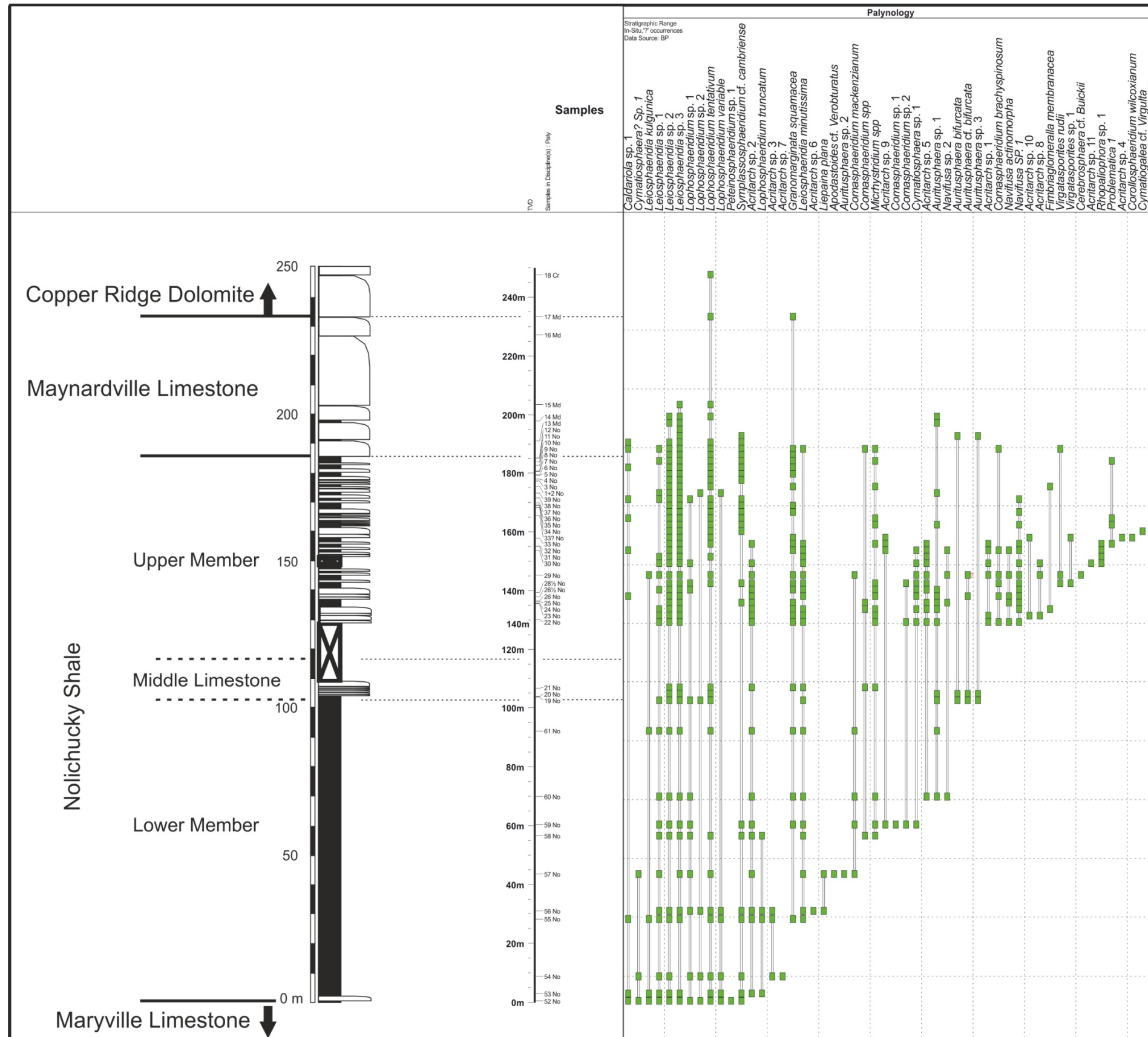
- Tommotskij yarus i problema nizhnej granitsy kembriya [Tommotian Stage and the Cambrian lower boundary problem]*, 74-76. Nauka, Moscow.
- Volkova, N. A. 1969b. Akritarkhi severo-zapada Russkoj platformy [Acritarchs of the north-western Russian Platform]. *In: Rozanov, A. Yu. et al.: Tommotskij yarus i problema nizhnej granitsy kembriya [Tommitian Stage and the Cambrian lower boundary problem]*, 224-236. Nauka, Moscow.
- Volkova, N. A. 1974. Akritarkhi iz pogranychnykh sloev nizhnego-srednego kembriya zapadnoj Latvii [Acritarchs from the transitional Lower-Middle Cambrian beds in the western Latvia]. *In: Biostratigrafiya i paleontologiya nizhnego kembriya Evropy i Severnoj Azii [Biostratigraphy and palaeontology of the Lower Cambrian in Europe and northern Asia]*, 194-262. Nauka, Moscow.
- Volkova, N. A. 1990. Middle and Upper Cambrian acritarchs in the East-European Platform. *Academy of Sciences of the USSR, Transactions no. 454*: 116 pp. (in Russian).
- Volkova, N. A. & Golub, I. N. 1985. Novye akritarkhi verkhnego kembriya Leningradskoy oblasti (Ladozhskaya svita) [New Upper Cambrian acritarchs from the Leningrad Oblast (Ladoga Formation)]. *Paleontologicheskii Zhurnal*, 19(4): 90-98.
- Volkova, N. A. & Kirjanov, V. V. 1995. Regional Middle-Upper Cambrian stratigraphic scheme of the East European Platform. *Stratigraphy and Geological Correlation*, **3**: 66-74.
- Volkova, N. A., Kirjanov, V. V., Piscun, L. V., Pashkyavichene, L. T., Jankauskas, T. V. 1979. Rastitelnye mikrofosili (Microflora). *In: Keller, B. M., Rozanov, A. Yu., editors. Paleontologiya verkhnedokembrijskikh i kembrijskikh otlozhenij Vostochno-Evropejskoj platformy (Upper Precambrian and Cambrian palaeontology of the East European Platform)*. Moscow: Nauka. p. 4-38 (in Russian).
- Volkova, N. A., Kirjanov, V. V., Piscun, L. V., Pashkyavichene, L. T., Jankauskas, T. V. 1983. Plant microfossils. *In: Urbanek, A., Rozanov, A. Yu., (editors). Upper Precambrian and Cambrian palaeontology of the East European Platform*. Warszawa: Wydawnictwa Geologiczne. p. 5-46.
- Vorob'eva, N. G., Sergeev, V. N. & Knoll, A. H. 2009. Diverse Ediacaran microfossils from the margin of the East European Platform. *Journal of Paleontology*, **83**: 161-196.
- Wahlenberg, G. 1821. Petrificata telluris Svecana examinata. *Nova Acta Regiae Societatis Scientiarum Upsaliensis*, **8**: 1-116, 293-297.
- Walcott, C. D. 1911. Middle Cambrian annelids. *Cambrian Geology and Paleontology II. Smithsonian Misc. Coll.* **57**: 109-144.
- Walker, K. R. & Byerly, D. W. 1985. Introduction to the Thorn Hill (U.S. Highway 25E) Stratigraphic Section, p. 1-5. *In: Walker, K. R. (Ed.), The geologic history of the Thorn Hill Paleozoic section (Cambrian-Mississippian) Eastern Tennessee*. Tennessee Department of Geological Sciences, Studies in Geology, 10.

- Walossek, D. 1993. The Upper Cambrian *Rehbachella* and the phylogeny of Branchiopoda Crustacea. *Fossils and Strata*, **32**: 1-202.
- Walossek, D. & Müller, K. J. 1998. Early arthropod phylogeny in light of the Cambrian 'Orsten' fossils. *In*: Edgecomb, G. D. (ed.), *Arthropod Fossils and Phylogeny*. Columbia University Press, New York. 185-231.
- Weber, L. J. 1988. Paleoenvironmental analysis and test of stratigraphic cyclicity in the Nolichucky Shale and Maynardville Limestone (Upper Cambrian) in central east Tennessee. Unpublished Ph.D. dissertation. University of Tennessee, Knoxville. 389 pp.
- Welsch, M. 1986. Die Acritarchen der höheren Digermul-Gruppe, Mittelkambrium bis Tremadoc, Ost-Finnmark, Nord-Norwegen. (The acritarchs of the Upper Digermul Group, Middle Cambrian to Tremadoc, eastern Finnmark, northern Norway). *Palaeontographica Abteilung B*, **201**: 1-109.
- Westergård, A. H. 1922. Sveriges Olenidskiffer. *Sveriges Geologiska Undersökning, Avhandlingar och uppsatser*, Ser. Ca, **18**: 205 pp.
- Westergård, A. H. 1944. Borrningar genom Skånes alunskiffer 1941-42. *Sveriges Geologiska Undersökning, C*, **459**: 1-45.
- Westrop, S. R. 1986. Trilobites of the Upper Cambrian Sunwaptan Stage, southern Canadian Rocky Mountains, Alberta. *Palaeontographica Canadiana*, **3**. 179 pp.
- Wetzel, O. 1933. Die in organischer Substanz erhaltenen Mikrofossilien des baltischen Kreide-Feuersteins mit einem sedimentpetrographischen und stratigraphischen Anhang. *Palaeontographica*, **78**: 1-110.
- Wicander, R. 2007. Acritarchs and Prasinophyte Phycomata, short course, Joint Meeting of Spores/Pollen and Acritarch Subcommissions, **15**.
- Wicander, R. & Monroe, J. S. 2007. Historical geology: evolution of Earth and life through time, 5th edition. Thomson learning inc. USA. 274 pp.
- Wicander, R., Playford, G. & Robertson, E. B. 1999. Stratigraphic and paleogeographic significance of an upper Ordovician acritarch flora from the Maquoketa Shale, northeastern Missouri, U.S.A. *The Paleontological Society Memoir*, **51**: 1-38.
- Willman, S. 2009. Morphology and wall ultrastructure of Leiospheric and acanthomorphic acritarchs from the Ediacaran of Australia. *Geobiology*, **7**: 8-20.
- Willman, S. & Moczyłowska, M. 2007. Wall ultrastructure of an Ediacaran acritarch from the Officer Basin, Australia. *Lethaia*, **40**: 111-123.
- Willman, S. & Moczyłowska, M. 2008. Ediacaran acritarch biota from the Giles 1 drillhole, Officer Basin, Australia, and its potential for biostratigraphic correlation. *Precambrian Research*, **162**: 498-530.

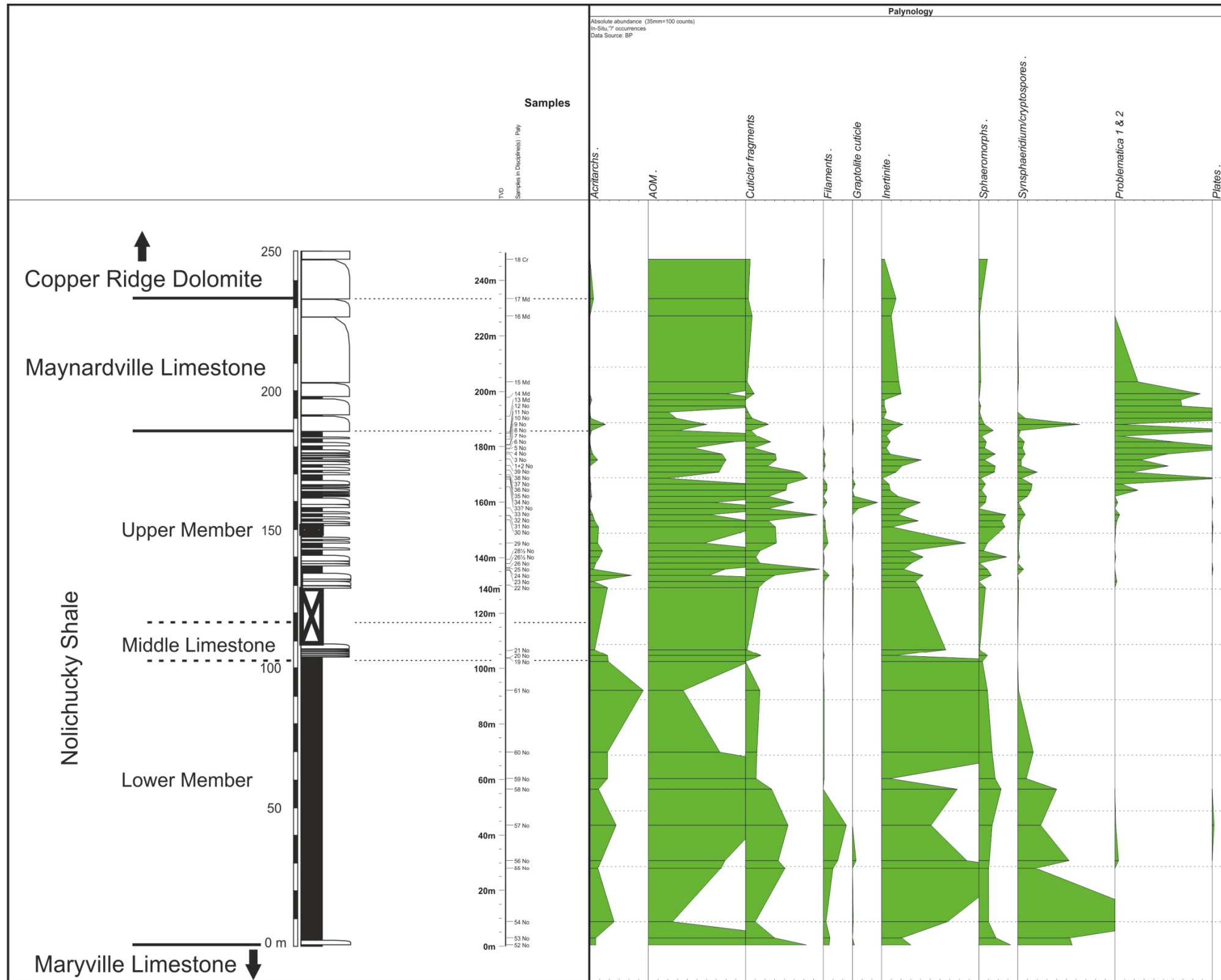
- Willman, S., Moczyłowska, M. & Grey, K. 2006. Neoproterozoic (Ediacaran) diversification of acritarchs: A new record from the Murnaroo 1 drillcore, eastern Officer Basin, Australia. *Review of Palaeobotany and Palynology*, **139**: 17-39.
- Wood, G. D. & Clendening, J. A. 1982. Acritarchs from the Lower Cambrian Murray Shale, Chilhowee Group of Tennessee, U.S.A. *Palynology*, **6**: 255-265.
- Wood, G. D. & Stephenson, J. T. 1989. Cambrian palynomorphs from the warm-water provincial realm, Bonneterre and Davis Formations of Missouri and Arkansas (Reelfoot Rift area): biostratigraphy, paleoecology and thermal maturity. In: Gregg, J.M., Palmer, J.R. & Kurtz, V.E. (Editors), *Field Guide to the Upper Cambrian of Southeastern Missouri: Stratigraphy, Sedimentology and Economic Geology*, Dept. of Geology and Geophysics, University of Missouri (Rolla). Geological Society of America Field Trip (Annual Meeting): 84-102.
- Xiao, S. 2002. Mitotic topologies and mechanics of Neoproterozoic algae and animal embryos. *Paleobiology*, **28** (2): 244-250.
- Xiao, S. & Knoll, A. H. 2000. Phosphatised animal embryos from the Neoproterozoic Doushantuo Formation at Weng'an, Guizhou, South China. *Journal of Paleontology*, **74**: 767-708.
- Xiao, S., Zhang, Y. & Knoll, A. H. 1998. Three-dimensional preservation of algae and animal embryos in a Neoproterozoic phosphorite. *Nature*, **391**: 553-558.
- Yan Yuzhong. 1982. *Schizofusa* from the Chuanlinggou Formation of Changcheng System in Jixian County. *Bulletin of the Tianjin Institute of Geology and Mineral Resources*, **6**: 1-7.
- Yang, Rui-Dong & Yin, Lei-Ming. 2001. Acritarch assemblages from the Early-Middle Cambrian Kaili formation of East Guizhou Province and biostratigraphic implication. *Acta Micropalaeontologica Sinica*, **18**: 55-69 (in Chinese with English abstract).
- Yao, J., Xiao, S., Yin, L., Li, G. & Yuan, X. 2005. Basal Cambrian microfossils from the Yurtus and Xishanblaq Formations (Tarim, northwest China): systematic revision and biostratigraphic correlation of *Micrhystridium*-like acritarchs. *Palaeontology*, **48** (4): 687-708.
- Yin, C. Bengtson, S. & Yue, Z. 2004. Silicified and phosphatised *Tianzhushania*, Spheroidal microfossils of possible animal origin from the Neoproterozoic of South China. *Acta Palaeontol Pol*, **49**: 1-12.
- Yin, L. 1986. Acritarchs. In: Chen Jun-Yuan (Ed.), *Aspects of Cambrian-Ordovician boundary in Dayangcha*, China. China Prospect Publishing House, Beijing, 314-373.
- Yin, L. 1997. Acanthomorphic acritarchs from Meso-Neoproterozoic shales of the Ruyang Group, Shanxi, China. *Review of Palaeobotany and Palynology*, **98**: 15-25.
- Yin, L & Yuan, X. 2007. Radiation of Meso-Neoproterozoic and early Cambrian protists inferred from the microfossil record of China. *Palaeogeography, Palaeoclimatology, Palaeoecology*, **254**: 350-361.

- Yin, L., Zhu, M., Knoll, A. H., Yuan, X., Zhang, J. & Hu, J. 2007. Doushantuo embryos preserved inside diapause egg cysts. *Nature*, **446**: 661-663.
- Young, T. P., Gibbons, W. & McCarroll, D. 2002. *Geology of the country around Pwllheli*. Memoir for 1:50,000 Geological Sheet 134 (England and Wales). British Geological Survey. 145pp.
- Young, T., Martin, F., Dean, W. T. & Rushton, A. W. A. 1994. Cambrian stratigraphy of St Tudwal's Peninsula, Gwynedd, northwest Wales. *Geological Magazine*, **131**: 335-360.
- Zang, W. L. 1992. Sinian and Early Cambrian floras and biostratigraphy on the South China Platform. *Palaeontographica* **B224**: 75-119.
- Zang, W. L. 2001. Acritarchs, *Palaeontological Institute of the Russian Academy of sciences. Transactions* **282**: 74-85.
- Zang, W. L., Jago, J. B. & Lin, T. R., 1998. Early Cambrian acritarchs, trilobites and biostratigraphy in South Australia. *Geological Society of Australia*, **49**: 493 (abstracts).
- Zang, W. L., Jago, J. B. & Lin, T. R., 2001. Early Cambrian acritarchs, trilobites and archaeocyathids from Yalkalpo 2, eastern Arrowie Basin, south Australia. *Department of Primary Industry and Resources, South Australia, Report Book 2001/0002*, 1-41.
- Zang, W. L., Jago, J. B., Alexander, E. M., Paraschivoiu, E., 2004. A review of basin evolution, sequence analysis and petroleum potential of the frontier Arrowie Basin, South Australia. *In: PESA Eastern Australian Basins Symposium II, Adelaide*. 243-256.
- Zang, W. L., Moczyłowska, M., Jago, J. B. 2007. Lower Cambrian acritarch assemblage zones in South Australia and global correlation. *Memoirs of the Association of Australian Palaeontologists*, **33**: 141-177.
- Zang, W. L. & Walter, M. R. 1992a. Late Proterozoic and Cambrian microfossils and biostratigraphy, Amadeus Basin, central Australia. *Memoirs of the Association of Australian Palaeontologists*, **12**: 134 pp.
- Zang, W. L. & Walter, M. R. 1992b. Late Proterozoic and Early Cambrian microfossils and biostratigraphy. northern Anhui and Jiangsu, central-eastern China. *Precambrian Research*, **57**: 243-323.
- Zhang, X., Shu, D., Li, Y. & Han, J. 2001. New sites of Chengjiang fossils: crucial windows on the Cambrian explosion. *Journal of the Geological Society*, **158 (2)**: 211-218.
- Zhang, Y., Yin, L. Xiao, S. & Knoll, A. H. 1998. Permineralized fossils from the terminal Proterozoic Doushantuo Formation, South China. *Palaeontological Society Memoir*, **50**: 52 pp.

- Zhao, Y.-L., Qian, Y. & Li, X.-S. 1994. *Wiwaxia* from Early-Middle Cambrian Kaili Formation in Teijinh Guizhou. *Acta Palaeontologica Sinica*, **33**: 359-366.
- Zhao, Y., Zhu, M., Babcock, L. E., Yuan, J., Parsley, R. L., Peng, J., Yang, X. & Wang, Y. 2005. Kaili Biota: a taphonomic window on diversification of metazoans from the basal Middle Cambrian: Guizhou, China. *Acta Geologica Sinica*, **79**: 751-765.
- Zhu, M. Y., Babcock, L. E. & Peng, S. C. 2006. Advances in Cambrian stratigraphy and paleontology: integrating correlation techniques, paleobiology. *Palaeoworld*, **15**: 217-222.
- Ziegler, A. M., Bambach, R. K., Parrish, J. T., Barret, S. F., Gierlowski, E. H., Parker, W. C., Raymond, A., Sepkoski J. J. 1981. Paleozoic biogeography and climatology. *Paleobotany, Paleoecology and Evolution* Vol. 2. Niklas, K. (Ed.) Praeger. 231-266.
- Yli ska, A., Szczepanik, Z. & Salwa, S. 2006. Cambrian of the Holy Cross Mountains, Poland; biostratigraphy of the Wi niówka Hill succession. *Acta Geologica Polonica*, **56**: 443-461.
- Yli ska, A., Szczepanik, Z. 2009. Trilobite and acritarch assemblages from the Lower–Middle Cambrian boundary interval in the Holy Cross Mountains (Poland). *Acta Geologica Polonica*, **59**: 413–458.



StrataBugs Chart 1 Stratigraphic range/occurrence of acritarchs for the Nolichucky Shale, Maynardville Limestone and Copper Ridge Dolomite at Thorn Hill.



StrataBugs Chart 2 - Palynofacies. Absolute abundances of acritarchs, AOM, cuticular fragments, filaments, graptolite cuticle, inertinite, sphaeromorphs, *Synsphaeridium/cryptospores* and Problematica 1 & 2 through the Nolichucky Shale, Maynardville Limestone and Copper Ridge Dolomite.